A Novel, Improved Throughput Bioassay for Determining the Relative Speed of Antimalarial Drug Action using Fluorescent Vitality Probes

A thesis submitted in fulfilment of the

requirements for the degree of

Doctor of Philosophy

In Biochemistry

Rhodes University

By

Dustin Laming

Abstract

Malaria is one of the most prevalent diseases in Africa and *Plasmodium falciparum* is widely accepted as the most virulent of the malaria parasite species, with a fatality rate of 15 – 20 % of reported cases of infection. While various treatments have been accepted into early stage clinical trials, there has been little progress towards a proven vaccine. Pending a long-term solution, endemic countries rely heavily on the development of innovative drugs that are not only efficacious but are also quick acting. Traditional methods of evaluating antimalarial killing speeds via morphological assessments are inherently flawed by tedious, subjective interpretations of the heterogenous parasite morphology encountered in routine parasite culture conditions. This has led to the introduction of alternative assay formats to determine how rapidly compounds act on parasites *in vitro*: a parasite reduction ratio (PRR) assay that measures the recovery of parasite cultures from drug exposure; determining the shift in IC_{50} values of compounds when dose-response assays are carried out for different time periods; a bioluminescence relative rate of kill (BRRoK) assay that compares the extent to which compounds reduce firefly luciferase activity in transgenic parasites. Recent whole cell *in vitro* screening efforts have resulted in the generation of chemically diverse compound libraries such as the Medicines for Malaria Venture's Pathogen Box, which houses 125 novel compounds with *in vitro* antiplasmodial activity. Assessing the relative killing speeds of these compounds would aid prioritizing fast-acting compounds that can be exploited as starting points for further development. This study aimed to develop a bioassay using the calcein-acetoxymethyl and propidium iodide fluorescent vitality probes, which would allow the relative speed of drug action on *Plasmodium falciparum* malaria parasites to be assessed and ranked in relation to each other using a quantitative, improved throughput approach. Initially applied to human (HeLa) cells, the assay was used to compare the relative speeds of action of

potential anti-cancer compounds by fluorescence microscopy. Subsequently adapted to *P. falciparum*, the assay was able to rank the relative speeds of action of standard antimalarials by fluorescence microscopy and two flow cytometry formats. Application of a multiwell flow cytometer increased throughput and enabled the assessment of experimental compounds, which included a set of artemisinin analogs and 125 antimalarial compounds in the MMV Pathogen Box. The latter culminated in the identification of five rapidly parasiticidal compounds in relation to the other compounds in the library, which may act as benchmark references for future studies and form the basis of the next generation of fast acting antimalarials that could be used to combat modern, resistant malaria.

Acknowledgements

To Prof Heinrich C. Hoppe, working with you over two degrees and seven years has been a true privilege. Through your guidance and mentorship, I have learnt not only to become a better scientist but a better person. I am proud to call you both supervisor and friend.

To the meneers, Lance Ho, Shane Flanagan, Greg Woolf and Chris Thorpe, thanks for helping keep me sane throughout the journey. To all the memories with you boys, it's been an incredible ride!

To my family, Roy and Jenny Laming, Connor and Tamika, your support throughout the years has been invaluable. Mom and Dad, I can only hope that I can make you fractionally as proud of me as I am to call you my parents. This PhD is as much a tribute to you as it is a success for me and I dedicate this thesis to you.

Table of Contents

Abstract 2
Acknowledgements 4
Table of Contents 5
List of Abbreviations 9
List of Figures 13
List of Tables 19
Chapter 1 – General Introduction 20
1.1 - Overview 20
1.2 - Life Cycle of malaria parasite 22
1.3 - Geographic Distribution and Impact of malaria 26
1.4 – Prophylaxis and Vaccine Progress 28
1.5 – Standard drug classes 30
1.5.1 - Quinolines 31
1.5.2 - Antifolates 35
1.5.3 - Artemisinins 37
1.6 - Antimalarial drug discovery 42
1.6.1 – Challenges 42
1.6.2 – Gametocytes and transmission-blocking approaches 44
1.6.3 – Asexual blood stages and current drug development 49
1.7 - *In vitro* assessment of antimalarial efficacy 58
1.8 – Fluorescent vitality staining 65
1.8.1 - Tetramethylrhodamine 68
1.8.2 - Hydroethidine 68
1.8.3 – Calcein-acetoxymethyl Ester 70
1.8.4 - Propidium Iodide 71
1.9 – A novel, quantitative, relative killing-speed bioassay for *Plasmodium falciparum*. 72
Chapter 2 – Vitality Probe Dynamics in HeLa cells 76
2.1 - Introduction 76
2.2 - Materials and Methods 78

2.2.1 - Mammalian (HeLa) cell culture and preliminary fluorescent vitality probe staining. 78
2.2.2 – Drug IC_{50} determination using an *in vitro* cytotoxicity assay. 80
2.2.3 – Fluorescence microscopy based relative killing speed assay. 80
2.2.4 – Plate-based fluorescence assay. 81
2.2.5 – ATP assay. 81
2.2.6 – Resazurin-based *in vitro* cytotoxicity assay. 82
2.3 - Results 83
2.3.1 - Fluorescent vitality probe staining in mammalian cells. 83
2.3.1.1 - Calcein-AM. 83
2.3.1.2 - Propidium Iodide 85
2.3.1.3 – TMRE. 86
2.3.1.4 – Hydroethidine. 87
2.3.2 – Compound IC_{50} determination using an *in vitro* cytotoxicity assay. 89
2.3.3 – Fluorescence microscopy-based relative killing speed assay. 92
2.3.4 – Plate-based fluorescence assay. 105
2.3.5 – ATP assay. 108
2.3.6 – Resazurin-based *in vitro* cytotoxicity assay. 110
2.3.7 – Results summary 112
2.4 – Discussion 114
2.4.1 - Fluorescent vitality probe staining in mammalian cells 115
2.4.3 – Vitality probe based cytocidal relative speed assays. 118
2.4.4 – ATP and resazurin-based assays. 127
2.5 – Conclusion 129
Chapter 3 – A Novel Bioassay to Measure the Relative Killing Speed of Antimalarials using Fluorescent Vitality Probes 131
3.1 - Introduction 131
3.2 - Materials and Methods 133
3.2.1 - Thawing cryopreserved cultures. 133
3.2.2 - Maintenance of *P. falciparum* 3D7 cultures. 133
3.2.3 - Parasite culture synchronization. 135
3.2.4 - Parasite culture cryopreservation. 135

3.2.5 – Determination of drug IC_{50} values using the Plasmodium lactate dehydrogenase (pLDH) assay. 136
3.2.6 – Fluorescent vitality probe analysis of drug-treated *P. falciparum* malaria parasites using fluorescence microscopy. 137
3.2.7 - Flow Cytometry analysis of drug-treated parasites stained with fluorescent vitality probes. 139
3.2.8 – Calcein-AM analysis of drug-treated parasites using filter tubes and plate fluorimetry. 141
3.2.9 - ATP Assay. 141
3.3 – Results 143
3.3.1 - Calcein-AM. 144
3.3.2 - Propidium Iodide 146
3.3.3 – TMRE. 148
3.3.4 – Hydroethidine. 149
3.3.5 - Drug IC_{50} values using the Plasmodium lactate dehydrogenase (pLDH) assay. 150
3.3.6 – Relative killing speed assay on panel of antimalarials using vitality probes. 153
3.3.7 – Improved quantification with flow cytometry. 157
3.3.8.1 – Calcein-AM and PI control samples. 162
3.3.8.2. – Analysis of standard antimalarial compounds. 167
3.3.9 - Adaptation of calcein-AM for use in a multi-well plate fluorimeter by employing filter tubes. 169
3.3.10 - Filter tube-based ATP Assay. 171
3.4 – Discussion 175
3.4.1 - Fluorescent vitality probe staining and optimization in *P. falciparum.* 175
3.4.2 – Relative killing speed assay on panel of antimalarials using vitality probes and fluorescence microscopy. 179
3.4.3 - Adapting the fluorescence assay to flow cytometry. 187
3.4.4 - Filter tube-based assays. 191
3.5 – Conclusion 193
Chapter 4 – Application of the Calcein-AM/Propidium iodide Relative Speed of Action Analysis to Experimental Antimalarial Compounds 195
4.1 – Introduction 195
4.2 – Materials and Methods 197

4.2.1 – Experimental compound assessment using calcein-AM/propidium iodide and flow cytometry 197
4.2.2 – Haemolysis assay 198
4.2.3 – Recovery assay 198
4.3 – Results 200
4.3.1 – Standard antimalarial assessment at 10 µM 200
4.3.2 – Assessment of a set of novel artemisinin analogs 203
4.3.3 – Assessment of a set of indolyl-3-ethanone ether antimalarials 207
4.3.4 – Assessment of the MMV 'Pathogen Box' 210
4.3.5 – Recovery assay 215
4.3.5.1 – Recovery assay using standard antimalarials 216
4.3.5.2 – Recovery assay using the slowest and fastest acting compounds in the Pathogen Box 218
4.4 – Discussion 220
4.4.1 – Standard antimalarial assessment at 10 µM 220
4.4.2 – Assessment of a set of novel artemisinin analogs 222
4.4.3 – Assessment of a set of indolyl-3-ethanone ethers 225
4.4.4 – Assessment of the MMV 'Pathogen Box' 227
4.4.5 – Recovery assay 230
4.5 – Conclusion 231
Chapter 5 – Concluding Discussion 233
Appendix 240
References 255

List of Abbreviations

4-AQ	4-aminoquinoline
ACT	Artemisinin-based combination therapy
AM	Acetoxymethyl
AMP	Adenosine monophosphate
APAD	3-Acetylpyridine adenine dinucleotide
APADH	3-Acetylpyridine adenine dinucleotide, reduced
ATP	Adenosine triphosphate
BD	Becton Dickinson
BFA	Brefeldin A
BSA	Bovine serum albumin
CFDA-SE	Carboxyfluorescein diacetate succinimidyl ester
CM	Complete Medium
CRISPR	Clustered Regularly Interspaced Short Palindromic Repeats
CSP	Circumsporozoite protein
DAPI	4,6-diamidino-2-phenylindole
ddH_2O	Double distilled water
DDT	Dichlorodiphenyltrichloroethane
DHA	Dihydroartemisinin
DHPS	Dihydropteroate synthase
DHFR	Dihydrofolate reductase
DHODH	Dihydroorotate dehydrogenase
DMEM	Dulbecco's Modified Eagle Medium
DMSO	Dimethyl sulfoxide

DNA	Deoxyribonucleic acid
EDTA	Ethylenediaminetetraacetic acid
FACS	Fluorescence-activated cell sorting
FITC	Fluorescein isothiocyanate
G6PD	Glucose-6-phosphate
GEF	Guanine nucleotide exchange factor
GFP	Green fluorescent protein
GPCR	G protein-coupled receptor
GTP	Guanosine-5'-triphosphate
HE	Hydroethidine
HEPES	N-2-hydroxyethylpiperazine-N'-2-ethanesulfonic acid
HIV	Human Immunodeficiency Virus
HPLC	High Performance Liquid Chromatography
HPPK	7,8-dihydro-6-hydroxymethylpterin-pyrophosphokinase
iRBC	Infected red blood cell
IRS	Indoor residual spraying
LL	Lower left
LLM	Limited liability company
LR	Lower right
LSM	Larval source management
MB	Methylene Blue
MIC	Minimum inhibitory concentration
MMV	Medicines for Malaria Venture
MPRR	Modified Parasite Reduction Ratio
MSF	SYBR Green I-based fluorescence

NADH	Nicotinamide adenine dinucleotide + hydrogen
NADPH	Nicotinamide adenine dinucleotide phosphate
NBT	Nitro tetrazolium blue
PBS	Phosphate-buffered saline
PES	Phenazine ethosulphate
P. falciparum	*Plasmodium falciparum*
PfSUB-1	Plasmodium falciparum subtilisin-like protease 1
PI	Propidium iodide
pLDH	Plasmodium lactate dehydrogenase
PPi	Pyrophosphate
PRR	Parasite Reduction Ratio
RAF	Rapidly accelerated fibrosarcoma
RBC	Red blood cell
RFU	Relative fluorescence units
RHX	Radioactive hypoxanthine
RLU	Relative luminescence units
RNA	Ribonucleic acid
ROS	Reactive oxygen species
RPMI	Roswell Park Memorial Institute
SERCaP	Single encounter radical cure and post-treament prophylaxis
SP	Sulphadoxine-pyrimethamine
TCAMS	Tres Cantos Antimalarial Set
TCP	Target Candidate Profile
TMRE	Tetramethylrhodamine
TPP	Target Product Profile

TRITC	Tetramethyl rhodamine iso-thiocyanate
UL	Upper left
UR	Upper right
USA	United States of America
UV	Ultraviolet
WHO	World Health Organization
WI	Wisconsin

List of Figures

Figure 1: Life cycle of malaria parasite showing both asexual and sexual life stages.

Figure 2: Light microscope images of Giemsa-stained *P. falciparum* parasites depicting the sequential intraerythrocytic life cycle.

Figure 3: *P. falciparum* malaria transmission regions as of 2017.

Figure 4: Global regions with the most widespread chloroquine resistance (indicated in red) in *Plasmodium falciparum.*

Figure 5: Distribution of sulphadoxine-pyrimethamine resistance in *Plasmodium falciparum.*

Figure 6: Artemisinin Combination Therapy resistance distribution in South-East Asia as of 2017.

Figure 7: Diagrammatic representation of fluorescent vitality probes and their area of intracellular sequestration.

Figure 8: Calcein-AM (5 µg/mL) and DAPI (2 µg/mL) staining of Hela cells treated with 100 µM gramicidin S for 30 min alongside untreated ('Normal') cells.

Figure 9: PI (20 µg/mL) and DAPI (2 µg/mL) staining of Hela cells treated with 100 µM gramicidin S for 30 min alongside untreated cells.

Figure 10: TMRE (0.05 µg/mL) and DAPI (2 µg/mL) staining of Hela cells treated with 100 µM gramicidin S for 30 min alongside untreated cells.

Figure 11: Hydroethidine (3 µg/mL) and DAPI (2 µg/mL) staining of Hela cells treated with 100 µM gramicidin S for 30 min alongside untreated cells.

Figure 12: Dose-response curves for novobiocin, etoposide, 17 AAG and brefeldin A against HeLa cell samples.

Figure 13: Dose-response curves for Golgicide, VER 155008, nav2729 and emetine against HeLa cell samples.

Figure 14: Tri-probe staining of compound-treated HeLa cells using PI (20 µg/mL), Calcein-AM (5 µg/mL) and Hoechst 33342 (5 µg/mL): 8 hours.

Figure 15: Killing speed for each test compound represented as average cell viability assessed by fluorescence microscopy after an eight-hour drug treatment.

Figure 16: Tri-probe staining of compound-treated HeLa cells using PI (20 µg/mL), Calcein-AM (5 µg/mL) and Hoechst 33342 (5 µg/mL): 16 hours.

Figure 17: Killing speed for each test compound represented as average cell viability assessed by fluorescence microscopy after a 16-hour drug treatment.

Figure 18: Tri-probe staining of compound treated HeLa cells using PI (20 µg/mL), Calcein-AM (5 µg/mL) and Hoechst 33342 (5 µg/mL): 24 hours.

Figure 19: Killing speed for each test compound represented as average cell viability assessed by fluorescence microscopy after a 24-hour drug treatment.

Figure 20: Calcein-AM fluorescence intensity of drug treated HeLa cells after 8, 16 and 24-hours.

Figure 21: Relative luminescence units (RLU) for the panel of cytotoxic compounds reflecting the ATP levels after an 8, 16 and 24-hour drug-treatment of HeLa cells.

Figure 22: Relative fluorescence units (RFU) for the panel of cytotoxic compounds representing population vitality after eight hours of drug treatment in HeLa cells, using resazurin as viability indicator.

Figure 23: Fluorescence microscopy of calcein-stained control and gramicidin D treated parasites.

Figure 24: Fluorescence microscopy of calcein-stained RBCs and saponin-treated trophozoites.

Figure 25: Fluorescence microscopy of propidium iodide-stained gramicidin D-treated and untreated control parasites.

Figure 26: Fluorescence microscopy of PI and calcein-stained merozoites.

Figure 27: Fluorescence microscopy of TMRE-stained control and gramicidin D-treated parasites.

Figure 28: Fluorescence microscopy of hydroethidine-stained control and gramicidin D-treated parasites.

Figure 29: Dose-response curves of the five *P. falciparum* 3D7 antimalarial drug compounds used in the study.

Figure 30: Dual probe staining of *P. falciparum* 3D7 parasites using PI (3.3 µg/mL) and calcein-AM (1 µg/mL).

Figure 31: Speed of drug action for each test compound represented as percentage viable parasites visualized by fluorescence microscopy after an 8-hour drug treatment.

Figure 32: Flow cytometric dot plot of Hoechst (1 µg\mL, 10 min) stained pRBCs and RBCs.

Figure 33: Flow cytometry histograms of gramicidin D (0.1 nM) treated pRBCs stained with PI (3.3 µg/mL) (A) and calcein-AM (1 µg/mL) (B).

Figure 34: Flow cytometry histogram comparison of the model antimalarial drugs and their respective killing speeds, measured as PI positive events after an eight-hour treatment.

Figure 35: Flow cytometry histogram comparison of the model antimalarial drugs and their respective killing speeds, measured as calcein-AM positive events after an eight-hour treatment.

Figure 36: Dot plots for control samples for the calcein-AM study depicting 100 000 events per panel generated by a Becton Dickinson ACCURI^{TM} C6 Plus flow cytometer.

Figure 37: Dot plots for control samples for the PI study depicting 100 000 events per panel generated by a Becton Dickinson ACCURI^{TM} C6 Plus flow cytometer.

Figure 38: Calcein-AM (green) and PI (red) fluorescent events recorded using a Becton Dickinson ACCURI^{TM} C6 Plus flow cytometer as a measure of drug stress after eight hours of treatment.

Figure 39: RFU (as an indication of killing speed) obtained from calcein-AM stained parasites after 8 hours of drug treatment using a filter tube-based assay.

Figure 40: RLU (Relative luminescence units) reflecting the ATP levels in drug-treated parasites obtained from cultures treated with standard antimalarial compounds.

Figure 41: Dot plots for the control samples depicting 100 000 events per panel generated by a Becton Dickinson ACCURI™ C6 Plus flow cytometer.

Figure 42: Mean fluorescent events recorded by Becton Dickinson ACCURI™ C6 Plus flow cytometer and representing 100 000 *P. falciparum* cells per sample after an eight-hour drug treatment at 10 µM.

Figure 43: Chemical structures of the panel of novel artemisinin analogs acquired from Richard Haynes (North West University).

Figure 44: Mean fluorescent events recorded by Becton Dickinson ACCURI™ C6 Plus flow cytometer and representing 100 000 *P. falciparum* cells per sample after an eight-hour drug treatment at 10 µM.

Figure 45: Qualitative examination of haemolysis observed post compound treatment in *P. falciparum.*

Figure 46: RBC counts indicative of hameolysis observed post treatment with the individual compounds at 10 µM for eight hours.

Figure 47: Fastest and slowest acting antimalarial-like compounds in the Pathogen Box according to the PI/calcein-AM fluorescent event ratios.

Figure 48: Chemical structures of the five most rapidly cidal compounds according to the novel fluorescent probe assay identified via their MMV Pathogen Box code.

Figure 49: Chemical structures of the five slowest acting parasiticidal compounds according to the novel fluorescent probe assay identified by their MMV Pathogen Box code.

Figure 50: Haemolysis assay of the five most rapid and five slowest acting Pathogen Box antimalarial compounds identified in the novel speed-of-action assay.

Figure 51: Recovery assay conducted on standard antimalarial compounds.

Figure 52: Pathogen Box recovery assay conducted on the 5 slowest and 5 most rapid acting antimalarial compounds in the Pathogen Box.

List of Tables

Table 1: Respective incubation time and concentrations implemented for each fluorescent probe in conjunction with HeLa cells.

Table 2: Maximum excitation and emission wavelengths of the fluorescent vitality probes used.

Table 3: Experimental IC_{50} values of the eight test compounds obtained in cytotoxicity assays performed in technical duplicate in each of three distinct biological replicates.

Table 4: Respective incubation times and final concentrations implemented for each fluorescent probe treatment of *P. falciparum* parasites.

Table 5: Experimental IC_{50} values of the five test compounds obtained in pLDH assays, compared to cited literature values.

Table 6: Slowest vs. fastest acting compounds in the Pathogen Box according to the killing speed assay and their associated IC_{50}'s.

Chapter 1 – General Introduction

1.1 - Overview

Malaria is one of the most prevalent diseases in Africa and is caused by parasites of the genus *Plasmodium*. Described as a 'prehistoric' parasite, its associated symptoms have been documented as early as 2700 BC, but it wasn't until 1880 that Charles Louis Alphonse Laveran identified the instrumental agent as a parasite (Cox, 2010; Sullivan, 2017). Various *Plasmodium* species have been identified with differential geographic distributions, including *Plasmodium ovale* (widely encountered in tropical Africa), *Plasmodium malariae* (generally observed as a coinfection with *P. falciparum* in sub-Saharan Africa and South America), and *Plasmodium vivax* (predominantly observed in South America) (Autino *et al.,* 2012). These species have been shown to have low levels of drug resistance and rarely cause fatalities (Janneck *et al*., 2011). By contrast, the *Plasmodium falciparum* species is widely accepted as the most virulent and prevalent, particularly in sub-Saharan Africa, with a fatality rate of 15 – 20% of reported cases of infection (Mace *et al*., 2011; Pacifici, 2018). It is often the case that when an individual becomes symptomatic of malaria, their health can deteriorate rapidly, with some of the more severe symptoms including renal failure, pulmonary edema, anemia and coma (cerebral malaria), made increasingly difficult to treat by the parasite's resistance to multiple antimalarial drugs (Janneck *et al*., 2011; Sypniewska *et al.*, 2017). Cerebral malaria is of particular concern in children with as many as 500 000 occurrences a year, often resulting in death due to rapid onset of fever and resultant coma within 1-3 days (Holmberg *et al.,* 2017). Although the etiology of cerebral malaria is not definitively known, it is currently hypothesized that infected erythrocytes sequester in cerebral capillaries, resulting in an inflammatory response in the central nervous system (Holmberg *et al.*, 2017).

According to the World Health Organization's (WHO) annual malaria report, no significant progress had been made in reducing the number of global malaria infection cases between 2015 and 2017 (World Malaria Report, 2018). Of the infected individuals, 61% of those that resulted in death in 2017 occurred in children under the age of 5 (World Malaria Report, 2018) which, due to their developing immune systems, have been identified as the most susceptible to the disease (Black *et al.,* 2003; Wendel *et al.,* 2017). While various treatments have been accepted into early stage clinical trials, progress towards a proven vaccine has been discouraging. Until a long-term solution is found, endemic countries rely heavily on the development of rapidly acting, innovative drugs with acute efficacy to complement vector control programs aimed at preventing disease transmission via the mosquito vector.

1.2 - Life Cycle of malaria parasite

Plasmodium transmission to Human (Fig. 1) occurs via the bite of the female mosquito of the genus *Anopheles*, whereby the parasite is initially transferred to the liver and subsequently invades the host red blood cells (RBCs) where it develops through ring, trophozoite and schizont life stages (Fu *et al.*, 2010).

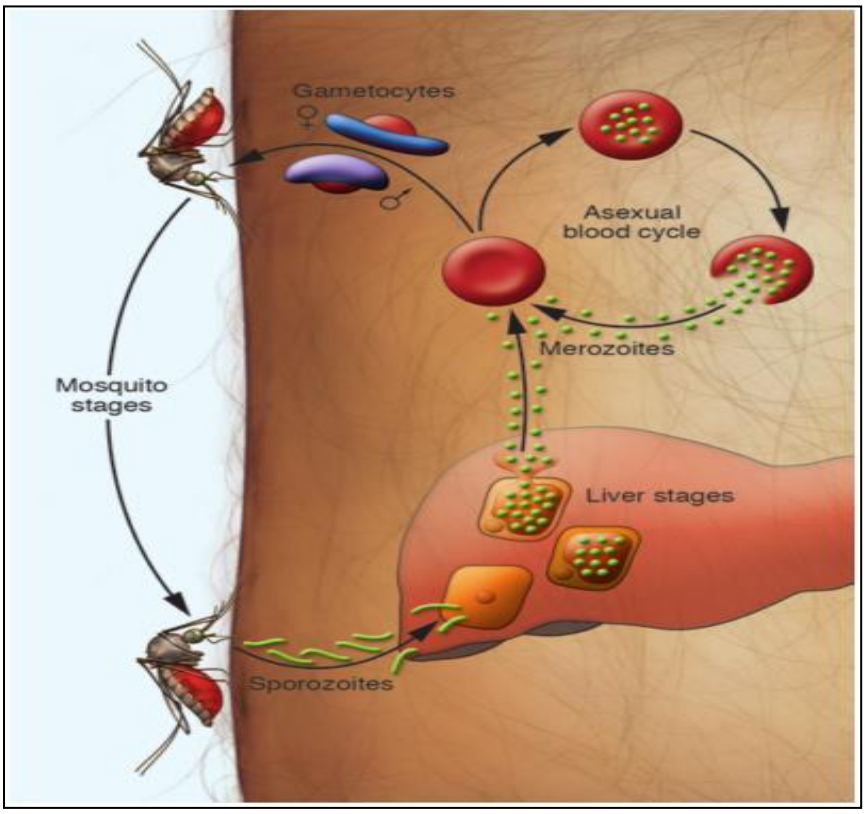

Figure 1: Human Life cycle of malaria parasite showing both asexual and sexual life stages. The asexual blood stage is the most commonly studied and accounts for the acute parasitic infection and accompanying symptoms (Wellems *et al*., 2009).

The female *Anopheles* mosquito produces eggs throughout her life and requires relatively large amounts of proteins for their production. These proteins are acquired from the blood they feed on, making them a model vector for malaria transmission (Miller *et al.*, 1994; Molina-cruz *et al.*,

2017). Part of the feeding process involves the mosquito injecting salivary fluid containing anti-coagulants into the blood of the host and, if infected with malaria parasites, allows the transfer of sporozoites into host tissue or directly into the blood stream (Baldacci and Menard, 2004; Singh *et al.,* 2017). The sporozoites then travel to the liver where they infect liver cells and begin dividing asexually into merozoites, marking the onset of the asexual life cycle (Grimberg, 2011; Singh *et al.,* 2017). Once significant replication has taken place, the cells swell and pressure overload results in rupture releasing the merozoites into the bloodstream where each single merozoite will infect a RBC and initiate the intraerythrocytic stage of the life cycle.

When inside the host RBC, the merozoite adopts a flattened morphology where the cellular organelles are found around the periphery of the parasite while the center contains only a thin layer of cytoplasm (Bannister *et al.,* 2000; Oikonomou and Jensen, 2017). Under light microscopy this morphology takes on the appearance of a 'ring', hence the name 'ring-stage parasite'. The ring stage occurs from 0 – 20 hours (Fu *et al.,* 2010) as the RBC is slowly altered, while a strict set of genes responsible for parasite metabolism are transcribed (Srivastava *et al.,* 2016). The primary mode of asexual blood-stage parasite metabolism involves glycolysis and the digestion of haemoglobin internalized from the surrounding host RBC cytoplasm. A byproduct of haemoglobin digestion is the release of haem, which is packed into inert crystals called haemozoin as a detoxification mechanism (Grimberg, 2011). The latter occurs during the trophozoite stage (20 – 36 hours) where metabolism is exponentially increased. It has been observed that lactic acid production in a trophozoite stage infected RBC is increased up to 100-fold in relation to an uninfected RBC and that the observed hyperlactatemia is assumed to be a result of increased parasite metabolism via anaerobic glycolysis. (Pfaller *et al.,* 1982; Mehta *et al.,* 2006; Marchetti *et al.,* 2015).

Once the host RBC haemoglobin has been fully metabolised, the mature trophozoite initiates large scale protein and DNA synthesis and nuclear division and enters the schizont stage (Srivastava *et al.*, 2016; Stanojcic *et al.*, 2017). After a period of 36-48 hours and once DNA and organelle replication are complete, the new cellular components are organized into independent foci and, after segmentation, produce new daughter merozoites. Following rupture of the infected RBC, each merozoite is then able to infect a new RBC and so maintain the intraerythrocytic stage of the parasite life cycle (Cowman and Crabb, 2006; Abkarian *et al.*, 2011).

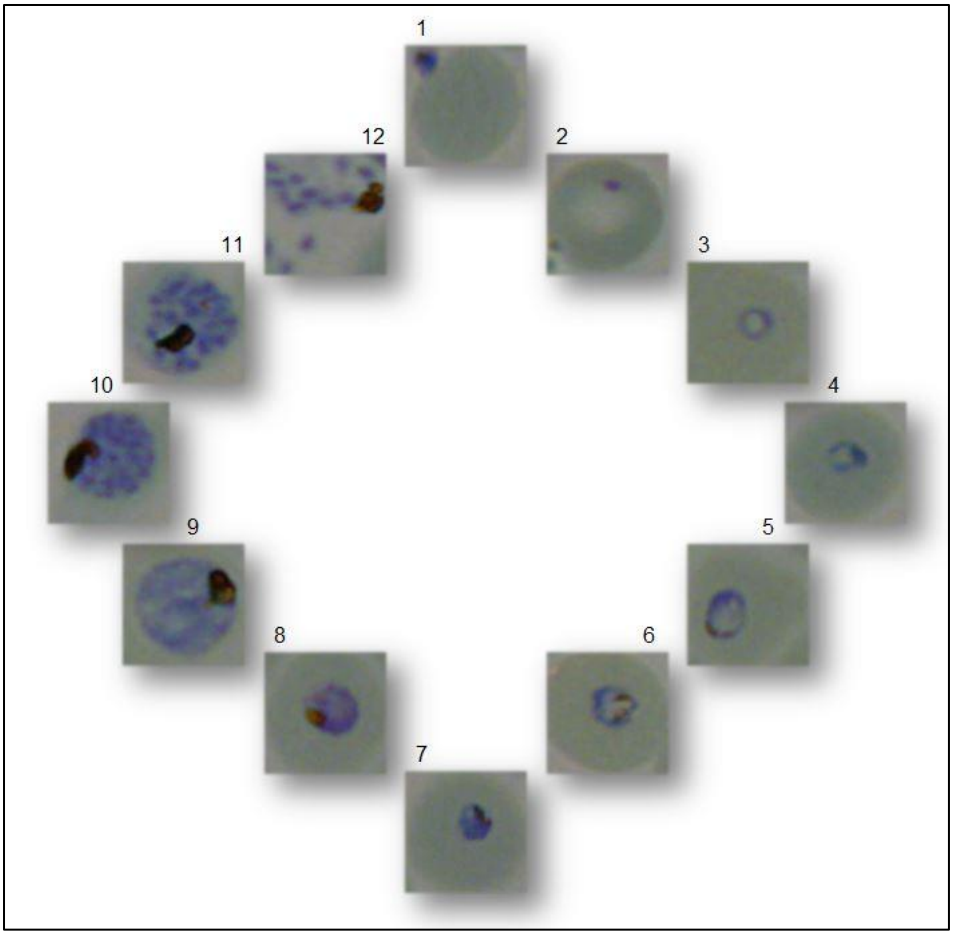

Figure 2: Light microscope images of Giemsa-stained *P. falciparum* parasites depicting the sequential intraerythrocytic life cycle. The cycle is initiated by the invasion of a merozoite into a host RBC (1-2). Once inside, the early stage parasite forms a ring-shaped structure and initiates hemoglobin metabolism (3-5). As the parasite matures it enters the trophozoite stage and metabolism is exponentially increased (6-9). The parasite then undergoes asexual replication as it enters the schizont phase (10-11) and approximately 48 hours post RBC invasion the host cell ruptures releasing daughter merozoites into the bloodstream (12).

Alternatively, some trophozoites may differentiate into male or female gametocytes and initiate the sexual stage of infection. The signal by which this process occurs is due to a number of influencers including parasite stress (Fivelman *et al.*, 2007; Gebru *et al.*, 2017) as well as specific epigenetic factors and transcriptional regulators (Josling and Llinas, 2015). In the case of *P. falciparum*, gametocyte differentiation is observed only a few weeks after erythrocyte infection (Fivelman *et al.*, 2007; Gebru *et al.*, 2017). As gametocytes are incapable of producing male and

female gametes within the human host, they differentiate only when extracted by another mosquito. The gametes fuse to form a zygote in the mosquito midgut, which (as an ookinete) penetrates the gut and forms and oocyst attached to the gut lining in the hemocoel. Multiple cell divisions occur in the oocyst and the resulting sporozoites are deposited into the salivary glands of the mosquito from where they are transferred to a new human host when the mosquito takes its next bloodmeal (Chimaka *et al.,* 2017).

1.3 - Geographic Distribution and Impact of malaria

As all malaria parasite species make use of the female *Anopheles* mosquito as a vector, it has been shown that malaria endemic regions often significantly overlap with the *Anopheles* mosquito's ideal environment (Hay *et al.,* 2009; World Malaria Report, 2016). This relates to the tropic regions of the world (Fig. 3) where people are at highest risk of contracting the parasite (Hay *et al.,* 2009; World Malaria Report, 2018). Important to note is that developing countries dominate these tropical regions and the high levels of poverty and inadequate healthcare lead to increased problems in controlling transmission.

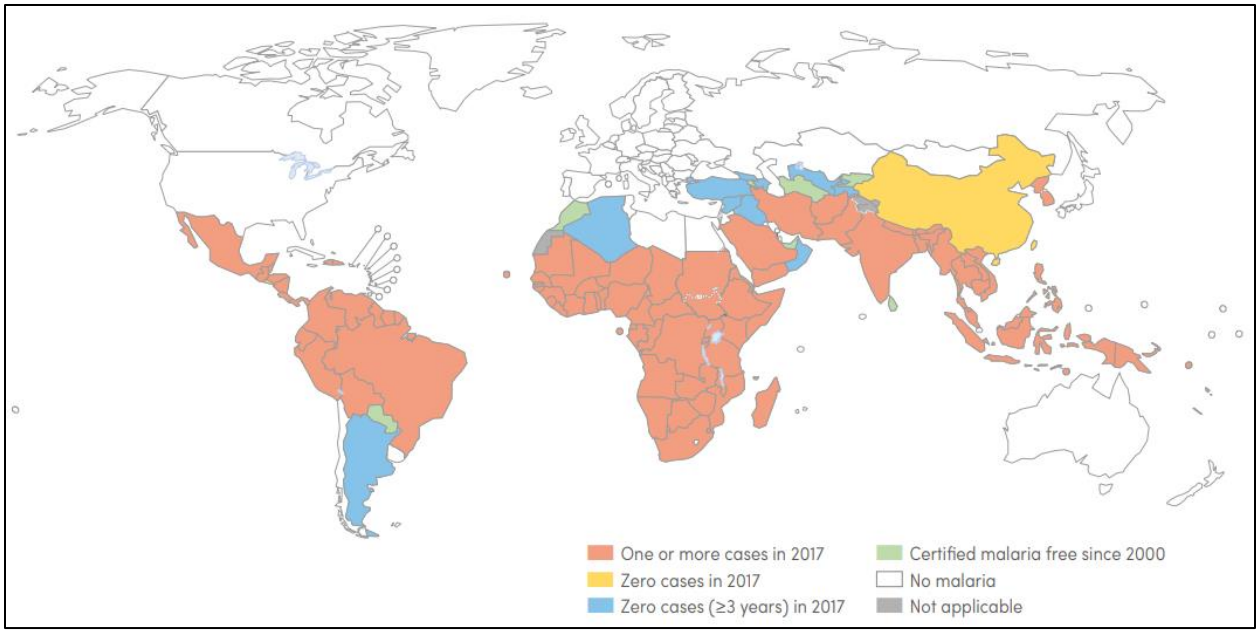

Figure 3: *P. falciparum* malaria transmission regions as of 2017. Countries with zero cases of new malaria parasite infections over at least three years were considered malaria free. China and El Salvador both reported zero cases of infection in 2017 (World Malaria Report, 2018).

From a South African perspective, it has often been the ideology that preventative measures need only be taken when travelling to central Africa. This is true in the sense that the regions in the country with the highest prevalence of malaria are along the border with Mozambique. However, this notion is rapidly becoming obsolete as Tonnang and company showed that, due to climate change, distribution patterns of the *Anopheles* mosquito have been expanding to the east and south-east coasts of South Africa (Tonnang *et al.*, 2010). South Africa is fortunate in relation to other developing countries in Africa and Asia in the sense that it has relatively well-developed health care infrastructure and is more economically robust, therefore being able to better implement malariacontrol measures.

1.4 – Prophylaxis and Vaccine Progress

Development of innovative means of malaria control has been slow. In order to prevent parasite infection, prophylactic approaches such as the use of insecticide treated bed nets, indoor residual spraying and larval source management are used. In terms of bed nets, the primary observable complication involves a lack of patient compliance for bed net use as a study conducted in Kenya showed 14% of children under five issued with bed nets had not utilized them (Atieli *et al.*, 2011). Secondarily, a lack of maintenance strategies in place for bed nets has led to reduced use after their issue (Tizifa *et al.,* 2018). Besides bed net use, the long-term application of insecticides to the indoor surfaces of homes resulted in killing the mosquitoes on contact or repelling them from the indoor environment. Termed indoor residual spraying (IRS), it has been effective in the control of malaria in some of the most endemic regions, with a protective efficacy in Tanzania and Pakistan of 54 and 88% respectively (Pluess *et al.,* 2010). Problems with IRS are primarily two-fold – firstly, it can be costly, as often multiple applications are required for long term vector prevention and secondly, there are often health risks associated with the insecticides used (e.g. the neurodegenerative and carcinogenic links previously observed with dichlorodiphenyltrichloroethane (DDT) use (Beard, 2006)) (Tizifa *et al.,* 2018).

Larval source management (LSM) involves habitat control (often aquatic) for the *Anopheles* vector to prevent mosquito maturation (Fillinger and Lindsay, 2011; Tizifa *et al.,* 2018). The most effective LSM method to date has been larviciding – the introduction of chemical or biological insecticides to aquatic mosquito environments. Although a promising method of vector control the process is costly and to date not feasible for routine use in third world countries (Tizifa *et al.,* 2018).

IRS and bed netting are still the most effective ways of preventing malarial infection - LSM remains in its infancy and has yet to show the major success the former have (Ridley, 2001; Tizifa *et al.,* 2018). These approaches are of further concern, however, with the emergence of insecticide resistant mosquito vectors and therefore requires constant monitoring as well as novel, environmentally friendly insecticide and insecticide-combination treatments (Klausner and Alonso, 2004; Tizifa *et al.,* 2018). Recent advances in genetic manipulation and the development of CRISPR/cas9 gene editing have opened new potential for genetic modification of *Anopheles* mosquitoes, i.e. releasing mosquitos resistant to the malaria parasite into the environment to outcompete the indigenous populations (Greenwood, 2017).

Besides vector control, another strategy for combating malaria prior to acquisition of the parasite is the use of a vaccine. However, a target specific vaccine has yet to leave developmental stages, therefore this option is currently unavailable in malaria treatment. Only a single vaccine has progressed as far as stage 3 clinical trials - RTS,S/AS01 (Agnanji *et al.*, 2012). The vaccine targets the sporozoite life stage of the parasite to prevent liver stage infection and therefore halts successful parasite transmission to a new host (Chaudhury *et al.,* 2017). The circumsporozoite protein (CSP) is the most abundant protein on the surface of the sporozoite stage parasite and has been a leading target for potential vaccines, as is the case for RTS,S/AS01 (Sedegah *et al.*, 2013). Results have shown minor decreases in the risk of infection in babies vaccinated between 5 and 17 months of age (Agnanji *et al.,* 2012) and an upper limit of 50-60% protection in vaccinated malaria-naïve individuals (White *et al.,* 2013). Recent adaptations to the dosage regimen (from 0-1-2 month to 0-1-7 month) have shown significant improvements in vaccine efficacy – up to 86% (Chaudhury *et al.,* 2017). Although these results appear promising, higher efficacy levels are required to contest the mortality rate observed for malaria. Other vaccines do exist but are at least

5-10 years in development behind RTS,S/AS01. Recently the promising vaccine PfSPZ underwent clinical trials, but it too was met with sub-optimal results. The vaccine is comprised of attenuated, live *P. falciparum* sporozoites and was developed by a group in Maryland, USA. Results have shown that healthy adults experienced only 33% reduction in infection in relation to placebo groups (Sissoko *et al.,* 2017).

The final broad method of malaria parasite control is that of drug treatment, the key to which is early diagnosis and rapid efficacy as malaria is an acute infection (as opposed to a chronic infection like HIV). If the disease is left unchecked, hospitalization is required. As malaria is extremely prevalent in poor and developing countries with severe shortages in adequate health care, this provides a major challenge to current control measures. Poor economic development leads to limited access to drugs and trained staff and with reports of increasing vector resistance to insecticides and the lack of a vaccine, drug treatment remains the last line of defense against the parasite.

1.5 – Standard drug classes

Since synthetic chemicals were introduced for malaria control over 70 years ago, only a small number of drugs (belonging to three classes) have reached the market and with increasing reports of resistance, there is a drive to alter and combine the existing antimalarials to create better drug formulations. The main classes (historic and current) of antimalarial drugs are discussed below. This includes quinolines (chloroquine and mefloquine), antifolates (sulfadoxine in combination with pyrimethamine) and artemisinins. Although these drugs are all to a larger or lesser extent compromised by resistance, artemisinins in combination with partner drugs remain the mainstay of malaria treatment and mefloquine is one of the standard partners. Chloroquine is obsolete due

to resistance, but additional 4-aminoquinolines that share its mode of action are in clinical development or have been approved for use, notably amodiaquine as a partner drug for artesunate. In addition, suladoxine and pyrimethamine have also been approved for use in combination with amodiaquine (Medicines for Malaria Venture global portfolio of antimalarial medicines: https://www.mmv.org/research-development/mmv-supported-projects). It is thus useful to briefly review these drug classes here.

1.5.1 - Quinolines

Quinine was originally extracted from cinchona bark in the 1800s and was often the go-to drug for severe forms of malaria (Grimberg and Mehlotra, 2011; Brown, 2017). Though poorly tolerated as an oral formulation with attendant side-effects (including severe anemia, liver damage and contribution to birth defects if taken during pregnancy), quinine motivated the subsequent development of synthetic quinolines. Chloroquine (a derivative of quinine) has historically been the most widely used antimalarial due to its high rate of success and low cost. Mechanistically it is widely accepted that it accumulates in the parasite food vacuole where the digestion of haemoglobin takes place (Chinappi *et al.,* 2010; Bounaadja *et al.,* 2017). As a weak base, chloroquine is uncharged at neutral pH and diffuses across the parasite membranes into the food vacuole. Here it becomes ionized due to the acidic pH of the vacuole and trapped, thus accumulating in the organelle (Yayon *et al.,* 1985; Tewari *et al.,* 2017). RBC cytoplasm which is predominantly composed of haemoglobin is ingested by the parasite by endocytosis and delivered to the food vacuole. Proteases exist within the food vacuole which digest the haemoglobin, releasing haem - a toxic moiety to malaria parasites (Yazon *et al.,* 1984; Tewari *et al.,* 2017). The parasite then sequesters the haem into a haemozoin crystal, resulting in haem detoxification. Chloroquine is proposed to disrupt the sequestration process, resulting in a build-up of toxic haem

and resultant cell death (Chinappi *et al.,* 2010). This was confirmed for example in studies using transmission electron microscopy, whereby chloroquine treatment in trophozoite-stage parasites resulted in a decrease in hemozoin and proportional increase in toxic haem, which correlated directly with parasite cell death (Combrinck *et al.,* 2013).

Unfortunately, chloroquine has become essentially redundant due to widespread resistant strains covering a majority of malaria endemic areas (Fig. 4).

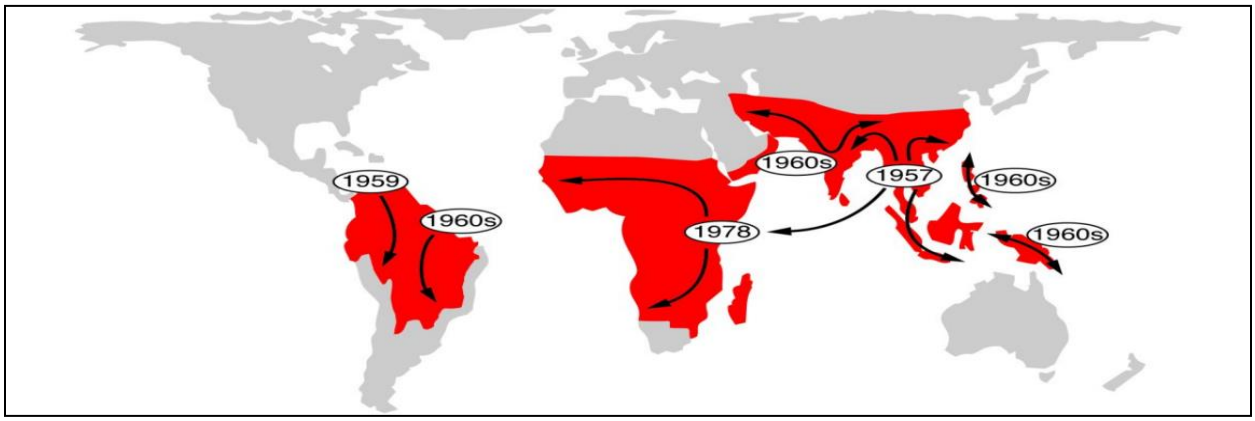

Figure 4: Global regions with the most widespread chloroquine resistance (indicated in red) in *Plasmodium falciparum*. Initial resistance is shown to have originated in South-East Asia and spread rapidly (indicated by arrows) across Africa and South America (Wellems *et al.,* 2009).

As with its mechanism of action, the mode by which resistant parasites deal with an influx of chloroquine has been hypothesized by a variety of studies. Initial mechanisms proposed included the development of a permeability barrier around the food vacuole disallowing chloroquine sequestration (Hancock, 1987) or an enzyme which perhaps inactivates chloroquine (analogous to antibiotic metabolism by β-lactamases) (Neu, 1987). Krogstad and associates (1988) suggested a mechanism whereby resistant *P. falciparum* parasites have adapted a process for rapid efflux of chloroquine. This efflux is then absent or significantly reduced in wild-type parasites. To enable the chloroquine efflux, it is primarily accepted that chloroquine resistant strains of malaria

parasites are caused by mutations in two genes associated with the parasite food vacuole – a chloroquine resistance transporter (*Pfcrt*) and the multidrug resistance transporter-1 (*Pfmdr1*), with *Pfcrt* mutations being a stronger predictor of resistance than *Pfmdr1* mutations (Mohammed *et al.,* 2013). Both *in vitro* and clinical resistance has been observed with the specific *Pfcrt*-K76T mutation and it was shown that the removal of this mutation from resistant strains led to wild-type levels of chloroquine sensitivity (Lakshmanan *et al.,* 2005). Current updates accept that the presence of mutant *Pfcrt* as well as the recently observed P-glycoprotein homologue 1 (*P-gh1*, a gene product of *Pfmdr1* and similar to *Pfcrt* in the sense that it is a transporter protein residing in the parasite digestive vacuole membrane) are responsible for chloroquine-resistant malaria strains. The mutated proteins have an enhanced affinity for chloroquine, allowing rapid efflux of chloroquine from the food vacuole and thus preventing the drug from reaching sufficient concentrations to disrupt haem detoxification (Skrzypek and Callaghan, 2017).

Mefloquine is a quinoline methanol derivative used as both a therapeutic and prophylactic antimalarial. Due to its more potent activity compared to chloroquine, it was quickly marketed under the name Lariam™ by Hoffmann-La Roche for U.S. military deployment to malaria endemic regions. In contrast to chloroquine, it has a longer half-life allowing for a single weekly dose, thereby reducing the risk of non-compliance. Early studies suggested a similar mechanism as that of chloroquine i.e., like chloroquine, mefloquine may interfere with detoxification of haem resulting from parasite haemoglobin metabolism, preventing growth and resulting in cell death. This had been proposed to occur either by mefloquine binding directly to haem (Dorn *et al.,* 1998) or inhibiting the polymerization of haem to haemozoin (Sullivan *et al.,* 1998). A later study showed that mefloquine and chloroquine may both affect parasite endocytosis of haemoglobin, albeit at different stages. Mefloquine inhibited host cell cytoplasm ingestion, while chloroquine appeared

to act later by blocking the delivery of ingested cytoplasm to the food vacuole (Hoppe *et al.,* 2004). This differential effect on the endocytic pathway suggests different modes of action for chloroquine and mefloquine, or at least that mefloquine has additional targets that are not shared by chloroquine. Recently, new evidence has suggested that mefloquine acts as a protein synthesis inhibitor, whereby the drug was found to bind directly to the GTPase of the 80S ribosome in the parasite. In the same study, mutagenesis of the mefloquine-binding residues resulted in increased resistance to the drug and aided in confirming this as one of the primary killing mechanisms of mefloquine (Wong *et al.,* 2017).

Unlike chloroquine, mefloquine use is often associated with side-effects, particularly cognitive disturbances. Gap junction proteins (connexins) are involved in various cognitive functions with one such protein, Cx36, being responsible for proper neuron functioning in several brain regions (Cruickshank *et al.,* 2004). The Cruickshank group proposed evidence to suggest mefloquine was able to block Cx36 channels in neuroblastoma cells and, importantly, did so with minimal nonspecific interactions (ensuring proper gap protein functioning in other brain areas). These observations are still being investigated and indications in recent studies suggest mefloquine to indeed be antagonistic to the Cx36 connexin, as well as being able to inhibit insulin secretion (Seemann *et al.,* 2017).

Chloroquine and mefloquine have been shown to not only contrast in mechanism, but also in drug resistance. Previous studies have observed that various mutations in the multidrug resistance gene (*Pfmdr1*) are responsible for a major part of the resistance seen in mefloquine resistant parasites (Cravo *et al.,* 2003), with only one of these having been associated with resistance to chloroquine – N86Y (Eyase *et al.,* 2013). A group in India observed that sampled local isolates that did not contain mutated *Pfmdr1* N86Y were not able to display resistance to mefloquine (in comparison

to N86Y mutated *Pfmdr1* parasite strains in which mefloquine was significantly less effective – Sharma *et al.,* 2017). A study conducted a year later confirmed the presence of an amplified *pfmdr1* gene (including N86Y, Y184F and F1226Y mutations) in as much as 49% of malaria patients in a clinical study in Cambodia (Rossi *et al.,* 2018). Although it appears universally agreed that other mechanisms of mefloquine resistance exist that do not involve *Pfmdr1*, they have yet to be observed or reported.

1.5.2 - Antifolates

Antifolates are compounds that inhibit the enzymatic synthesis of folates that are required as co-factors in purine and amino acid synthesis. Antifolates were developed as a more adept means of combating leukaemia - folic acid was observed to be an important factor in the spread of leukaemia and thus led to the first folate analogue, aminopterin, which demonstrated a drastic increase in remissions in cancer patients and a landmark for cancer chemotherapy (Farber *et al.,* 1948). This success led to the use of this class of drugs in the treatment of other rapidly dividing cells such as parasites. The antifolate class of drugs used to counter *P. falciparum* can be divided into two groups – those which target the parasitic enzyme dihydropteroate synthase (DHPS; class I antifolates) and those which target dihydrofolate reductase (DHFR; class II antifolates) (Nzila, 2006). These are two key enzymes in the pathway that coverts GTP and *para*-aminobenzoic acid into tetrahydrofolate. Arguably the best recognized of the antimalarial antifolates is pyrimethamine which belongs to class II and as such counters the parasitic DHFR and inhibits DNA and amino acid synthesis (Hurwitz *et al*., 1981).

Typically, antifolates are used as combination therapies that combine class I (sulfonamides, *e.g.* sulphadoxine and sulfalene) and class II (*e.g.* pyrimethamine) antifolates in a single formulation.

Sulphadoxine-pyrimethamine (SP) is, to date, the most commonly used antimalarial in the preventative treatment of malaria in pregnancy (Walker *et al.,* 2017) and is also largely used in preventative treatment in infants (Okell *et al.,* 2017). Malaria parasites, being rapidly dividing cells, have an increased demand for nucleotide precursors for DNA synthesis. By blocking folate synthesis using antifolates (like SP) there is decrease in tetrahydrofolate, a resultant decrease in conversion of serine to glycine, reduced synthesis of thymidylate, and ultimately a decrease in parasite DNA production (Verhoef *et al.,* 2017).

Combinations of class I and class II antifolates (e.g. co-trimoxazole, a combination of sulfamethoxazole and trimethoprim) are also widely used for combating a wide range of other bacterial, fungal and parasitic diseases. However, in these diseases as well as malaria, use of antifolates is threatened by the emergence and spread of resistance caused by point mutations in DHFR and DHPS that reduce the affinity of the enzymes for the drugs. As was the case with the quinolines, resistance emerged in South America and Southeast Asia and subsequently spread to remaining malaria endemic regions (Fig. 5).

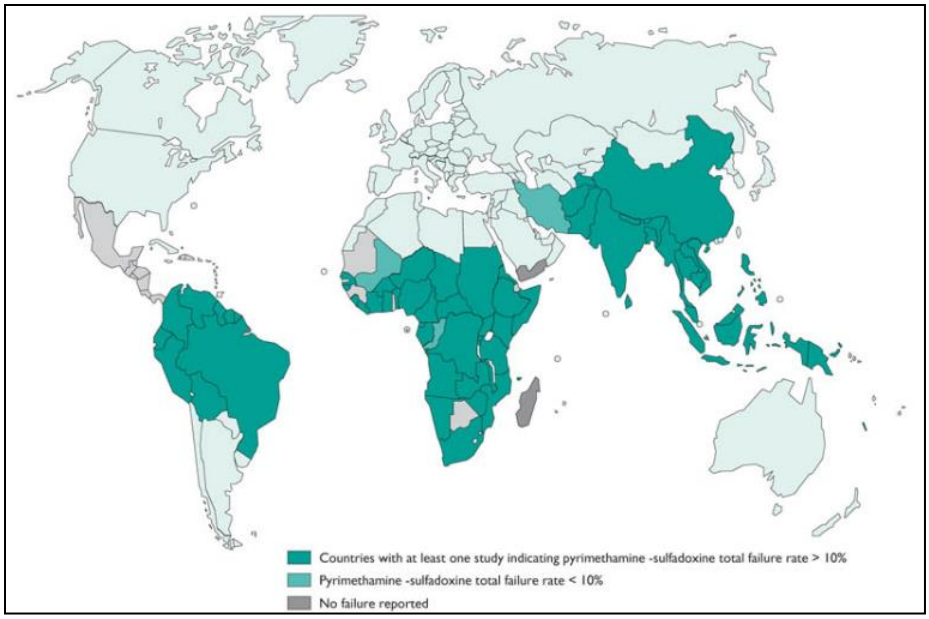

Figure 5: Distribution of sulphadoxine-pyrimethamine resistance in *Plasmodium falciparum*. Regions affected correlate with those showing resistance to quinoline derived drugs (Anderson, 2003).

Pyrimethamine resistance has been associated with various point mutations in the parasite DHFR gene with the most effective documented being S108N, which has been shown to cause a 7-50-fold increase in *in vitro* IC_{50} (Jovel *et al.,* 2017). Mutations in the parasite DHPS have also been associated with resistance (Abdul-Ghani *et al.,* 2013) and a combination of mutations in the DHFR and DHPS encoding genes have resulted in highly resistant parasites (Jovel *et al.,* 2017). Point mutations in the parasite multidrug resistant protein (Pfmdr1), presumably resulting in more efficient drug efflux from the parasite, have also previously been associated with SP resistance (Dahlstrom *et al.,* 2009).

1.5.3 - Artemisinins

The current global standard for malaria treatment is the use of artemisinin and its derivatives. Like quinine which generated the quinoline class of compounds, artemisinin is also derived from a plant, the qinghao herb (*Artemisia annua*), and was initially used as a treatment for fevers in

traditional Chinese medicine (Klayman, 1985). In 1977 the structure of artemisinin was solved and provided the basis of a chemical scaffold which could be modified to improve solubility and synergy with other antimalarial drugs (Klayman, 1985). To date, artemisinin is still extracted from the *Artemisia* herb and, with its derivatives, comprises the last and most effective line of defense against modern, resistant malaria parasite strains. Reasons for its versatility include the fact that its administration can take one of several routes – intramuscular, intravenous, intrarectal and oral (Hien, 1994; Krishna *et al.*, 2004). It has a relatively short half-life in comparison to other common antimalarials – the active metabolite has an elimination half-life of approximately 1 hour (Krishna *et al.,* 2004) - and it has been shown to be effective against strains of malaria parasite that are highly resistant to chloroquine (Agbenyega *et al.,* 2000). Artemisinins have also been shown to impede the broadest range of malaria parasite life stages being effective against rings, trophozoites and early stage schizonts (ter Kuile *et al.*, 1993; Angus *et al.*, 1997; Zhang *et al.*, 2017) while artesunate and artemether have shown efficacy against gametocytes (Roth *et al.,* 2018).

To date, the mechanism of action of artemisinin has been proposed by several studies, often with conflicting findings, and as such is still not conclusive. The strongest case was originally suggested by the Meshnick group whereby the bioactivation and derivation of artemisinin-associated trioxane dimers are triggered by iron (II) and subsequently generate toxic oxygen radicals (Meshnick *et al.,* 1993; O`Neill *et al.,* 2010). This bioactivation of artemisinins endoperoxide bridge is dependent on a rich source of iron and hence provides selectivity of artemisinin towards parasite infected RBCs – the parasites metabolism of haemoglobin into nontoxic haemozoin generates an abundance of iron (II) and iron (III) inside the parasite food vacuole. (O`Neill *et al.,* 2010). Activated oxygen damage is then observed via lipid peroxidation, protein oxidation and alkylation amongst others. Iron chelators have been shown to have an antagonistic effect on artemisinins

activity providing further evidence of the importance of iron in the mechanism of the drug (Meshnick *et al.,* 1993). Cleavage of the endoperoxide bridge may also produce artemisinin-haem adducts which prevents haemozoin formation and hence results in an accumulation of toxic haem in the parasite cell (Wang *et al.,* 2015). Alternatively, it has been suggested that the drug may target a specific protein or enzyme. Work in this area has shown artemisinin to inhibit the falcipain protein family - cysteine proteases that promote haemoglobin degradation (Pandey *et al.,* 1999; O'Neill *et al.,* 2013). Studies have also reported observing artemisinins ability to depolarize the membrane potential of the parasite and result in apoptosis (Antoine *et al.,* 2014). There has also been evidence to propose that the artemisinin-associated free radical production directly resulted in mitochondrial breakdown (Li *et al.,* 2005).

Due to the emergence of resistance to previous antimalarials over an arguably short time, the WHO has recommended the use of artemisinin combination-based therapies (ACT). ACT involves making use of artemisinin or several related endoperoxide antimalarials in combination with drugs with longer half-lives and spanning different classes which have been shown to rapidly eliminate *P. falciparum* infections (as is the case with artesunate-mefloquine) (Dondorp *et al*., 2010). This is done so that the more long-lived partner drug can combat any remaining parasites after initial artemisinin activity and, by using a combination of drugs with different modes of action, to significantly reduce the probability of selecting parasites that are simultaneously resistant to both. There are currently five ACTs recommended by the WHO (artemether-lumefantrine, artesunate-mefloquine, artesunate-amodiaquine, dihydroartemisinin-piperaquine and artesunate-sulphadoxine-pyrimethamine) which have shown to be rapidly effective against multidrug-resistant parasites as well as gametocytes (van Vugt *et al.,* 2002; Kavishe *et al.,* 2017). Each combination has been shown to be effective in different regions (depending on the predominant

strain of resistant parasites) with artesunate-mefloquine still extensively used in Southeast Asia and dihydroartemisinin-piperaquine in western Cambodia (Kavishe *et al.,* 2017). Artemether-lumefantrine is mostly used in Africa where artemisinin-mefloquine is less effective.

Although resistance to artemisinin has emerged, evidence of its mechanism has only recently become clear. The kelch propeller domain of the protein encoded by gene K13 is a *Plasmodium* specific gene and has become a marker for artemisinin resistance. *P. falciparum* isolates collected in Vietnam between 2009 and 2016 resulted in the detection of eight separate point mutations in the propeller domain of the K13 gene. These mutations were found to be associated with reduced effectiveness of dihydroartemisinin, specifically in ring-stage parasites (Thuy-Nhien *et al.*, 2017). ACT resistance has also been reported, although often to the non-artemisinin partner drugs, with the upregulation of the multidrug resistance marker *Pfmdr1* playing a major role. Due to its widespread use in Southeast Asia, artesunate-mefloquine is now met with highly resistant parasite strains and mefloquine use in isolation has little effect (Nosten *et al.,* 2000; Kavishe *et al.,* 2017).

Chloroquine and pyrimethamine resistance can be traced back to the same origin – Cambodia - where in both cases the resistant strains swept across Africa and killed millions of people (White, 2010).

Recent data has shed light on further expansion of ACT resistance in the Greater Mekong region of Cambodia. The area has shown increasing failure rates after treatment with four different ACTs (Fig. 7), a trend that has spread to Thailand and the People's Democratic Republic of Lao (resistant to three ACTS), Vietnam (resistant to two ACTs) as well as to Myanmar and the Yunnan Province of China (resistant to one ACT). Monitoring of the therapeutic efficacy of ACT therapies in these regions has been lax and only recently has been shortened to every two years by national treatment

policies (Narain and Sall, 2016). With artemisinin resistance threatening to become a new reality with origins in Southeast Asia and a lack of new compounds leaving the drug discovery pipeline, social and economic impact may be catastrophic. Renewed funding has prompted malaria drug research after more than 10 years of abeyance, but the drug development process is slow.

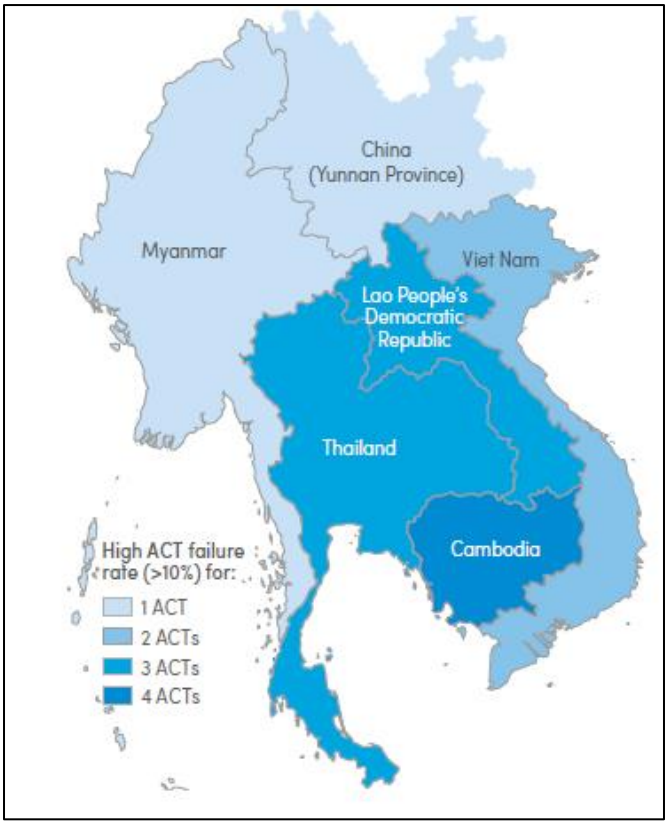

Figure 6: Artemisinin Combination Therapy resistance distribution in South-East Asia as of 2017. The region with the largest number of failing ACT therapies is Cambodia – often the origin of antimalarial resistance (World Malaria Report, 2018). Ascending shade of blue represents the failure of one, two, three and four ACT's respectively.

1.6 - Antimalarial drug discovery

1.6.1 – Challenges

The erythrocytic (RBC) stages of the malaria parasite are responsible for malaria symptoms and persistence of an infection in individuals (at least in the case of *P. falciparum*), hence the primary goal of antimalarial therapy is the discovery of compounds that rapidly eradicate these stages. Fortuitously, the erythrocytic cycle can be readily mimicked in *in vitro* cell cultures for drug screening purposes. The first straight-forward procedure to be published for the asexual culture of *P. falciparum* was by Trager and Jensen (1976) using standard mammalian cell culture media components supplemented with human serum and erythrocytes. It has since been optimized and refined to become a standardized protocol. Some of these advancements include the use of AlbuMax II (an albumin-rich fraction prepared from bovine serum) instead of human sera, as well as using a specialized low oxygen/high carbon dioxide gaseous atmosphere (1% O_2, 94% N_2 and 5% CO_2) with which more successful growth has been shown (McNamara *et al*., 2006).

Resistance to current drug measures continues to evolve and limits our ability to combat the disease. Antimalarial drug discovery is an extremely challenging process due to the environments in which the drugs are most needed. This is since malaria endemic areas are some of the poorest in the world and access to suitable health care is limited or non-existent. As such, any novel antimalarial compound must be well tolerated by the patient and have minimal side effects (Burrows *et al.,* 2013). This also leads to the necessity for the drug to be readily available for oral administration, often in a rural setting. One of the primary reasons for drug resistance is the lack of patient compliance over the full period of therapy. It is therefore necessary to provide a treatment that will act quickly and last approximately three days with as few dosing's as possible.

Single-dose therapy is the ideal that is being sought (Burrows *et al.,* 2013). The drugs should also be used in conjunction with other drugs (as is the case with artemisinin) to reduce the risk of resistance. Finally, the drugs should be inexpensive (less than $ 0.1 per treatment to produce, as was the case with chloroquine) (Gelb, 2007).

In 2013, Burrows *et al*. published a set of guidelines for new drug molecules (target candidate profiles – TCPs) and medicines (target product profiles – TPPs) to meet for them to be considered effective novel therapies (Burrows *et al.,* 2013). The candidate referred to in TCP defines a single molecule/compound that has, at minimum, progressed to preclinical trials. These candidates were then further defined by the parasite life stage on which they act – TCP-1 candidates rapidly clear the parasite asexual blood stages (using artesunate as a rapid speed of kill benchmark which novel TCP-1 candidates should ideally match, or at a minimum, rival that of chloroquine (Burrows *et al.,* 2013). TCP-3 candidates show activity against hypnozoites, the dormant liver stages that are particularly relevant in *P. vivax* infections. TCP-4 candidates act against hepatic schizonts, while TCP-5 and TCP-6 candidates block parasite transmission by targeting parasite gametocytes and the mosquito vector respectively (Burrows *et al.,* 2017). Prior to the defining standards of the TPP, the optimal medicinal product was defined in 2011 as being a single-dose cure that additionally accounted for post-treatment prophylaxis (SERCaP, malERA Consultative Group on Drugs, 2011). SERCaP thus refers to a drug that is able to clear all asexual blood stage parasites as well as transmissible gametocytes in a single dose or exposure. A TPP defines a final product that may contain multiple active candidates and is divided between TPP-1 (case management or chemotherapy) and TPP-2 (chemoprotection) profiles. A TPP-1 product may treat acute malaria and use a combination of TCP-1 candidates to rapidly clear asexual stage parasites, combined with TCP-5 candidates to reduce transmission, as well as for severe cases of malaria where a single,

fast-acting TCP-1 candidate may be considered. A TPP-2 product would be administered when an individual plans on entering an area with high malaria prevalence and would generally contain a combination of TCP-1 and TCP-4 candidates (Burrows *et al.,* 2017).

The current gold standard TCP-1 drug used in severe malaria, artesunate, is not without its pitfalls. Aside from the aforementioned drug resistance, it has been linked with haemolysis (Rolling *et al.,* 2015) and is unstable in aqueous solution (Burrows *et al.,* 2017). The latter feature leads to a short half-life *in vivo* and partly motivates the need for a longer half-life partner drug to eradicate parasites surviving initial artesunate exposure (Morris *et al.*, 2011). With continuously increasing resistance to historic and modern day antimalarials, the rapid clearance time for fast-acting drugs is under threat, and provides further motivation for the identification of novel, rapidly cidal TCP-1 candidates. In addition to rapid clearance similar to (or better than) artesunate, allowing the possibility of a single-dose regimen, challenges that an ideal TCP-1 candidate is expected to meet include clinical single-dose efficacy against all known resistant strains, very low susceptibility to acquired resistance, no drug-drug interactions with anti-TB or anti-retroviral therapeutics (motivated by the extent of TB, malaria and HIV co-infections in malaria endemic countries), a 50-fold window between antimalarial therapeutic concentrations and those at which adverse effects are observed, simple formulations suitable for endemic countries and low cost (Burrows *et al.*, 2017).

1.6.2 – Gametocytes and transmission-blocking approaches

As formulated in the TPP-1 requirements, in addition to eradicating the parasite asexual erythrocytic stages, there is also an imperative to develop drugs capable of suppressing or destroying sexual stage parasites (gametocytes) to prevent transmission. Even if the asexual stages

are successfully eradicated, gametocytes may persist in the bloodstream for weeks (White, 2017). This means that an individual that has been cured of malaria symptoms may still be infectious and capable of transmitting parasites to the mosquito vector and then onward to other humans (White, 2017). Gametocytes develop through five distinct maturation stages (I-V) over the course of 10-11 days with only late-stage gametocytes (V) being able to initiate gamete formation and sexual reproduction when taken up by a feeding mosquito (Demanga *et al.,* 2017). The difficulty which exists when attempting to culture and isolate gametocytes significantly hampers drug development directed towards the sexual stage of the parasite. This contrasts with the relative ease it takes to generate asexual parasite cultures. Currently protocols to produce mature gametocyte cultures require intricate synchronization procedures as well as the addition of either stimulatory/inhibitory factors (Delves *et al.,* 2016). Recent advances have resulted in a protocol that can produce mature gametocytes that can be routinely cultured in 15 days and, although complex, allows functionally viable gametocytes to be used to evaluate transmission-blocking drugs *in vitro* (Delves *et al.,* 2016). A method for culturing gametocytes was established and made use of nutrient starvation combined with a systematic drop in haematocrit over a period of ten days to induce gametocytogenesis (Reader *et al.,* 2015). The method was replicated across three independent studies and provides a foundation on which to base gametocytocidal activity assays.

Emerging resistance to the artemisinin derivatives, toxicity concerns surrounding primaquine-induced haemolysis, as well as recent advances in gametocyte culture and assay techniques, has prompted renewed vigour in the search for novel gametocytocidal compounds to add to the ones currently used – primarily artesunate, artemether, methylene blue and the two 8-aminoquinolines primaquine and tafenoquine (Chen *et al.,* 2015; Birkholtz *et al.,* 2016). The current TCP-5 (gametocytocidal candidate compound) reference compound is primaquine which, in combination

with an effective ACT for parasite asexual stage clearance, is the most effective gametocytocide and compound for the post-treatment preventation of gametocyte circulation and proliferation (Bronner *et al.,* 2016). Mechanistically, it has been proposed that primaquine may promote oxidative stress in the parasite by interacting with enzymes responsible for reducing oxidative damage (Giovanella *et al.,* 2015). In combination with chloroquine, it has been shown to reduce the effects of chloroquine resistance *in vitro* (Egan, 2006). Despite it being the frontline of defense against *P. falciparum* gametocytes, primaquine is used with caution due its haemolytic effects observed in individuals with glucose-6-phosphate (G6PD) deficiency (Chen *et al.,* 2015; Bronner *et al.,* 2016; Burrows *et al.,* 2017). Studies have shown the haemolytic effects to be dose-dependent with a single primaquine dose of 0.40 mg/kg producing a large haemoglobin drop in individuals that had a G6PD deficiency in relation to those that did not (Bronner *et al.,* 2016). The WHO therefore recommends a treatment concentration of 0.25 mg/kg (in combination with an ACT) to outweigh the potential haemolytic effects while maintaining gametocytocidal activity (World Health Organization, 2018).

With the emergence of primaquine resistance in recent years, alternatives have been sought to reduce the load on primaquine as the primary gametocytocidal compound (Thomas *et al.,* 2016). Tafenoquine is an 8-aminoquinoline like primaquine and has been shown to have comparable efficacy to primaquine while being longer acting, with the added advantage of being better tolerated in a single dose regimen (Thomas *et al.,* 2016). Its relatively slow action has required it to be administered alongside a more rapid acting artemisinin-based compound in an ACT therapy. Although championed for its activity against gametocytes, tafenoquine is also active against the hepatic and asexual stages in both *P. falciparum* and *P. vivax* (Campo *et al.,* 2015; Ebstie *et al.,* 2016) satisfying both TCP-1, TCP-4 and TCP-5 candidate profiles. Mechanistically it has been

shown to disrupt parasite mitochondrial function via the inhibition of cytochrome C reductase, which results in elevated reactive oxygen species (Carbalho *et al.,* 2010). Like chloroquine, it has also been shown to inhibit haematin formation (Vennerstrom *et al.,* 1999). As is the case with primaquine, tafenoquine has shown evidence of haemolysis in individuals who are G6PD-deficient, although at higher doses than primaquine (Rueangweerayut *et al.,* 2017). The haemolytic effects combined with its relatively slow action help prompt the ongoing search for novel transmission blocking drugs.

The search for novel transmission-blocking compounds has the additional allure that if compounds are dual-active against both the sexual and asexual parasite stages, several antimalarial TCPs may be met, although with increased risk for resistance if used as a single compound (Burrows *et al.,* 2011; Burrows *et al.,* 2013; Leroy *et al.,* 2014). Recently several high-throughput assays have been developed to assess large chemical libraries for transmission-blocking potential in the hopes that novel compounds showing gametocytocidal activities may be found, as has been the case in studies that have identified active hits in the 'Malaria Box' (Plouffe *et al.,* 2016) as well as larger libraries (Duffy and Avery, 2013). The Tres Cantos Antimalarial Set (TCAMS) was recently screened against gametocytes and over 400 compounds were identified with activities < 2 μM (Miguel-Blanco *et al.,* 2017). Of these compounds, 276 showed promising activity against both the sexual and asexual parasites stages from which suitable drug scaffolds can be identified and prioritized for further study (Miguel-Blanco *et al.,* 2017).

One such hit is the synthetic trioxolane OZ439 (artefenomel) which has shown promise to be fast-acting against stage V gametocytes in a sub-micromolar range (Delves *et al.,* 2012; Duffy and Avery, 2013; Bolscher *et al.,* 2015). Containing a similar chemical core to that of artemisinin, it is the second trioxolane to advance to clinical trials where it was observed to be well tolerated in

volunteers and is being further developed to work in combination treatment with ferroquine and/or piperaquine (Phyo *et al.,* 2016). Artefenomel's similarity to artemisinin also comes with a limitation in the sense that it may share similar resistance patterns to that of artemisinin in the future. The elimination half-life of artefenomel (46-62 hours) greatly exceeds that of other peroxide antimalarials (e.g. artesunate – 0.8-1.3 hours (Morris *et al.,* 2011), dihydroartemisinin – 0.9-1.2 hours (Tarning *et al.,* 2012)). This relatively slow elimination rate would provide longer protection against the development of drug resistance in any fast-acting partner drug – as would be the case if used in conjunction with an artemisinin derivative in an ACT. Crucially, it also provided evidence of dual- species activity, showing rapid parasite clearance of the asexual blood stages of both *P. falciparum* and *P. vivax,* which suggests the potential for a single-dose malaria cure when combined with a partner compound to reduce the risks of resistance (Phyo *et al.,* 2016).

In a recent study the Delves group made use of the *P. falciparum* dual gamete formation assay (*Pf*DGFA) coupled with high-throughput screening to track the effects of a library of chemically diverse compounds on gametocyte transmission (Delves *et al.,* 2018). The assay proved to be effective in predicting transmission-blocking activity comparable to the current gold standard for measuring gametocyte transmission – the standard membrane feeding assay (SMFA). The study culminated in identifying a novel sulphonamide scaffold (N-4HCS) that rapidly arrested male gamete formation and blocked transmission *in vivo* in murine models (Delves *et al.,* 2018). The novel transmission-blocking compound has been suggested as a new transmission-based chemotherapeutic to be used to develop new ACTs.

In contrast to *P. falciparum* which only infects the liver in the initial 1-2 weeks prior to initiating the erythrocytic cycle, other malaria parasite species (notably *P. vivax*) persist in the liver as dormant hypnozoites that cause regular recurrences of erythrocytic infection in an individual even

in the absence of mosquito transmission and after the initial symptoms have been cleared by drug treatment targeting the erythrocytic stages. This motivates the search for compounds acting on liver-stage hypnozoites, i.e. TCP-3 candidates (Mikolajczak *et al.,* 2015). In the case of *P. falciparum*, liver-stage active compounds (TCP-4) may also be useful as prophylactics by eradicating an infection prior to the initiation of the pathogenic erythrocytic cycle, which would contribute to the TPP-2 goals. However, even more so than the search for gametocytocidal drugs, this is hampered by the lack of a tractable *in vitro* model that simulates liver infection. It requires the generation of gametocytes in culture, infection of mosquitoes, harvesting sporozoites from the mosquito salivary glands and using them to infect liver cell lines. To avoid the use of mosquitoes, attempts are also being made to simulate the mosquito developmental cycle for the generation of sporozoites *in vitro*. In the case of *P. vivax,* this is further hampered by the lack of a continuous *in vitro* culture method for the parasites. To some extent, the use of mouse models may be more tractable (mosquitoes are fed on infected mice to generate sporozoites for liver cell line infection) (Meister *et al.,* 2011; Gural *et al.,* 2018).

1.6.3 – Asexual blood stages and current drug development

Although chloroquine itself as a chemotherapeutic agent has become obsolete due to large scale resistance, analogs of the drug are still currently being pursued effectively as potential antimalarial drugs. Studies conducted on 4-aminoquinolines (4-AQ; the compound class to which chloroquine belongs) have shown that the 4-AQs with shorter (2-3 carbons) and longer (10-12 carbons) side chains than chloroquine are active against chloroquine resistant strains of *P. falciparum* (De *et al.,* 1996)). AQ13 is an example of a compound in this group of drugs that contains a three-carbon side chain and has been shown to be effective against chloroquine-resistant strains of the *P. falciparum* parasite (De *et al.,* 1998; Koita *et al.,* 2017). Importantly, AQ13 showed no observable

recrudescence, pharmacokinetics similar to chloroquine and was more effective than artemether-lumefantrine in alleviating fever in patients with uncomplicated *P. falciparum* malaria in a phase II trial by Koita *et al.* (2017), although parasite clearance was slower. Overall the conclusion was drawn that AQ-13 was non-inferior to artemether-lumefantrine.

Previous success with the 4-AQs includes ferroquine, the most successful of the chloroquine derivatives, which has been used both in combination with artesunate as well as a monotherapy in humans (Wani *et al.,* 2015; Wells and Hooft van Huijsduijnen, 2015; Held *et al.,* 2015). Ferroquine has been shown to function as chloroquine, whereby a buildup of ferroquine in the parasite prevents haemozoin formation resulting in a buildup of toxic haem and resultant cell death (Christensen, 2009). Additionally, ferroquine's iron core, stabilized between two aromatic rings, may alternate between the ferric and ferrous states and hence generate toxic free radicals (Chavain *et al.,* 2008). It has been shown to be significantly more active than chloroquine in mouse models (Kondratskyi *et al.,* 2017) and has shown activity against parasites that are resistant to amodiaquine and piperaquine *in vitro* (Marfurt *et al.,* 2011). Therefore, although the parent chloroquine may be all but redundant, there is still a need for additional chloroquine analogs that can be used together with faster acting antimalarials for new combination therapies.

Napthoquine was developed for clinical use in the 1990's and hence is one of the more historic 4-AQs. With a slow efficacy rate and long-half life (23 days), it has been used in combination with artemisinin as an effective ACT in patients (marketed as ARCO) (Moore *et al.,* 2016). Although not fully elucidated, napthoquine's mechanism of action is thought to have the same basis as chloroquine (and the 4-AQs) by inhibiting the sequestration of toxic haem (Sullivan *et al.,* 1996; Moore *et al.,* 2016). Studies have shown the 4-AQs to have weak gametocytocidal affects, but a recent study by Cabrera *et al*. showed that napthoquine was more effective than other 4-AQs

against late-stage gametocytes, additionally showing synergism with primaquine resulting in a potent combination against both sexual and asexual parasite stages *in vitro* (Cabrera and Cui, 2015). Due to its long-half life and slow relative speed of action, napthoquine has been used as an effective prophylactic, proving to be more effective than primaquine in this regard (Wu *et al.*, 2001).

Phenotypic screening, i.e. the screening of synthetic or natural compound collections against parasites in culture and subsequent testing in mouse models, has become the predominant approach for malaria drug discovery. However, target-based drug discovery has become a topic of interest since the sequencing of the parasite and human genomes and promising drug targets have already been identified, including protein kinases and falcipains, to name a few (Grimberg and Mehlotra, 2011). Target-based drug discovery provides an opportunity to purposefully design compounds ("rational drug design") that potentially inhibit the target, provided the 3-dimensional structure of the target protein is known or can be predicted using *in silico* homology modelling techniques and a suitable assay for target activity is available for screening purposes (Mishra *et al.,* 2017). Amongst others, additional advantages include the opportunity to select targets that are absent in humans or structurally sufficiently dissimilar from human homologues to minimize the probability of toxicity or side-effects, and the potential to predict the likelihood of resistance due to point mutations in the target protein (Mishra *et al.,* 2017). Nonetheless, phenotypic screening using parasite cultures remains a powerful approach for the identification of antimalarial compounds, particularly when employed in high-throughput screening using large synthetic chemical libraries. This has for example been demonstrated by Gamo *et al.* (2010) in a screening campaign by GlaxoSmithKlein which identified more than 13,000 compounds with low micromolar activities against cultured *P. falciparum*. A selection of representative chemotypes of these compounds is

available to researchers from the Medicines for Malaria Venture (MMV) (the "Malaria Box") for further development and exploitation (Spangenberg *et al.,* 2013).

The phenotypic screening approach has resulted in the discovery of some potent compounds (some with novel mechanisms of action), which have also been shown to be active in patients (Burrows *et al.,* 2017). Of these is the prior mentioned artefenomel, alongside other such compounds like KAF156 and DSM265 (Kuhen *et al.,* 2014; McCarthy *et al.,* 2017; Burrows *et al.,* 2017). DSM265 was originally discovered during a target-based study to develop inhibitors to the parasites dihydroorotate dehydrogenase (DHODH) which is responsible for pyrimidine biosynthesis (McCarthy *et al.,* 2017). The drug was found to have a high selectivity over the human DHODH orthologue and was long-acting, maintaining the minimum inhibitory concentration (MIC) in patients for over eight days (McCarthy *et al.,* 2017). Its antiplasmodial activity has been shown to be comparable to that of mefloquine and chloroquine while its relatively slow speed of action was compared to that of atovaquone and pyrimethamine in patients (McCarthy *et al.,* 2017; Llanos-Cuentas *et al.,* 2018). DSM265 is also attractive for use in chemotherapy as an addition to a TPP-2 profile medicine as its long half-life and high individual tolerance make it an attractive short-term travel prophylactic. Therefore, DSM265 presents the potential for a single dose cure when used with a fast-acting partner drug in combination therapy, such as KAF156, which has the added advantage of no pre-existing drug pressure (Llanos-Cuentas *et al.,* 2018).

KAF156 is an imidazolopiperazine that has frontlined a new class of antimalarials and has shown efficacy in both hepatic and blood stages of *P. falciparum* and *P. vivax* malaria parasites in patients with a clearance concentration in the nanomolar range in patients (5 – 15 nM) (Kuhen *et al.,* 2014; White *et al.,* 2016). It has also been shown to have potential in prophylaxis and has been effective against gametocytes in humans (Leong *et al.,*2018). Although its mechanism is unknown,

alongside piperaquine's longer half-life it has been assessed as a potential combination therapy as piperquine-KAF156 (Leong *et al.,* 2018). Parasite killing speeds for KAF156 were found to be marginally slower than that of artemisinin and significantly slower than the spiroindolone KAE609 (a *Pf*ATP4 inhibitor, the target of the currently fastest acting group of antimalarials), but more rapid than mefloquine, atovaquone and sulfadoxine-pyrimethamine in patients (White *et al.,* 2016). To note is that the study conducted by White *et al*. observed parasite clearance with all currently known artemisinin-resistant parasites (parasite cell lines with *Pf*MDR, *Pf*CRT and K13 domain mutations) with no recrudescence (monitored over a period of 28 days).

Spiroindolones are a relatively novel class of antimalarials that have been shown to be fast acting (in relation to mefloquine and artemisinin) at low nanomolar concentrations against both *Plasmodium falciparum* and *vivax* (Rottman *et al.,* 2010). Mechanistically they have been shown to rapidly reduce parasite protein synthesis and improve on killing speed in comparison to both artemisinin and mefloquine (Rottman *et al.,* 2010). Studies conducted on humans have in fact shown one such compound, KAE609 (cipargamin), to be more effective than any known artemisinin (a clearance speed slightly faster than artesunate) with the additional benefit of being active in artemisinin-resistant *P. falciparum* parasites (White *et al.,* 2015). Cipargamin targets the parasite's *Pf*ATP4 which is situated on the parasite membrane and responsible for Na^+ efflux/ H^+ influx and consequentially low cytosolic pH (Spillman *et al.,* 2013; Spillman *et al.,* 2015). By disrupting *Pf*ATP4, cipargamin generates an increase in alkalization in the parasite cytosol which in turn increases osmotic fragility of the parasite membrane and results in cell swelling and eventual apoptosis (Dennis *et al.,* 2018). These effects were found to be immediate and with as little as 10 nM of cipargamin *in vitro* by Dennis *et al*. confirming the extreme rapidity of the drug observed by White *et al*. (White *et al.,* 2015; Dennis *et al.,* 2018).

In 2013 the lipid kinase, phosphatidylinositol 4-kinase (PI4K), was identified as an antimalarial drug target by the novel class of antimalarials – imidazopyrazines (McNamara *et al.,* 2013). The class of compounds were shown to be rapidly effective in the inhibition of the asexual blood stage parasites of *P. falciparum* and *P. vivax* in mouse models as well as in hepatic and gametocyte stages, suggesting high potential for the fulfillment of the SERCaP profile (McNamara *et al.,* 2013). This also suggests that PI4K is a critical regulatory enzyme in the parasite. The imidazopyrazines exerted their effect by interacting with the ATP-binding site of PI4K, reducing the formation of phosphatidylinositol 4-phosphate in the parasite (McNamara *et al.,* 2013). Although not definitive, the imidazopyrazines have been shown to disrupt Rab11A-mediated membrane trafficking in the blood stages of *P. falciparum*. In so doing, a late step in merozoite development is blocked via disruption of plasma membrane invagination (McNamara *et al.,* 2013; Burke *et al.,* 2014). MMV390048 is a potent inhibitor of PI4K which was discovered using phenotypic whole-cell screening and exhibited activity across all blood stages as well as in gametocytes for transmission blocking approaches in animal models (Paquet *et al.,* 2017). Although it does show the potential for prophylaxis, no activity was observed in late-stage hypnozoites however, which prevents the drug from being championed as a radical, as was the case with the PI4K inhibitor KDU691 (Zeeman *et al.,* 2016). Of note was that MMV390048 was found to be rapid acting as well as maintained a long half-life, with a putative 80-100 mg dose being sufficient to maintain therapeutic plasma levels for 8 days in humans (Paquet *et al.,* 2017).

During the intra-erythrocytic maturation of the parasite from ring through to schizont stage, there is a systematic increase in tyrosine phosphorylation of an erythrocyte membrane protein, band 3 (Pantaleo *et al.,* 2010; Lasondor *et al.,* 2012). This increase in tyrosine phosphorylation is directly proportional to a weakening of the RBC membrane, putatively in preparation of eventual

merozoite release (Ferru *et al.,* 2011). The *P. falciparum* genome does not encode for any tyrosine kinase and hence it is suggested that the tyrosine phosphorylation observed to occur on band 3 may occur by either the host RBC tyrosine kinase or an alternative parasite kinase capable of tyrosine phosphorylation (Solyakov *et al.,* 2011; Graciotti *et al.,* 2014). In testing this hypothesis in patient blood samples, the Kesely group identified imatinib (a tyrosine kinase inhibitor used in cancer chemotherapy) as being able to inhibit the RBC tyrosine kinase (or alternatively a parasite kinase with multi-specificity) which in turn arrested the parasite life cycle by preventing its emergence from the RBC (Kesely *et al.,* 2016). Importantly, imatinib is already well studied and established and generally non-toxic. Furthermore, the fact that it does not target any known specific parasite enzyme makes mutation-resistance unlikely.

One of the greatest challenges in severe cases of malaria is the high parasite loads and proportional blockage of the patient's microvasculature's (Ponsford *et al.,* 2012). Parasitised RBCs encountered in severe forms of malaria characteristically bind to the vascular endothelium forming 'rosettes' (Bruneel *et al.,* 2010). Sevuparin is an antiadhesive polysaccharide drug that has been shown to hinder merozoite invasion of RBCs and also disrupt the rosetting of pRBCs, thereby restoring blood-flow in humans (Maitland, 2015; Leitgeb *et al.,* 2017). Based on studies by Leitgeb *et al*. it is a rapidly cidal compound showing significant efficacy within the first hour of treatment in patients, rivaling the most rapid acting antimalarials (Leitgeb *et al.,* 2017). It is therefore suggested that it be used in combination with slower acting compounds as a combination therapy, such as atovaquone and proguanil (Leitgeb *et al.,* 2017). The first effects of artesunate are observed in four hours making sevuparin significantly more rapid and an important addition to the treatment options against severe forms of malaria (Klonis *et al.,* 2013).

Attempts to target the parasite mitochondrion resulted in the development of atovaquone, specifically targeting *cytochrome b* in the *bc*1 complex and disrupting the electron transport chain by mimicking ubiquinone (Fry and Pudney, 1992; Goodman *et al.*, 2017). Inhibition of the *bc*1 complex leads to loss of mitochondrial function coupled with a reduction in pyrimidine synthesis (Nixon *et al.*, 2013). Atovaquone has shown significant activity against both asexual and sexual stages of the parasite and is coupled with proguanil in a combination therapy in humans (Nixon *et al.*, 2013). Proguanil, although ineffective against malaria parasites independently, shows synergy with atovaquone (Nixon *et al.*, 2013; Goodman *et al.*, 2017). Atovaquone-resistance emerged as early as clinical trials as a result of only targeting one enzyme and the relatively low mitochondrial energy requirements during the blood stages of the parasite (Nixon *et al.*, 2013; Goodman *et al.*, 2017). Although resistance to the drug is widespread, it is important to note that the resistance mutations do not allow survival in the vector phase, whereby the defective mitochondria inhibit the parasites requirement for full respiration (Goodman *et al.*, 2016). Coupled with its proven efficacy in parasite transmission blocking, atovaquone-proguanil has been used for mass administration and is well tolerated in children and pregnant women (Nixon *et al.*, 2013). Asexual-stage parasite killing speed has been shown to be slow in relation to artemisinin as well as chloroquine, and along with its exceptional safety profile, makes it better suited for use as a prophylactic (Biagini *et al.*, 2012).

As it could take many years before a novel antimalarial that fulfills the SERCaP profile is successful in drug trials, there are currently a variety of alternative measures being used to slow the increase of virulent, drug-resistant malaria parasite strains. It has been shown that the removal of a drug to which parasites have become resistant (such as chloroquine) from administration is able to bring back drug-sensitive strains and eventually replace drug-resistant strains in most of

the infected human population due to the increased fitness of sensitive strains (Mishra *et al.,* 2017). However, sensitivity to the respective drugs may require up to 10 years to return (Kublin *et al.,* 2003; Mishra *et al.,* 2017). Alternatively, drugs presently used to treat other diseases can be repurposed to treat malaria if they show respectable activity. This has for example been suggested with antiretrovirals used commonly to treat HIV as well as anti-cancer drugs such as SU-11274 and Bay 43-9006 (Grimberg *et al.,* 2009). Additional examples may be the antibiotics doxycycline and fosmidomycin. The former is not useful for treatment but is occasionally used as a prophylactic by travelers to malaria endemic areas, while fosmidomycin has shown promising results against the schizont parasite stage (Mobo-Ngoma *et al.,* 2016). Additionally, fosmidomycin has been combined with piperaquine to provide an effective non-artemisinin-based combination therapy for acute *Plasmodium* infection, as well as for prophylaxis (Mobo-Ngoma *et al.,* 2016).

A favoured alternative to rescue the utility of existing antimalarials includes synthetically altering the existing compounds to preserve drug efficacy while simultaneously reducing or avoiding pre-existing resistance (Vangapandu *et al.,* 2007; Mishra *et al.,* 2017). This has been shown to be effective in the case of mefloquine and chloroquine. There is also the option of drug hybridization, whereby two class distinct compounds are covalently linked to circumvent the issue of single drug resistance. The idea is to generate a hybrid compound capable of acting on multiple targets, thus reducing the risk of resistance, similar to the motivation behind combination therapy. An example is artemisinin-quinine based hybrids in which strong activity was shown against chloroquine-resistant strains of *P. falciparum* (Walsh *et al.,* 2007; Held *et al.,* 2015).

Marine and plant natural compounds are sought after due to their historical medicinal properties - the clear majority of existing drugs for all indications are based on natural compounds or derivatives thereof (Atanasov *et al.,* 2015). This was exemplified by the discovery of artemisinins

and quinolines for malaria treatment (Shen, 2015). Advantages of this approach include the use of traditional medicine practices to guide the selection of appropriate plants and the "privileged structures" of natural compounds (they have a propensity for binding to proteins since they are metabolites produced by enzymes and/or act as substrates of enzymes). In addition, organisms commonly produce compounds to combat competitors or pathogens that can be re-purposed as anti-infectives (Burketova *et al.,* 2015). Natural compounds are also thought to occupy a larger "chemical space" than synthetic compounds, i.e. more compound diversity may be accessed by pursuing natural products libraries vs. synthetic chemical libraries (McKerrow, 2015). The latter, however, may also be a disadvantage – active natural compounds may be difficult/costly/impossible to synthesize, thus requiring continuous harvesting from the natural source (as exemplified by artemisinin) (McKerrow, 2015). Natural product drug discovery is also a lengthy process requiring collection and species identification of source organisms, repeated extraction, fractionation and screening and isolation and structural elucidation of the active compounds (Ginsburg *et al.,* 2011).

1.7 - *In vitro* assessment of antimalarial efficacy

With an increase in *in vitro* efficiency of malaria parasite culture comes a concomitant need for the development of adept ways of studying parasite sensitivity to antimalarial compounds. The original technique is the use of the Giemsa stain in combination with microscopic examination of blood smears for parasite diagnosis (Fleischer, 2004). Although this technique has provided much of the data on parasite vitality in culture, it is prone to misdiagnosis and subjective interpretation (Grimberg, 2011).

The use of radioactive hypoxanthine (RHX) attempted to improve on the use of a microscope as the RHX would be incorporated into the parasite DNA as it was synthesized (Desjardins *et al*., 1979). Erythrocytes don't synthesize polynucleotides, hence RHX incorporation is a specific indicator of parasite levels in cultures. Although a marked improvement over microscopy, enabling the simultaneous assessment of multiple compounds in 96-well plates for screening purposes, RHX is not without its drawbacks i.e. the need for a radioactive H^3-purine and specialized instrumentation, notably suitable scintillation counters (Desjardins *et al*., 1979). An alternative screening method assesses parasite enzyme activity as a surrogate indicator of parasite numbers in culture following compound exposure, e.g. the plasmodium lactate dehydrogenase (pLDH) assay. This assay is based on the difference noted in the *P. falciparum* enzyme which rapidly reduces 3-acetyl pyridine adenine dinucleotide (APAD) in the reaction to produce pyruvate from lactate, in comparison to the human LDH enzyme where the same reaction occurs 200 times slower (Makler and Hinrichs, 1993).

$$APAD + lactate \longrightarrow APADH + pyruvate$$

Reduced APAD in turn is quantified using colorimetric tetrazolium-based reagents. The assay thus selectively detects parasite pLDH vs. host RBC LDH in culture. The pLDH assay has become commonly used as an alternative to the RHX assay due to its relative simplicity and lack of a requirement for radioactive containment procedures and scintillation counters (only a standard multiwell spectrophotometer is required). Notably, the pLDH assay format was selected for the high-throughput antimalarial screening of an approx. 2 million compound library at the Tres Cantos campus of GlaxoSmithKline (Gamo *et al.*, 2010).

Measuring ATP levels in cells may be a means for determining cell viability in cultures. ATP quantification in mammalian cells can be performed using isolated mitochondria and fluorometry (Tatuch and Robinson, 1993; Houstek *et al.,* 1995; Wanders *et al.,* 1996). However, a robust and convenient way to measure ATP in both live cells and isolated mitochondria makes use of the luciferin-luciferase reaction whereby luminescence is measured to detect photons released during the ATP-dependent conversion of luciferin to oxyluciferin catalyzed by firefly luciferase (Lyman and DeVincenzo, 1967; Manfredi *et al.,* 2002):

$$Luciferase + luciferin + ATP + O_2 \longrightarrow luciferase + oxyluciferin + AMP + PPi + CO_2 + light.$$

This reaction is exploited in commercially available kits (e.g. Promega's Cell-Titer-Glo and BacTiter-Glo) to quantify ATP levels in mammalian and bacterial cell cultures as a measure of cell viability. Previous studies have indicated that the luciferin-luciferase reaction is effective in measuring ATP levels in asexual and sexual stages of *P. falciparum* parasites (Khanaani and Ginsburg, 1989; Peatey *et al.,* 2012). Further developments in the field have seen Khan *et al.* (2012) explore the possibilities of utilizing native parasite ATP levels as an indication of drug stress and if the quantification of ATP levels would be suggestive of the speed of antimalarial drug action. The study observed an initial increase in ATP levels in the parasite during drug treatment, suggesting that the harmful effects of the drugs triggered an increase in metabolic activity and subsequent elevated ATP levels in response. In converse, decreased ATP levels would indicate a decline in parasite metabolism and viability (Khan *et al.,* 2012). However, a significant complication in measuring ATP levels as an indication of parasite viability in cultures is the background contribution of ATP found in the RBCs which obscures parasite-specific signals and necessitates the removal of RBC components from samples by saponin lysis and centrifugation

procedures. This renders ATP measurement impractical in plate-based compound screening experiments.

Fluorescence -based drug screening procedures have been developed and make use of the fact that host RBCs lack DNA and hence parasite growth in cultures can be measured using fluorescent nucleic acid stains such as SYBR Green and DAPI. The SYBR Green I-based fluorescence assay has been used to monitor drug efficacy and associated resistance and involves lysing infected RBCs in culture post drug-treatment using saponin (a nonlethal detergent that permeabilises the host RBC membrane) after which the SYBR green fluorescent probe is added to the culture sample and relative fluorescence units (RFU) are determined per sample in a multi-well plate reader (Smilkstein *et al.,* 2004; Johnson *et al.,* 2007). The assay allows for a reliable, high-throughput, automated, plate-based method to measure malaria parasite susceptibility to current and novel antimalarial drugs (Johnson *et al.,* 2007). Linked to flow cytometry, these assays can be used to provide quantitative screens based on an exact parasite cell count in patient samples as well as cultures.

Although the pLDH, Sybr Green-I based, and RHX plate-based assays provide an effective means to conduct medium- to high-throughput screens for antimalarial compounds, there are disadvantages. Compounds are typically added to cultures in 96-well plates and residual parasite levels determined using the assays after a 48-96 hour period. These assays are not stage specific and there is no clear way of accurately determining the actual speed of drug action on the parasite, although an exception may be comparing the IC_{50}s obtained for an individual compound in 24-, 48- and 72-hour assays, as described by Le Manach *et al.* (2013; further discussed below). The latter factor (speed of action) has become increasingly crucial due to aspects such as poor health care and patient compliance in malaria endemic regions and has become a key component expected

of TCP-1 candidates, as described earlier. As stated earlier, the introduction of a single-dose treatment regimen is ideal, but a drug that fulfills the specifics required from an ideal SERCaP profile has not yet been developed. Rapid-action drugs also provide opportunities to combat the severe forms of malaria where prompt activity is crucial to prevent patient death. Historic methods for determining speed-of-death in malaria parasites hinged on using light microscopy with Giemsa stained blood smears of parasite cultures to examine the deterioration in parasite morphology during drug treatment. This technique was labor intensive, time consuming and prone to subjective interpretation i.e. determining viable cells from non-viable - it is impossible to achieve an accurate quantification of parasite viability. Therefore, a need for new techniques to quantitatively assess the speed of antimalarial compound and drug action in parasite cultures led to three novel speed of action assays being developed (Sanz *et al.,* 2012; Le Manach *et al.,* 2013; Ullah *et al.,* 2017). Prioritizing the development of rapid acting antimalarials will i) rapidly alleviate patient symptoms, ii) improve patient compliance and simultaneously reduce dosage required thereby reducing cost and iii) reduce the parasite's opportunity to develop resistance mutations due to prolonged exposure of live parasites to the drug (Burrows *et al.,* 2017; Ullah *et al.,* 2017).

To directly address these considerations, Sanz *et al.* (2012) developed the Parasite Reduction Ratio (PRR) assay to accurately assess the speed of action of antimalarial compounds *in vitro*. A further motivation for developing the PRR assay is that normal assays that rely on metabolic activity (Hypoxanthine incorporation), enzyme content (pLDH assay) or DNA content (SYBR Green assay) may either overestimate the speed of action (parasites are metabolically suppressed and inactive, but able to recover when drug pressure is removed) or underestimate it (pLDH enzyme and parasite DNA present in the culture, even though the parasites are dead) (Sanz *et al.,* 2012). In the assay, parasite cultures are exposed to the drugs for 24 – 120 hours. Culture aliquots are

removed at 24-hour time-points during this period, limiting dilution performed and culturing continued for an additional 4 weeks. This allows enumeration of the number of parasites remaining in the drug treated cultures at the various time-points and a calculation of the ratio (PRR value) of starting parasitaemia vs. decrease in that parasitaemia 48-hours later (representative of a single asexual life cycle). Studies making using of the PRR assay have shown large variances in compound killing speed with artemisinin proving to be significantly more rapid acting than clindamycin – a PRR with a magnitude of 10^3-10^4 vs. 10 respectively (Sanz *et al.,* 2012). A more succinct version of the assay was also developed and measured parasite viability after 72-hours of drug treatment to account for compounds with an observable lag phase and successfully identified atovaquone as being slow acting. Importantly, this assay version justified the use of a single-time point at which parasite viability could be measured, and hence identify rapid-acting compounds in a panel (Sanz *et al.,* 2012).

Although regarded as the gold standard for determining the *in vitro* speed of action of blood-stage antimalarial drugs, the drawback of the PRR assay is that it takes 4 weeks to obtain the results. Le Manach *et al.* used this as a motivation to introduce an alternative assay which made use of the PRR as well as a modified version of the standard [^{3}H]-hypoxanthine incorporation assay to group a set of standard antimalarial drugs, as well as three novel antimalarial compounds, into two groups – fast- and non-fast-acting (Le Manach *et al.,* 2013). In this assay, the hypoxanthine incorporation method is used to determine the IC_{50} values of compounds using 24-, 48- and 72-hour incubations respectively, and calculating the ratios of the IC_{50}s. Compounds displaying IC_{50} ratios close to 1 (little difference between the 24 hour IC_{50} and later IC_{50}s) are regarded as fast acting, while compounds that have larger ratios (lower IC_{50}s during a 72h incubation) are regarded as slow.

Using IC_{50} data as a measure of parasite killing speed may also in itself be risky as compound IC_{50}s often differ depending on parasite life stage and when measured on different occasions.

The Le Manach assay does not make fine distinctions between drug action speeds (e.g. chloroquine and artesunate are indistinguishable in the assay). More importantly, both the PRR and Le Manach assays are limited in throughput (seven compounds were compared with each other in both the published assays). This is not ideal for scenarios where researchers wish to simultaneously compare the potential speed of action of larger compound libraries (dozens to hundreds of compounds) in a relatively short space of time, in order to triage compounds for further studies. This is the need addressed by the assay developed in this thesis. Interestingly, the identical consideration also motivated Ullah *et al.* (2017) to develop a bioluminescence relative speed of kill (BRRoK) assay (Ullah *et al.*, 2017). The assay takes advantage of a phenomenon noted by Khan *et al* (2012) – that firefly luciferase activity in transgenic parasites expressing the enzyme is highly sensitive to drug pressure, possibly due to a relatively fast turnover and short half-life of the enzyme in living cells, and this could be exploited to assess the relative speeds of action of antimalarials. In the Ullah study, trophozoite stage parasites were exposed to test compounds for six hours and luciferase activity compared to untreated controls. Using standard antimalarials, the results were found to correlate well with that obtained by Sanz *et al.* using the PRR assay, and the assay was then employed to interrogate the Malaria Box compound collection to identify fast acting compounds. In the published study, the BRRoK assay identified compounds as being slow (atovaquone-like), moderate (pyrimethamine-like) and fast (artemisinin-like) acting. Previously described DSM265 and KAE609 were identified to be slow- and moderate- to fast-acting respectively based on these classifications, while the fastest acting PfATP4 inhibitor in the Malaria Box was found to be the spiroindolone MMV396749 (Ullah *et al.*, 2017).

Ullah *et al.* acknowledge the fact that their assay is limited in the requirement for transgenic parasites and that complete kill cannot technically be demonstrated in six hours. Therefore, the BRRoK assay is unable to identify a direct measure of the relative killing speed of antimalarials, as is rather the case with the PRR assay. Instead it is capable of discriminating between slow- and fast-acting drugs such that compounds that fulfill the criteria for TCP-1 candidates can be identified in a shorter time frame than any previously published speed of kill assay (Ullah *et al.*, 2017). The study described in this thesis proposes a new bioassay which addresses the same concerns as the BRRoK assay, i.e. being able to compare the speed of action of relatively large numbers of compounds in a short time-frame (8 hours in this case) to perform triage of possible TCP-1 candidates. The speed of action of rapid compounds prioritized in the assay may then be subjected to the PRR assay for confirmation. It does not rely on a metabolic read-out or enzyme (pLDH or luciferase) or DNA content to assess parasite viability or require transgenic parasites, but uses fluorescent vitality probes sensitive to membrane integrity (permeability) to definitively distinguish between viable and compromised populations of drug treated parasites.

1.8 – Fluorescent vitality staining

Innovation in the fields of molecular and cellular biology has provided a plethora of means to study individual cellular structures and functions. The introduction of fluorescent probe compounds has allowed researchers to selectively target and visualize various cellular activities and structures in real time i.e. cellular membranes, organelles, proteins and nucleotides. Some fluorescent compounds are engineered to distinguish between viable and non-viable cells and are termed vitality probes.

There are primarily three modes of vitality probe staining – nuclear, mitochondrial and cytoplasmic. Cytoplasmic staining involves engineering fluorescent compounds such as calcein and hydroethidine into neutral molecules by the addition of an acetoxymethyl group. The neutral probe can freely permeate cell membranes and subsequently be converted into their fluorescent products via cytoplasmic esterases (Fig. 7A and 7C). These compounds are then retained by the cell due to their ensuing negative charge. Mitochondrial membrane potential has a significant impact on the integrity and activity of these organelles and can be altered by a variety of intra- and extra-cellular signals. As such, probes have been developed, such as tetramethylrhodamine (TMRE), to act as indicators of mitochondrial membrane potential and ultimately cellular stress (Lyons and Parish, 1994). These probes are often positively charged and readily cross cellular and mitochondrial membranes where they are retained in healthy mitochondrial matrices (Fig. 7B). An accumulation of probe hence causes an increase in fluorescence. Nuclear staining involves fluorescent probes with aromatic amino groups such as propidium iodide (PI) which interacts with DNA and RNA directly to produce fluorescence. PI molecules intercalate within the double helix while probes like 4',6-diamidino-2-phenylindole (DAPI) interact with the minor groove of the DNA. These probes are negatively charged and cannot readily permeate cellular membranes. A loss of membrane integrity is the foremost indicator of cellular death and hence these probes can be used to detect cellular degradation (Fig. 7D).

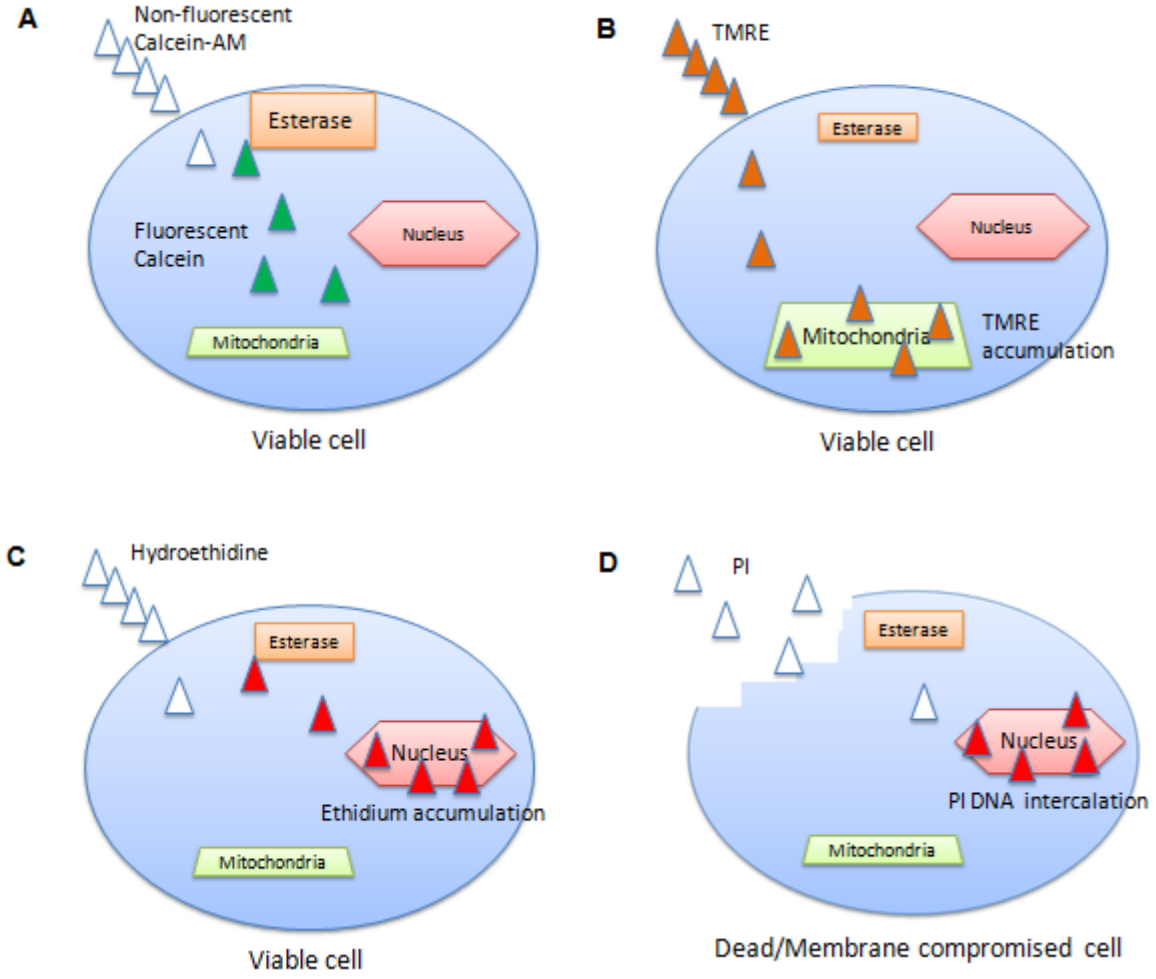

Figure 7: Diagrammatic representation of fluorescent vitality probes and their area of intracellular sequestration. A – Calcein-AM freely permeates cellular membranes and is cleaved by intracellular esterases to green fluorescent calcein. B – TMRE readily permeates cellular membranes and is retained by healthy mitochondria exhibiting orange fluorescence. C – Hydroethidine freely permeates cellular membranes and is cleaved to ethidium which subsequently intercalates with the DNA and produces red fluorescence. D – Propidium iodide is only able to permeate membrane compromised cells where it binds directly to the DNA nucleotides and produces red fluorescence.

1.8.1 - Tetramethylrhodamine

Mitochondrial membrane potential is required for maintaining functions like Ca^{2+} uptake. Spontaneous depolarization and subsequent loss of this potential was first studied using TMRE (Loew *et al.,* 1993). TMRE can cross the membranes of viable mitochondria and due to this potential is retained in the matrix of the mitochondria. As such a rapid increase of orange fluorescence can be detected while a loss of fluorescence can be attributed to unhealthy/dead mitochondria and hence provides an indication of oxidative or general cell stress (O`Reilly *et al.,* 2003). TMRE has been used very rarely for applications other than mammalian cell staining. The dye has become popular in tracking mitochondrial staining and sorting apoptotic and damaged cells from healthy cells via flow cytometry, as was the case for example in samples of THP-1 monocytic cells (McFarlin and Gary, 2017). In studies where it has been employed for malarial cells it has been used as a probe to detect the presence of the parasite (Enderle *et al.,* 1997). Similarly, it was used to develop a fluorescence-based assay for use in screening for inhibitors of a malarial protease PfSUB-1, whereby TMRE was used to assess the parasites morphological response to said inhibitors with a decrease in fluorescence attributed to an effective anti-PfSUB-1 response (Blackman *et al.,* 2002). In other studies, TMRE has been employed to monitor the membrane potential of mitochondria in malaria parasite infected red blood cells and their response to novel semi-synthetic endoperoxides in comparison to artemisinin (Antoine *et al.,* 2013).

1.8.2 - Hydroethidine

Hydroethidine (alternatively known as dihydroethidium) is a common superoxide detector and is synthesized via the reduction of an ethidium cation (Zielonka *et al.,* 2005; Sikora *et al.,* 2017). As such it has been mostly used in studies requiring an intracellular superoxide probe that does not

contribute to the generation of additional superoxide species (Zielonka *et al.,* 2005; Sikora *et al.,* 2017). A neutral molecule that freely permeates cells, the reaction between hydroethidine and superoxide yields a strong red fluorescence. The cationic ethidium product then becomes retained by the cell due to its charge and intercalation with DNA. Its natural cell permeability and retention by viable cells has led hydroethidine to be popular as a vitality probe. After incubation of live human melanoma and murine fibrosarcoma cells with hydroethidine it was shown that an oxidised form of hydroethidine can be visualized as blue fluorescence in the cytoplasm, as well as red fluorescence in the nucleus (Bucana *et al.,* 1986; Pena *et al.,* 2017). It was observed that accumulation of the dye depended largely on the metabolic state of the cell, with compromised cells exhibiting a significantly reduced amount of fluorescence (Bucana *et al.,* 1986; Pena *et al.,* 2017).

Use of hydroethidine in parasites was first completed in *Babesia bovis (B. Bovis),* whereby an assay was developed to measure growth and viability of intraerythrocytic protozoa. The red fluorescence generated by ethidium-DNA intercalation allowed for the use of flow cytometry to distinguish erythrocytes infected with viable parasites from uninfected erythrocytes and dead parasites. It was shown to be effective in observing the effect of parasite-specific drugs and the subsequent decline in parasite viability (Wyatt *et al.,* 1991). It was later applied to several *Plasmodium* species including *P. berghei* and *P. yoelii* (Cruz *et al.,* 2012) and *P. falciparum* (Elloso *et al*., 1994), although its reliability as a vitality probe for malaria paasites has been reported to be questionable (Engelbrecht and Coetzer, 2012). Recently the probe has been used to track the process of host cell rupture and subsequent removal of the parasite from the RBC (Collins *et al.,* 2017) as well as to track parasite growth during the assessment of a novel vaccine candidate (CyRPA) (Favuzza *et al.,* 2017).

1.8.3 – Calcein-acetoxymethyl Ester

The acetoxymethyl ester of calcein (calcein-AM) is a non-fluorescent hydrophobic compound that diffuses across the membranes of cells (Tenopoulou *et al*., 2007). Hydrolysis occurs in the cytoplasm via esterases to produce calcein, a strongly green fluorescent alcohol which is well retained by the cell. It is unable to permeate cellular or organelle membranes once cleaved and hence appears as a cytosolic fluorescence. The exception is when calcein-AM is introduced into cell suspensions at a significantly high concentration such that it oversaturates intracellular esterases allowing enough time to diffuse across organelle membranes. Due to its fluorescence intensity and retention, calcein-AM has begun to replace more conventional probes such as fluorescein. The calcein-AM assay has previously been established as a technique to measure the cellular 'labile iron pool' in the cytosol (Cabantchik *et al*., 1996; Kakhlon *et al*., 2002; Esposito *et al*., 2002; Glicktein *et al*., 2005) and has been extensively used as a mammalian cell viability assay. These cases have included measuring multidrug resistance in cancerous mouse embryonic fibroblasts (Lin *et al*., 2002), and it has also been employed as a prokaryotic bacterial stain used in the observation of biofilm permeabilization effects (Carlson *et al*., 2008). It has been used to measure cell viability using flow cytometry for mammalian natural killer cells (Jang *et al*., 2012), plant pathogenic bacteria (Chitarra *et al.*, 2006) and parasite species such as *Plasmodium berghei* (Kenthirapalan *et al.*, 2012). Although it has been primarily marketed as a mammalian cell stain, with optimization it has been used to measure changes in parasite morphology using fluorescence microscopy in *P. falciparum* (Esposito *et al*., 2010), as well as diagnostically as a general parasite detection probe (Wissing *et al.*, 2002; Gelhaus *et al*., 2008).

1.8.4 - Propidium Iodide

A red fluorescent molecule and well-known polynucleotide intercalator, propidium iodide (PI) has been used extensively in mammalian cells (Stewart and Stewart, 1994; O'Brien and Bolton, 1995), bacteria (Vesey *et al.,* 1994), and protozoa (Mossallam 2010). PI is commonly used to detect the presence of dead cells due to its membrane impermeability and hence exclusion from viable cells. Once inside a compromised cell it binds to DNA by intercalating between the bases at a ratio of one dye molecule per 4-5 base pairs of DNA (Suzuki *et al.,* 1997). It is capable of staining both DNA and RNA and, once bound, fluorescence intensity is magnified at least 20-fold. It has also been widely used in malarial parasites where it was utilized as an indicator in the isolation of *P. falciparum* by flow cytometry (Boissiere *et al.,* 2012; Jang *et al.,* 2013), to detect changes in parasite morphology due to the antiplasmodial activity of plant steroids derived from *Solanum nudum* (Lopez *et al.,* 2010), as a tracker of cerebral malaria cell death (Swanson *et al.,* 2016), as well as diagnostically as an indicator of general parasite cell death (Hemmer *et al.,* 2005).

As PI is only capable of staining the nuclei of dead or compromised cells and calcein-AM is a viable cell stain, they have both previously been used in conjunction as a dual stain assay. This was in an effort to measure the physiological status of the biphenyl degrading bacterium *C. testeroni* (Hiraoka and Kimbara, 2002). To date there is no evidence to suggest previous studies have been conducted using a combination of PI and calcein-AM in *P. falciparum* or parasites at all.

1.9 – A novel, quantitative, relative killing-speed bioassay for *Plasmodium falciparum*.

The fluorescent probes described have worked well in mammalian cells for a variety of research-based applications but have been used to a lesser degree in parasites owing to the need to adapt their staining protocols for use in protozoan organisms cultured in suspensions. To date they have been used to detect parasite viability following treatment with experimental compounds, i.e. in a time-independent manner. Using fluorescent vitality probes and microscopy, a time-dependent assay could be generated in an effort to expand on the screening procedure for novel antimalarials. This would allow for screenings to not only include an indication of parasite sensitivity to the compound/drug in question but to provide an indication of the relative speed of drug action.

Artemisinin, its derivatives, and the combination therapies in which it is used, have had large scale success and this is predominantly due to their swift action (Balint, 2001). Victims of the acute form of the disease, especially in third world countries, rely greatly on drugs with a rapid onset of action, where the use of compounds with longer action half-lives can lead to the onset of severe symptoms and death. The additional complication of patient compliance through the full course of drug treatment only further enhances the need for a single dose, rapid acting antimalarial drug. The need to accurately and quantitatively determine the speed of drug action on malarial parasites, with a priority to match or exceed the rapidity of artemisinin and current ACTs, has been addressed in studies that have produced the PRR, Le Manach and BRRoK assays. As stipulated before, with the BRRoK assay, the motivation for the development of the assay described in this thesis is to enable a rapid (8 hours) relative speed of action assessment of larger libraries of compounds, e.g. the Malaria Box or Pathogen Box. Unlike the BRRoK assay which relies on comparative effects of compounds on luciferase activity in transgenic parasites, the assay detects compromisedmembrane integrity (free diffusion of fluorescent probes into or out of parasites)

which conceivably should more definitively distinguish between viable and irreversibly compromised parasites. It also does not rely on transgenic parasites and could thus in principle be applied to e.g. clinical isolates or parasite species not susceptible to genetic manipulation with current methodologies (for instance *P. vivax*)

One means for quantifying fluorescent probe levels in cells is by flow cytometry. The clear majority of flow cytometry used to assess malaria parasite growth and development has been conducted with the use of nucleic acid stains (Karl *et al*., 2009). Traditionally, cytometry investigations on malaria parasites have been conducted on the premise that uninfected RBCs lack DNA (Grimberg, 2011). Therefore, diagnostic tests can be performed by comparing the ratio of RBCs that stain positive for DNA compared to the total number of RBCs and hence an accurate parasitaemia can be achieved. Previous studies by Karl *et al* (2009) show this to be an efficient technique by making use of the nucleic acid dye SYBR Green to assay for parasitized RBCs over uninfected cells. Furthermore, they made the comparison of cytometry in measuring parasite drug sensitivity to conventional methods i.e. the hypoxanthine incorporation assay and light microscopy with Giemsa staining and concluded that cytometry not only provided a more quantitative result but was also less labour intensive (Karl *et al*., 2009). Studies using the stains discussed in section 1.8 have previously been published although often to identify parasites in solution, and not necessarily for their viability-defining characteristics. TMRE has been shown to be effective in identifying parasites via their mitochondria using flow cytometry and hence measure apoptosis speeds but was not used to actively track the decline in parasite viability (Jones *et al.*, 2009). This is similar to studies that identified and enumerated pRBCs using calcein-AM and PI coupled with flow cytometry (Clark *et al.*, 2013; Jang *et al.*, 2014). Hydroethidine on the other hand has been

used to track a progessional decline in parasite viability over time using flow cytometry (Chevalley *et al.,* 2010; Varela *et al.,* 2014).

To enumerate parasites in culture following drug treatment, this study proposed to use flow cytometry to quantify the accumulation of fluorescence due to vitality probes in cultured parasites at a specific time as a means for rapidly determining the relative speed of action of antimalarial compounds. To achieve this, the following experimental aims were pursued:

1. Confirm the staining patterns of four well characterized fluorescent vitality probes in mammalian cells via microscopy.
2. Assess the extent to which the probes can be used in combination to differentiate between live and dead HeLa cells and their subsequent ability to rank a set of known anticancer agents according to their speeds of action using fluorescence microscopy.
3. Compare the HeLa cell fluorescence microscopy data to alternative assay techniques for measuring anticancer drug killing speeds including a fluorescent probe, plate reader-based assay as well as resazurin- and ATP-based assays.
4. Adapt the probe staining procedures from mammalian cells for use in *P. falciparum* 3D7 strain parasites such that fluorescence microscopy can be used to provide qualitative confirmation of the relative killing speed of a panel of standard antimalarial drugs.
5. Develop a quantitative method for assessing the relative killing speed of a panel of antimalarial drugs using the vitality probes in combination with flow cytometry.
6. Explore additional assay techniques with which to measure antimalarial drug action, including the ATP assay developed by Khan *et al.* (2012).

7. Assess experimental antimalarial compounds, notably the Pathogen Box, using the novel assay and identify any ‘hit’ compounds that show rapid efficacy.
8. Compare the novel assay to a recovery assay to account for any recrudescence across a single parasite life cycle.

Chapter 2 – Vitality Probe Dynamics in HeLa cells

2.1 - Introduction

This study aimed to use fluorescent vitality probes to definitively distinguish between viable and compromised drug treated populations at a specified time interval such that panel of drugs could be ranked as a measure of speed of kill in relation each other. A dual method of staining was applied and involved cytoplasmic staining of viable cells with the readily fluorescent compound calcein, modified into a neutral molecule by the addition of an acetoxymethyl group (calcein-AM). Calcein can freely permeate cell membranes and subsequently be converted into its fluorescent counterpart via cytoplasmic esterases, which is then retained by healthy cells. The second probe, propidium iodide (PI), is a nuclear stain containing aromatic amino groups which interact with nucleotides directly to produce red fluorescence. PI is negatively charged and cannot readily permeate cellular membranes. A loss of membrane integrity allows for the subsequent influx of fluorescent PI and it therefore acts as an indicator of cellular death.

Two alternative probes, TMRE and hydroethidine, were also assessed for their ability to distinguish between viable and non-viable cells. Since these probes are marketed for use in mammalian cells, fluorescence microscopy was first used to assess the behavior of the probes in viable/compromised cultured mammalian (HeLa) cells. Based on the results, calcein-AM and PI were selected for further study in *P. falciparum* parasites (chapters 3 and 4). Additionally, to determine if the probes could be used to assess the relative speed of action of compounds, a panel of eight anticancer compounds were assayed against HeLa cells which were subsequently stained with PI and calcein-AM and then analyzed using fluorescence microscopy. The compounds included two Hsp90 inhibitors (novobiocin and 17AAG), one Hsp70 inhibitor (VER 155008) two

ADP-ribosylation factor 1 (Arf1) inhibitors (brefeldin A and Golgicide), one ADP-ribosylation factor 6 (Arf6) inhibitor (nav2729) and two apoptosis inducers (emetine and etoposide). The ranking of compounds observed in the probe-based microscopy assays were then compared to three additional assays: i) A plate-based assay of probe-stained cells using a fluorimeter; ii) a modified version of the resazurin-reduction assay and iii) an ATP-based assay in an effort to rank the compounds in order of killing speed. This was done in order to determine if the combination of the two probes could also be applied to assess the relative speed of action of compounds that have potential anti-cancer therapy modes of action.

2.2 - Materials and Methods

2.2.1 - Mammalian (HeLa) cell culture and preliminary fluorescent vitality probe staining.

Probes supplied by Sigma-Aldrich (Steinheim, Germany) were used to prepare stock solutions (1 mg/mL). Calcein-AM and PI were solubilized in double distilled water (ddH_2O) while TMRE and hydroethidine were solubilized in dimethyl sulfoxide (DMSO) after which they were stored at -20°C. HeLa cells (Cellonex, South Africa) were cultured under sterile conditions in Dulbecco's modified eagle medium (DMEM) with Ultraglutamine and 4.5 g/L glucose (Lonza, Belgium) supplemented with 10% heat-inactivated fetal bovine serum and antibiotics (penicillin/streptomycin/amphotericin B – Sigma-Aldrich, Germany) in T75 flasks with vented caps in a 37^{o}C, 5% CO_2 incubator. When cells were near confluence, they were detached from the flask in trypsin-EDTA (Lonza, Belgium), pelleted and resuspended in fresh DMEM culture medium. After counting the cells using a light microscope and hemocytometer, 1 mL of 10^5 cells (per well) were transferred into the wells of a 24 well culture plate containing 12 mm round glass coverslips and allowed to incubate at 37^{o}C in a 5% CO_2 incubator overnight. Upon incubation, the culture medium was removed, and the cells were washed twice in phosphate-buffered saline (PBS) (Sigma-Aldrich, Germany). To simulate compromised cellular vitality, a series of wells were incubated in phosphate-buffered saline (PBS) containing 100 µM gramicidin S for 30 min. Untreated control wells containing healthy cells remained under standard culture conditions for this time. The PBS (and drug if applicable) was then removed and the respective fluorescent probes (in PBS) were added to the cells according to Table 1 and allowed to incubate at 37^{o}C for the indicated times.

Table 1: Respective incubation time and concentrations implemented for each fluorescent probe in conjunction with HeLa cells.

Fluorescent probe	Concentration (µg/mL)	Incubation Time (min)	Reference
Propidium Iodide	20	30	Hui, Z. 2012
DAPI/Hoechst33342	2	15	Saha *et al.*, 2013
Hydroethidine	3	10	Forkink *et al.*, 2010
Tetramethylrhodamine	0.05	10	Dikov and Hahn, 2013
Calcein-AM	5	30	Schoonen *et al.*, 2005

Staining solutions were then removed, and cells were washed twice with PBS. After PBS removal the coverslips were transferred to microscope slides and observed on a ZEISS Axiovert fluorescence microscope using a 40x objective and the UV (DAPI/Hoechst33342), blue (calcein-AM) and green (PI, TMRE, hydroethidine) excitation channels based on the excitation and emission peaks in Table 2.

Table 2: Maximum excitation and emission wavelengths of the fluorescent vitality probes used.

Fluorescent probe	Excitation/Emission maxima (nm)
Propidium Iodide	535/617
DAPI/Hoechst33342	358/461
Hydroethidine	535/610
Tetramethylrhodamine	548/573
Calcein-AM	490/520

2.2.2 – Drug IC_{50} determination using an *in vitro* cytotoxicity assay.

HeLa cells cultured as described above were plated in 96-well plates at a cell density of $1x10^4$ cells/well (120 µL) and grown overnight. Three-fold serial dilutions of the eight test compounds starting at 100 µM and performed in duplicate were incubated with the cells for an additional 48 hours, and cell viability in the wells assessed by adding 20 µL of 0.54 mM resazurin in PBS for an additional 2-4 hours. Fluorescence readings (excitation 560 nm, emission 590 nm) obtained for the individual wells were converted to % cell viability relative to the average readings obtained from untreated control wells. Plots of % cell viability vs. log[compound] were used to determine IC_{50} values for each compound by non-linear regression using GraphPad Prism (v. 5.02).

2.2.3 – Fluorescence microscopy based relative killing speed assay.

HeLa cells cultured as described above were plated in 96-well plates at a cell density of $1x10^4$ cells/well and grown overnight. Each well was treated with novobiocin (1.7 mM), etoposide (100 µM), 17 AAG (130 µM), brefeldin A (7 µM), Golgicide (80 µM), VER 155008 (140 µM), emetine (300 nM) and nav2729 (100 µM) (working solutions prepared in complete DMEM medium) in the panel for 8, 16 and 24 hours at 37^{o}C and 5% CO_2. A control sample was left untreated. After the incubations, wells were treated with a combination of PI (20 µg/mL), calcein-AM (5 µg/mL) and Hoechst 33342 (2 µg/mL) according to Table 1 and allowed to incubate at 37^{o}C for 30 min. Staining solutions were then removed, and cells were washed twice with PBS buffer to remove residual probe. The plate was transferred to a ZEISS Axiovert fluorescence microscope and viewed using a 40x objective and the UV (DAPI/Hoechst33342), blue (calcein-AM) and green (PI) excitation channels based on the excitation and emission spectra in Table 2. Experiments were completed in duplicate

2.2.4 – Plate-based fluorescence assay.

HeLa cells were seeded in a 96-well black plate at a concentration of 1 x 10^4 cells per well and incubated overnight at 37°C and 5% CO_2. Each well was treated with novobiocin (1.7 mM), etoposide (100 µM), 17 AAG (130 µM), brefeldin A (7 µM), Golgicide (80 µM), VER 155008 (140 µM), emetine (300 nM) and nav2729 (100 µM) (working solutions prepared in complete DMEM medium) in the panel for 8, 16 and 24 hours at 37°C and 5% CO_2. A control sample was left untreated. After the incubations, wells were treated with calcein-AM according to Table 1 and allowed to incubate at 37°C for 30 min. The staining solutions were then removed, and cells were washed twice with PBS buffer. An unstained control was included to correct for any background fluorescence and the RFU of this control was subtracted from the RFU of the treated wells. The plate was transferred to a Spectramax M3 microplate reader (Molecular Devices, USA) and analyzed for fluorescence emission as per Table 2.

2.2.5 – ATP assay.

HeLa cells were seeded in a 96-well, white-walled, clear bottom plate at a concentration of 1 x 10^4 cells per well and incubated overnight. Each well was treated with novobiocin (1.7 mM), etoposide (100 µM), 17 AAG (130 µM), brefeldin A (7 µM), Golgicide (80 µM), VER 155008 (140 µM), emetine (300 nM) and nav2729 (100 µM) (working solutions prepared in complete DMEM medium) in the panel for 8, 16 and 24 hours at 37°C and 5% CO_2. Control samples included an untreated well as well as wells without cells. At each time point, cells were lysed with 0.5% Triton-X100 in PBS after which the luciferase enzyme reagent provided in the CLS II ATP Bioluminescence Assay Kit (Roche Diagnostics) was added (50 µL) to each respective well. Luminescence in each well was measured in a Spectramax M3 microplate reader (Molecular

Devices, USA) to measure residual HeLa cell associated ATP. An ATP assay standard (provided for in the kit) was run alongside each timepoint to control that the luciferase enzyme reagent was active.

2.2.6 – Resazurin-based *in vitro* cytotoxicity assay.

HeLa cells were seeded in a 96-well, clear plate at a concentration of 1 x 10^4 cells per well and incubated overnight. Test compounds were incubated with the cells at novobiocin (1.7 mM), etoposide (100 µM), 17 AAG (130 µM), brefeldin A (7 µM), Golgicide (80 µM), VER 155008 (140 µM), emetine (300 nM) and nav2729 (100 µM) (working solutions prepared in complete DMEM medium) in the panel for 8, 16 and 24 hours at 37^{o}C and 5% CO_2 after which the drugs were removed and fresh complete DMEM culture medium added to the cells. Cell viability in the wells was assessed by adding 20 µL of 0.54 mM resazurin in PBS for an additional 2 hours. The plate was transferred to a Spectramax M3 microplate reader (Molecular Devices, USA) and fluorescence readings (excitation 560 nm, emission 590 nm) obtained for the individual wells were converted to % cell viability relative to the average readings obtained from untreated control wells. Additional controls included a sample of resazurin in media without cells. At each time point a row of wells were treated with serially diluted concentrations of emetine to generate a dose-response curve by plotting log[compound] vs. % parasite viability to obtain an IC_{50} (50% inhibitory concentration) by non-linear regression analysis using GraphPad Prism (v. 5.02). Obtaining an emetine IC_{50} in line with literature values (~40 nM (Grollman and Jarkovsk, 1975)) would confirm the resazurin assay to be working as expected.

2.3 - Results

2.3.1 - Fluorescent vitality probe staining in mammalian cells.

Although shown to be able to stain their respective cellular elements in other organisms including bacteria (Vesey *et al.*, 1994) and protozoa (Mossallam 2010), the probes explored in this study are more widely marketed for use in mammalian cells and have been used extensively in conjunction with fluorescence microscopy, flow cytometry and fluorimeter spectroscopy. Before proceeding to employing the probes with *P. falciparum* parasites, they were therefore first applied to human cells to determine their staining patterns and efficacy under our culture and experimental conditions and to be able to draw parallels between their behavior in mammalian cells and malaria parasites, respectively.

Briefly, HeLa cells were incubated with the relevant probe staining solutions in separate wells and incubated at 37^{o}C and 5% CO_2 as follows – calcein-AM (5 µg/mL) for 30 min; PI (20 µg/mL) for 30 min; hydroethidine (3 µg/mL) for 10 min; TMRE (0.05 µg/mL) for 10 min; DAPI (2 µg/mL) for 15 min. Visualization was conducted on a ZEISS Axiovert fluorescence microscope. In the instances where it was necessary to simulate compromised cellular vitality (to control for a drug treated culture), respective wells were incubated in 100 µM of Gramicidin S for 30 min prior to probe staining. Gramicidin S was selected due its significant toxicity to human cancer cells in culture for concentrations exceeding 70 µM as well as its rapid activity (Nir-Paz *et al*., 2002).

2.3.1.1 - Calcein-AM.

The acetoxymethyl ester of calcein, calcein-AM, was seen to freely permeate cell membranes and was cleaved to green fluorescent calcein. The probe was then retained well by healthy cells, while a marked decrease in fluorescence was observed in gramicidin S treated cells (Fig. 8). The extent

of calcein fluorescence intensity was thus observed to disappear as cellular vitality was compromised by drug action. Interestingly, DAPI positive cells were observed in greater quantity after drug treatment which coincided with a decrease in calcein staining. This agrees with published work whereby DAPI was observed to penetrate living cell membranes poorly and hence was used as a dead cell indicator (Wallberg *et al.*, 2016). There also appeared to be no dual staining of any cells with each stained cell containing either DAPI or calcein. The staining pattern of the cleaved calcein was observed to have no preferential subcellular localization and instead was spread evenly through the cytoplasm and nuclei of the HeLa cells.

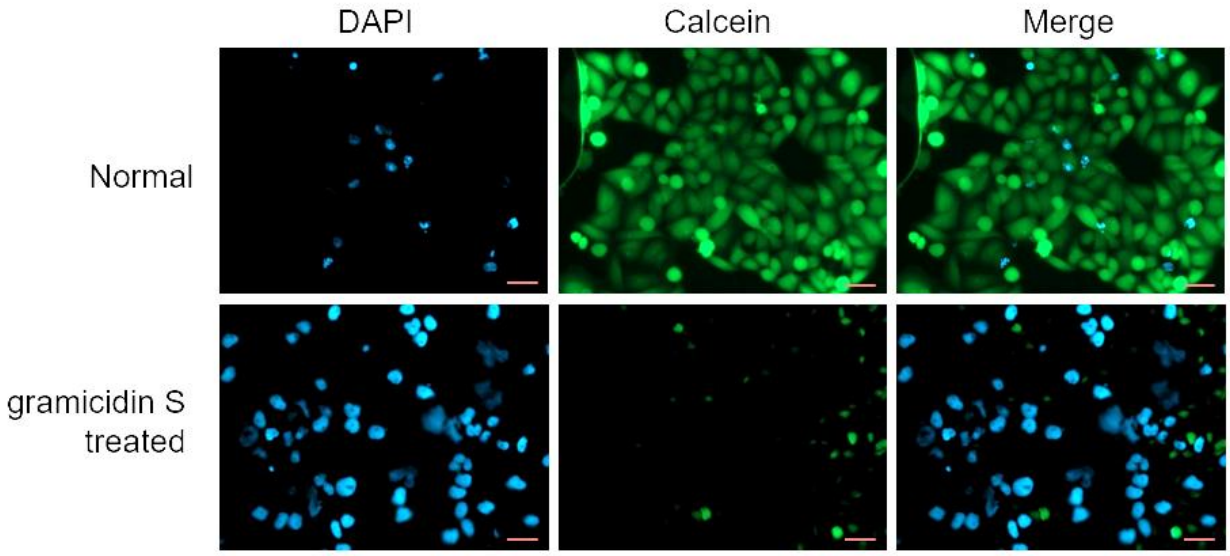

Figure 8: Calcein-AM (5 µg/mL) and DAPI (2 µg/mL) staining of Hela cells treated with 100 µM gramicidin S for 30 min alongside untreated ('Normal') cells. To simulate healthy cell conditions the 'Normal' cells were incubated in media at 37°C and 5% CO_2 during the period of 'gramicidin S treatment. Total probe incubation time was 30 min to allow for both optimal DAPI and calcein-AM staining. Scale bars represent 40 µm.

2.3.1.2 - Propidium Iodide.

Although requiring minor optimization with adjustments to staining concentration and incubation time, PI proved useful in acting as a vitality probe and showed significant fluorescence intensity in Gramicidin S-treated, compromised cells (Fig. 9, bottom panel). A small number of PI positive cells were also observed in untreated 'normal' cell populations (Fig. 9, top panel), likely representing non-viable cells present under normal culture conditions. As was found in the calcein staining experiments where DAPI and calcein displayed inverse staining patterns (calcein staining decreased in Gramicidin S-treated cells and *vice versa* with DAPI), drug treated cells showed a significant increase in DAPI staining. As expected, the DAPI and PI staining coincided exactly since they both stain the DNA in cell nuclei. It also suggests that, like PI, DAPI may act as a vitality probe for HeLa cells, only accumulating in the nuclei of compromised cells.

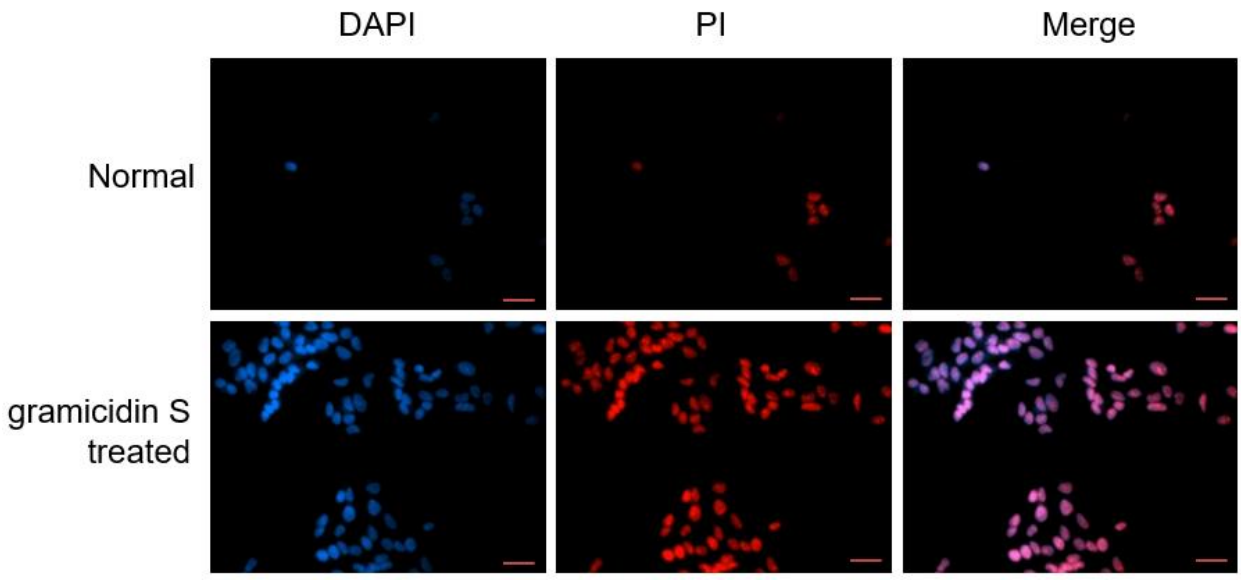

Figure 9: PI (20 µg/mL) and DAPI (2 µg/mL) staining of Hela cells treated with 100 µM gramicidin S for 30 min alongside untreated cells. To simulate healthy cell conditions the 'Normal' cells were incubated in media at 37ºC and 5% CO_2 during the period of gramicidin S incubation. Total probe incubation time was 30 min to allow for both optimal DAPI and PI staining. Scale bars represent 40 µm.

2.3.1.3 – TMRE.

TMRE is marketed as a fluorescent mitochondrial probe that accumulates in mitochondria based on their membrane potential. Given the dependence of the latter on general cell viability, TMRE may thus also be used as vitality probe that preferentially stains healthy cells. TMRE extensively stained untreated HeLa cells, though the probe appeared to be present throughout the cell cytoplasm and nuclei and not limited to mitochondria (Fig. 10, top panel). The gramicidin S-treated sample showed an increase in DAPI-stained nuclei in addition to 'ghost-like' staining of a large proportion of the HeLa cells, where DAPI staining was not confined to the nucleus but diffusely stained cell contents (Fig. 10, bottom panel). DAPI 'ghost' cells may represent instances where gramicidin S treatment not only compromised plasma membrane integrity, but disrupted nuclei, causing genomic DNA diffusion throughout the cell. Nonetheless, TMRE staining in the gramicidin S-treated samples appeared indistinguishable from the untreated samples, suggesting that TMRE was incapable of discriminating between healthy and compromised cells under our experimental conditions.

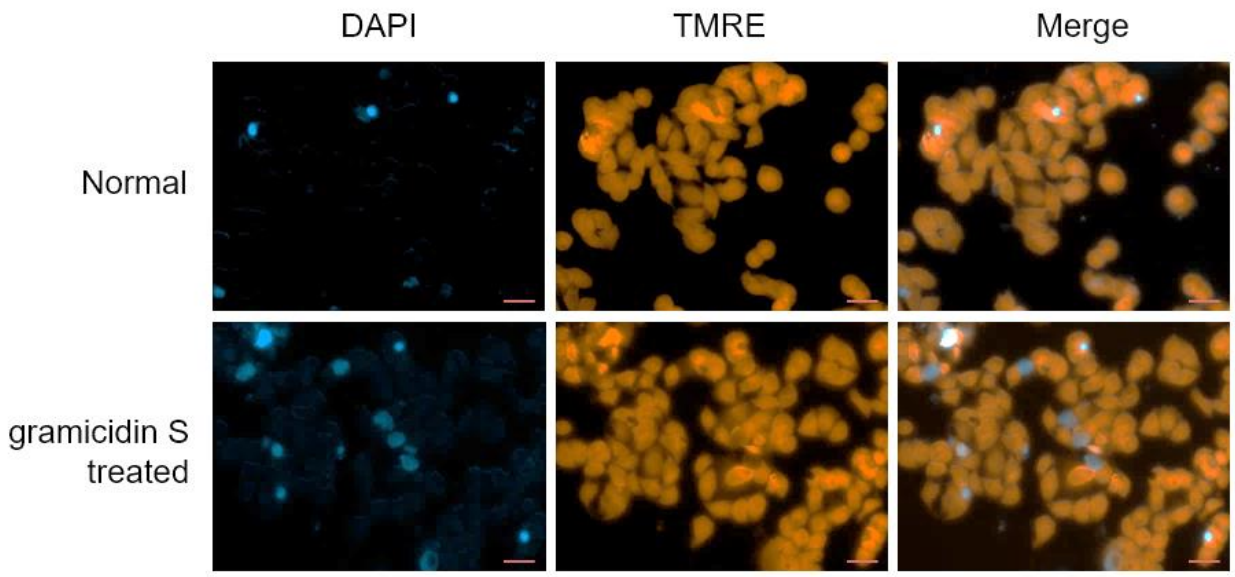

Figure 10: TMRE (0.05 µg/mL) and DAPI (2 µg/mL) staining of Hela cells treated with 100 µM gramicidin S for 30 min alongside untreated cells. To simulate healthy cell conditions the 'Normal' cells were incubated in media at 37°C and 5% CO_2 during the period of incubation for the 'gramicidin S treated' cells. Total probe incubation time was 15 min to allow for both optimal DAPI and TMRE staining. Scale bars represent 40 µm.

2.3.1.4 – Hydroethidine.

Hydroethidine was designed as a neutral molecule which readily diffuses across cell membranes and is cleaved by cellular esterases to form a charged product which is retained in the cell and emits fluorescence upon DNA binding. It should therefore act as a vitality probe by preferentially staining viable cells with intact membranes and pools of esterases. Indeed, extensive hydroethidine staining of untreated HeLa cells was observed, though staining was not limited to the cell nuclei (Fig. 11, top panel). However, although a significant increase in DAPI staining occurred in gramicidin S treated cells, hydroethidine staining appeared unchanged from the untreated cell sample (Fig. 11, bottom panel). In addition, in the untreated cell sample, DAPI-stained cells that likely represent non-viable cells present under normal culturing conditions also retained hydroethidine staining. Alteration of the hydroethidine staining protocol (concentration and

incubation time) did not prevent the staining of non-viable cells. In conclusion, hydroethidine appeared to be unable to distinguish between healthy and compromised HeLa cells under our experimental conditions.

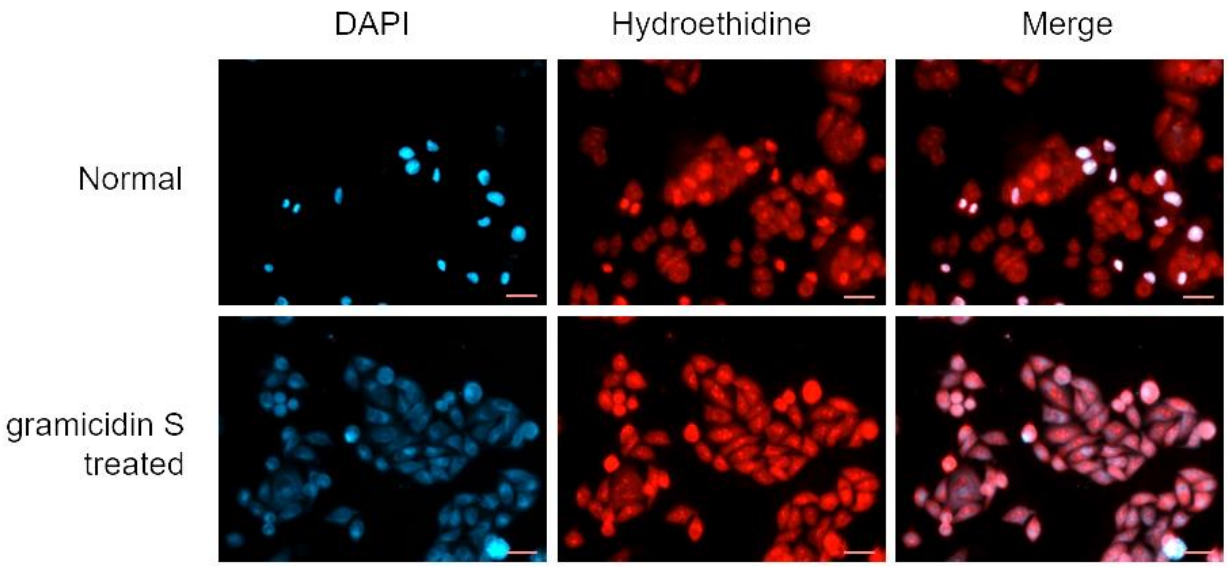

Figure 11: Hydroethidine (3 µg/mL) and DAPI (2 µg/mL) staining of Hela cells treated with 100 µM gramicidin S for 30 min alongside untreated cells. To simulate healthy cell conditions the 'Normal' cells were incubated in media at 37ºC and 5% CO_2 during the period of gramicidin S incubation. Total probe incubation time was 15 min to allow for both optimal DAPI and hydroethidine staining. Scale bars represent 40 µm.

Having established that calcein-AM and PI were suitable vitality indicators for distinguishing between nonviable/viable HeLa cells (while TMRE and hydroethidine were not), the probes were put forward for use in conjunction with a panel of known cytotoxic compounds. This was to assess whether the probes were able to distinguish between live and dead cells at specific time points (8, 16 and 24 hours) and hence give an indication of the relative killing speed of each compound. Before this could be conducted it was necessary to confirm the compound efficacies against the HeLa cells to obtain a guideline of the concentrations to be used in subsequent experiments.

2.3.2 – Compound IC_{50} determination using an *in vitro* cytotoxicity assay.

The cytotoxicity of experimental compounds was assessed using the resazurin reduction assay alongside a well-documented apoptosis inducer in the form of emetine as a control standard (which was also included in the subsequent relative speed of action assessment panel). Resazurin is a cell permeable compound that is blue in solution and capable of uptake in viable cells where it is readily metabolized (reduced) providing a fluorescent, pink product – resorufin. The number of viable cells in a sample may then be assessed as a direct relation to the resorufin produced which can be quantified using a microplate reader and 560 nm excitation / 590 nm emission wavelengths (McMillian *et al.*, 2002). The IC_{50} values for the individual drugs were calculated from the average percentage viability across duplicate experiments of each serially diluted concentration to obtain a single dose-response curve per compound using GraphPad Prism v5.02. (Fig. 12 & 13, Table 3).

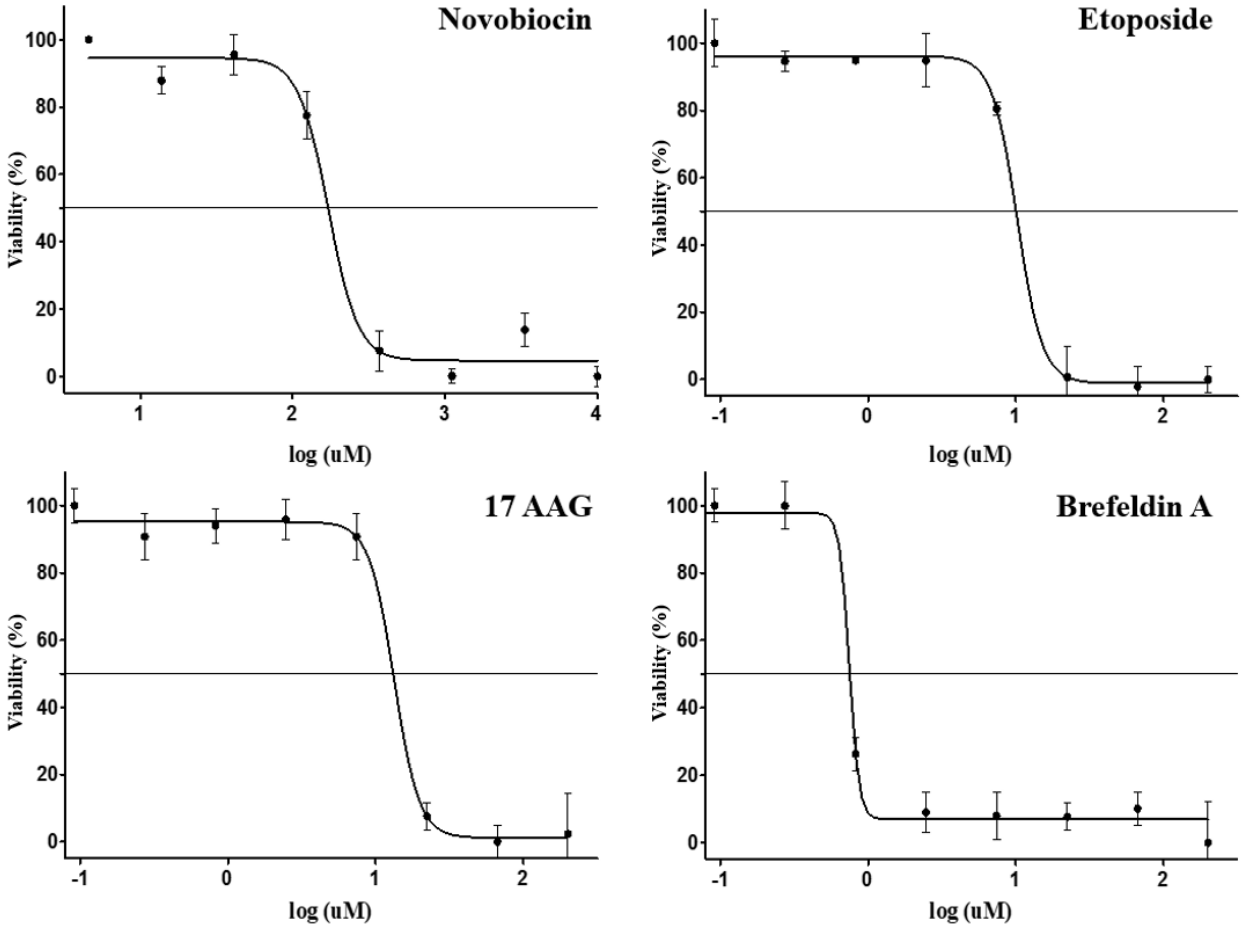

Figure 12: Dose-response curves for novobiocin, etoposide, 17 AAG and brefeldin A against HeLa cell samples. Confluent HeLa cells were grown in DMEM and plated in a 96-well, clear-plastic microplates at 1 x 10^4 cells/ well (120 µL) and then incubated at 5% CO_2, 37ºC for 24 hours. Three-fold serially diluted concentrations of the panel of compounds were added to separate respective wells before incubation at 5% CO_2, 37ºC for a further 48 hours. Resazurin was added to each well and allowed to incubate for 3 hours before quantification at 560 nm/ 590 nm in a Spectramax M3 microplate reader. Cytotoxicity assays were performed on three separate occasions with each being in duplicate and dose-response curves plotted using GraphPad Prism v5.02. Each data point represents an average viability at that concentration ± standard error. IC_{50} values for three dose response curves per compound were averaged and tabulated in Table 3. The curves are representative of a single IC_{50} experiment.

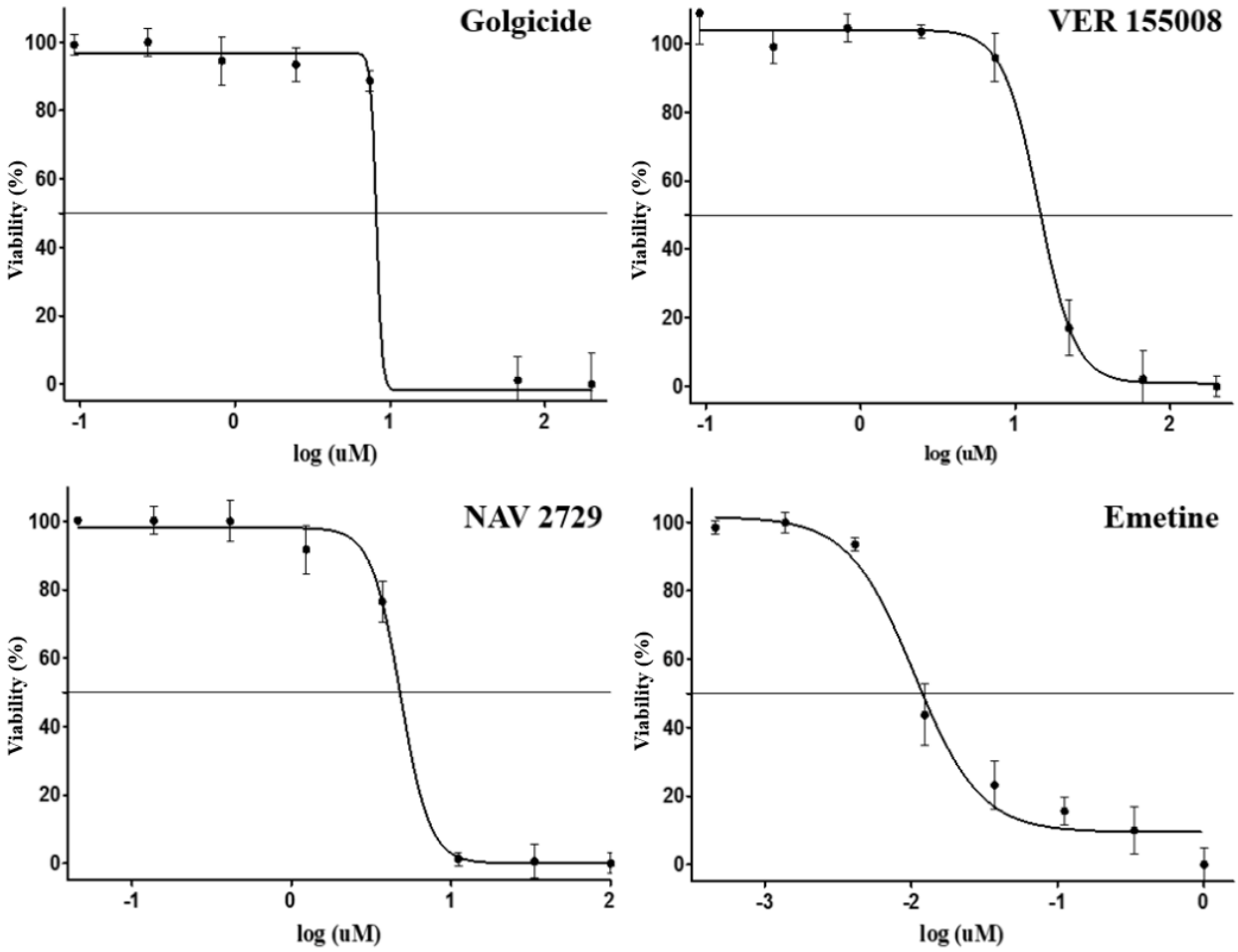

Figure 13: Dose-response curves for Golgicide, VER 155008, nav2729 and emetine against HeLa cell samples. Confluent HeLa cells were grown in DMEM and plated in a 96-well, clear-plastic microplates at 1 x 10^4 cells/ well (120 µL) and then incubated at 5% CO_2, 37ºC for 24 hours. Three-fold serially diluted concentrations of the panel of compounds were added to separate respective wells before incubation at 5% CO_2, 37ºC for a further 48 hours. Resazurin was added to each well and allowed to incubate for 3 hours before quantification at 560 nm/ 590 nm in a Spectramax M3 microplate reader. Cytotoxicity assays were performed on three separate occasions with each being in duplicate and dose-response curves plotted using GraphPad Prism v5.02. Each data point represents an average viability at that concentration ± standard error. IC_{50} values for three dose response curves per compound were averaged and tabulated in Table 3. The curves are representative of a single IC_{50} experiment.

Table 3: Experimental IC_{50} values of the eight test compounds obtained in cytotoxicity assays performed in technical duplicate in each of three distinct biological replicates.

Compound	**IC_{50} (µM) ± Standard Deviation**
Novobiocin	171 ± 9.2
Etoposide	10 ± 2.3
17 AAG	13 ± 1.3
Brefeldin A	0.7 ± 0.052
Golgicide	8 ± 0.24
VER 155008	14 ± 2.8
Nav2729	10 ± 0.52
Emetine	0.03 ± 0.001

2.3.3 – Fluorescence microscopy-based relative killing speed assay.

Although TMRE and hydroethidine appeared to be ineffective vitality probes for HeLa cells when evaluated using fluorescence microscopy and gramicidin S to compromise cell integrity, the two probes that showed the most effective staining patterns for the purposes of this study were PI and calcein-AM which were able to selectively stain compromised and viable cells, respectively. Using the latter two probes, a potentially novel microscopy-based, relative drug killing speed assay for mammalian cells was explored. The concept was to expose HeLa cells cultured in 96-well plates to a series of compounds and use fluorescence microscopy to assess the level of cell staining with calcein-AM and PI. The extent to which cell viability was compromised (increased PI or decreased calcein fluorescence) during a defined period of compound exposure provided an indication of the relative speed of cell toxicity manifestation of the individual compounds. This assay was conducted on a panel of eight compounds that had previously been proposed as inhibitors of cancer

cell viability, and included apoptosis inducers, chaperone inhibitors and Arf1 & Arf6 GTPase inhibitors.

The panel was incubated with HeLa cells in 96-well plates for eight hours at a concentration of 10 x IC_{50} before removal and subsequent incubation with calcein-AM, PI and Hoechst 33342 for 30 min. The probes were used in each drug treated sample to visually gauge the cytotoxic effects of each compound over 8- 16- and 24-hour periods. Calcein, PI and Hoechst staining intensity in the treated cell populations was observed using fluorescence microscopy and fluorescence filters suitable for the excitation/emission peaks specified in Table 2 to determine to what degree the compounds were capable of compromising cell viability in each incubation period.

In eight hours, there was little observable difference between the untreated control and samples treated with novobiocin, etoposide and 17AAG. All three samples showed large scale calcein-positive cells and little to no indication of any that were PI-positive (Fig. 14, top 4 panels) ($p>0.05$ when quantifying and comparing calcein-AM and PI staining levels of control and treated samples – see Fig. 15). By contrast, brefeldin A, Golgicide and VER 155008 showed similar fluorescent patterns with an observable fraction of cells appearing to stain PI-positive, although the majority of the cells remained calcein-positive (Fig. 14, middle panels) ($p<0.05$ when comparing calcein-AM and PI staining levels of treated cells with control cells – see Fig. 15). Golgicide treatment had more of an impact on the calcein-positive cells with some cells showing reduced calcein staining (a 'ghost-like' appearance) – an indication of partial leaching of calcein out of the cells after drug stress. Treatment with emetine and nav2729 showed a stark contrast in fluorescence patterns in relation to the rest of the compound panel. Large scale PI-positive cell staining was observed in both drug-treated samples which complemented a significantly reduced number of calcein-positive cells (Fig. 14, bottom panels) ($p<0.05$ when comparing calcein-AM and PI

staining levels of emetine or nav2729 treated cells with brefeldin A, Golgicide or VER 155008 treated cells – see Fig. 15). Of the two compounds, nav2729 appeared to have more of an effect on the number of calcein-positive cells in eight hours, although the difference did not reach statistical significance ($p>0.05$ when calcein-AM staining in nav2729 and emetine treated cells are compared - Fig. 15).

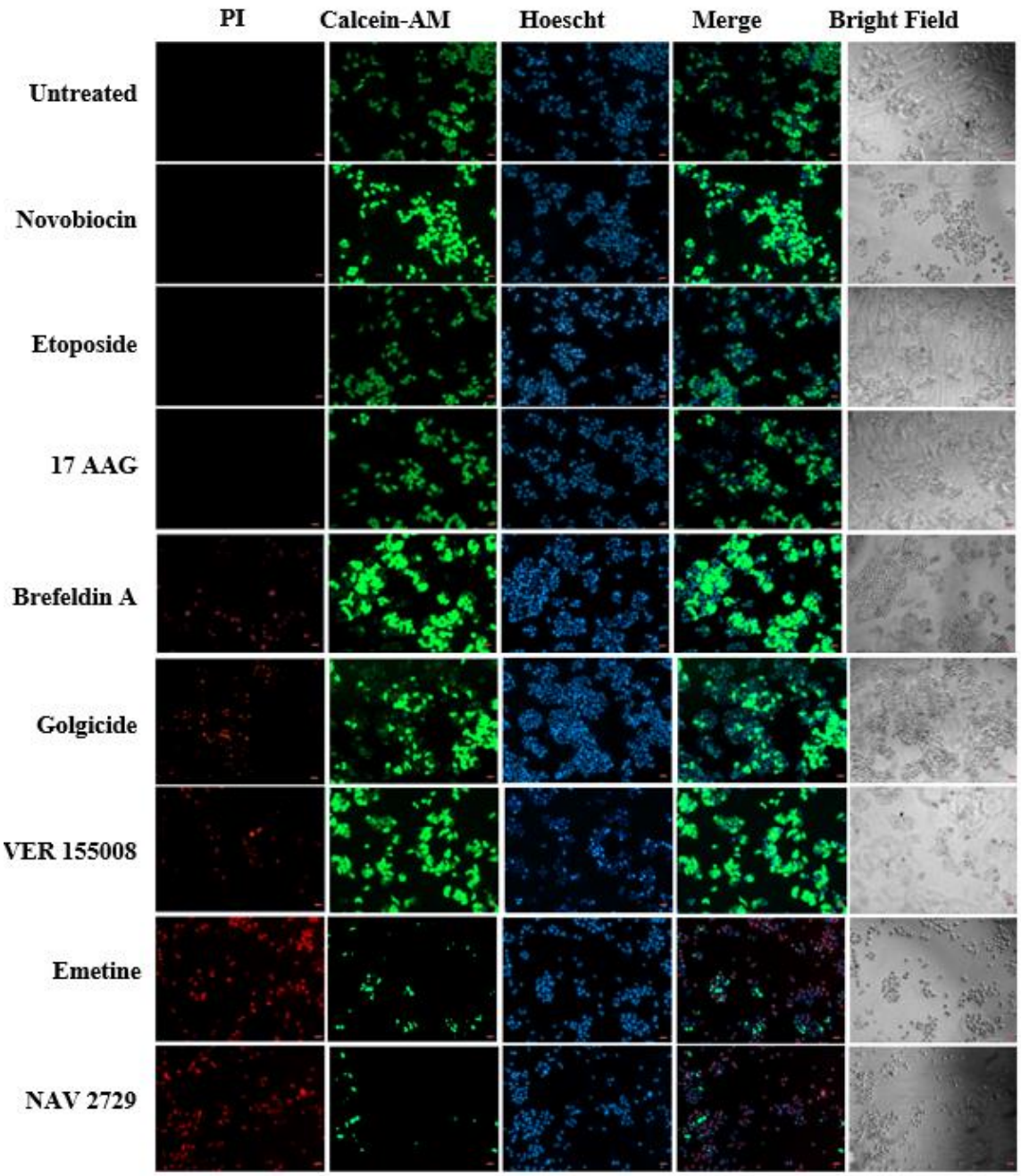

Figure 14: Tri-probe staining of compound-treated HeLa cells using PI (20 µg/mL), Calcein-AM (5 µg/mL) and Hoechst 33342 (5 µg/mL) for 8 hours. Untreated HeLa cells were cultured in routine conditions while test samples were treated for eight hours with novobiocin (1.7 mM), etoposide (100 µM), 17 AAG (130 µM), brefeldin A (7 µM), Golgicide (80 µM), VER 155008 (140 µM), emetine (300 nM) and nav2729 (100 µM) before staining with PI, calcein-AM and Hoechst33342. Analysis via fluorescence microscopy was done on a ZEISS AxioVert fluorescence microscope. Scale bars represent 20 µm.

ImageJ v1.49 coupled with the Cell Counter plugin was used to quantify each field of stained HeLa cells. The prevalence of dead cells per field was defined as:

$$\left[\frac{PI\ (+)\ cells}{Hoechst\ (+)\ cells}\right] drug\ treated / \left[\frac{PI\ (+)\ cells}{Hoechst\ (+)\ cells}\right] untreated$$

This then provided a quantified ratio of the number of dead cells (PI-positive) in each drug treated sample compared to the number of dead cells in the untreated, healthy cell sample. In the same way the prevalence of live cells per field was defined as:

$$\left[\frac{Calcein\ (+)\ cells}{Hoechst\ (+)\ cells}\right] drug\ treated / \left[\frac{Calcein\ (+)\ cells}{Hoechst\ (+)\ cells}\right] untreated$$

Like the PI quantification this provided a ratio of the number of live cells (calcein-positive) in each drug treated sample compared to the number of live cells in the untreated, healthy cell sample. This provided an indication of the remaining cellular viability in each drug treated sample after 8, 16 and 24 hours of treatment. As shown in Fig. 15, a decrease in calcein-positive viable cells compared to the untreated controls was mirrored by a comparable increase in PI-positive, compromised cells. Based on this analysis, after eight hours of treatment, the compounds could be clearly arranged into 3 groups: slow acting (novobiocin, etoposide, 17 AAG), moderate killing speed (brefeldin A, Golgicide, VER 155008) and rapid killing speed (emetine, nav2729), with novobiocin being the slowest and nav2729 being the fastest. The resultant efficacy of the compounds at 8 hours could thus be ranked as novobiocin ~ etoposide ~ 17 AAG < brefeldin A ~ Golgicide ~ VER 155008 < emetine ~ nav2729 on an increasing scale.

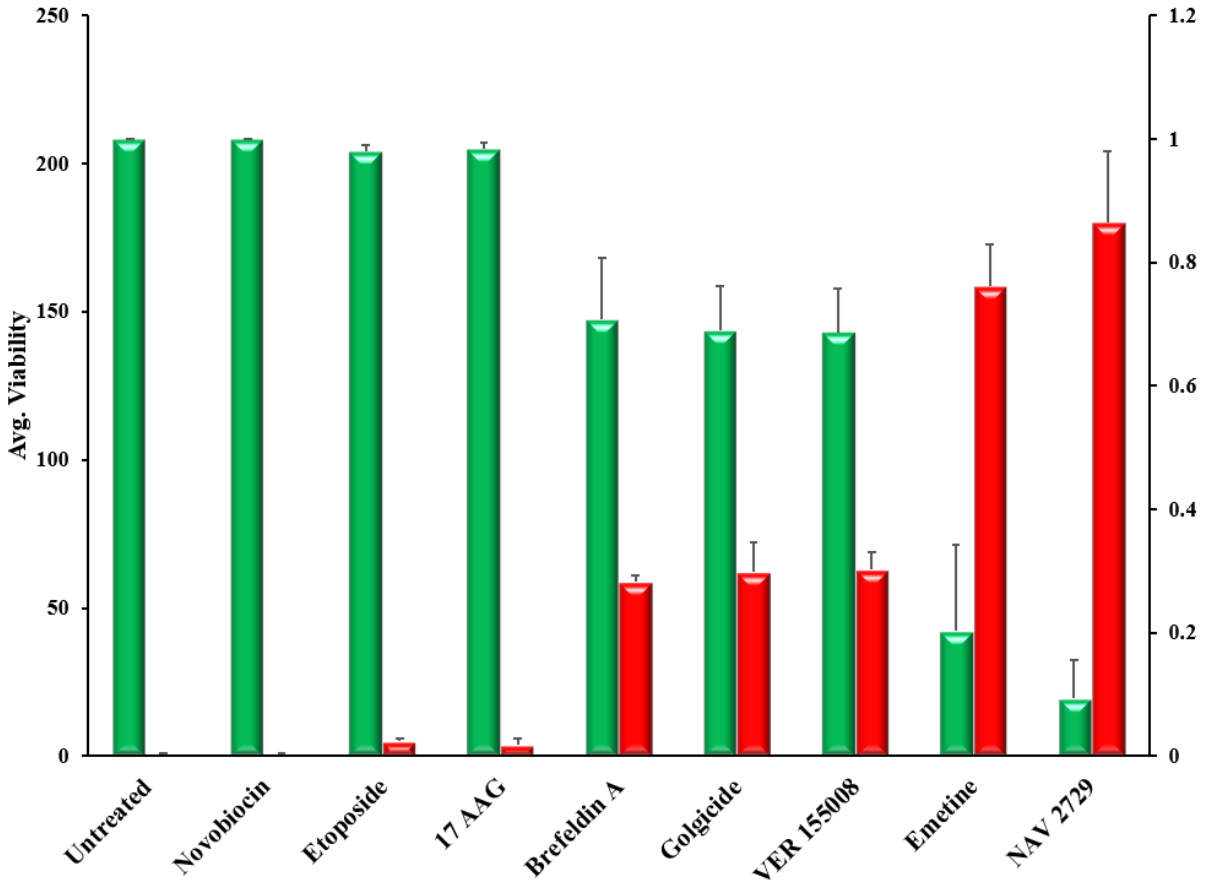

Figure 15: Viability indices for each test compound represented as average cell viability assessed by fluorescence microscopy after an eight-hour drug treatment. HeLa cells were treated with novobiocin (1.7 mM), etoposide (100 µM), 17 AAG (130 µM), brefeldin A (7 µM), Golgicide (80 µM), VER 155008 (140 µM), emetine (300 nM) and nav2729 (100 µM), stained with calcein-AM (5 µg/mL - green), PI (20 µg/mL - red) and Hoechst 33342 (5 µg/mL). Images were captured with a Zeiss AxioVert fluorescence microscope and stained cells counted using ImageJ v1.49 and the Cell Counter plugin (De Vos, Academic Neurology, University of Sheffield). Cell counts were used to calculate average cell viability as the ratio of PI-positive cells (treated) to PI-positive cells (untreated) - left Y-axis and the ratio of of calcein-positive cells (treated) to calcein-positive cells (untreated) – right Y-axis. Error bars represent standard deviation across the five fields.

After 16 hours of treatment, novobiocin and the untreated control culture displayed limited signs of PI staining, as was seen after eight hours, and the large majority of cells remained calcein-positive (Fig. 16, top two panels; Fig. 17) ($p>0.05$ when comparing PI and calcein-AM staining in

treated and control cells), suggesting that novobiocin is incapable of affecting HeLa cell viability within 16 hours. By contrast, although etoposide and 17 AAG only caused a minor increase in PI positive cells after 8 hours, by 16 hours they exhibited similar staining patterns with both showing a marked increase in PI-positive cells compared to the eight-hour treatment period and untreated control cells ($p<0.05$ when comparing PI staining in treated and control 8 hour samples). Furthermore, both compounds showed comparable decreases in calcein-AM stained cells and an increase in the number 'ghost-like' calcein-positive cells (Fig. 16, 3rd and 4th panels; Fig. 17). This confirmed that they were faster acting than novobiocin but required a 16-hour incubation to exert a prominent cell compromising effect, as opposed to the other compounds which displayed the same effect after only 8 hours. Treatment with brefeldin A, VER155008 and Golgicide showed an increase in PI-positive staining in the 16-hour treatment period as compared to eight hours where $p<0.05$ when comparing PI staining across the two time points. There was no significant decrease in calcein-AM staining from eight to 16-hours for these drugs ($p>0.05$ in these cases) (Fig. 16 and 17). Although emetine and particularly nav2729 showed a large-scale decrease in the number of PI-positive cells compared to the 8-hour time-point and the other compounds in the panel (with the exception of novobiocin), this was due to a decrease in the overall observable number of HeLa cells in the samples as judged by Hoechst staining and bright field microscopy (Fig. 16, bottom two panels), likely due to complete destruction of cells by a 16-hour exposure to these compounds. Nav2729 had the fewest calcein-positive cells after 16 hours consistent with a near collapsed HeLa cell culture. The remaining calcein-positive cells might represent sub-populations of HeLa cells that were resistant to emetine and nav2729 action.

Since the ImageJ cell counting approach (Fig. 17) did not take into account the reduction in cell numbers due to drug action but only compared the PI and calcein staining ratios of remaining

treated vs. untreated cells, it might lead to an under-estimation of the total impact of individual compounds on the cultures after 16 hours or longer of treatment. The faster acting drugs (emetine and nav2729) resulted in a fewer number of cells available for staining after 16 hours. Nonetheless, it suggested that a finer distinction could be made between the compounds in the slow acting group – etoposide and 17 AAG were clearly more rapid acting than novobiocin, while of the fast-acting compounds, nav2729 was now clearly distinguishable as faster than emetine. Therefore, a proposed efficacy ranking at 16 hours was novobiocin < etoposide < 17 AAG < brefeldin A < Golgicide ~ VER 155008 < emetine < nav2729.

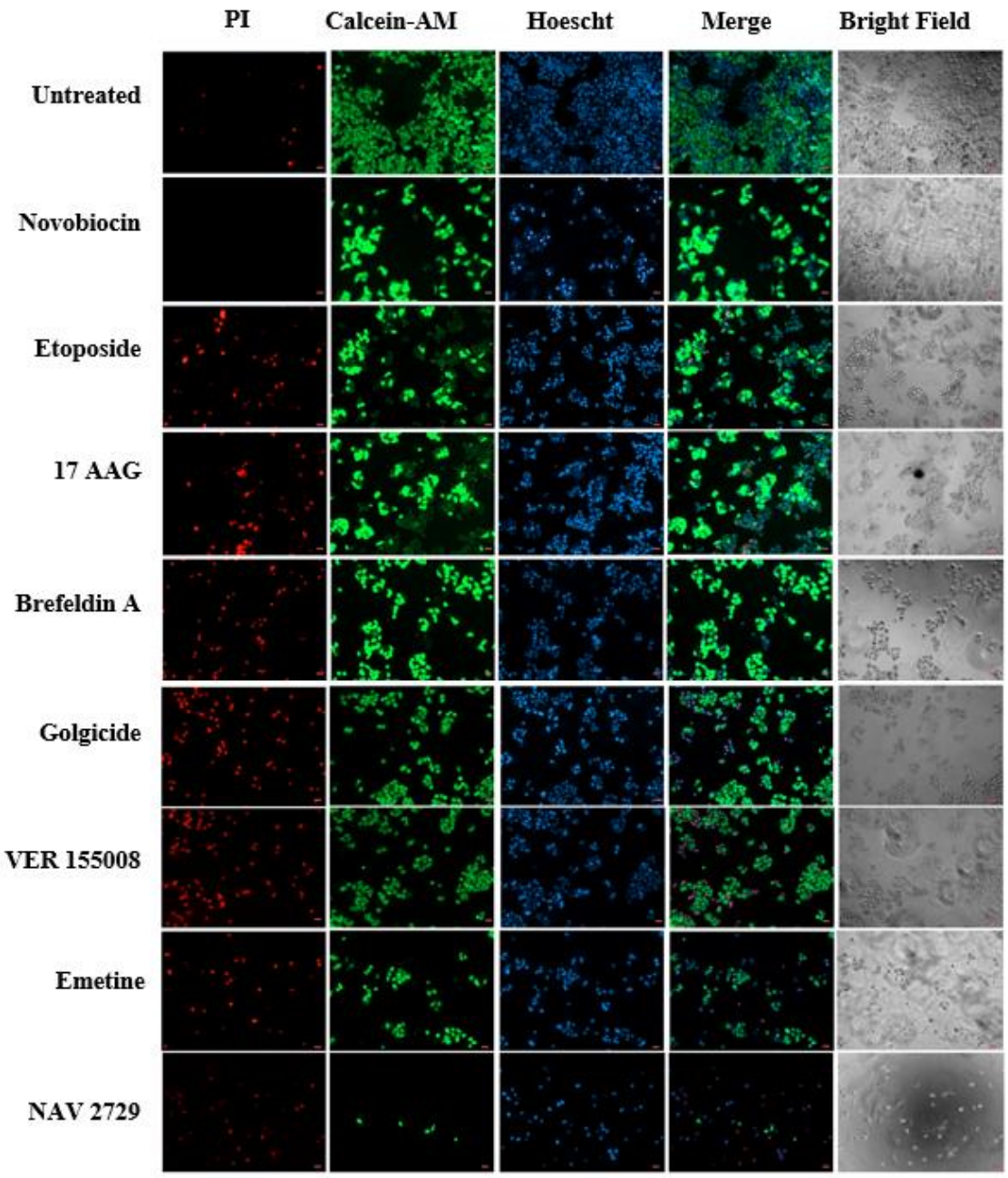

Figure 16: Tri-probe staining of compound-treated HeLa cells using PI (20 µg/mL), Calcein-AM (5 µg/mL) and Hoechst 33342 (5 µg/mL) after 16 hours. Untreated HeLa cells were cultured in routine conditions while test samples were treated for 16 hours with novobiocin (1.7 mM), etoposide (100 µM), 17 AAG (130 µM), brefeldin A (7 µM), Golgicide (80 µM), VER 155008 (140 µM), emetine (300 nM) and nav2729 (100 µM) before staining with PI, calcein-AM and Hoechst33342. Analysis via fluorescence microscopy was done on a ZEISS AxioVert fluorescence microscope. Scale bars represent 20 µm.

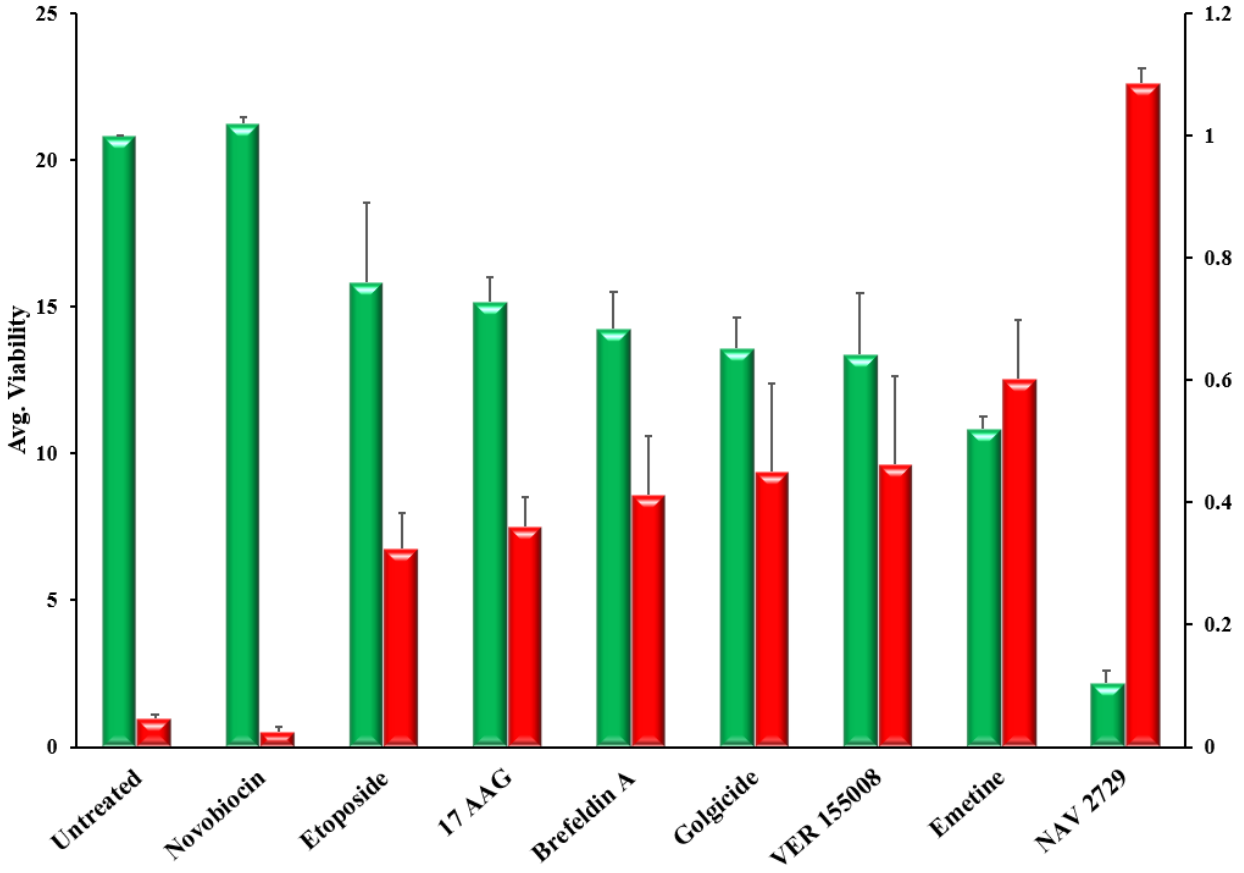

Figure 17: Viability indices for each test compound represented as average cell viability assessed by fluorescence microscopy after a 16-hour drug treatment. HeLa cells were treated with novobiocin (1.7 mM), etoposide (100 µM), 17 AAG (130 µM), brefeldin A (7 µM), Golgicide (80 µM), VER 155008 (140 µM), emetine (300 nM) and nav2729 (100 µM), stained with calcein-AM (5 µg/mL - green), PI (20 µg/mL - red) and Hoechst 33342 (5 µg/mL). Hoechst 33342 (5 µg/mL). Images were captured with a Zeiss AxioVert fluorescence microscope and stained cells counted using ImageJ v1.49 and the Cell Counter plugin (De Vos, Academic Neurology, University of Sheffield). Cell counts were used to calculate average cell viability as the ratio of PI-positive cells (treated) to PI-positive cells (untreated) - left Y-axis and the ratio of of calcein-positive cells (treated) to calcein-positive cells (untreated) – right Y-axis. Error bars represent standard deviation across the five fields.

The final treatment period of 24 hours was the point at which novobiocin appeared to be effective in increasing the number of drug-affected, PI-positive cells, although many calcein-positive cells was still observed (Fig. 18, 2nd panel). Compared to the untreated control, this was the first time

point the two samples produced different staining patterns. The untreated control showed more calcein-positive cells, although the difference was not statistically significant ($p>0.05$), as well as a lower number of PI-positive cells ($p<0.05$ when comparing PI stained treated and control cells). Etoposide and 17 AAG again appeared to have similar killing speeds with an increase in PI-positive and decrease in calcein-positive cells compared to 16 hours of treatment. Brefeldin A, Golgicide and VER 155008 displayed similar killing speeds with only residual PI and calcein stained cells due to comprehensive destruction of cells in the respective culture wells, followed by emetine and then nav2729. Similar to the 16-hour treatment period, there were thus significant differences in overall cell count across drug treated samples and determining the ratio of calcein or PI-stained cells in treated vs. untreated cells (Fig. 19) may not accurately reflect the true impact of the compounds on the cultures. This analysis is thus an approximation of killing speed which was determined to be novobiocin < etoposide < 17 AAG < brefeldin A < Golgicide < VER 155008 < emetine < nav2729.

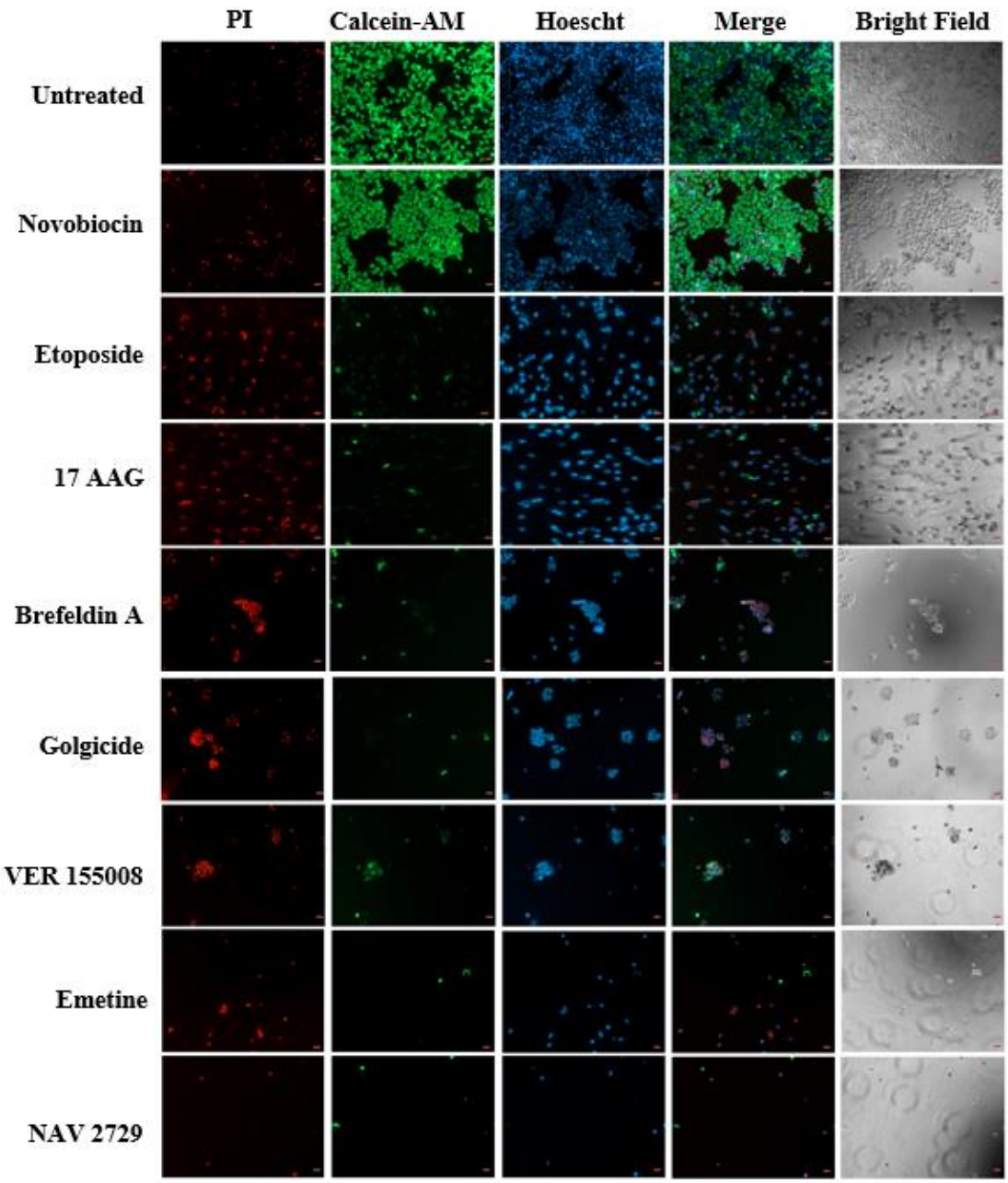

Figure 18: Tri-probe staining of compound treated HeLa cells using PI (20 µg/mL), Calcein-AM (5 µg/mL) and Hoechst 33342 (5 µg/mL) after 24 hours. Untreated HeLa cells were cultured in routine conditions while test samples were treated for 24 hours with novobiocin (1.7 mM), etoposide (100 µM), 17 AAG (130 µM), brefeldin A (7 µM), Golgicide (80 µM), VER 155008 (140 µM), emetine (300 nM) and nav2729 (100 µM) before staining with PI, calcein-AM and Hoechst33342. Analysis via fluorescence microscopy was done on a ZEISS AxioVert fluorescence microscope. Scale bars represent 20 µm.

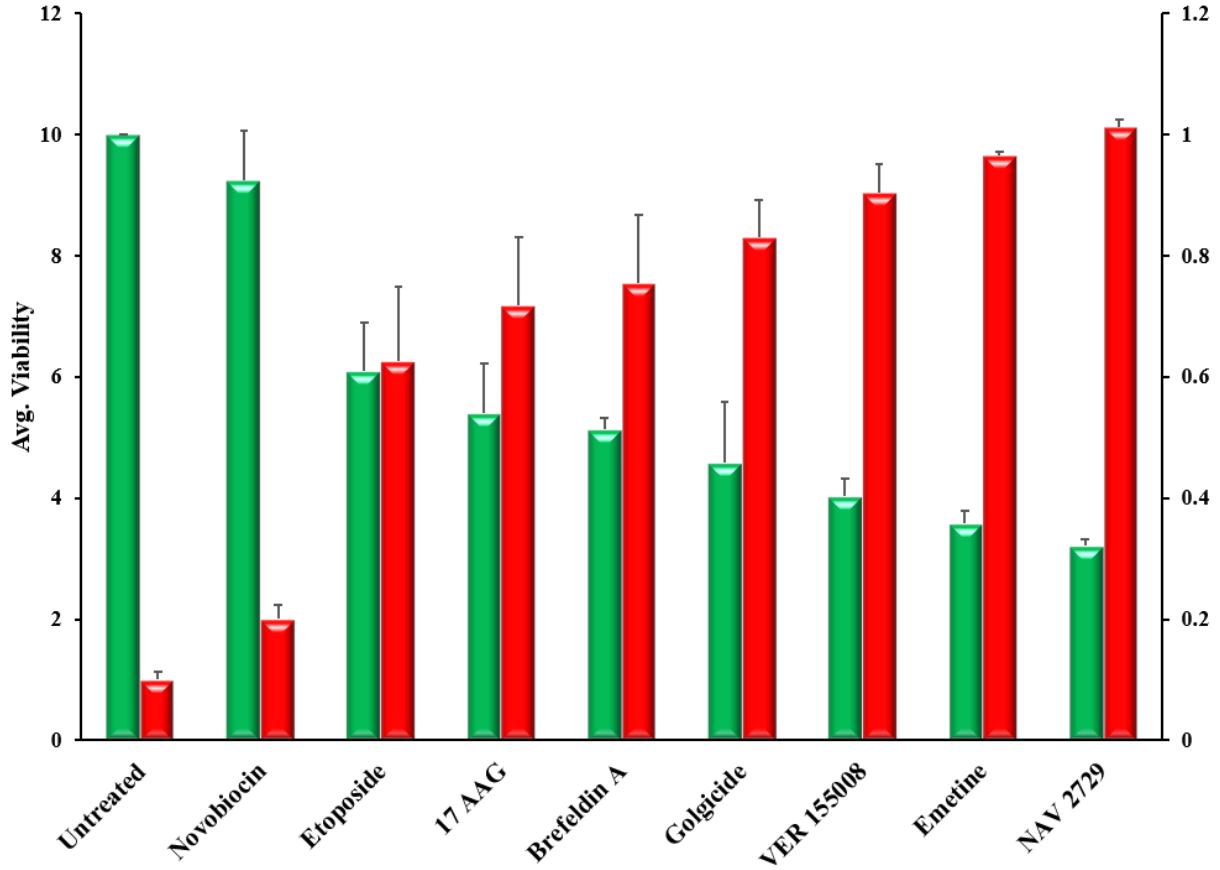

Figure 19: Viability indices for each test compound represented as average cell viability assessed by fluorescence microscopy after a 24-hour drug treatment. HeLa cells were treated with novobiocin (1.7 mM), etoposide (100 µM), 17 AAG (130 µM), brefeldin A (7 µM), Golgicide (80 µM), VER 155008 (140 µM), emetine (300 nM) and nav2729 (100 µM), stained with calcein-AM (5 µg/mL - green), PI (20 µg/mL - red) and Hoechst 33342 (5 µg/mL). Hoechst 33342 (5 µg/mL). Images were captured with a Zeiss AxioVert fluorescence microscope and stained cells counted using ImageJ v1.49 and the Cell Counter plugin (De Vos, Academic Neurology, University of Sheffield). Cell counts were used to calculate average cell viability as the ratio of PI-positive cells (treated) to PI-positive cells (untreated) - left Y-axis and the ratio of of calcein-positive cells (treated) to calcein-positive cells (untreated) – right Y-axis. Error bars represent standard deviation across the five fields.

2.3.4 – Plate-based fluorescence assay.

Using fluorescence microscopy and the PI and calcein-AM probes to rank a series of cytotoxic compounds according to relative killing speed proved successful and nav2729 was identified as being the most rapid acting and novobiocin the slowest. However, the microscopy analysis itself as well as the image processing and additional tools required for quantification (ImageJ) limits the assay throughput. Therefore, the assay was adapted for use in a fluorimeter in an attempt to increase throughput and immediately quantify the levels of calcein/PI staining in drug treated samples.

The assay was conducted in the same way as the microscopy assay but instead of a microscope, the plate was transferred to a Spectramax M3 microplate reader (Molecular Devices) for analysis using the excitation/emission wavelengths described in Table 2. Drug treated samples were compared to an untreated healthy cell sample at each time point (8, 16 and 24 hours) with a control sample left untreated before calcein-AM staining and analysis using a Spectramax M3 microplate reader.

During the study it was noted that samples stained with PI and Hoechst provided erratic fluorimeter readings with no consistency between sample reads. In some instances, there appeared to be spikes in fluorescence intensity regardless of drug treatment that could not be accounted for. Only calcein-AM staining provided consistent and reproducible data that correlated with treated/untreated/unstained samples. Although only based on one fluorescent probe (calcein-AM), the efficacy observed with the compounds at the 8-hour time point (Fig. 20) mirrored that obtained using fluorescence microscopy (Fig. 15) and also discriminated between three groups of compounds: slow acting (novobiocin, etoposide, 17 AAG), moderate acting (brefeldin A,

Golgicide, VER 155008) and fast acting (emetine, nav2729). At 16 hours, the results also confirmed the corresponding microscopy analysis (Fig. 17) in showing that, though classified as slow acting at 8 hours, etoposide and 17 AAG were faster acting than novobiocin.When comparing calcein-AM staining after treatment with brefeldin A, goligicide and VER155008 for 8 and 16 hours in the microscopy analysis, the change in the number of calcein-AM positive cells was not significantly different ($p>0.05$ in all three cases). However, when using a plate-based approach and a fluorescence reader (Fig. 20), there is a larger observable difference when making the same comparison ($p<0.05$ in all three cases). A ranking of novobiocin < etoposide ~ 17AAG < brefeldin A ~ Golgicide < VER155008 < emetine < nav2729 was thus based on the readings obtained for eight and 16 hours, while 24 hours proved too long a treatment time to provide an indication on individual, relative drug killing speeds due to a substantial loss of fluorescent signals, likely due to cell destruction (except in the case of novobiocin; Fig. 20).

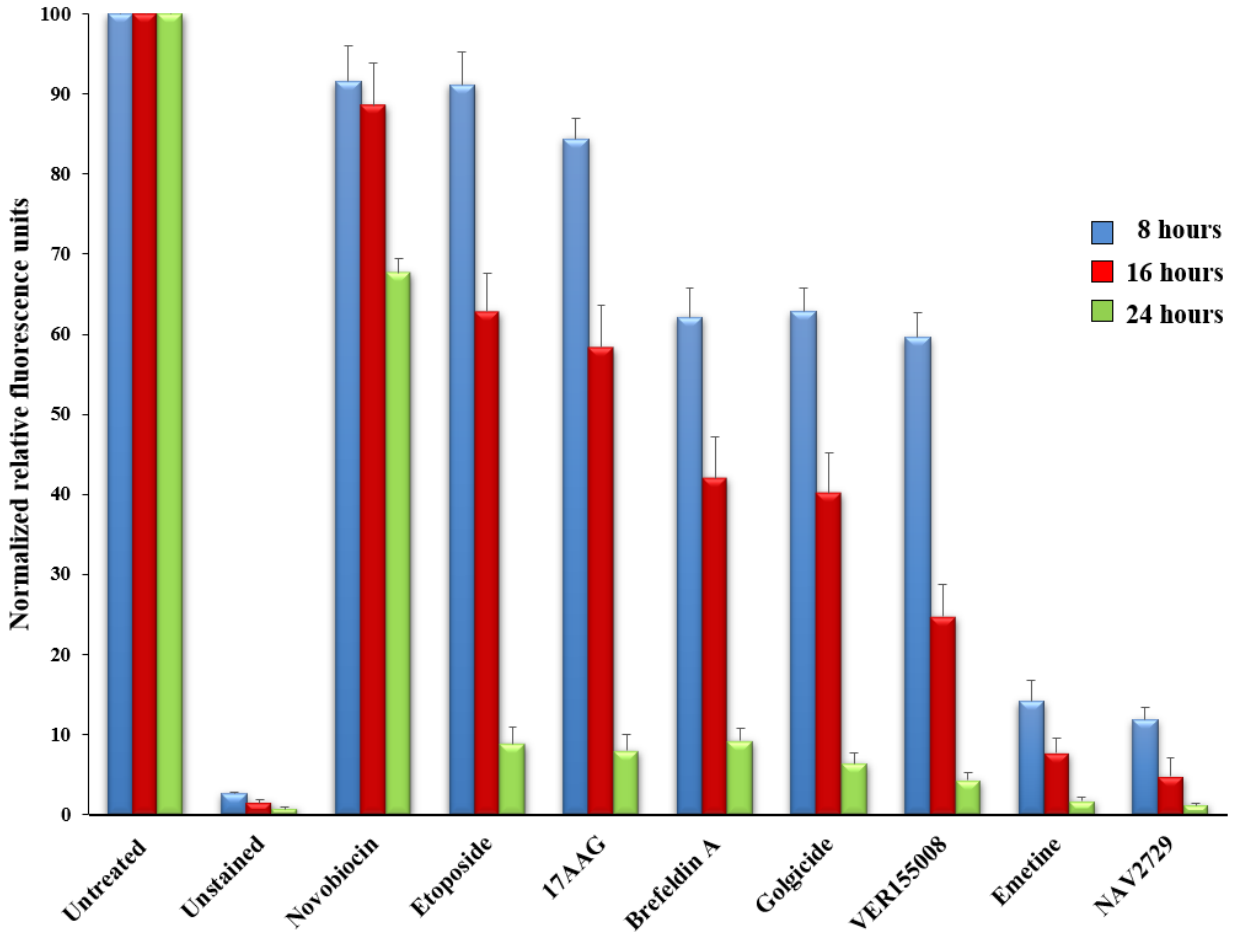

Figure 20: Calcein-AM fluorescence intensity of drug treated HeLa cells after 8, 16 and 24-hours. HeLa cells cultured in 96-well plates were incubated with 10 x IC_{50} of the respective drug compounds which included novobiocin (1.7 mM), etoposide (100 µM), 17 AAG (130 µM), brefeldin A (7 µM), Golgicide (80 µM), VER 155008 (140 µM), emetine (300 nM) and nav2729 (100 µM) for 8,16 or 24-hours, stained with calcein-AM (5 µg/mL) and calcein fluorescence read on a Spectramax M3 microplate reader. Relative fluorescence readings in drug treated wells were expressed as percentage of HeLa cell growth inhibition in relation to the untreated control ± standard deviation (three independent biological repeats in duplicate).

2.3.5 – ATP assay.

As an alternative to using fluorescent probes to detect changes in levels of drug stress, an assay was designed that quantified ATP levels in drug treated populations of HeLa cells in relation to a healthy cell sample. An ATP Bioluminescence Assay Kit (Roche Diagnostics) was used for the quantitative detection of ATP by luciferase driven bioluminescence. This allowed changes in the number of viable cells across drug treatment time points to be tracked and correlated directly to the relative killing speed of the panel of cytotoxic compounds obtained with the fluorescent probes and as such represented an attempt to obtain independent verification of the relative speeds. Briefly, the panel of test compounds were incubated in standard conditions with HeLa cells in 96-well plates for 8, 16 and 24 hours at a concentration of 10 x IC_{50} before compound removal and cell lysis. Luciferase enzyme and substrate (luciferin) were added to each sample and the relative luminescence units measured in a Spectramax M3 microplate reader. Drug treated samples and their associated residual ATP was compared to a healthy cell sample, while luciferase reagent and Triton X-100 lysis buffer was added to wells without cells to control for background luminescence.

When replicating the assay to improve on precision, the ATP levels in individually drug treated samples appeared to fluctuate significantly. Although novobiocin remained the slowest acting compound and emetine and nav2729 the fastest (Fig. 21), the other five compounds interchanged rankings across replicate assays. In particular, etoposide and 17 AAG (classified in the fluorescent probe assays as slow acting) could not be as confidently distinguished as slower acting than brefeldin A and Golgicide (classified as moderate acting) at the 8-hour time-point, and in the fast-acting group, neither could nav2729 be distinguished as faster acting than emetine. It was therefore difficult to generate a confident ranking over the full set of compounds according to relative killing speed. As with the plate-based fluorescence assay, though, VER155008 did appear to be faster

acting than the fellow “moderate” compounds (brefeldin A and Golgicide) at 16 hours. A tenuous ranking based on the 16-hour time-point was observed as novobiocin < etoposide < 17AAG < BFA ~ Golgicide < VER155008 < emetine ~ nav2729 (Fig. 21). By 24 hours, the compounds had affected cell viability to the extent that ATP signals had essentially been reduced to background levels.

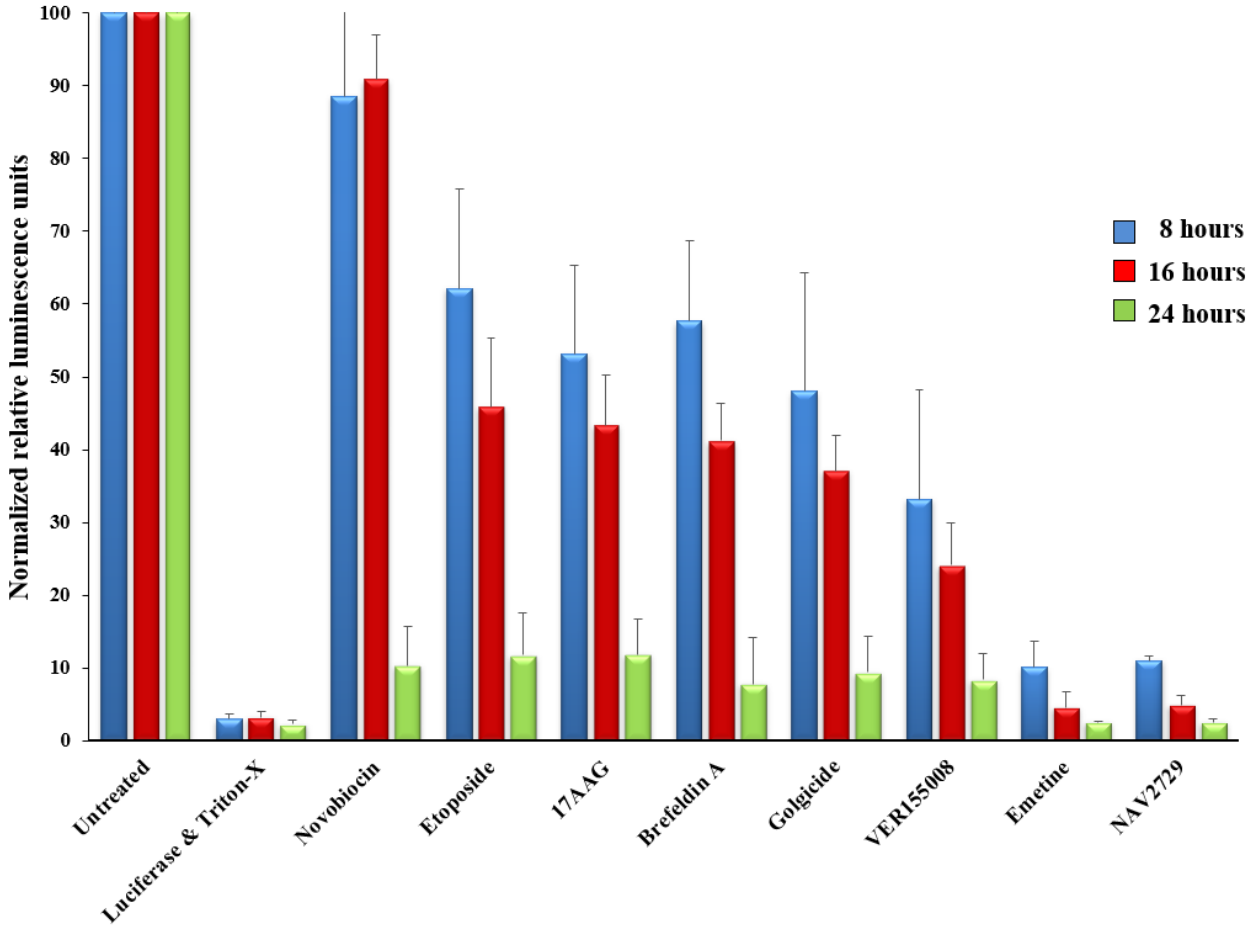

Figure 21: Relative luminescence units (RLU) for the panel of cytotoxic compounds reflecting the ATP levels after an 8, 16 and 24-hour drug-treatment of HeLa cells. HeLa cell samples were treated with test compounds at 10 x IC_{50} concentration which included novobiocin (1.7 mM), etoposide (100 µM), 17 AAG (130 µM), brefeldin A (7 µM), Golgicide (80 µM), VER 155008 (140 µM), emetine (300 nM) and nav2729 (100 µM). Test samples were compared to untreated cells and empty (cell-free) wells as controls. RLU readings in drug treated wells were expressed

as percentage of HeLa cell growth inhibition in relation to the untreated control ± standard deviation (representative of a single biological sample in technical triplicate).

2.3.6 – Resazurin-based *in vitro* cytotoxicity assay.

In this study (section 2.3.2), IC_{50} values were obtained using a standard cytotoxicity assay in the form of the resazurin reduction assay. Briefly, the assay relies on the conversion of freely cell permeable resazurin (blue) to resorufin (pink) by reducing compounds (e.g. NADH and NADPH) in cells. Resorufin can be readily quantified by absorbance or fluorescence in a plate reader (fluorescence was used in this instance). The number of viable cells in a sample could therefore directly correlate to the resorufin produced and conclusions can be made on compound toxicity. Conceivably, exceptions may occur where compounds affect the redox status of cells, i.e. reduce NADH/NADPH levels without overtly compromising cell viability. In this study, the assay was further adapted to assess the series of compounds in the cytotoxicity panel at single concentrations (10 x IC_{50}) to gauge their effect on the ability of treated cells to reduce resazurin at each of the three time points (8, 16 and 24 hours). This was done to determine if the assay could provide insight into relative compound killing speeds and how this compared to the results obtained with the fluorescent vitality probes.

HeLa cells were plated in a 96-well, clear-plastic microplates at 1 x 10^4 cells per well and then incubated at 5% CO_2, 37^{o}C for 24 hours before test compounds were added at 10 x IC_{50} concentrations before further incubation at 5% CO_2, 37^{o}C for 8, 16 or 24 hours. Resazurin was thereafter added for an additional two hours after removal of the drugs and cell viability was assessed via the quantification of resorufin fluorescence at 560 nm/590 nm (excitation / emission) in a Spectramax M3 microplate reader.

The resazurin-based cytotoxicity assay proved to be both sensitive enough to measure changes in HeLa cell population vitality after treatment with the different drugs as well as reproducible across triplicate experiments. Importantly, the trend of the fastest acting compounds found in the microscopy, plate-based calcein-AM, and ATP assays (emetine and nav2729) through to the slowest acting (novobiocin) was mirrored in this assay (Fig. 22). As with the ATP assay, a difference between the resazurin assay and the microscopy/calcein-AM plate-based assay results at the 8-hour time-point was that etoposide and 17 AAG appeared faster acting than novobiocin, while VER155008 appeared faster acting than brefeldin A and Golgicide ($p<0.05$ in both cases). This may reflect that compound action induced a drop in ATP or NADH/NADPH levels before cell viability was irreversibly compromised, leading to disruption of membrane integrity and increased calcein or PI permeability. With the exception of novobiocin and etoposide, at the 24-hour time point the compounds had reduced cell viability almost to background levels (Fig. 22).

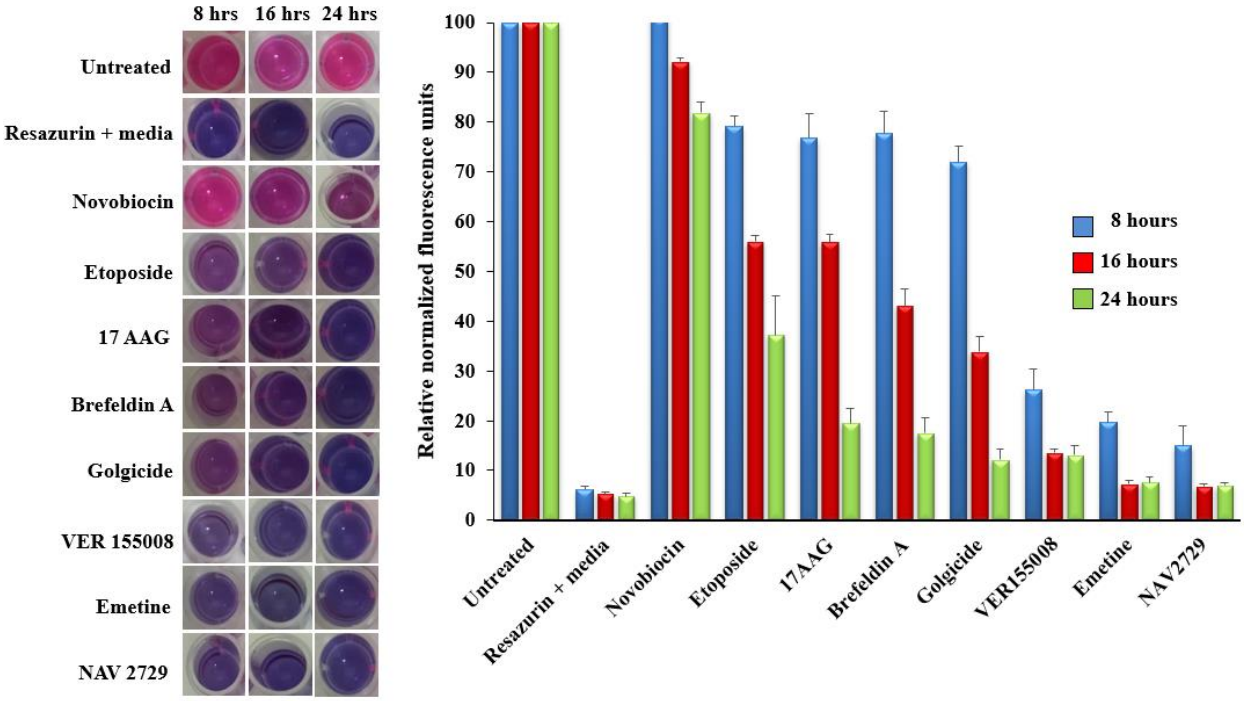

Figure 22: Relative fluorescence units (RFU) for the panel of cytotoxic compounds representing population vitality after eight hours of drug treatment in HeLa cells, using resazurin as viability indicator. HeLa cell samples were treated with test compounds at 10 x IC_{50} concentration which included novobiocin (1.7 mM), etoposide (100 µM), 17 AAG (130 µM), brefeldin A (7 µM), Golgicide (80 µM), VER 155008 (140 µM), emetine (300 nM) and nav2729 (100 µM). After adding resazurin, fluorescence was measured in a plate reader (Exc_{560}/Em_{590}). Controls used were wells containing untreated cells, and wells without cells (resazurin + media). RFU in drug treated wells were expressed as percentage of HeLa cell growth inhibition in relation to the untreated control ± standard deviation (three independent biological repeats in technical duplicates).

2.3.7 – Results summary

In summary, analysis of the compound panel by fluorescence microscopy and plate-based fluorimetry yielded very similar results. After 8 hours of treatment, the compounds were arranged into three groups: slow acting (novobiocin, etoposide, 17AAG), moderate acting (BFA, Golgicide, VER155008) and fast acting (emetine, nav2729). By 16 hours, of the slow compounds, etoposide

and 17AAG had shown themselves to be faster acting than novobiocin, while of the moderate compounds, VER155008 appeared faster acting. For comparison, the compounds were assessed by two alternative possible relative speed of action assays (ATP and resazurin). Overall the results confirmed those obtained with the fluorescent probes, except that the relatively faster action of etoposide and 17AAG vs. novobiocin and of VER155008 vs. BFA and Golgicide was already apparent at the 8-hour time-point (for comparative purposes, the results obtained with the various assay formats are shown together in Appendix 12)

2.4 – Discussion

As discussed in Chapter 1, one of the ideal criteria for a TCP-1 (asexual blood stage) antimalarial drug candidate is a rapid parasiticidal action that allows single-dose regimens to become feasible. This emphasis has led to the development of several speed of action assays to improve on traditional morphological evaluation of micrsocopy slides, notably the PRR assay (recovery from drug exposure by parasite cultures; Sanz *et al.*, 2012), comparison of IC_{50} values obtained by exposing parasite cultures to test drugs for different time periods (Le Manach *et al.*, 2013) and, primarily to compensate for the limited throughput of the above assays, the BRRoK assay (reduction in luciferase activity in transgenic parasites due to compound action; Ullah *et al.*, 2017) The approach in this study was to use fluorescent vitality probes to definitively distinguish between viable and compromised drug treated populations at a specified time interval such that panel of compounds could be ranked as a measure of speed of kill in relation to each other.

Before proceeding to malaria applications, the work described in this chapter assessed the staining patterns of four fluorescent vitality probes both in healthy HeLa cell cultures as well as drug treated populations. This was done to unambiguously quantify viable and non-viable/compromised cultures during drug treatment such that novel compounds can be ranked in relation to killing speed. Additionally, a panel of eight anticancer compounds were assayed against HeLa cells which were subsequently stained with PI and calcein-AM and then analyzed using a plate-based fluorimeter as well as fluorescence microscopy. These assays were then compared against a modified version of the resazurin reduction assay as well as an ATP-based assay.

2.4.1 - Fluorescent vitality probe staining in mammalian cells

The fluorescent vitality probes selected for use have been predominantly marketed for mammalian cell studies, although shown to be able to stain their respective cellular elements in other organisms including bacteria (Vesey *et al.*, 1994), and protozoa (Mossallam, 2010). Although these probes have been used in *Plasmodium* parasites, it has been as a screening tool to determine drug efficacy, i.e. to enumerate the number of parasites remaining after drug treatment (as opposed to determining the relative speed of drug action), or for diagnostic purposes to detect parasites in blood samples. The studies also often make use of flow cytometry instead of fluorescence microscopy. To understand their innate staining patterns (factors like staining intensity and quenching susceptibility) and gain familiarity with their use, it was therefore elected to first assess their staining patterns in mammalian cells prior to their use in *P. falciparum* parasites.

Gramicidin S treated cells showed a significant increase in DAPI staining and a distinct decrease in fluorescent calcein. The staining pattern of the cleaved calcein was observed to have no subcellular localization and instead encompassed the entirety of the HeLa cell. This would suggest the concentration was unnecessarily high such that intracellular esterases were becoming oversaturated and allowing for the calcein to cross organelle membranes as previously observed by Tenopoulou *et al*., (2007). This was dismissed after significantly lower concentrations either failed to produce fluorescence or the fluorescence signal was weak but still retained by the whole cell. Hence it was determined that the calcein-AM probe functioned as would be expected in mammalian HeLa cells.

PI has been used extensively to track a visual reduction in cellular vitality and cell degradation. This study observed that drug-treated cells showed an increase in DAPI staining and a co-localized

increase in PI staining. If a cell was unhealthy but appeared still to be viable, then PI was either not able to enter the cell or the subsequent fluorescent signal was low. This is comparable to a study conducted in papillary thyroid carcinoma cells whereby PI was used to probe for dead cells and DAPI used to visualize the entirety of the cell population by observing the staining patterns in compromised nuclei (Infanger *et al.,* 2006). The staining patterns observed by the Infanger group (2006) closely resemble those observed in this study and therefore PI satisfied the purpose of acting as a suitable viability probe in mammalian HeLa cells.

TMRE stained, drug-treated cells showed a minor increase in DAPI staining compared to healthy populations whereby no marked difference was observed between drug-treated and healthy TMRE test samples. An important note is that gramicidin S is lytic, cationic and amphipathic and the scenario exists whereby it may have bound to TMRE and hence limited the drug activity against the cellular and mitochondrial membranes, although further investigation with alternative cytotoxic compounds is required for any confirmation. If TMRE could be optimized to localize to the mitochondria as previous diagnostic studies have confirmed (Loew *et al.,* 1993; Collins *et al.,* 2002) then this could allow for less dual probe interaction. It was therefore decided that TMRE would not be suitable as an indication of cellular vitality in any mammalian cell studies but would however be assessed in *P. falciparum* to compare staining patterns.

Of the four vitality probes chosen the most promising prior to scrutiny was hydroethidine. Extensive studies have been conducted on the probe as a vitality marker, including work done in mammalian cells (Zielonka *et al.,* 2005) and parasites (Elloso *et al.,* 1994; Cruz *et al.,* 2012). Nonetheless, the staining patterns could not be optimized sufficiently to provide a reliable vitality indicator in HeLa cells in this study. Drug treated cells showed large scale DAPI fluorescence as well as co-localization with hydroethidine. Untreated cells showed minimal DAPI fluorescence

coupled with high fluorescence intensity in hydroethidine positive cells. The marked sequestration of fluorescence in drug treated cells was unexpected as previous studies have shown that the accumulation of the probe depends heavily on the metabolic state of the cell, with compromised cells exhibiting a significantly reduced amount of fluorescence (Bucana *et al.*, 1986). The co-localization with DAPI would support the conclusion that these cells were indeed membrane compromised but still retained the hydroethidine stain, a result not found in other studies. There exists the potential that gramicidin S treatment somehow leads to compromised cells that retain the ability to be stained with both hydroethidine and TMRE and as such does not conform with expected staining patterns. As was the case with TMRE, hydroethidine was temporarily discarded as a suitable vitality indicator for mammalian cells but would still be pursued in parasites to compare staining patterns.

2.4.2 – Drug IC_{50}'s using an *in vitro* cytotoxicity assay

Having found that calcein-AM and PI could discriminate between unaffected and compromised HeLa cells using gramicidin S, the question addressed was whether they would be applicable to other cytotoxic compounds and could be used to rank compounds with respect to their relative speeds of action. An interest in our group and those of collaborators is exploring chaperones and ADP-ribosylation factor (Arf) GTPases as drug targets for cancer. Standard inhibitors of these target classes were thus chosen for analysis and included novobiocin and 17AAG (heat-shock protein 90 inhibitors), VER 155008 (hsp70 inhibitor) and brefeldin A, Golgicide and nav2729 (Arf GTPase inhibitors). Etoposide and emetine were also included since they are regularly used as positive control standards in cytotoxicity/anti-cancer screens. The IC_{50} values for the panel of cytotoxic compounds used in this study have been previously reported but it was important to assess their effective concentrations on the available HeLa cell stocks to ensure that i) the drug

stocks used in this study were active; ii) that the HeLa cells had not altered their susceptibility to the drugs due to extensive sub-culturing. Generally, the IC_{50} values obtained agreed closely with published results although some deviations were observed. Of the Hsp90 inhibitors, novobiocin treatment resulted in the highest IC_{50} observed (as well as overall in the panel) at 170 µM, which was lower than reported in previous studies: ~ 3 mM (McConnell *et al.,* 2015) and 250 µM (Allan *et al.*, 2006) in HeLa cells. Contrastingly, 17 AAG displayed a much lower IC_{50} at 10 µM, comparing well to literature – 10 µM in HeLa cells (Du *et al.,* 2008). The Hsp70 inhibitor VER 155008 has been described to be effective at 20 µM in A375 cells (Budina-Kolomets *et al.,* 2014) which is slightly higher than the observed IC_{50} in this study at 13 µM. Of the toxicity standards, etoposide aligned well with literature (1-10 µM in HeLa cells) at an IC_{50} of 10 µM (Fu *et al.,* 2008). The significantly cytotoxic emetine displayed the lowest IC_{50} in the panel at 30 nM, again showing similarity to the cidal effects reported in other studies at 40 nM (Grollman and Jarkovsk, 1975). Of the two Arf1 GTPase inhibitors, brefeldin A proved toxic at lower concentrations with an IC_{50} of 0.7 µM compared to Golgicide's 8 µM. Brefeldin A was significantly more toxic against the HeLa cells used in this study when compared with literature values (~ 30 µM in HeLa cells according to Zhang *et al.,* (2012)) while Golgicide was slightly less effective when compared with a study conducted by Saenz (2009) that observed an IC_{50} of 3.3 µM in Vero cells. Finally, treatment with the experimental Arf6 GTPase inhibitor, nav2729, resulted in a 10 µM IC_{50} which is higher than the reported 1.5 µM (Yoo *et al.*, 2016).

2.4.3 – Vitality probe based cytocidal relative speed assays.

Evidence of previous studies using a fluorescence microscopy or a fluorimeter to measure relative drug speeds of cytocidal action coupled with vitality probes could not be found. Therefore, the panel of eight cytotoxic drugs, with varying mechanisms of action, were selected for a pilot assay

using calcein-AM/PI and fluorescence microscopy. This was followed up with a plate-based fluorimetry assay in an attempt to accelerate data acquisition. The latter produced inconsistent fluorescence readouts for PI and Hoechst staining, but calcein-AM produced results that were highly comparable with the microscopy analysis. The plate-based calcein-AM assay may thus be a tractable alternative to assessing relative compound speed of action in mammalian cells which avoids the requirement for fluorescence microscopy sample preparation and analysis. The relative compound speeds found are discussed in relation to their modes of action and relevance for therapeutics research below.

Chaperones, notably heat-shock protein 90 (Hsp90), have become attractive targets for anti-cancer therapy development (Sydor *et al.,* 2006; Yang *et al.,* 2017). This is due to their vital role in folding nascent or denatured cellular proteins and maintaining their functional conformations. This function becomes particularly relevant in cancer cells that are exposed to proteome-damaging cell stress (e.g. hypoxia, nutrient deprivation and rapid growth). Pertinent in this regard is the essential role of Hsp90 in protecting the functional status of oncoproteins involved in tumorigenic signal transduction pathways (Rajabi and Kufe, 2017). Of the eight compounds in the panel, two were Hs90 inhibitors - novobiocin and 17AAG. Originally purified in 1970 from *Streptomyces hygroscopicus* (DeBoer *et al*., 1970), geldanamycin is the prototypical Hsp90 inhibitor. Its main mode of action is to inhibit the ATPase activity of the N-terminal domain of Hsp90 through competitive binding with ATP (Grenert *et al*., 1997; Obermann *et al*., 1998). Additionally, it was found that the drug was capable of myeloma cell growth inhibition via apoptosis signal induction (Jurczyszyn *et al.,* 2014). 17-allyamino-17-demethoxygeldanamycin (17AAG) was the first derivative of geldanamycin to progress to clinical trials for cancer chemotherapy due to its reduced liver toxicity compared to geldanamycin (Neckers and Workman, 2012, Guo *et al*., 2005).

As with geldanamycin, 17AAG inhibits Hsp90 ATPase activity and causes a destabilization of its oncogenic client proteins, for example the AXL receptor tyrosine kinase (Gnana *et al*., 2013). In addition to subverting the ability of Hsp90 to maintain functional client proteins, it has been shown to inhibit the association between Hsp90 and heat shock factor-1 (a transcription factor regulating Hsp expression), resulting in increased transcription of Hsp70 and Hsp40 (Ho *et al.,* 2013). This is relevant since cells may be able to compensate for loss of Hsp90 function by upregulating other chaperones. 17AAG has been used previously in combination with both calcein-AM and PI to assess live/dead cells post drug treatment (Internet 2) which suggest it is compatible with the probes.

Like geldanamycin and 17AAG, virtually all Hsp90 inhibitors target the N-terminal domain ATPase activity. By contrast, novobiocin (an aminocoumarin antibiotic used to treat gram positive bacterial infections) inhibits Hsp90 function by binding to an ATP-binding site at the C-terminus of Hsp90 and disrupting Hsp90 dimerization which is required for Hsp90 function (Marcu *et al*., 2000). It has thus become a model compound for exploring C-terminal domain Hsp90 interaction as a potential approach for cancer therapy. It also causes a reduction in key Hsp90 oncogenic client proteins, *e.g.* the kinase Raf-1 (Marcu *et al*., 2000) and an inhibition of cancer cell viability, *e.g.* the proliferation and migration of human breast cancer cells (Luo *et al*., 2010). The drug has been used extensively in studies coupled with PI as a dead cell marker and effective indicator of novobiocin cidal effects (Luhrmann *et al.,* 1998; Shawna *et al.,* 2010; Wu *et al.,* 2015) as well as with calcein-AM (Lai *et al.,* 2007; Lebedeva *et al.,* 2011) again suggesting compatibility with the probes used in this study.

Under scrutiny of the novel assay, the two Hsp90 inhibitors had little impact on the HeLa cells over the eight-hour time period, and calcein positive/PI negative cell ratios were equivalent to

untreated controls. At 16 hours, 17AAG produced a large increase in PI-positive staining with a corresponding reduction in calcein-positive cells, while novobiocin-treated cells remained unaffected. By 24 hours, novobiocin showed the first signs of cytocidal effects on the HeLa cells, but large numbers of calcein-positive cells remained, while 17AAG produced predominantly PI-positive and correspondingly less calcein-positive cells. This would suggest that the binding of novobiocin to the ATP-binding site in the C-terminus of Hsp90 and disruption of Hsp90 dimerization leads to a less rapid onset of HeLa cell decline than N-terminal inhibition of the ATPase activity of Hsp90 (17AAG).

Overall, novobiocin was observed to be the slowest acting drug in the panel while 17AAG was only moderately faster. This suggests that targeting Hsp90 in HeLa cells results in late onset of cell death compared to other drug targets. One possibility is that it is due to a slow decline in Hsp90 client protein levels after Hsp90 inhibition and partial compensation of the reduced client levels by related proteins. For example, in terms of novobiocin specifically, the drug has been shown to not abolish, but rather diminish the activity of the Hsp90 protein kinase client Raf-1 (Marcu *et al.,* 2000). This may not produce enough of a significant early effect to observe a rapid adverse cellular response. Additionally, there are three RAF-kinases families and gradual loss of functional Raf-1 (a member of the A-RAF family) may result in upregulation of B- and C-RAF kinases to diminish the drug effect (Durrant and Morrison, 2018). Likewise, the Hsp90 client protein AXL receptor tyrosine kinase which is affected by 17AAG treatment (Gnana *et al.,* 2013) belongs to the TAM family of receptor tyrosine kinases which includes Tyro3, AXL and Mer that are overexpressed in several cancer types (Krishnamoorthy *et al.,* 2013). AXL decline may thus be compensated by increased expression of Mer and Tyro3. Another possible reason for the relatively slow manifestation of cell decline by the Hsp90 inhibitors is the notion that Hsp90 ‘buffers’ the cell

proteome against denaturation in the face of stresses that are experienced in *in vivo* tumours (e.g. hypoxia, nutrient depravation, drug and immune action) that may not be relevant in *in vitro* cultures. It would be interesting to determine if simulation of these stressors in cultures enhance the speed of action of the Hsp90 inhibitors.

In addition to Hsp90, Hsp70 is also being explored as a chaperone target for cancer treatment. Included in the panel in this study was the Hsp70 inhibitor VER 155008 which competes with ATP at the nucleotide binding site of Hsp70 (Schlecht, *et al*., 2013) and other members of the Hsp70 family (HSc70 and Grp78) (Ernst *et al*., 2016) and is cytotoxic to cancer cells (Budina-Kolomets *et al*., 2014). It has previously been used in HeLa cells at concentrations similar to this study: 20 µM (Budina-Kolomets *et al*., 2014) and 50 µM (Boroughs *et al*., 2011). VER 155008 was more rapid acting than the Hsp90 inhibitors with several PI-positive cells evident after eight hours and was ranked as the third fastest compound in the panel. This would suggest that Hsp70 is a more attractive drug target over Hsp90 when assessing compounds for rapidity. Hsp90 is more specialized in the client proteins it interacts with and as such a larger number of client proteins rely on Hsp70 and related family members for folding (Saibil, 2013), which might explain the more rapid effect of Hsp70 inhibition on cell viability.

A novel drug target being investigated for cancer treatment is the small GTPase ADP-ribosylation factor 1 (Arf1) (Schlienger *et al.,* 2014). Its most well-explored role is to mediate the formation of COPI vesicles for the trafficking of secretory proteins in the Golgi apparatus (Dodonova *et al.,* 2017). The canonical Arf1 inhibitor is brefeldin A (BFA), a fungal metabolite that inhibits the guanine-nucleotide exchange factor (GEF)-mediated activation of Arf1 and a consequent inhibition of COPI protein transport and a collapse of the Golgi apparatus (Waxse *et al.,* 2017). This results in the inhibition of protein secretion (Misumi *et al*., 1986) and eventual cellular

apoptosis which may be mediated by the formation of reactive oxygen species (Shao *et al*., 1996; Lee *et al*., 2013). BFA and its derivatives have shown an inhibition of cancer cell proliferation *in vitro* and in mouse models (Guo *et al.,* 2017) and has previously been used in cell lines that were visualized using both calcein-AM alone (Sharaf el dein *et al*., 2009) and in conjunction with PI (Deniaud *et al*., 2008). The compound Golgicide was originally identified during a screen for novel small molecules that protected cells from the harmful effects of the Shiga toxin (a potent bacterial toxin found in *Shigella dysentriae* and some strains of *Escherichia coli*) and acts in a manner identical to BFA. It binds to the same site as BFA on Arf1, causing a dissociation of Arf1 and COPI from Golgi membranes and a collapse of secretory traffic through the Golgi (Saenz *et al.,* 2009; Linden *et al.,* 2010). Evidence of Golgicide's use in studies coupled with PI could be found (Ohashi *et al.,* 2011; Naydenov *et al*., 2012), but not with calcein-AM. Given their shared mechanisms of action, it was gratifying to note that they produced an almost identical response in HeLa cells and ranked together in the middle of the panel in terms of speed of action. They thus act as mutual controls to confirm the ability of the assay to distinguish relative speed of action. It can also be hypothesized that the reliance of cancer cells on the transport of newly synthesized secretory proteins to their cellular destinations via the Golgi and loss of this function results in a marked cytocidal effect within 8 hours which is more rapid than Hsp90 inhibition, but not as comprehensive as disruption of protein folding due to Hsp70 inhibition.

While Arf1 GTPase regulates secretory protein trafficking through the Golgi apparatus, Arf6 is involved in the endocytic pathway, mediating the formation of endocytic vesicles and recycling of endocytosed membrane and proteins back to the plasma membrane. In addition, it regulates actin cytoskeleton dynamics and it may also be involved in signal transduction pathways. Oncogenic mutations in two of the G protein-coupled receptors (GPCRs), GNAQ and GNA11, have been

shown to be causative agents in uveal melanoma (O'Hayre et al., 2013) and their discovery has led to the investigation into several downstream signaling pathways that may be attractive drug targets (Yoo *et al.,* 2017). Arf6 is activated by a range of Arf-guanine nucleotide exchange factors (Arf-GEFs) and has been identified as a GPCR signaling effector whereby GPCRs associate with Arf-GEFS to activate Arf6 (Laroche *et al.,* 2007). Arf6 has been shown to be a central mediator in β-catenin signaling as well as endocytosis and recycling of membrane receptors including GPCRs (Chen *et al.,* 2003). Blocking Arf6 with a small inhibitor like nav2729 has reduced uveal melanoma cell proliferation in murine models suggesting a therapeutic strategy for GPCR mediated diseases (Yoo *et al.,* 2017). Using homology modeling and molecular docking studies it was proposed that nav2729 associates with Arf6 in the GEF binding site which subsequently blocked all known downstream signaling pathways of oncogenic GNAQ (including β-catenin signaling) (Yoo *et al.,* 2017). This activity was observed using low micromolar concentrations with IC_{50}'s ranging from 1 – 3.4 µM (Yoo *et al.,* 2017).

In this study nav2729 was observed to be the fastest acting compound in the panel with large scale PI-positive staining, and subsequent dead cells, observed after eight hours of treatment. At 16 hours only residual calcein staining was observed indicating an almost complete HeLa cell population collapse. Arf6 inhibition has been shown to inhibit the downstream signaling pathways of the oncogenic GPCRs leaving potentially none/few alternative pathways with which cellular proliferation can occur in GPCR-mediated tumorigenesis. This blanket inhibition would target the primary point of GPCR signaling responsible for oncogenesis and hence prevent the cascade of signaling pathways e.g. uveal melanoma oncogenesis. In addition to GPCR signaling, there is the dependence of cells on Arf6 to maintain the endocytic pathway for nutrient import and protein recycling/degradation, as well as the role of Arf6 in actin dynamics which may affect cell

attachment and division (Humphreys *et al.*, 2013). As a result, it is perhaps not surprising that nav2729 has such a significantly more rapid killing speed compared to other compounds in the panel.

Of the two well established cytotoxicity standards and apoptosis inducers included in the panel (emetine and etoposide), emetine displayed a rapid speed of cytocidal action which approached that of nav2729. A drug used in the treatment of dysentery and acute amebic hepatitis, emetine has been extensively studied with effective concentrations as low as 0.1 μg/mL (Rogers, 1912). The primary downfall of its use in amebiasis was its relatively high cytotoxicity and subsequent myocardial cellular damage (Rollo, 1975). Emetine is the active compound found in ipecac syrup (used in emergencies involving poisonings and induces vomiting in the patient) and mechanistically has been shown to partially affect DNA synthesis, whereas protein biosynthesis is irreversibly affected post treatment (Grollman, 1968). The latter has been attributed to the binding of emetine to the 40S ribosomal subunit and as such has been used for studies into protein degradation in cells (Jimenez *et al.*, 1977). It was further discovered that emetine causes irreversible inhibition of the rate-limiting step in glycolysis (Combs *et al.*, 1992). Emetine has also been shown to be effective in combatting trophozoite-stage malaria parasites (Hany *et al.*, 2017). Furthermore, the drug has been used in conjunction with calcein-AM across widely varying organisms to assess toxicity, including prostate cancer cell lines (Bamji *et al.*, 2015), while PI has been used to track emetine toxicity in patients with cystic fibrosis (Gelman *et al.*, 2002). It has also recently been used in combination with both PI and calcein-AM in diagnostic double staining assays (Kikuta *et al.*, 2017). Due to its potent cytotoxicity, it is highly cytocidal in HeLa cells at concentrations of 100 nM – 1 μM (Gilead and Becker, 1971) or even lower at 40 nM (Grollman and Jarkovsky, 1975). What aspect of its mechanism contributes most decisively to its relatively

rapid speed of action is not clear, but conceivably both inhibition of protein synthesis and glycolysis are likely to have an almost immediate effect on cell viability.

In contrast to emetine, etoposide was found to be relatively slow acting in the assays and had little to no effect on cell viability at 8 hours of treatment. First synthesized in 1966, etoposide is derived from the podophyllotoxin and was only permitted for use in chemotherapy in 1983 (Hande, 1998). Since then it has been extensively used in various treatments including leukaemias, lymphomas and dense tumors and was the leading prescribed anticancer drug globally until the emergence of the taxanes (Hande, 1998). Mechanistically, it targets DNA topoisomerase II function (Montecucco *et al.*, 2015) and is thought to increase the number of topoisomerase II DNA cleavage sites, thus turning the host's topoisomerase II into its own cellular toxin and resulting in an increasingly disjointed genome (Walker and Nitiss, 2002; Fredholm *et al.*, 2003). It has also been shown to have a high affinity for histones, thus providing evidence that chromatin can also be targeted by the drug (Chamani *et al.*, 2014). With relevance to this study is that etoposide has been used together with PI (Chan *et al.*, 2013) as well as calcein-AM (Sirenk *et al.*, 2015), or with both in a phenotypic assay approach to measure cell viability (Hammerstein *et al.*, 2016).

Since etoposide targets DNA topoisomerase II and possibly chromatin organization, its effects will likely be experienced most acutely during the DNA replication process and cellular proliferation. The doubling time of HeLa cells is approximately 24 hours (Lu *et al.*, 2018) which would result in a delayed onset of cell death and confirms the relative speed of action for etoposide according to the microscopy results. The largest proportion of PI-positive (dead) cells were observed only after 24 hours of etoposide treatment.

2.4.4 – ATP and resazurin-based assays.

Having employed the fluorescent probes in fluorescence microscopy and plate-based formats to rank compounds in terms of relative speeds of cytocidal action, the question arose to what extent the ranking agrees with alternative plate-based assays that could conceptually be employed for this purpose. In contrast to normal cells that generate much of their ATP through oxidative phosphorylation, cancer cells are far less efficient in generating their ATP through aerobic glycolysis – the Warburg effect (Martinez *et al.*, 2018). One theory behind this is that it may to be a strategy to avoid cell death in low oxygen tumour environments, and toxic exposure due to the presence of cytotoxic agents that damage mitochondria (Fadaka *et al.*, 2017). It is well established that intracellular ATP levels are directly related to human cancer cell viability and correlate with drug effects on the number of cells and ATP levels (Ahmann *et al.*, 1987), though, to our knowledge, it has not been employed to compare the speeds of action of compound panels in mammalian cells. In this study, a simple assay was designed to compare ATP levels of drug treated HeLa cell populations after 8-, 16- and 24-hour intervals using an ATP bioluminescence assay kit (a Roche Diagnostics kit was used in this study, but numerous suppliers provide equivalent luciferase-based kits).

Unfortunately, for reasons that are not apparent, results obtained in the ATP-based assay fluctuated across replicates, although novobiocin's relatively slow speed of action and the rapid cytocidal effect of emetine and nav2729 when compared to the rest of drugs in the panel were reproduced. The remaining six drugs in the panel appeared to interchange their killing speed ranking across repeat assays. From this perspective, the use of the fluorescent probes appears to be a more rigorous approach for determining the relative speed of action of compounds against mammalian cells.

Resazurin is a dye that has been extensively used to measure cell viability to determine the cytotoxicity of compounds in mammalian cells (Putnam *et al.,* 2002; Emter and Natsch, 2015; Rodriguez-Corrales and Josan, 2017), as well as other organisms e.g. trypanosomal parasites (De Rycker *et al.,* 2016) and mycobacteria (Kumar *et al.,* 2018). The dye itself is weakly fluorescent and only when reduced in the presence of reductase enzymes in viable cells does it produce a highly fluorescent pink product, resorufin (Csepregi *et al.,* 2018). Therefore, in the presence of toxic compounds, a reduction in cell viability correlates with a diminished conversion of resazurin to resorufin. Often referred to as the Alamar Blue assay, this assay method has been popular as it is cost-effective, reliable, sensitive and non-toxic to the cells themselves (Czenkaska, 2011). While it is normally used to determine the toxicity of compounds (including IC_{50} values, as was done in this study), to our knowledge it has not been employed to compare the speeds of compound cytocidal action. When employed in this fashion in this study by measuring resorufin fluorescence in drug-treated HeLa cell populations after 8, 16 and 24 hours, novobiocin again proved to be the slowest acting compound and nav2729 and emetine the fastest. At the eight-hour time point novobiocin treated cells appeared to produce a slightly elevated RFU in relation to the untreated control sample. This is due to novobiocin appearing to be ineffective (according to this assay) at eight hours and hence simulated a 'healthy' cell sample. As such the RFU appeared like that of the untreated control with a minor fluctuation above control levels due to biological system dynamics.

The assay was highly reproducible and the compound ranking obtained reflected that of the microscopy and calcein-AM plate-based assays, but with one interesting observation: of the slower compounds, the faster speed of 17AAG and etoposide (relative to novobiocin) was only apparent after 16 hours using the fluorescence probes, but was already revealed at 8 hours in the resazurin assay, and the same applied to the speed of VER155008 compared to the moderate compounds

(BFA and Golgicide; this was also observed with the ATP assay). A possible explanation is that the drug pressure and metabolic disruption exerted by the compounds causes a decrease in cell reducing agents (e.g. NADH, NADPH) that can convert resazurin to resorufin before cell membrane integrity is eventually compromised sufficiently to allow access to PI or prevent the accumulation of calcein. The resazurin assay would thus be more sensitive in terms of detecting drug pressure. An interesting question is whether the decrease in reducing capacity detected by resazurin is irreversible (i.e. would inevitably lead to cell death), compared to the membrane disruption detected by the fluorescent probes which likely reflects cells that have been terminally compromised.

2.5 – Conclusion

Calcein-AM and PI were selected as appropriate (and complimentary) fluorescent probes for assessing residual HeLa cell viability after exposure to Gramicidin S and using fluorescence microscopy. Importantly, they were able to rank the speed of action (in terms of how efficacious the compounds were to cause a decline in cell viability) of 8 cytotoxic compounds after only 8 hours of incubation. Of interest was that the speed of action ranking was exactly reproduced by using a plate reader rather than fluorescence microscopy – a considerably faster quantification method – although this was only achieved using calcein-AM (PI yielded erratic results by this approach). Of further interest was that the simple, cost-effective and rapid resazurin assay normally used to assess compound cytotoxicity could also be used to obtain a relative speed of action ranking. Broadly speaking, the ranking obtained agreed with that revealed by the fluorescent probes, except that drug action was detected earlier (e.g. the more rapid action of 17AAG and etoposide vs. novobiocin was already revealed at 8 hours as opposed to 16 hours), possibly due to a decrease in cellular reducing ability occurring before irreversible degradation of membrane

impermeability. Although the ATP assay ranked compounds in same order as that obtained with the resazurin assay, it yielded less reproducible results between technical and biological repeats and is not recommended for speed of action assessments in future assessments. In terms of the compounds used, of the chaperone inhibitors, inhibition at the C-terminal domain (dimerization) of Hsp90 only revealed cytocidal effects at 24 hours (novobiocin), while inhibition of N-terminal Hsp90 ATPase activity (17AAG) had a faster cytocidal action. Inhibition of Hsp70 function (VER155008) had a more profound speed of action, likely indicative of the wider range of client proteins that rely on Hsp70 for folding than Hsp90. Inhibition of Arf1 GTPase function (BFA, Golgicide) already revealed significant reduction of cell viability at 8 hours, which may be diagnostic of the critical reliance of rapidly growing cells on the trafficking of newly synthesized secretory proteins through the Golgi apparatus. More significantly, Arf6 GTPase inhibition (nav2729) had an extremely rapid cytocidal effect. While it is not clear exactly why this may be the case, it could be a result of the pleiotropic functions of Arf6 in endocytosis, actin cytoskeleton dynamics and oncogenic GPCR signaling. Of the two reference cytotoxic compounds, emetine was considerably faster acting than etoposide, likely due to inhibition of glycolysis (on which cancer cells are particularly reliant due to the Warburg effect) and protein synthesis, as opposed to the topoisomerase and histone effects exerted by etoposide which may only become relevant during DNA replication and cell division.

Chapter 3 – A Novel Bioassay to Measure the Relative Killing Speed of Antimalarials using Fluorescent Vitality Probes

3.1 - Introduction

One of the principal reasons for drug resistance and treatment failure is the lack of patient compliance over the full period of therapy. It is therefore necessary to provide a treatment that will act quickly and ideally in a single dose. This points to a need to accurately and quantitatively determine the relative killing speed of novel antimalarials with the priority being to match or exceed the speed of action of artemisinin, the current gold standard in malaria treatment, as stipulated in the TCP-1 requirements.

To complement the gold standard PRR assay with a more rapid and higher throughput method for interrogating compound libraries, this study explored the development of a novel bioassay using fluorescent vitality probes which would allow the relative speed of drug action on malaria parasites to be assessed i) rapidly (in relation to current assay techniques) and ii) in a quantitative manner. This is following on from the work described in Chapter 2 which suggested that PI and calcein-AM were able to robustly and reproducibly distinguish between viable and compromised HeLa cells as well as separate and rank a panel of anticancer compounds according to relative speed of action.

Fluorescence based assays that make use of DNA intercalating dyes have long been used to measure malaria parasite growth susceptibility to drug compounds. They include the PicoGreen, YOYO-1 and, arguably the most common, SYBR Green assays (Bennet *et al.,* 2004; Corbett *et al.,* 2004; Banieckie *et al.,* 2007). These assays are highly sensitive and allow for rapid

quantification and assessment of anti-parasite drug efficacy *in vitro*, but they fail to account for the speed of individual drug action in their described formats. The study described in this chapter evaluated the development of a novel bioassay in which the relative speed of drug action on malaria parasites was assessed in a quantitative manner using fluorescence microscopy in combination with fluorescent vitality probes. Optimizations on this novel assay were then made by i) generating a more rapidly quantifiable bioassay and ii) increasing the throughput using flow cytometry. The assay was conducted on a panel of six well established antimalarials – chloroquine, mefloquine, doxycycline, methylene blue, gramicidin D and artemisinin.

3.2 - Materials and Methods

3.2.1 - Thawing cryopreserved cultures.

Frozen 3D7 strain *P. falciparum* culture glycerol stocks (see section 3.2.4. below) were thawed by hand and the parasite-infected RBC suspensions were transferred to a 15 mL tube. Thawing Solution A (12% [w/v] NaCl in water) was added dropwise under constant agitation to the thawed culture at 0.2x the volume of the RBC suspension. Thawing Solution B (1.8% NaCl in water) was added at 2x the volume of the RBC suspension dropwise and under agitation. After being allowed to stand for 3 min, the suspension was centrifuged at 460 x g for 3 min and the supernatant aspirated off. Fresh, uninfected RBCs (blood type O+) were added to the infected RBC pellet at a ratio of 1:1 and the cells resuspended in 5 mL complete RPMI 1640 culture medium (section 3.2.2) (Rhodes University ethics clearance 2011Q4-1 for using human volunteer donor blood for culturing *P. falciparum*). The freshly prepared, 4 % haematocrit culture was transferred to a T25 solid capped culture flask. The parasitaemia of these freshly thawed starter cultures varied over the range 1 – 10%. The flask was suffused with a special gas mixture (5% CO_2, 5% O_2, 90% N_2), sealed, placed in a 37^{o}C shaking incubator (LM-4000 shaker incubator, Already Enterprises, Taiwan) and agitated at 45 rpm.

3.2.2 - Maintenance of *P. falciparum* 3D7 cultures.

Cultures were maintained according to an adaptation of the procedure by Trager and Jensen (1977) in T75 sealed culture flasks containing an atmosphere of 5% CO_2, 5% O_2, 90% N_2 (special gas mixture supplied by Afrox, South Africa) and agitated at 45 rpm in a 37^{o}C shaking incubator. The complete culture medium used for parasite maintenance consisted of RPMI 1640 medium containing 25 mM HEPES and 2 mM L-glutamine (Lonza), further supplemented with 0.5% (w/v) Albumax II (Thermo Fisher Scientific), 22 mM glucose, 0.65 mM hypoxanthine and 0.05 mg/mL gentamicin. Cultures were routinely maintained at

approximately 3% parasitaemia (percentage of parasite-infected RBCs) and 3% haematocrit (percentage [v/v] of human RBCs in the medium). The RBCs were obtained from blood drawn from volunteer donors in EDTA-containing vacuum tubes (Rhodes University ethical clearance: 2011Q4-1). The whole blood was transferred to a 50 mL tube, centrifuged at 460 x g for 5 min and the serum supernatant and buffy coat layer aspirated off and discarded. The RBC pellet was washed in complete culture medium and stored at 4^{o}C for up to one month. Cultures were removed from the flasks daily and placed in 50 mL tubes for centrifugation at 460 x g. The spent medium was aspirated off and a Giemsa-stained smear on a microscope slide was prepared from the pelleted parasitized RBCs and viewed using a light microscope fitted with a 100x oil-immersion objective. To prepare the slides, a drop of suspended cultured red blood cells was removed from the culture, placed on a microscope slide and a thin blood smear prepared. The smeared blood cells were allowed to air dry on the slide for 10 – 30 seconds, after which the cells were fixed by adding a layer of methanol on the slide for an additional 10 – 30 seconds. The methanol was poured off and the slide covered with a layer of Giemsa solution [a 1:10 dilution of Giemsa stain (Sigma-Aldrich) in phosphate-buffered saline] for 5 minutes. After pouring off the staining solution, the slide was rinsed under running tap water and allowed to air dry before microscopy. The smears were used to assess parasitaemia and quality of parasite morphology. As was required to maintain a healthy cell culture, a portion of the cultured RBC pellet was discarded and replaced with fresh RBCs to adjust the parasitaemia and haematocrit. The RBC pellet was resuspended in 20 mL of fresh culture medium and returned to the T75 flask. The flask was filled with the special gas mixture, sealed and returned to the 37^{o}C shaking incubator.

3.2.3 - Parasite culture synchronization.

To ensure that all parasites in the culture were at the same morphological and metabolic life stage it was necessary to synchronize the culture every two weeks.

All experimentation was conducted using mid- to late-stage trophozoites. As malaria parasite cultures contain a mixture of ring, trophozoite and schizont life stages, it was necessary to treat the culture with sorbitol to induce synchronous development (Lambros and Vanderberg, 1979). Cultured RBCs containing predominantly ring stage parasites were centrifuged at 460 x g for 3 min and the pellet was resuspended in 5% (w/v) sorbitol in water for 5 min at ambient temperature. The parasite-infected RBCs (pRBCs) containing only ring-stage parasites were then pelleted by centrifugation, resuspended in 20 mL of complete RMPI 1640 culture medium and transferred to a T75 flask which was filled with the special gas mixture, sealed and replaced in the 37^{o}C shaking incubator.

3.2.4 - Parasite culture cryopreservation.

To ensure a stable supply of parasites for culture maintenance, frozen culture stocks were prepared on a regular basis. A culture containing predominantly ring-stage parasites was transferred to a 15 mL tube and centrifuged at 460 x g for 3 min. The supernatant was discarded, and the pelleted pRBCs were resuspended by the drop-wise addition of an equal volume of ice-cold culture medium containing 28% (v/v) glycerol, 0.9% (w/v) NaCl and 4.2% (w/v) sorbitol. The suspension was transferred to a 1.5 mL cryotube on ice and the cryotube stored at -80^{o}C.

3.2.5 – Determination of drug IC_{50} values using the Plasmodium lactate dehydrogenase (pLDH) assay.

To obtain dose-response curves for test compounds and drug IC_{50} values, pLDH assays were conducted with a method adapted from Makler *et al.*, (1993). Working solutions (100 µM) made from drug stocks (20 mM - Appendix 7) and a 2% haematocrit, 2% parasitaemia culture containing healthy, trophozoite stage *P. falciparum* 3D7 parasites were used for the assay. Three-fold serial dilutions of the test compounds in complete culture medium were prepared in triplicate wells in a 96-well plate. An equal volume (100 µL) of the parasite culture was added to the wells and the plate was transferred to an air-tight container, gassed using the special gas mixture (5% CO_2; 5% O_2; 90% N_2) and allowed to incubate at 37^oC for 48 hours. Negative (background) control wells contained uninfected RBCs, while positive control wells contained parasite cultures not exposed to drug compounds. After incubation, the cells in the wells were resuspended by pipetting and 20 µl of each sample was transferred to a separate 96-well plate containing 100 µl per well of Malstat solution (55 mM Tris, 0.22 M L-lactic acid, 0.17 mM acetylpyridine adenine dinucleotide [APAD; Sigma-Aldrich], 0.2% [v/v] Triton X-100, pH 9.0). Twenty µl NBT/PES solution (1.96 mM nitrotetrazolium blue chloride, 0.24 mM phenazine ethosulphate) was added to each well and the plate was left in the dark for 10 – 30 min to allow colour development before the absorbance was measured at 620 nm in a Spectramax M3 microplate reader (Molecular Devices). The mean absorbance value obtained in the background control wells was subtracted from all the other absorbance readings and the percentage parasite viability in drug-treated wells calculated relative to the mean absorbance reading obtained for positive control (untreated) wells:

$$\text{Parasite viability (\%)} = \left[\frac{(\text{Avg. absorbance of drug treated samples}) - \text{Avg. absorbance negative control})}{\text{Avg. absorbance postive control}}\right] * 100$$

Dose-response curves were prepared by plotting log[compound] vs. % parasite viability and IC_{50} (50% inhibitory concentration) values determined by non-linear regression analysis using GraphPad Prism (v. 5.02).

3.2.6 – Fluorescent vitality probe analysis of drug-treated *P. falciparum* malaria parasites using fluorescence microscopy.

Synchronised cultures containing trophozoite-stage parasites at 2-5% parasitaemia were used for fluorescent probe analysis. A culture removed from a T75 culture flask was centrifuged at 460 x g for 3 min and the supernatant removed. The pelleted RBCs were resuspended in culture medium to 10% (v/v) and distributed in microfuge tubes (0.5 mL suspension per tube). To simulate compromised parasite viability, gramicidin D was added to pRBC samples to a concentration of 0.1 nM, the tubes were briefly gassed with special gas mixture, sealed and incubated at 37^{o}C in a heating block for 30 min. Control samples were set up in parallel, but without addition of gramicidin D. After incubation, the cells were pelleted, washed once in incomplete medium, resuspended in 0.5 mL complete medium containing vitality probes (as per the concentrations outlined in Table 4 - vitality probe stocks are detailed in Appendix 8), gassed and allowed to incubate at 37^{o}C. Probe concentrations and incubation times were adapted and optimized according to patterns observed in the mammalian cell staining and are provided in Table 4. In cases where more than one probe was used per sample simultaneously, the incubation time was extended to accommodate both.

Table 4: Respective incubation times and final concentrations implemented for each fluorescent probe treatment of *P. falciparum* parasites.

Fluorescent probe	Concentration (µg/mL)	Incubation Time (min)
Propidium Iodide	3.3	15
DAPI	0.7	15
Hydroethidine	1	10
Tetramethylrhodamine	0.05	10
Calcein-AM	1	30

After incubation, the RBCs were pelleted, the supernatants removed, and the cells were washed twice with culture medium (except in the case of calcein-AM, where RBCs were resuspended in saponin (0.1% [w/v] in PBS) to lyse the RBC membranes before pelleting and continuing with washing). After removal of the culture medium supernatant, a small amount of the RBC pellet was transferred to a microscope slide, covered with a coverslip and observed on a ZEISS AxioVert fluorescence microscope fitted with a Zeiss AxioCam MRm monochrome digital camera, using a 100x oil-immersion objective and the UV excitation filter for DAPI, FITC (blue) excitation filter for Calcein-AM and TRITC (green) excitation filter for propidium iodide, tetramethylrhodamine and hydroethidine.

To assess the relative speeds at which a panel of standard antimalarial compounds compromise parasite viability, the above procedure was expanded to include 8-hour incubations with test compounds prior to probe staining and analysis by fluorescence microscopy. Compounds were added to 0.2 mL cultures (2-5% parasitaemia, 10% haematocrit) in microfuge tubes. The compounds were added to final concentrations of 10x their previously determined IC_{50} concentrations (determined in section 3.3.5) as follows: artemisinin – 160 nM; methylene blue – 120 nM; doxycycline – 120 µM; chloroquine – 125 nM; mefloquine – 95 nM. Gramicidin D

was used at 0.1 nM – a suitably parasiticidal concentration previously obtained with the 3D7 strain of *P. falciparum* (Khan *et al.,* 2012). The samples were gassed and placed in a 37^{o}C heating block for eight hours. Post incubation the cells were washed once in culture medium, resuspended in medium containing a mixture of 1 µg/mL calcein-AM, 3.3 µg/mL PI and 0.7 µg/mL DAPI, gassed and allowed to incubate at 37^{o}C for 30 min. Saponin (0.1% [w/v] in PBS) was added to the stained suspensions after which staining solutions were removed by centrifugation. The parasite pellets were washed twice with culture medium and analysed by fluorescence microscopy.

3.2.7 - Flow Cytometry analysis of drug-treated parasites stained with fluorescent vitality probes.

FACS Aria II

In order to ensure all FACS staining events were representative of parasites alone, pRBCs were pelleted and split between two Eppendorf tubes containing complete media. One sample was treated with 1 µg/mL Hoechst33342 (stains nucleic acid irrespective of cellular vitality) for 10 min prior to analysis while the other remained untreated. Analysis was done using a FACS Aria II flow cytometer and gating's were established to isolate pRBCs from other RBCs. After it was established that saponin lysis was required to remove the parasites from the RBCs so as not to encounter the issue of RBCs staining positive with calcein, Hoechst staining was omitted.

Parasite drug incubations were carried out as described in section 3.2.6 above. Fluorescent probe staining with calcein-AM and PI was carried out as per Table 4 after which staining solutions were removed from the parasitized RBCs via centrifugation and the cell pellet washed twice with culture medium. All stained samples were resuspended in saponin (0.1% [w/v] in PBS) to lyse RBC membranes before pelleting the parasites and resuspending them in 0.5 mL culture medium. Samples were transferred to a flow cytometry round bottom test tube before

analysis using a FACS Aria II flow cytometer (Becton Dickinson). The calcein-AM fluorescence was analysed using a 488 nm excitation laser and emission recorded in the 530/30 filter channel, while the 622 nm laser was used to excite PI and emission recorded in the 660/20 filter channel. A total of 100 000 events were recorded for each sample and the data was analysed using FlowJo software (FlowJo, LLC, Ashland, Ore.). Dot plots were generated depicting parasite cell counts as a measure of fluorescent events – PI positive (indicating dead cells) and calcein-AM positive (indicating live cells).

ACCURI™ C6 Plus flow cytometer

To enhance throughput, the flow cytometry analysis was adapted to a multiwell plate format. After drug incubation, independent probe staining with either PI or calcein-AM, saponin lysis and resuspension of the cells in culture medium, samples were transferred to a 96-well, clear plate (0.2 mL per well) and placed in an ACCURI™ C6 Plus flow cytometer (Becton Dickenson) for analysis. The calcein-AM was excited at 488 nm and emission recorded in the 530/30 filter channel, while the 622 nm laser was used to excite PI and emission recorded in the 660/20 filter channel. A total of 100 000 events were recorded for each sample and the data was analysed using Becton Dickinson Accuri C6 Plus (64-bit) software. Dot plots were generated depicting parasite cell counts as a measure of fluorescent events – PI positive (indicating dead cells) and calcein-AM positive (indicating live cells). Sampling was automated via a robotic arm with a shaking procedure implemented between each sample read.

3.2.8 – Calcein-AM analysis of drug-treated parasites using filter tubes and plate fluorimetry.

Trophozoite-stage parasite cultures were treated with test compounds in microfuge tubes as detailed in section 3.2.6. and the pRBCs pelleted by centrifugation in a microfuge. The pellets were resuspended in 0.5 mL PBS containing 1 µg/mL calcein-AM and incubation at 37ºC continued for 30 min. The RBCs were washed twice in PBS and resuspended in 0.5 mL PBS containing 0.3% (w/v) saponin and 0.5% (w/v) BSA to lyse RBC membranes. The lysates were transferred to Spin-X HPLC micro centrifuge filter tubes containing 0.45 µm nylon filters (Sigma-Aldrich). The lysates were allowed to settle for 5 min after which the filter tubes were centrifuged at 1050 x g for 3 min and the filtrate discarded. PBS containing 0.5% (v/v) Triton X-100 (0.5 mL) was added to lyse the parasites trapped on the filters, after which the tubes were again centrifuged 1050 x g for 3 min. The filtrates were transferred to the wells of a 96-well black plate and calcein fluorescence measured in a Spectramax M3 microplate reader (Molecular Devices) using excitation/emission wavelengths of 488 nm and 530 nm, respectively. Controls included in the experiments consisted of background control samples (uninfected RBCs), positive control samples (cultures that were not exposed to drug treatments) and unstained samples.

3.2.9 - ATP Assay.

The assay was adapted from the procedure developed by Khan *et al.*, 2012. Parasite cultures in microfuge tubes were incubated with test compounds for 8 hours as described in section 3.2.6 after which the RBCs were washed in PBS and lysed by resuspension in 0.5 mL PBS containing 0.3% saponin and 0.5% BSA. The lysates were transferred to Spin-X HPLC micro centrifuge filter tubes (0.45 µm nylon filter) and allowed to settle for 5min after which the filter tubes were centrifuged at 1050 x g for 3 min and the filtrate discarded. The parasites trapped

on the filters in the tubes were washed in PBS, after which the filters were placed in fresh microfuge tubes and a 1:1 mixture of PBS and CellTiter-Glo reagent (Promega) was added to the top of each filter. The samples were centrifuged at 1050 x g for 3 min and the filtrates transferred to a white-walled, clear bottom 96-well plate. Luminescence in each well was measured in a Spectramax M3 microplate reader to measure residual parasite-associated ATP.

3.3 – Results

Although the probes selected for use in the development of the vitality assay are predominantly marketed for mammalian cell use, they have all been used to some extent in parasites, although often to quantify parasite numbers after prolonged drug treatment in end-point drug efficacy assays (Hemmer *et al.*, 2005; Esposito *et al*., 2010; Antoine *et al.*, 2013; Collins *et al.*, 2017). In Chapter 2, four vitality probes were assessed for their ability to distinguish between viable and compromised HeLa cells. Using fluorescence microscopy and gramicidin S treatment to compromise cells, it was found that PI and calcein-AM were able to robustly and reproducibly act as suitable vitality indicators whereas TMRE and hydroethidine were unsuccessful. All four probes were, however, assessed for their ability to stain *P. falciparum* 3D7 parasites and to elucidate if the stains were indicative of cellular viability. It was found that, presumably due to morphological and biochemical differences in *P. falciparum* cells, the HeLa cell methods could not be directly applied, but optimization was required with regards to probe concentration and treatment period to achieve reliable staining methods.

Briefly, parasite cultures of between 2-5% parasitaemia were pelleted and resuspended to 10% (v/v) parasitized RBC solutions in complete culture medium staining with vitality probes using concentrations and incubation times as per Table 4 (section 3.2.6). A small volume of the pRBC pellet was transferred to a microscope slide under a coverslip and observed on a ZEISS AxioVert fluorescence microscope. In instances where it was necessary to simulate compromised cellular vitality (to control for a drug-treated culture), respective samples were incubated with 0.1 nM gramicidin D for 45 min prior to staining.

3.3.1 - Calcein-AM.

Calcein-AM was observed to readily enter and be retained by healthy parasites. In contrast, membrane compromised parasites (post gramicidin D treatment) were unable to retain the probe and hence exhibited no fluorescence. Staining patterns covered the entirety of the parasite cytoplasm, excluding only the food vacuole (Fig. 23) and DAPI fluorescence intensity in parasite nuclei remained equal in both untreated and drug treated test samples. The calcein-AM concentration that yielded prominent parasite staining (1 µg/mL) was 5 times lower than that required for HeLa cells.

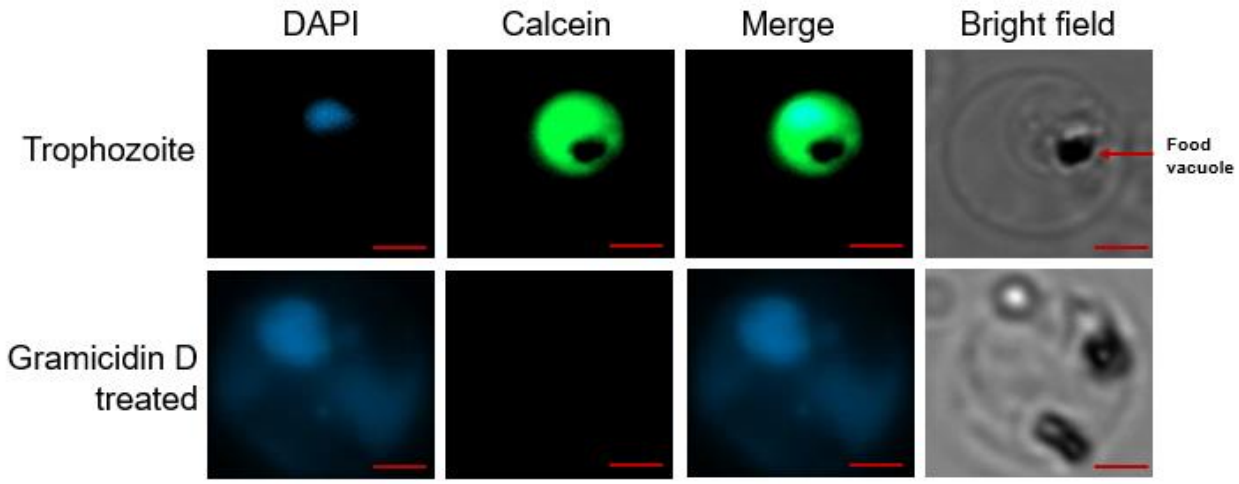

Figure 23: Fluorescence microscopy of calcein-stained control and gramicidin D treated parasites. An untreated control *P. falciparum* trophozoite-stage culture as well as a culture exposed to a 45 min treatment with 0.1 nM gramicidin D was stained for 30 min with calcein-AM (1 µg/mL) and DAPI (0.7 µg/mL), washed and viewed with a Zeiss AxioVert fluorescence microscope. The dark, unstained region in the trophozoite stage parasites represent the food vacuole, as denoted by the prominent haemozoin crystal in the bright field image, while the DAPI staining indicates the parasite nuclei. Scale bars represent 2 µm.

It was further observed that the calcein-AM staining was not always limited to the parasite, but instead was also found in the cytoplasm of infected and uninfected RBCs. Calcein-AM staining of a sample of uninfected RBCs yielded RBCs with the acetoxymethyl ester being cleaved in the cytoplasm and resultant large-scale fluorescent calcein in the RBC cytoplasm (Fig. 24A).

This staining pattern was similar in infected RBCs. Fig. 24B is a magnified image of a trophozoite-infected RBC with calcein fluorescence across the entirety of the RBC cytoplasm and a slightly more intensely stained trophozoite parasite. This has the potential for users to mistakenly classify an RBC as a healthy parasite and hence adds a misleading element. In addition, any fluorescence measurements using a flow cytometer or plate reader could deduce a signal from an RBC as a false positive parasite signal. Therefore, an additional saponin lysis step was included in the calcein-AM procedure to remove the variable of RBC staining (saponin is a detergent capable of selectively lysing RBC membranes, leaving parasites intact). Intact trophozoite-stage cultures were stained with calcein-AM (1 µg/mL) as normal, before the addition of 0.1% saponin in PBS for 5 min and centrifugation to remove the RBC lysate and leave a parasite pellet. With the inclusion of saponin treatment after staining and visualization, parasites were observed to retain the calcein-AM probe while the RBCs were disrupted to a significant enough extent that their fluorescence was eliminated (Fig. 24C).

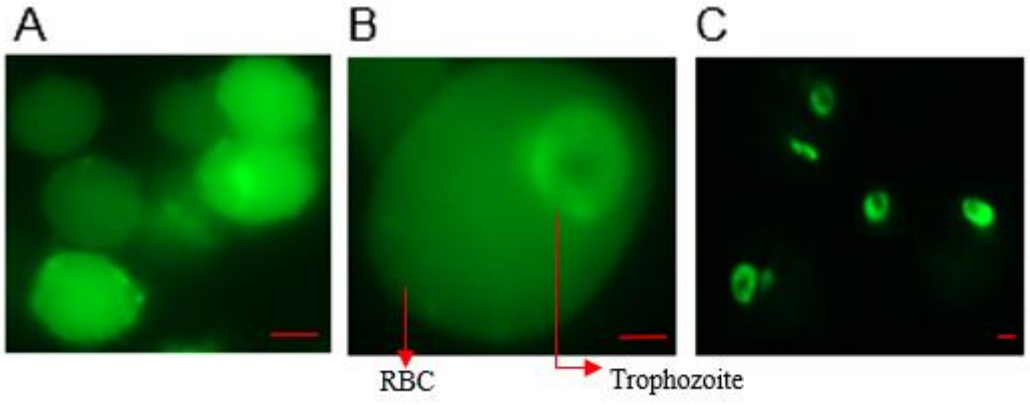

Figure 24: Fluorescence microscopy of calcein-stained RBCs and saponin-treated trophozoites. Calcein-AM (1 µg/mL) was used to stain uninfected RBCs (A), trophozoite-infected RBCs (B) and trophozoite-infected RBCs treated with 0.1% saponin to lyse RBC membranes (C). Scale bars represent 5 µm, 1 µm and 1 µm in A, B and C, respectively.

3.3.2 - Propidium Iodide.

In contrast to the calcein-AM staining pattern, PI fluorescence was only observed once parasite membrane integrity was sufficiently compromised. This required substantial optimization to obtain a gramicidin D concentration that provided sufficient impact on the cell membrane to observe a PI signal, while maintaining enough structural integrity such that the signal was retained long enough to provide satisfactory fluorescence images and the parasites were still morphologically intact and distinguishable under bright field (Fig. 25).

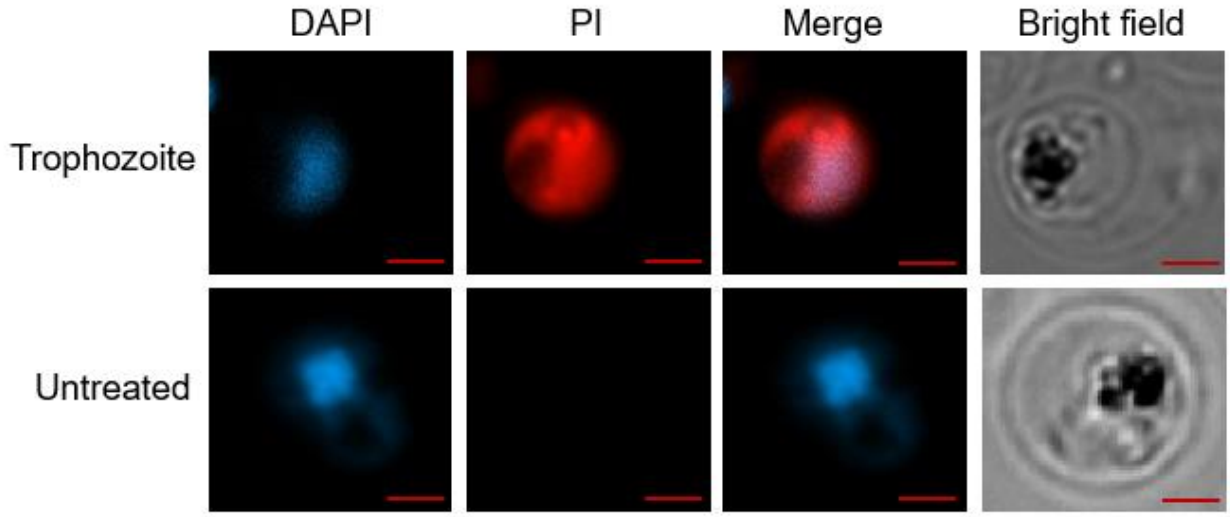

Figure 25: Fluorescence microscopy of propidium iodide-stained gramicidin D-treated and untreated control parasites. *P. falciparum* trophozoite-stage parasites were left untreated (bottom panel) or treated for 45 min with 0.1 nM gramicidin D (top panel) prior to a 15 min incubation with PI (3.3 µg/mL) and DAPI (0.7 µg/mL). After staining, cells were washed and viewed with a Zeiss AxioVert fluorescence microscope. Scale bars represent 2 µm.

A significantly lower concentration of PI was required for suitable parasite staining (3.3 µg/mL) compared to mammalian cell staining (20 µg/mL). This was similar to what was observed when moving from mammalian cell staining to parasites using calcein-AM. Consistent with what was found with mammalian cells, no PI was observed in healthy, untreated parasites (or RBCs), while significant PI accumulation was seen in gramicidin D treated trophozoites and schizonts (Fig. 25). Peculiarly, unlike mammalian cells, PI staining

was not only limited to the parasite nucleus (denoted by DAPI staining) but found throughout the parasite cytoplasm.

An interesting observation was that PI appeared to stain the matrix of healthy merozoites, the small invasive stages of the parasite that rupture from infected RBCs following completion of the parasite life cycle, whereas calcein-AM was not retained in these cells (Fig. 26). This could provide false positives for nonviable parasites. In probing viable vs. nonviable parasites using PI and/or calcein-AM staining, care should thus be taken not to include merozoites in the analysis. Note that the cells shown in the micrographs were untreated with gramicidin.

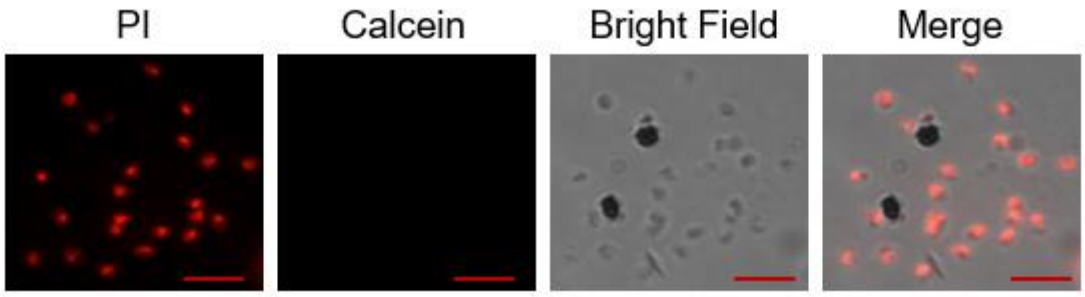

Figure 26: Fluorescence microscopy of PI and calcein-stained merozoites. staining of merozoite-stage *P. falciparum* 3D7 parasites. Parasites were allowed to grow past the trophozoite and schizont life stages in normal culture conditions and then pelleted, stained with PI (3.3 µg/mL) and calcein-AM (1 µg/mL) and observed with a Zeiss AxioVert fluorescence microscope. The image shows free-floating merozoites, positive for PI, and two dark hemozoin crystal remnants of schizonts that had completed merozoite formation and release. Scale bar represents 5 µm.

3.3.3 – TMRE.

TMRE was able to cross the membranes of healthy malaria parasites, however the probe was not seen to localize to the parasite mitochondria as was anticipated. As with mammalian cells, the probe appeared to be located throughout the cell cytoplasm and showed consistent fluorescence intensity across the parasite (except for the dark region occupied by the haemozoin crystal in the food vacuole; Fig. 27). Drug treatment with gramicidin D did not provide any change in staining patterns compared to healthy parasites (Fig. 27). Thus, unlike PI and calcein-AM, TMRE did not distinguish between gramicidin D treated and untreated parasites - both had similar staining patterns (a trend that was also observed in HeLa cells). Due to this consideration, it was decided to no longer continue pursuing TMRE as a suitable fluorescent vitality probe.

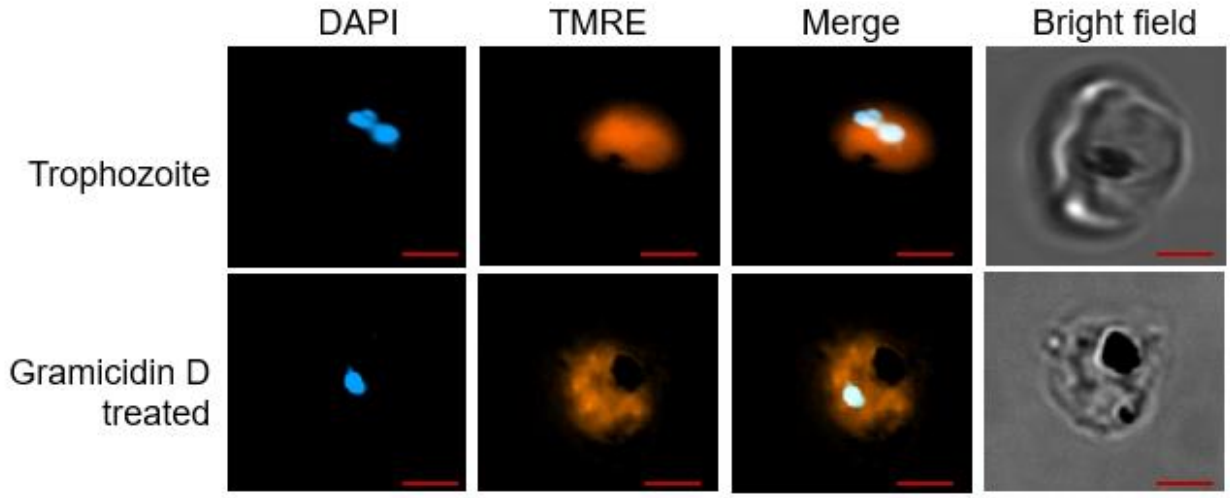

Figure 27: Fluorescence microscopy of TMRE-stained control and gramicidin D-treated parasites. Cultures of *P. falciparum* trophozoite-stage parasites were left untreated (top panel) or incubated with gramicidin D (0.1 nM) for 45 min, followed by staining for 10 min with TMRE (0.05 µg/mL) and DAPI (0.7 µg/mL). Cells were washed and viewed with a Zeiss AxioVert fluorescence microscope. Scale bars represent 2 µm.

3.3.4 – Hydroethidine.

Hydroethidine provided results similar to those observed in HeLa cells (with the exception that DAPI appeared unable to stain the nuclei of viable HeLa cells – in parasites, DAPI-staining was found in the nuclei of untreated and treated parasites in equal proportions). Hydroethidine fluorescence was not affected in either drug treated or healthy HeLa cells. In the *P. falciparum* parasites, hydroethidine staining was shown to extend beyond the nucleus into the parasite cytoplasm (Fig. 28). As found with HeLa cells, there was no decrease in fluorescence in the parasites after gramicidin D treatment (Fig. 28). The concentration of the probe was altered systematically, as well as the incubation temperature and time, however no change in staining pattern was noted between drug treated and healthy populations. Further assays were conducted with hydroethidine concentrations ranging from 3 to 6 µg/mL but failed to yield differential staining. Hence hydroethidine was discarded as a suitable vitality probe for use in this study.

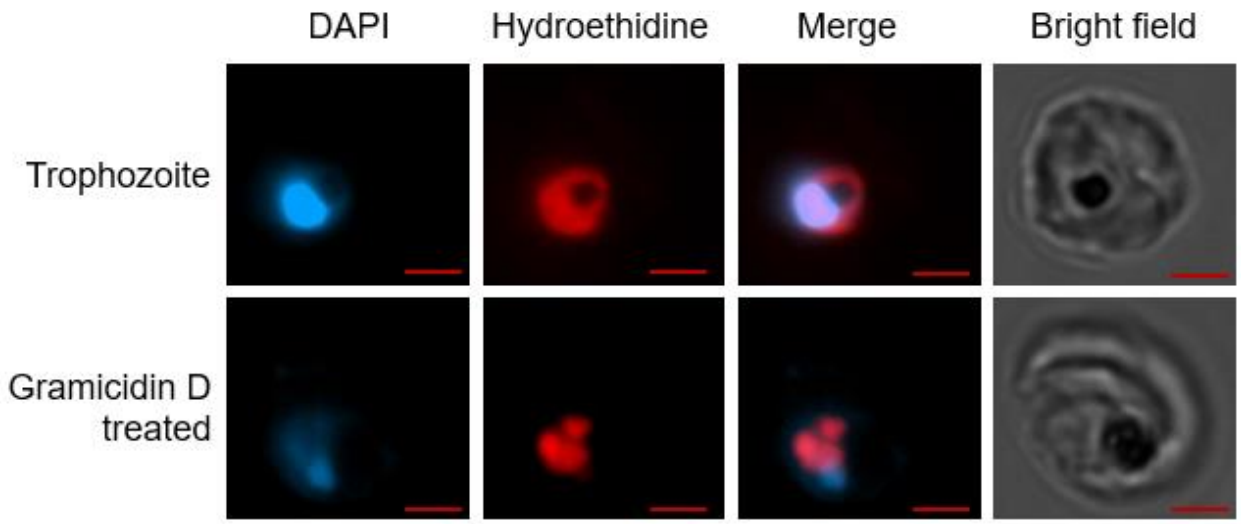

Figure 28: Fluorescence microscopy of hydroethidine-stained control and gramicidin D-treated parasites. Control (top panel) *P. falciparum* parasites and parasites exposed to 0.1 nM gramicidin D for 45 min were stained with hydroethidine (1 µg/mL) and DAPI (0.7 µg/mL) for 10 min, followed by washing and viewing with a Zeiss AxioVert fluorescence microscope. Scale bars represent 2 µM.

3.3.5 - Drug IC_{50} values using the Plasmodium lactate dehydrogenase (pLDH) assay.

Having established that calcein-AM and PI were promising probes for distinguishing viable/non-viable parasites (while TMRE and hydroethidine were not) using gramicidin D as a model parasite compromising agent, the next step was to determine whether use of the probes could be extended to other conventional antimalarial drugs. Before the fluorescent vitality assay could be conducted on currently used antimalarials, it was necessary to confirm their efficacy against the lab strain of *P. falciparum* 3D7 parasites and to obtain a guideline of the concentrations to be used in subsequent experiments. Drug concentrations resulting in 50% parasite cytotoxicity (IC_{50}) were determined using the Plasmodium lactate dehydrogenase (pLDH) cytotoxicity assay, which measures pLDH activity as a surrogate indicator of the numbers of parasites that survive drug treatment. The assay involves the pLDH-mediated conversion of APAD to APADH which subsequently reduces nitro blue tetrazolium to a formazan product which can be measured spectrophotometrically.

Parasite cultures (2% haematocrit, 2% parasitaemia) were incubated in 96-well plates with serial dilutions of the drug compounds chloroquine, mefloquine, artemisinin, doxycycline and methylene blue. Control solutions encompassed a negative control of unparasitized RBCs and a positive control of untreated, parasitized RBCs. After a 48-hour incubation, pLDH activity in individual wells was measured to enumerate surviving parasites, as detailed in section 3.2.7. The IC_{50} values for the individual drugs were calculated from dose-response curves obtained in triplicate (Fig. 29) and tabulated (Table 5).

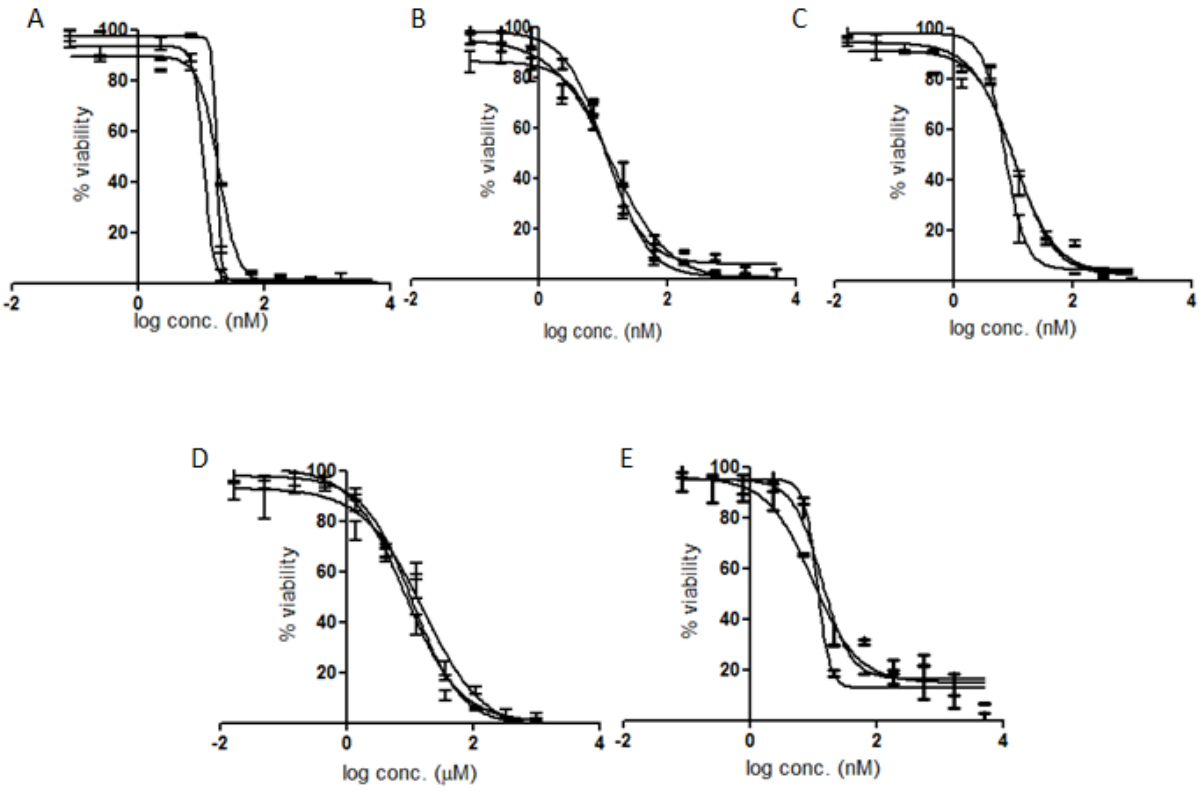

Figure 29: Dose-response curves of the five *P. falciparum* 3D7 antimalarial drug compounds used in the study. pLDH assays were performed on three independent biological samples in technical triplicate and dose-response curves plotted using GraphPad Prism v5.02. Errror bars indicate standard deviation of individual data points. A: Artemisinin; B: Chloroquine; C: Mefloquine; D: Doxycycline; E: Methylene blue.

Table 5: Experimental IC_{50} values of the five test compounds obtained in pLDH assays, compared to cited literature values.

Drug	**IC_{50}**	**Reference IC_{50}**
Artemisinin	16 nM	24 nM (Walcourt *et al.*, 2008)
Chloroquine	12 nM	14 nM (Moneriz *et al.*, 2011)
Mefloquine	9 nM	12 nM (Wisedpanichkii *et al.*, 2009)
Doxycycline	12 µM	11 µM (Fall *et al.*, 2011)
Methylene Blue	12 nM	2 nM (Okombo *et al.*, 2012)

The panel of drugs tested against the laboratory strain of 3D7 malaria parasite all gave similar IC_{50}s with doxycycline being the exception. Artemisinin's growth response curve (Fig. 29A) resulted in an IC_{50} of 16 nM (Table 5) which deviates only slightly from a cited literature value of 24 nM (Walcourt *et al.*, 2008). The two quinolines, chloroquine and mefloquine, provided IC_{50}'s of 12 and 9 nM (Table 5) which again agreed with previous studies at 14 nM (Moneriz *et al.*, 2011) and 12 nM (Wisedpanichkii *et al.*, 2009) respectively. In contrast to literature, the IC_{50} for methylene blue was higher at 12 nM as opposed to only 2 nM reported by Okombo *et al.*, 2012, while doxycycline provided an IC_{50} of 12 µM relating well to a published value of 11 µM (Fall *et al.*, 2011) (Table 5).

3.3.6 – Relative killing speed assay on panel of antimalarials using vitality probes.

With the calcein-AM and PI probes proving to work efficiently as vitality indicators in both HeLa cells and malaria parasites, a pilot relative killing speed assay was developed combining the probes with six well established antimalarials selected as test compounds to observe the staining patterns in parasites after an eight-hour drug treatment period. These patterns could then be quantitatively analyzed using a simple 'cell count' approach on a fluorescence microscope to provide an indication of the relative speed-of-action of each drug.

Briefly, an early stage trophozoite parasite culture was treated independently with the test compounds at 10-fold IC_{50} concentration and incubated at 5% CO_2, 5% O_2, 90% N_2 at 37^{o}C for eight hours. The cells were then incubated in calcein-AM and PI co-staining solutions at 37^{o}C for 30 min after which RBC membranes were lysed with saponin (to prevent calcein-AM staining of uninfected RBCs) and excess probe was washed off. A sample of the stained pellet was transferred to a microscope slide, wet-mounted under a coverslip and observed on a ZEISS AxioVert fluorescence microscope.

Upon eight hours incubation, it was observed that there was a clear decrease in the proportion of calcein-AM positive parasites with a corresponding increase in PI positive parasites when comparing slower vs. faster acting drugs (Fig. 30). The largest proportion of calcein-AM fluorescent (viable) parasites was observed in the doxycycline treated sample through to artemisinin which had the largest number of PI fluorescent (non-viable) parasites. Importantly, PI and calcein-AM fluorescence showed no co-localization and instead probed only dead and live cells, respectively. These patterns were compared to untreated, healthy parasites and gramicidin D treated parasites which acted as positive (viable) and negative (nonviable) controls, respectively. The positive control simulated optimal growth conditions over the eight-hour period, and this was evident in the large number of calcein-AM positive cells (Fig. 30,

untreated). The PI staining observed in the untreated sample comprised only 2% of the total parasite population and can be attributed to the occasional occurrence of nonviable parasites in normal cultures. The untreated control appeared similar to the staining patterns observed in the doxycycline treated sample, suggesting that the latter is the slowest acting drug.

In contrast, the gramicidin D-treated control was used to provide an indication of fluorescent patterns in a severely compromised parasite culture. The image shown in Fig. 30 (gramicidin D treated) is representative of what was observed in all fields of the treated sample - significant PI staining of all discernible parasites and minor calcein-AM staining fragments or RBC artefacts (occasional ‘ghosts’ that survived saponin treatment). The percent of viable parasites reached a maximum of 2% across all fields and hence provided insight into what to expect from a drug with rapid, potent efficacy. The staining pattern of the gramicidin-treated sample most closely resembled that obtained for the artemisinin sample.

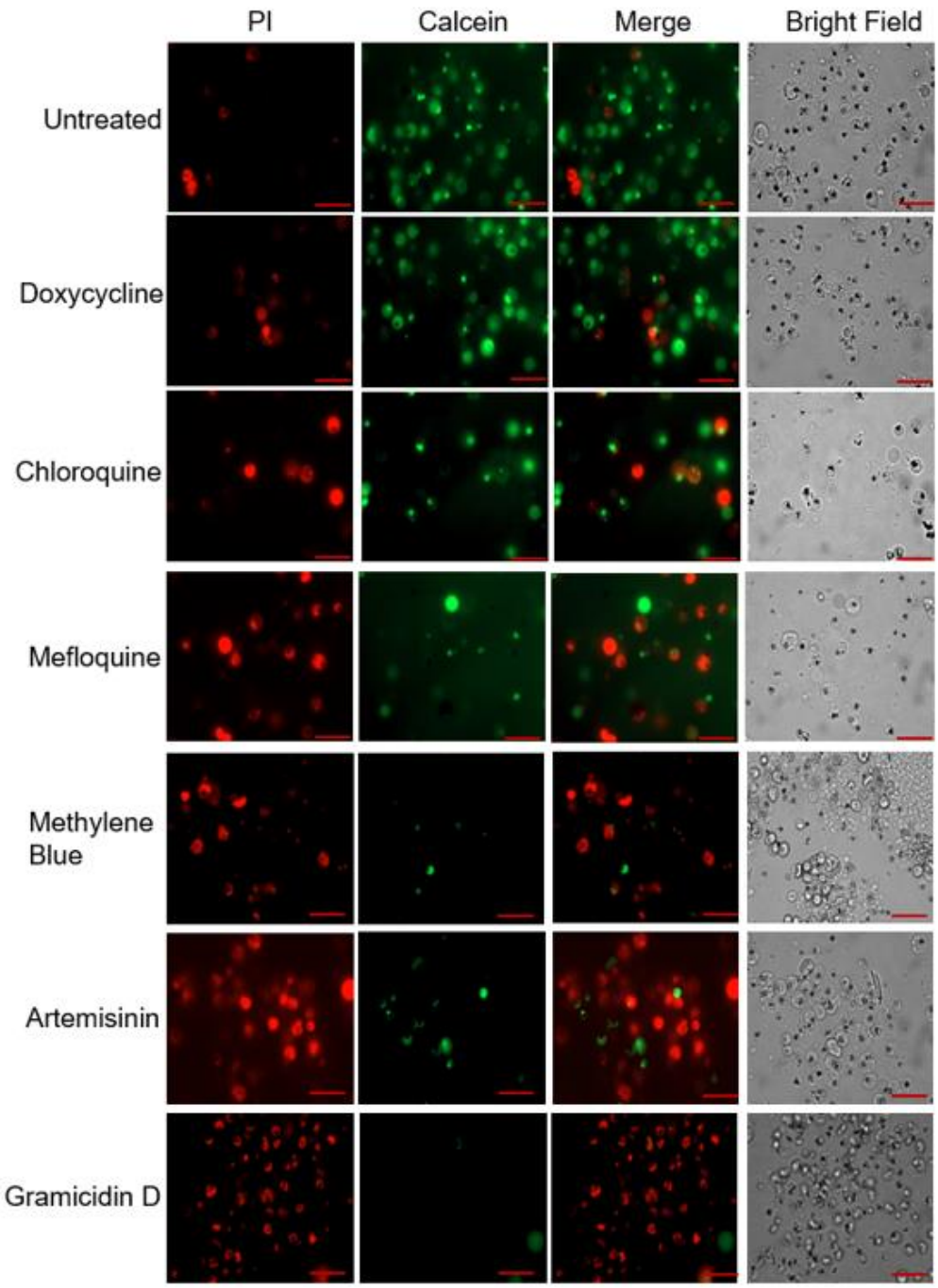

Figure 30: Dual probe staining of *P. falciparum* 3D7 parasites using PI (3.3 µg/mL) and calcein-AM (1 µg/mL). Parasites were untreated or treated for eight hours with doxycycline (100 µM), chloroquine (120 nM), mefloquine (90 nM) artemisinin (150 nM), methylene blue (120 nM) and gramicidin D (0.1 nM) respectively, after which they were stained with PI and calcein-AM, treated with saponin to lyse RBCs, washed and viewed by fluorescence microscopy on a ZEISS AxioVert fluorescence microscope. Scale bars represent 5 µm.

The total number of parasites per field was enumerated using ImageJ v1.49 and the Cell Counter plugin. Total parasites were defined as the sum of both green fluorescent (calcein-AM

positive, viable) and red fluorescent (PI positive, nonviable) cells. The ratio of green fluorescent cells (viable) to total parasite cell count was then calculated as a percentage, averaged from five distinct fields of view (Fig. 31).

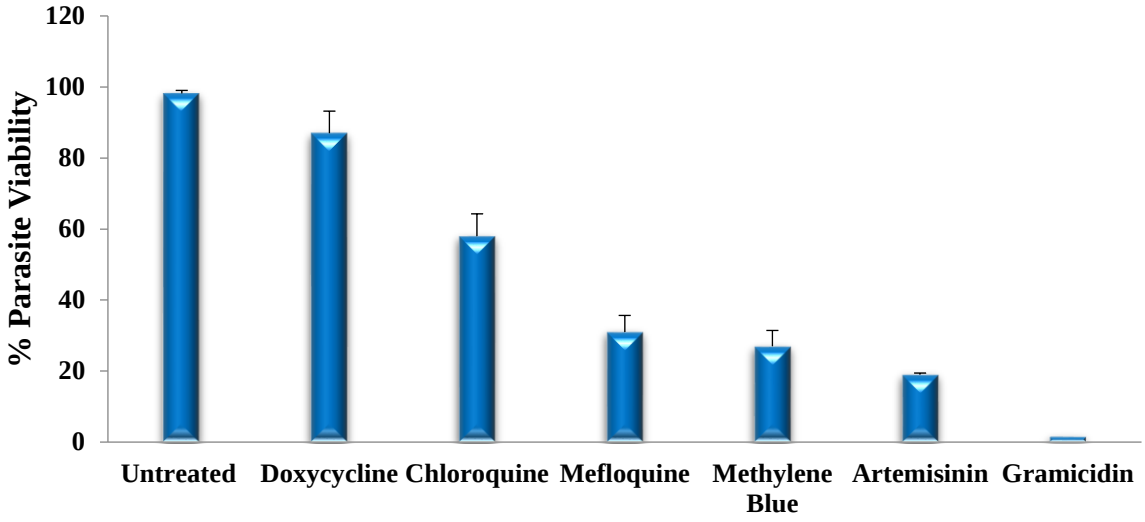

Figure 31: Speed of drug action for each test compound represented as percentage viable parasites visualized by fluorescence microscopy after an 8-hour drug treatment. Early trophozoite stage parasites were treated with doxycycline (100 µM), chloroquine (120 nM), mefloquine (90 nM), methylene blue (120 nM) and artemisinin (150 nM) for 8 hours, stained with calcein-AM and PI, the RBCs lysed with saponin and images of the parasites captured with a Zeiss AxioVert fluorescence microscope. The mean percentage parasite viability ± standard deviation across five fields was calculated as the ratio of (calcein positive parasite)/ (calcein positive + PI positive parasites) x 100 using ImageJ v1.49 and the Cell Counter plugin (De Vos, Academic Neurology, University of Sheffield).

Doxycycline, a member of the tetracycline antibiotic group, was observed to have been the least efficacious over 8 hours by a considerable margin in relation to the other test compounds, yielding only 11% nonviable (PI positive, calcein negative) parasites compared to the untreated control sample which contained 2% PI positives. It is thus evident that doxycycline has limited impact on the parasite population in an 8-hour period. With a mean parasite viability of 58%, chloroquine treatment resulted in more than half of the parasite population still maintaining calcein staining and recalcitrant to PI after the 8-hour period. Removal of the drug at this stage would suggest that some parasites would survive to replicate and maintain the infection. As a

member of the quinoline family it may have been expected that mefloquine would have a similar mechanism and similar killing speed to chloroquine. In this study it was found that mefloquine had a greater impact in relation to chloroquine with only 31% of parasites remaining viable after eight hours. In comparison to chloroquine, mefloquine was thus approximately twice as effective in the same period. Methylene blue shared a killing speed similar to mefloquine with 27% of the parasite population remaining viable, while the most effective drug was artemisinin with a substantial loss of 81% parasite viability after eight hours.

3.3.7 – Improved quantification with flow cytometry.

The pilot relative killing speed assay was able to quantitatively distinguish and rank a panel of well-established antimalarial compounds based on their speeds of action. However, quantification involved collecting images of stained parasites and counting viable/non-viable parasite numbers using ImageJ software. Therefore, to i) increase throughput and ii) simplify quantification, the novel assay was adapted for use in a flow cytometer using the same fluorescent vitality probes used in the microscopy study – calcein-AM and PI.

Before commencing with the analysis of drug-treated cultures, a gating experiment was carried out to distinguish between infected and uninfected RBCs in the samples. Briefly, a parasite culture of 5% parasitaemia was pelleted and split between two Eppendorf tubes containing complete media. One sample was treated with 1 µg/mL Hoechst 33342 for 10 min prior to analysis while the other remained untreated. Analysis was done using a FACS Aria II flow cytometer (Fig. 32). Hoechst was used as it is not dependent on cellular vitality and hence is able to stain any nucleic acid present. Upon the inclusion of Hoechst, a large increase in DNA stained, pRBCs emerged from the population (demarcated by the black outline in Fig. 32), thus segregating the total cell population into infected and uninfected cells.

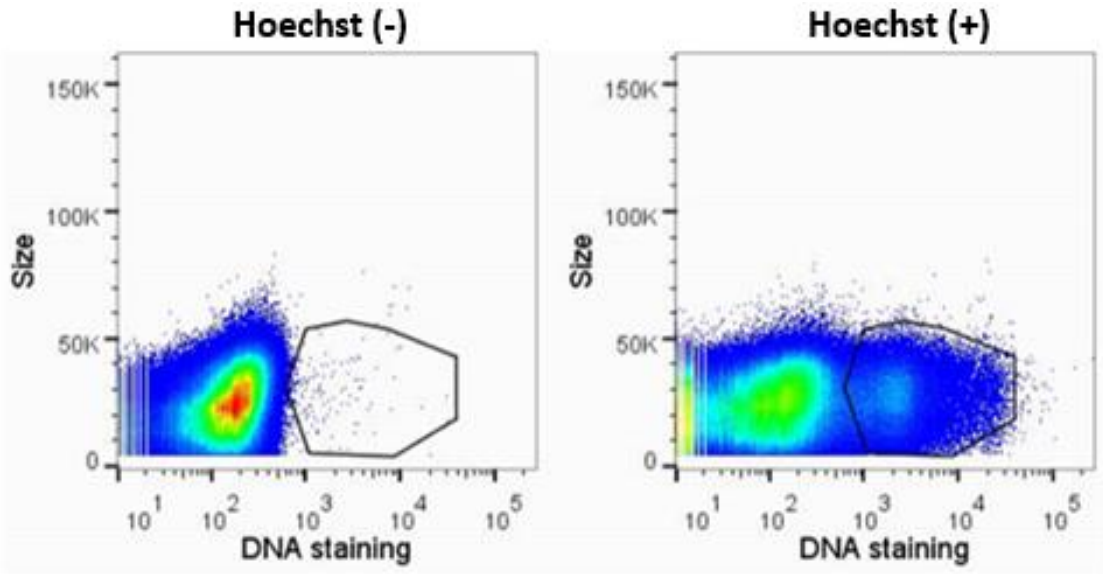

Figure 32: Flow cytometric dot plot of Hoechst (1 µg/mL, 10 min) stained pRBCs and RBCs. The gating (indicated by the black outline) depicts the pRBC population which emerges using the Hoechst DNA stain. The X-axis represents Hoechst fluorescence intensity and the Y-axis represents cell size. Analysed using FlowJo software (FlowJo, LLC, Ashland, Ore.).

Hoechst 33342 was included as a stain in subsequent experiments where analysis was conducted using the FACS Aria II. As such, all cells counted in further experiments using the FACS Aria II flow cytometer were only recorded if they fell within the pRBC gate in order to exclude the contribution of uninfected RBCs in the viable/non-viable parasite analyses.

A subsequent experiment was carried out to assess the ability of the flow cytometer to detect parasites stained with PI or calcein-AM and ensure the probes were able to distinguish between viable and nonviable cell populations using flow cytometry, as previously recorded with fluorescence microscopy. Parasite cultures were left untreated or treated by the addition of gramicidin D (0.1 nM, 45 min), followed by co-staining with PI (3.3 µg/mL), calcein-AM (1 µg/mL) and Hoechst 33342 (1 µg/mL) and analysis in a FACS Aria II flow cytometer (Fig. 33).

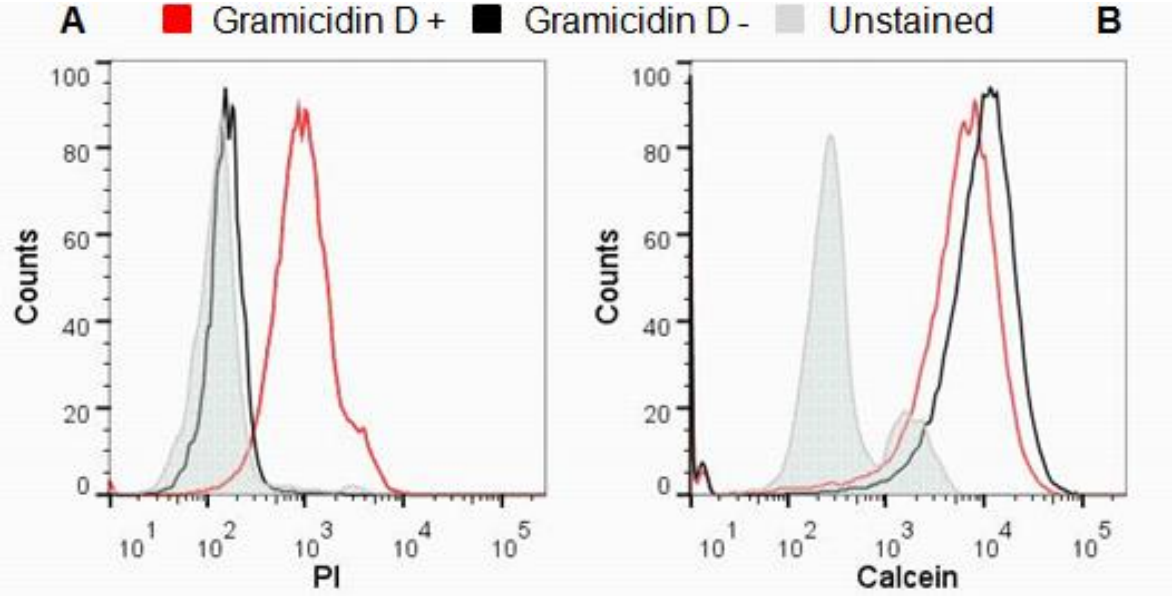

Figure 33: Flow cytometry histograms of gramicidin D (0.1 nM) treated pRBCs stained with PI (3.3 µg/mL) (A) and calcein-AM (1 µg/mL) (B). Treated samples are compared to unstained and untreated (Gramicidin D negative) control cultures. X-axis represents PI or calcein-AM fluorescence intensity and y-axis represents cell count.

Gramicidin D treated cells in panel A showed a significant increase in PI staining in relation to untreated and unstained controls, which is consistent with the PI staining of compromised parasites seen by fluorescence microscopy in previous experiments. In contrast, calcein-AM positive cells (panel B) show only a minor decrease in fluorescence intensity in the gramicidin D treated populations (in relation to the untreated control sample). This could have been attributable to calcein-AM being able to stain the matrix of the RBCs and hence provide false positives for healthy parasite cells, as was found in the fluorescence microscopy experiments (Fig. 24). This confirmed the necessity to remove the cytoplasm of RBCs in the sample by lysing RBC membranes using saponin prior to identifying live vs. dead parasite populations in calcein-AM stained samples. A saponin lysis step was thus included in subsequent experiments.

The microscopy relative killing speed assay was optimized for use in a flow cytometer by making use of the same set of standard antimalarial compounds. Hence, parasite cultures were

treated with artemisinin, chloroquine, doxycycline, methylene blue and mefloquine for eight hours, co-stained with PI, calcein-AM and Hoechst 33342, saponin treated and analyzed to gauge the change in staining patterns of PI and calcein-AM. A general trend of an increase in PI staining could be observed in cultures treated with the respective compounds (Fig. 34).

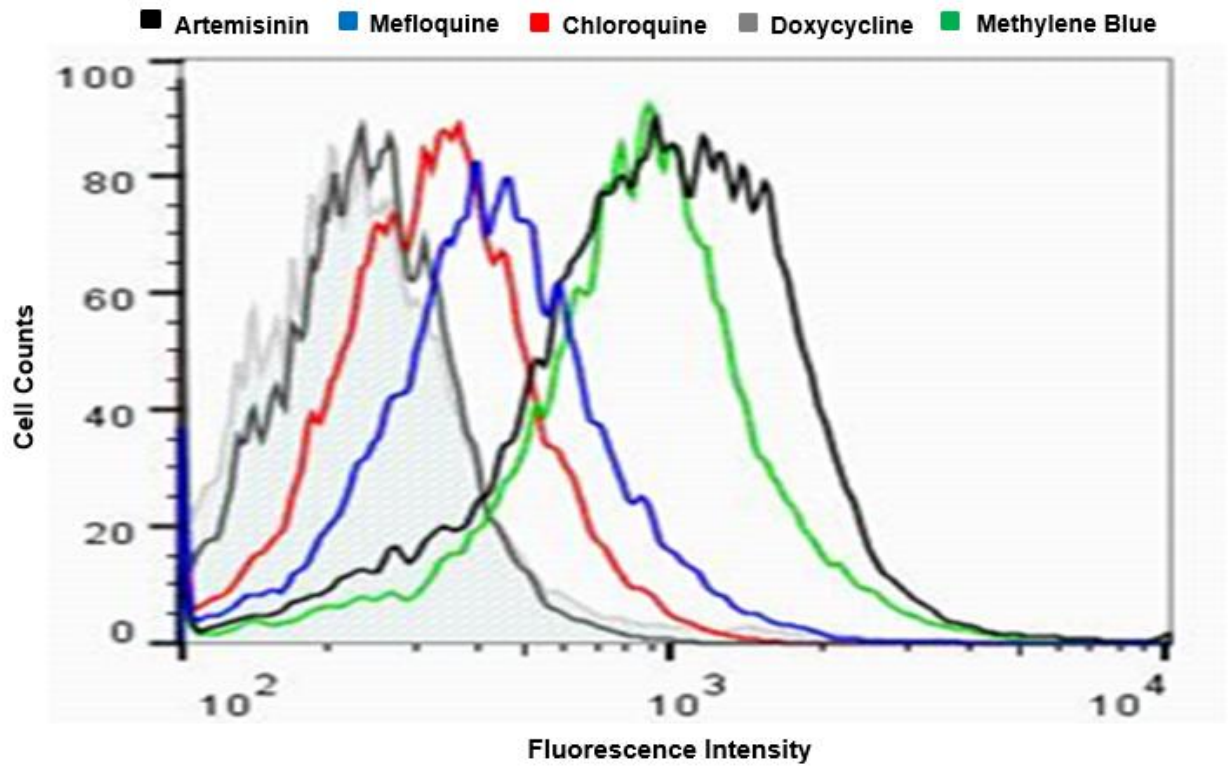

Figure 34: Flow cytometry histogram comparison of the model antimalarial drugs and their relative killing speeds, measured as PI positive events after an eight-hour treatment. Parasite cultures were treated with doxycycline (100 µM), chloroquine (120 nM), mefloquine (90 nM) artemisinin (150 nM) and methylene blue (120 nM) respectively. After eight hours, cultures were stained with PI (3.3 µg/mL), RBC membranes lysed with saponin and samples analysed using a FACS Aria II flow cytometer and FlowJo software (FlowJo, LLC, Ashland, Ore.). The shaded peak represents untreated parasites.

After eight hours of treatment, there was an increase in the PI signal received from the artemisinin treated sample (as expected from the quickest acting drug) which was closely followed by methylene blue. A similar staining trend was observed for chloroquine and mefloquine, with mefloquine showing a slightly greater signal at the 8-hour mark. Finally, as

anticipated, doxycycline showed very little antimalarial activity, with the PI staining intensity matching that of the untreated control.

Similarly, calcein-AM staining patterns were assessed and showed a similar trend to that of PI, albeit in reciprocal fashion. A general trend of a decrease in calcein-AM staining could be observed in treated parasites (Fig. 35) as a direct result of the killing speed of each drug in question.

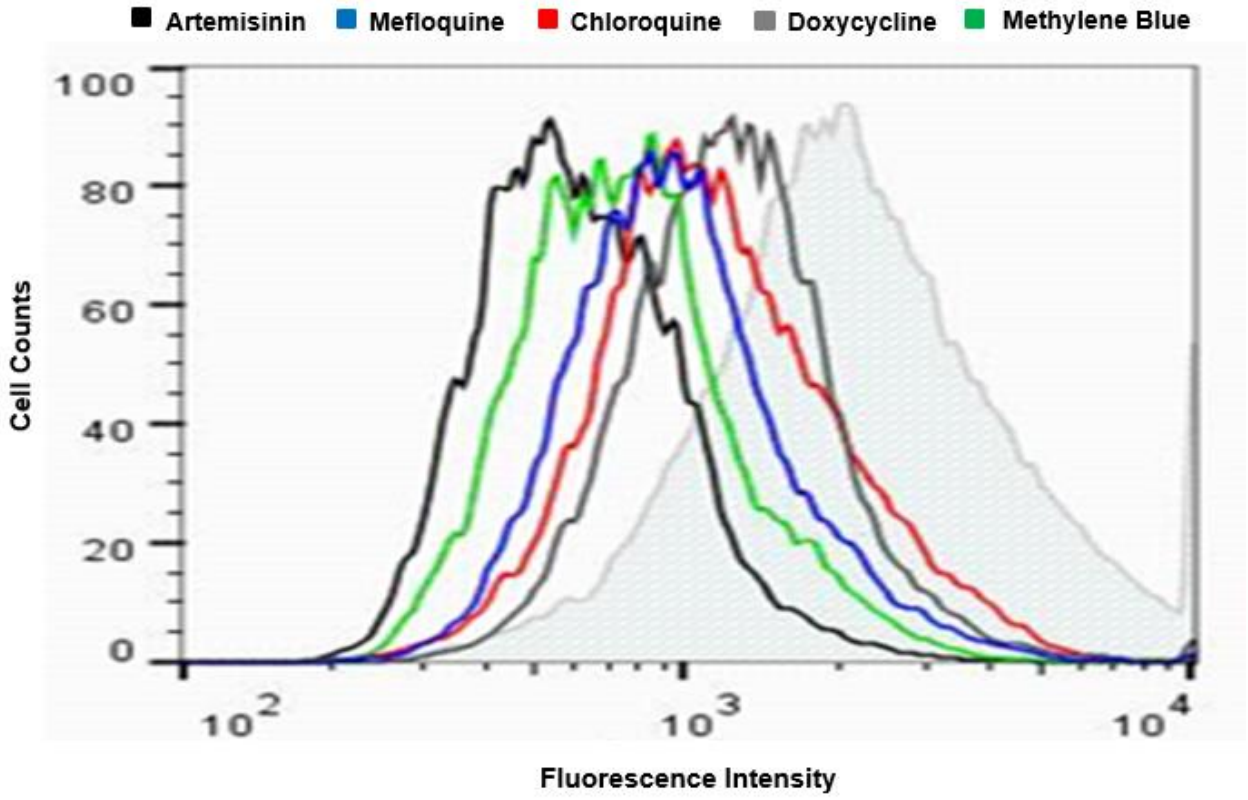

Figure 35: Flow cytometry histogram comparison of the model antimalarial drugs and their relative killing speeds, measured as calcein-AM positive events after an eight-hour treatment. Parasite cultures were treated with doxycycline (100 µM), chloroquine (120 nM), mefloquine (90 nM) artemisinin (150 nM) and methylene blue (120 nM) respectively. After eight hours, cultures were stained with calcein-AM (1 µg/mL), RBC membranes lysed with saponin and samples analysed using a FACS Aria II flow cytometer and FlowJo software (FlowJo, LLC, Ashland, Ore.). The shaded peak is representative of untreated parasites.

While PI staining increased as the parasite population showed signs of increased stress and eventual compromised membrane permeability due to drug treatment, the inverse was true for calcein-AM. Untreated cells were expected to have the highest calcein-AM staining and hence

indicate a healthy population. After eight hours of treatment artemisinin showed the quickest speed of action with the most significant decrease in calcein-AM staining. Methylene blue ranked in a close second followed by chloroquine and mefloquine with very similar trends. Finally, doxycycline showed very little deviation from the untreated sample, showing a predominantly healthy cell culture after eight hours of treatment.

3.3.8 – Flow cytometry: Increased throughput.

Although a ranking of the standard antimalarial compounds as a measure of relative killing speed was observed using the FACS Aria II flow cytometer and corroborated the fluorescence microscopy results, the two methods were not optimal for the simultaneous evaluation of multiple compounds (i.e. more than 5 or 6). The FACS Aria II was only capable of single sample analysis and hence the time between sampling may impact the parasites while they are outside of ideal culture conditions and as a result affect the staining patterns observed. The same consideration applied to the fluorescence microscopy approach. To improve on this and explore increasing overall throughput, the temporary placement of a Becton Dickinson ACCURI™ C6 Plus flow cytometer in our department by the local distributing company (Scientific Group) was exploited. Coupled with a robotic arm for automated sampling, the ACCURI was able to accommodate 96 well plates for multi-sample analysis, which reduced the inter-sample analysis time. This removed the human element between sampling and the method was explored using the panel of standard antimalarial compounds.

3.3.8.1 – Calcein-AM and PI control samples.

Preliminary analysis of the compounds in the Becton Dickinson ACCURI™ C6 Plus flow cytometer using the probes independently was done to ensure the fluorescent events were recorded in the correct channels and cross fluorescence would not be an issue. Parasite cultures were stained with calcein-AM (1 µg/mL), followed by saponin lysis and flow cytometry

analysis. Three control samples were analysed to establish gating limits (Fig. 36 A-C), and included unstained parasites, parasites stained with calcein and subsequently treated with a fixative and unfixed calcein-stained parasites. The dot plots obtained for the control samples (Fig. 36) represent 100,000 recorded fluorescent events (fluorescent cells) each. The y-axis represents calcein-AM-positive fluorescent events and staining intensity, i.e. the fluorescence intensity of individual cells measured using the calcein-AM channel (Exc_{488}/Em_{530}), while the x-axis represents the same but for the PI channel (Exc_{622}/Em_{660}). The unstained samples (Panel A) were used to generate gating parameters – the fluorescence intensity thresholds applied to the calcein-AM and PI channels to distinguish between fluorescence negative and positive events (the red lines in the individual dot plots) and allowed a baseline for comparison between fluorescent and non-fluorescent events recorded. Thus, all events recorded in quadrant Q1-LL (lower left) are non-fluorescent events, quadrant Q1-UL (upper left) represents all calcein-AM positive and PI negative events and Q1-LR (lower right) represents all PI-positive and calcein-AM negative events. Quadrant Q1-UR (upper right) represents all dual positive events (calcein-AM and PI-positive). These gating parameters were maintained through all subsequent experimentation using the Becton Dickinson ACCURI™ C6 Plus flow cytometer.

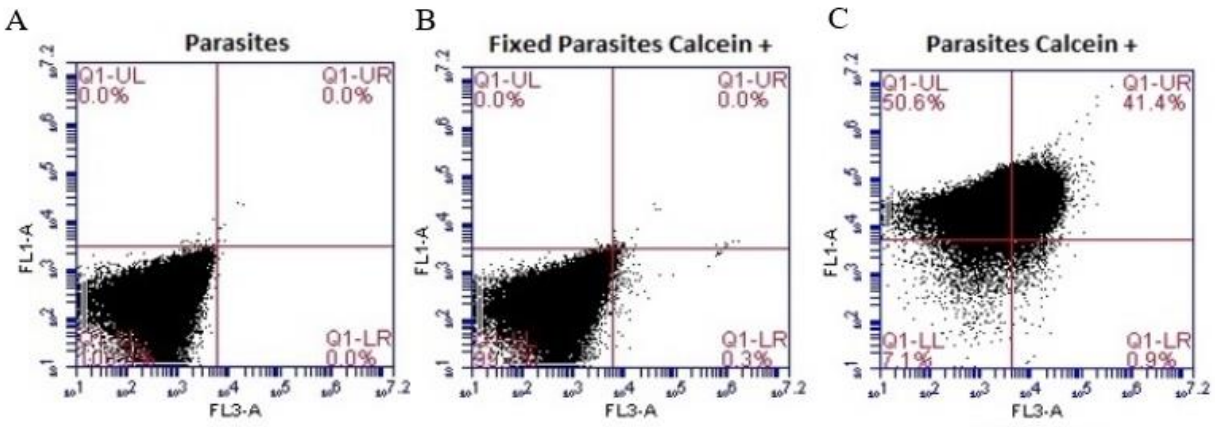

Figure 36: Dot plots for control samples for the calcein-AM study depicting 100 000 events per panel generated by a Becton Dickinson ACCURI™ C6 Plus flow cytometer. Panels A-C are representative of the three control samples run alongside the relative killing speed assay for the five standard antimalarials treated with calcein-AM (1 µg/mL). Panel A – RBC-free parasites obtained by saponin lysis, unstained; Panel B – Saponin lysed parasites treated with a fixative and then stained with calcein-AM; Panel C – Saponin lysed parasites (healthy) stained with calcein-AM. Y-axis (FL1-A) represents fluorescence intensity recorded in the calcein-AM channel; X-axis (FL3-A) represents PI fluorescence intensity of individual events. The vertical and horizontal red lines indicate the gating thresholds used to distinguish between non-fluorescent (Q1-LL quadrant), calcein-AM positive (Q1-UL), PI positive (Q1-LR) and dual positive (Q1-UR) cells. Analysis conducted using the Becton Dickinson Accuri C6 Plus (64-bit) software.

Panel A shows unstained parasites after saponin lysis of RBCs. This controls for any auto fluorescence of parasites and illustrates the rationale behind the gating used. Two calcein-AM stained controls were incorporated. The first was a sample of parasites obtained after saponin lysis of RBCs, stained with calcein-AM and subsequently treated with fixative (3% paraformaldehyde, 0.2% glutaraldehyde in PBS) (Panel B). The rationale was to explore whether parasite fixation would yield samples that could be stored prior to flow cytometry analysis. However, the fixed parasites were unable to retain the calcein-AM probe and hence provided a similar readout to the unstained controls. The fixation thus resulted in a permeabilized cell sample such that calcein-AM leaked out and PI was freely able to cross membranes (see Fig. 37 below for the PI analysis). Fixation therefore provided an additional calcein-AM-negative/PI-positive control. The second calcein-AM stained control contained healthy (untreated) parasites obtained by saponin lysis (panel C). This population generated a

large shift in fluorescence events into the upper quadrants (Q1-UR and Q1-UL). Important to note is that many of the calcein-AM positive events were recorded in the Q1-UR quadrant which is indicative of both calcein-AM and PI positive events, although this sample was not treated with PI. This suggests cross-fluorescence into the PI-positive channel. For analysis of the antimalarial compounds, events recorded in the Q1-UL and Q1-UR were thus combined to indicate calcein-AM positive cells. It further suggested that calcein-AM and PI co-staining was not advisable using the ACCURI flow cytometer, as it would provide false positives for PI-positive parasites.

In parallel with the calcein-AM gating experiment, control samples were stained with PI (3.3 µg/mL) and fluorescent events were recorded in the Becton Dickinson ACCURI™ C6 Plus flow cytometer using the same gating thresholds established with the calcein-AM samples (Fig. 37).

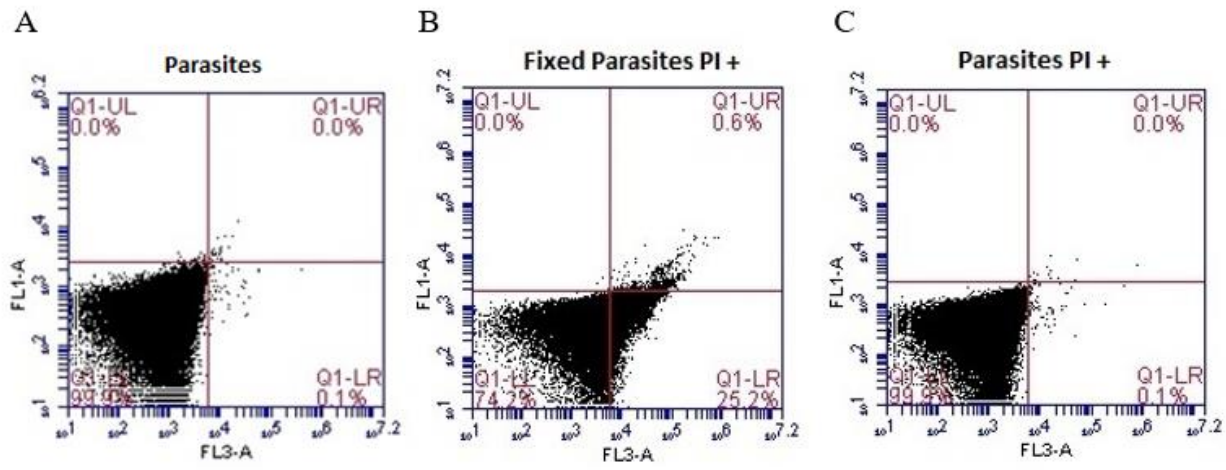

Figure 37: Dot plots for control samples for the PI study depicting 100 000 events per panel generated by a Becton Dickinson ACCURI™ C6 Plus flow cytometer. Panels A-C are representative of the three control samples analysed alongside the relative killing speed assay for the five standard antimalarials treated with PI (3.3 µg/mL). Panel A – unstained parasites removed from the RBC with saponin; Panel B – Parasites treated with a fixative and then PI; Panel C – Healthy parasites treated with PI. Y-axis (FL1-A) represents fluorescence intensity recorded in the calcein-AM channel; X-axis (FL3-A) represents PI fluorescence intensity of individual events. The vertical and horizontal red lines indicate the gating thresholds used to distinguish between non-fluorescent (Q1-LL quadrant), calcein-AM positive (Q1-UL), PI positive (Q1-LR) and dual positive (Q1-UR) cells. Analysis was conducted using the Becton Dickinson Accuri C6 Plus (64-bit) software.

Panel C indicates a healthy (untreated) parasite population stained with PI and, as expected, no fluorescent events were recorded outside the gates established (i.e. outside the lower left quadrant) and the fluorescence was similar to that obtained with unstained parasites (panel A), confirming PI's inability to enter healthy cells. This therefore ensured no background fluorescence would be recorded as false PI-positive cells. The calcein-AM experiment suggested that parasite fixation with paraformaldehyde/glutaraldehyde compromises parasite membrane integrity, and hence the ability to retain/exclude fluorescent probes. After the use of the fixative agent (membrane permeabilization) and subsequent PI treatment (Panel B), the number of fluorescent events in the PI-positive quadrant (Q1-LR) increased to 25.2% of the total population. Note that, unlike calcein-AM which yielded significant bleed-through fluorescence into the PI channel (Q1-UR), the PI positive events were more rigorously

confined to fluorescence events in the PI channel (Q1-LR). For analysis of antimalarial compounds, PI positive events were therefore restricted to those obtained in this quadrant.

3.3.8.2. – Analysis of standard antimalarial compounds.

In conjunction with the control samples, parasite cultures incubated with antimalarial compounds were analysed. Briefly, trophozoite stage cultures were treated with either artemisinin (160 nM), doxycycline (120 µM), chloroquine (125 nM), mefloquine (95 nM) or gramicidin D (10 nM) for eight hours before calcein-AM (1 µg/mL) or PI (3.3 µg/mL) staining. After staining, samples were saponin lysed and the parasite lysates were transferred to a 96 well, clear plate and analysed in a Becton Dickinson ACCURI™ C6 Plus flow cytometer. Using the gating thresholds established with the control samples, the samples treated with the five antimalarial compounds were assessed for total calcein-AM positive events (i.e. those recorded in the Q1-UL + Q1-UR quadrants) and total PI positive events (the Q1-LR + UR quadrants). The combined calcein-AM and PI results are shown in Fig. 38 (Dot plot images available in Appendix 13). As with the previous fluorescence microscopy and FACS Aria II analyses, decreasing calcein-AM fluorescent events and increasing PI events were considered diagnostic of drug action during the eight-hour incubation period.

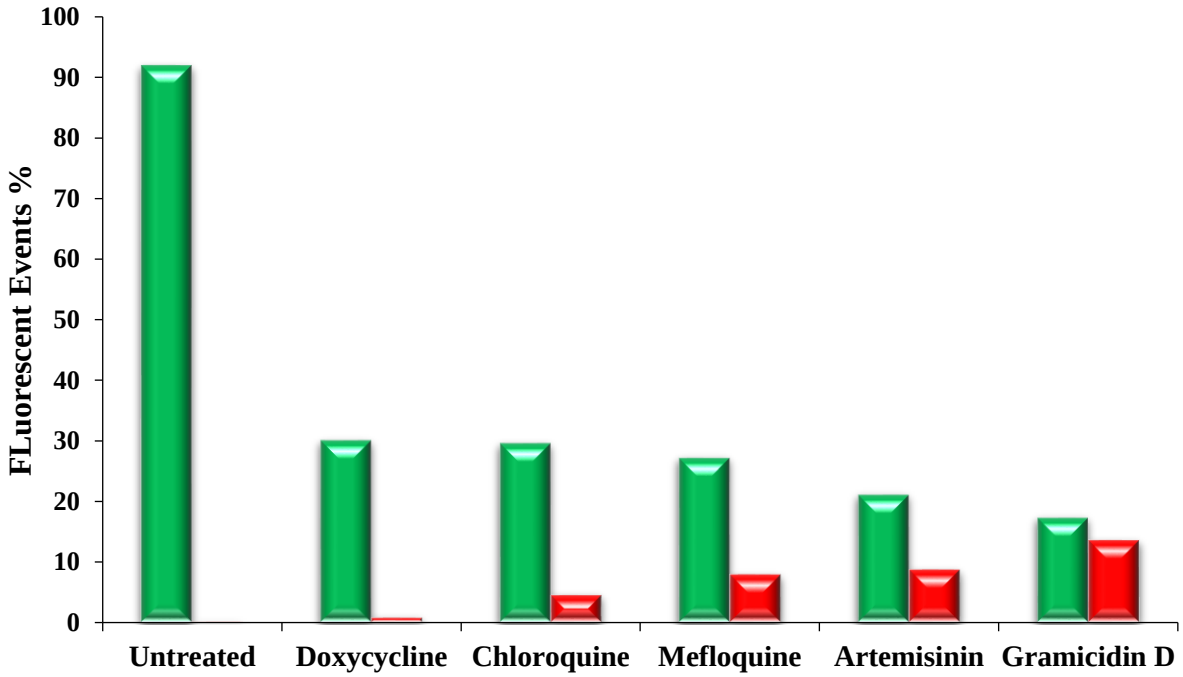

Figure 38: Calcein-AM (green) and PI (red) fluorescent events recorded using a Becton Dickinson ACCURI™ C6 Plus flow cytometer as a measure of drug stress after eight hours of treatment. Parasite samples were treated with artemisinin (160 nM), doxycycline (120 µM), chloroquine (125 nM), mefloquine (95 nM) or gramicidin D (10 nM) for eight hours and then stained with calcein-AM (1 µg/mL) or PI (3.3 µg/mL) after which they were saponin lysed. Two untreated control samples were included and stained with either calcein-AM or PI. Analysis was conducted using the Becton Dickinson Accuri C6 Plus (64-bit) software.

Encouragingly, the ranking of the speeds at which the compounds compromised parasite viability mirrored that obtained in the previous fluorescence microscopy and FACS Aria flow cytometry experiments. Doxycycline, the slowest acting compound and having almost no discernable effect in eight hours according to microscopy, was again the slowest acting compound in the panel, while gramicidin D had the biggest impact. The extent to which parasite viability was compromised during the eight-hour drug exposure followed the trend of doxycycline <chloroquine <mefloquine <artemisinin <gramicidin D (Fig. 38).

3.3.9 - Adaptation of calcein-AM for use in a multi-well plate fluorimeter by employing filter tubes.

Before proceeding to the analysis of the relative speed of action of experimental compounds using flow cytometry (Chapter 4), two alternative procedures were briefly explored – measuring calcein-AM accumulation in parasites by fluorimetry (this section) and measuring parasite ATP levels by luminometry (section 3.3.10 below). This was done for two reasons: to corroborate the relative speed of action of the standard antimalarial compounds obtained in this study thus far, and to investigate the possibility of bypassing the need for a flow cytometer.

The fluorescence retained by drug-treated and healthy parasites has been shown to be quantifiable via flow cytometry. To further reduce the economic impact on laboratories that may employ the novel relative killing speed assay (in its current state the assay requires access to a flow cytometer) the possibility of using a multi-well fluorimeter to quantitate calcein-AM in drug-treated parasite populations was explored. This approach was complicated by the fact that RBCs in the culture also accumulate calcein-AM and need to be removed by selective cell lysis (using saponin). Therefore, the development of a novel method for rapidly removing probe-stained parasites from saponin lysed red blood cells using microfuge tubes fitted with removable 0.45 µm filters (filter tubes) was explored.

Briefly, pRBC suspensions were treated with the same compounds in the panel at 10 x IC_{50} concentrations for eight hours in parallel with gramicidin D (0.1 nM) which was used to simulate a collapsed parasite population. Samples were stained with calcein-AM (1 µg/mL, 30 min) before RBC lysis using a 0.3% saponin, 0.5% BSA solution. The lysates were transferred to Spin-X HPLC micro centrifuge filter tubes and centrifuged, causing the RBC-associated calcein-AM to pass through the pores of the filters, while the calcein-stained, intact parasites remained trapped atop the filter. After discarding the filtrate, 0.5% Triton-X100 in PBS was

used to lyse the parasite cells to release parasite-associated calcein-AM (the assumption was made that uninfected RBC-derived calcein in the saponin lysate would not contribute to calcein released from the filter-trapped parasites, but was not controlled for). The final lysates were transferred to a 96- well microtiter plate and analysed in a Spectramax M3 microplate reader and the fluorescence was measured as Relative Fluorescence Units (RFU) (Fig. 39).

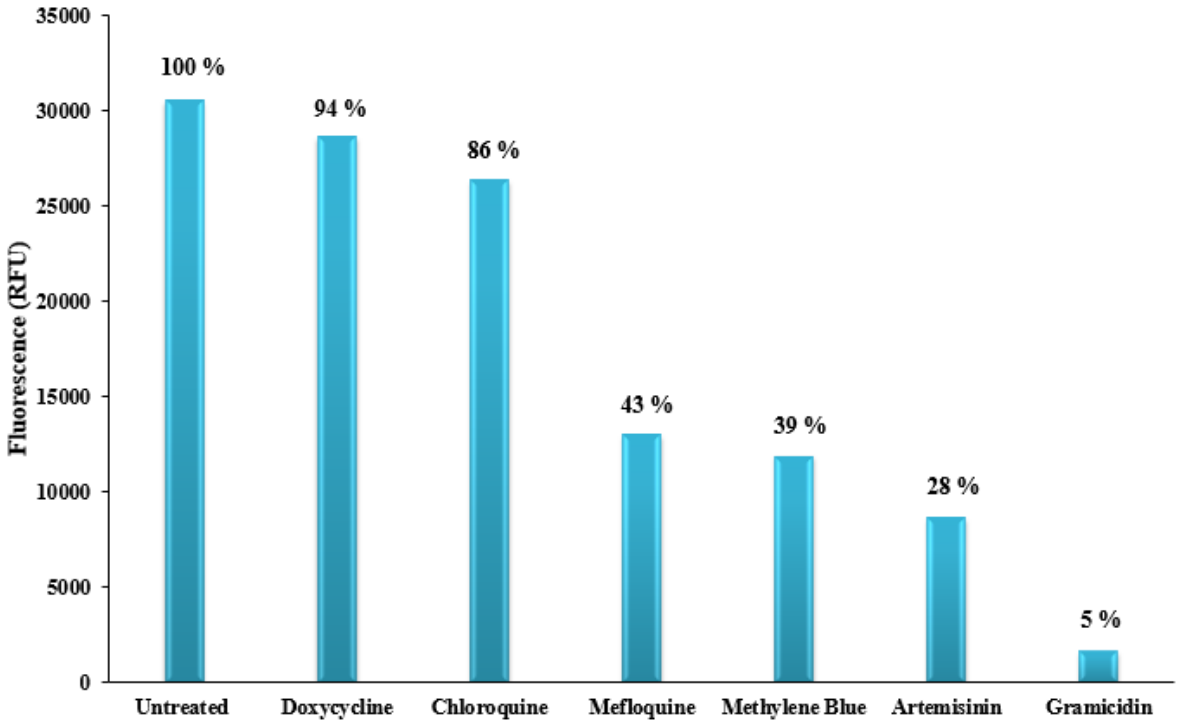

Figure 39: RFU (as an indication of killing speed) obtained from calcein-AM stained parasites after 8 hours of drug treatment using a filter tube-based plate fluorimeter assay. Parasite cultures were treated with doxycycline (100 µM), chloroquine (120 nM), mefloquine (90 nM), methylene blue (120 nM), artemisinin (150 nM) and gramicidin D (0.1 nM), prior to staining with calcein-AM (1 µg/mL, 30 min). After saponin lysis, lysates were centrifuged through 0.45 µm filters using filter tubes to remove RBC cytoplasm. Parasites trapped on the filters were lysed and parasite associated calcein-AM released by adding Triton X-100 and fluorescence (RFU) in the lysates measured in a multiwell plate fluorimeter (Exc_{488}/Em_{530}). RFU values were used to calculate percentage parasite viability for the respective samples (indicated above each bar in the graph) relative to the untreated control sample which represented 100% parasite viability. Note: Each viability as a measure of RFU is representative of single sample readings.

The drugs were ranked as measure of relative killing speed after eight hours of treatment using the untreated control as a baseline for a healthy, viable parasite population and the gramicidin

D treated sample as an indication of a collapsed parasite population. Doxycycline and chloroquine showed minor decreases in RFU (6% and 14% respectively) in relation to the untreated control, suggesting these two drugs had little impact on the parasites after an eight-hour period. Mefloquine and methylene blue had more significant reductions in RFU in relation to the untreated control with viabilities of 43% and 39% respectively. This was a significantly lower residual calcein-AM fluorescence compared to doxycycline and chloroquine. Artemisinin had the lowest RFU out of the test drug samples with 28% remaining parasite viability after eight hours and would suggest it was the most efficaceous drug in the panel over 8 hours, as seen in previous assays. Gramicidin D proved most effective with only 5% of parasites remaining after an eight-hour treatment.

3.3.10 - Filter tube-based ATP Assay.

In 2012 the Khan group identified an alternative, novel, quantitative assay for determining the kinetics of drug action in cultures by measuring changes in parasite ATP levels as a direct indication of drug stress (Khan *et al.,* 2012). As such, they made use of the firefly luciferase-based commercially available CellTiter-Glo Luminescent Cell Viability Assay kit (Promega) to assess the relative speed of action of a panel of antimalarials by quantifying the remaining ATP in drug-treated parasite cultures. However, similar to the requirement in the calcein-AM based assays, determining parasite associated ATP concentrations entails saponin lysis to remove background ATP found in the cytoplasm of RBCs in the culture samples. In the Khan *et al.* study, separation of the parasites from the RBC cytoplasm in the saponin lysates was achieved by centrifugation through a phthalate oil cushion. For the current study, the microfuge filter tubes (as described for the fluorescence filter tube assay in the previous section) were employed to remove RBC ATP and allow specific quantitation of parasite ATP.

As was done in the calcein-AM filter tube-based assay (section 3.3.9. above), drug compounds were used at 10x IC_{50} concentrations to treat parasite cultures for eight hours and gramicidin D (0.1 nM) was used to simulate a collapsed parasite population. Post-treatment the samples were lysed using a 0.3% saponin, 0.5% BSA solution after which the lysates were transferred to 0.45 µm Spin-X HPLC microcentrifuge filter tubes. The lysates were centrifuged and after discarding the filtrate (containing the ATP in lysed RBCs), the filters (containing intact parasites) were placed in fresh microfuge tubes and an equal volume of PBS and CellTiter-Glo reagent was added atop each filter. The CellTiter-Glo reagent lysed the parasites and the released ATP produced luminescence due to the presence of firefly luciferase and its substrate in the reagent. The lysates were transferred to a white-walled, clear bottom 96-well plate and the luminescence measured in a Spectramax M3 microplate reader to measure parasite-associated ATP. Luminescence was measured as Relative Luminescence Units (RLU) and is graphically illustrated for each drug-treated parasite sample in Fig. 40.

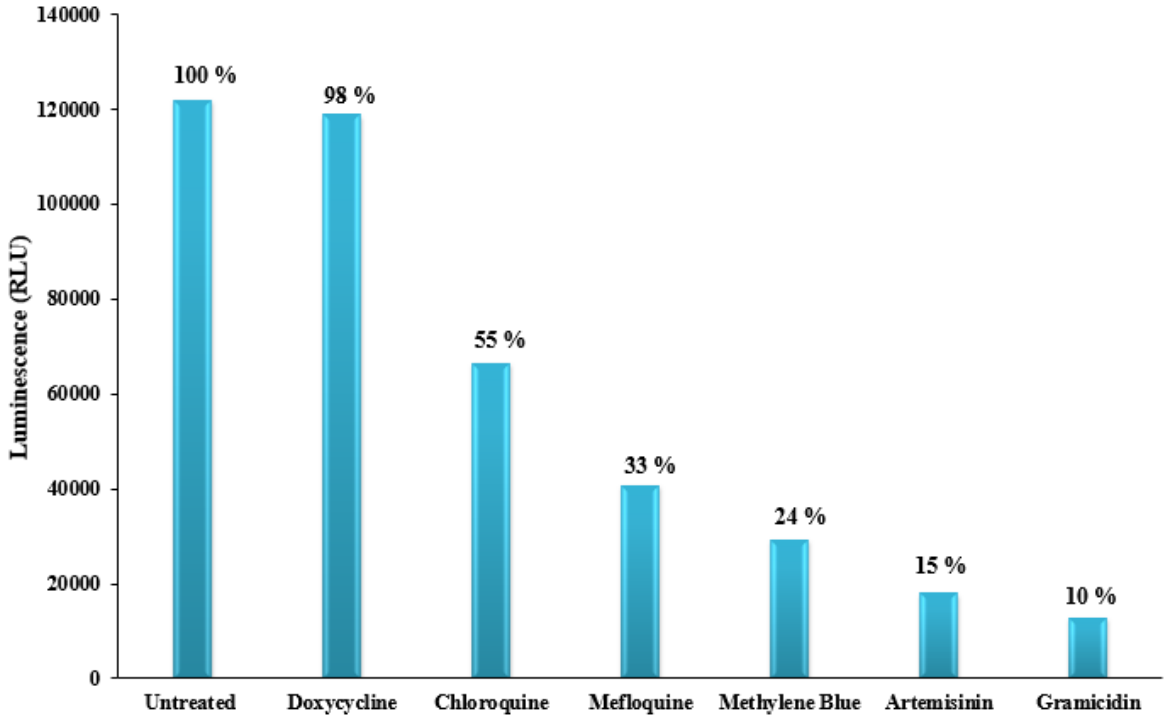

Figure 40: RLU (Relative luminescence units) reflecting the ATP levels in drug-treated parasites obtained from cultures treated with standard antimalarial compounds. Test samples were treated with doxycycline (100 µM), chloroquine (120 nM), mefloquine (90 nM), methylene blue (120 nM) and artemisinin (150 nM) for eight hours. Included were untreated and gramicidin D (0.1 nM) treated controls. Saponin lysates of the treated cultures were centrifuged through 0.45 µm filters using microfuge filter tubes. Parasites trapped on the filters were lysed by adding CellTiter-Glo reagent and ATP-dependent luminescence (RLU) measured in a multiwell luminometer after transferring the lysates to 96-well plates. Parasite viabilities (%) are indicated above each drug treatment, calculated relative to the RLU value obtained with the untreated control sample which represented 100 % parasite viability. Note: Each viability as a measure of RLU is representative of single sample readings.

The untreated control sample acted as a model healthy cell culture and the RLU associated with it (representing the level of residual ATP in the parasites) was deemed to represent 100% parasite viability, whereas gramidicin D treatment was indicative of a collapsed parasite population with an RLU translating into only 10% remaining parasite viability. Doxycycline appeared to have little effect on the parasites with an almost entirely viable cell culture of 98 % after eight hours of treatment. Chloroquine and mefloquine appeared to have significantly more impact with 55% and 33% parasite viability respectively. Methylene blue and artemisinin

provided the quickest killing speeds with only 24% and 15% remaining parasite viability, respectively, after eight hours of treatment.

3.4 – Discussion

With confirmation of the ability of PI and calcein-AM to distinguish between viable and nonviable HeLa cells (Chapter 2), this subsequent study explored the development of a novel bioassay using fluorescent vitality probes which would allow the relative speed of drug action on malaria parasites to be assessed rapidly and quantitatively. The assay was conducted on a panel of six well known antimalarials (chloroquine, mefloquine, doxycycline, methylene blue, gramicidin D and artemisinin) and was first established via fluorescence microscopy and then adapted for use in flow cytometry.

On a cautionary note, in this chapter and throughout the thesis we refer to the assay as being able to determine the relative speed of action of compounds and therefore being capable of discriminating fast acting and slow acting compounds, as was done by Le Manach *et al.* (2013) and Ullah *et al.* (2017). What is being measured is the efficacy of the compounds in lowering viable parasite levels at a single time-point (8 hours), which could conceivably lead to erroneous assumptions. This is further discussed in section 3.4.2. below.

3.4.1 - Fluorescent vitality probe staining and optimization in *P. falciparum.*

Calcein-AM staining in *P. falciparum* parasites showed fluorescent coverage of the parasite matrix and absence from the parasite food vacuole. Fluorescent signals observed in healthy trophozoites were found to be of sufficient quality at 1 µg/mL, five times lower than that required for HeLa cells in this study. This could perhaps be attributed to a higher activity of esterases required to cleave the calcein-AM precursor to its fluorescent cell-retained product in parasites. In addition, calcein-AM staining was not limited to the parasite, but instead stained the cytoplasm of infected and uninfected RBCs, as previously observed by Brostin *et al.*, 2005 where erythrocyte aging was tracked using calcein-AM. This would introduce subjectivity based on the user who may mistakenly classify a RBC as a healthy parasite. Furthermore, any

fluorescent measurements using a flow cytometer or plate reader would deduce a signal from a RBC as a parasite fluorescent signal. It was decided to therefore include an additional saponin lysis step which was found to be effective at lysing the RBC membranes and removing the calcein found in the RBC cytoplasm, while leaving intact, easily distinguishable fluorescent parasites. Although there appeared to remain RBC 'ghosts' (RBC membrane remnants surrounding intact parasites), their fluorescence intensity was significantly lower than that of the parasite cell and hence contributed negligibly to the overall fluorescence of the samples. Although the saponin lysis treatment adds an additional step to the assay and could be detrimental to the goal of producing a higher throughput procedure, it is essential for accuracy when extrapolating to a quantitative assay using flow cytometry.

A similar trend was observed when moving from mammalian cell staining to parasites in terms of probe concentration using propidium iodide. A significantly lower concentration of PI was required for adequate parasite staining (3.3 µg/mL) as opposed to mammalian cell staining (20 µg/mL). These decreases are significant in the sense that they reduce the economic impact of a new bioassay on laboratories wanting to establish screening procedures. The fluorescence signals were observed throughout the parasite, as opposed to being limited to the parasite nuclei, considering that PI is a nucleic acid stain. One possibility is that this reflects deterioration of the nuclear envelope and diffusion of chromatin into the parasite cytoplasm but is counter-indicated by the restriction of DAPI staining to the parasite nuclei. Alternatively, it may represent binding of PI to RNA molecules in the parasite cytoplasm. Other studies have made use of PI concentrations ranging from 5 µg/mL (Liu *et al.,* 2005) through to the most popular 10 µg/mL (Lopez *et al.,* 2010; Boissiere *et al.,* 2012) and up to 50 µg/mL (Contreras *et al.,* 2004). We found this to be unnecessary in combination with a 45 min 0.1 nM gramicidin D incubation, which provided sufficient membrane deterioration to allow for adequate PI staining. Lower gramicidin D concentrations or incubation times led to erratic PI staining with

PI often being unable to enter the cell. Higher concentrations or longer incubations with gramicidin D destroyed the parasites significantly, thereby not allowing for the retention of the stain due to excessive cellular damage.

An interesting discovery was that PI appeared to stain the matrix of healthy merozoites whereas calcein-AM was not retained in these RBC-free invasive forms of the parasite. The strong PI staining and lack of calcein-AM could provide false positives for nonviable parasites. It would have been expected that the merozoite membrane would be permeable to calcein-AM and once across the barrier would result in fluorescent green calcein. It could be hypothesized that the cellular machinery and esterases required for calcein-AM cleavage are not ubiquitously expressed. As such, calcein-AM may be able to cross the membrane of the merozoite but remain uncleaved, thus able to freely diffuse back into the extracellular space. However, if these enzymes are present and able to produce the fluorescent calcein product, it may also be able to leach out of the cell by other means (reduced lipophilicity/packing or pores in the merozoite membranes). Alternatively, merozoite membrane composition differs from the trophozoite stage parasite in the sense that merozoite membranes contain a thick 20 nm surface coat that encodes various marker proteins required for RBC invasion and immune evasion (Maitland and Molyneux, 2004). This variance in membrane composition may provide an alternative explanation for the inability of calcein to penetrate the coat and accumulate in merozoites. Conversely, it may account for PI's capability to cross viable merozoite membranes and provide intracellular fluorescence while it is excluded from viable trophozoite parasites (unless PI is binding directly to the surface of the protein coat, which couldn't be excluded based on the resolution of the microscope used).

Marketed as a mitochondrial membrane vitality stain and indicator of cellular degradation, TMRE was expected to be a suitable addition to the candidate probes to measure vitality in

malaria parasites. HeLa cell staining showed no specific localization and instead whole-cell, cytoplasmic staining, as well as potentially organelle staining. In contrast, TMRE was shown to have a moderate preference for regions in malaria parasites although it is unclear if this localization was mitochondria specific (morphologically, the staining does not resemble the typical patterns obtained when staining parasites with mitochondrial marker probes, e.g. Mitotracker) and staining patterns were mostly irregular. Studies that made use of the probe for measuring cellular apoptosis in *P. falciparum* have also shown staining patterns that are not typical of mitochondrial probes (Mutai and Waitumbi 2010) and instead appear to more closely resemble the HeLa cell staining observed in this study. This was not an isolated incident as, in a study conducted by the Kocken group that looked to assess novel methodology for live/dead parasite cell staining, it was found that in both *P. falciparum* and *P. knowlesi*- infected cultures, parasite vacuolar staining was observed in 'dead' parasites (Pasini *et al.*, 2013). Furthermore, the uptake of TMRE in other studies varied across life stages, with the ring stage showing the largest sequestration (Mutai and Waitumbi, 2010). While attempts were made to optimize the staining patterns in the parasite, focusing on incubation time and concentration of the probe, it was still observed to be able to stain both live and compromised cells in all cases, as was evident in HeLa cells. As such, it was decided to no longer continue pursuing TMRE as a suitable fluorescent vitality probe.

Although used previously in various organisms as a distinct indicator of cellular vitality, it was observed that, similar to HeLa cells, there was no decrease in hydroethidine fluorescence after drug treatment with gramicidin D. This probe had been extensively used as a vitality marker in both mammalian cells as well as malaria parasites according to published results (Krishan, 1975; Elloso *et al*., 1994; Cruz *et al.*, 2012) and hence additional optimizations were attempted to attain valid vitality properties. The concentration of the probe was altered systematically, as well as the incubation temperature and time, although no resultant change in staining patterns

was obtained. It has been reported that, in the trophozoite life stage of the parasite, a decline in fluorescence intensity is observed to accompany a decrease in parasite viability (Chevalley *et al.,* 2010). Although this study found staining patterns that closely resembled those published by the Chevalley group (2010), it was unable to show a change in those patterns after drug treatment. Furthermore, studies conducted on all life stages of the parasite provided the same outcome – high DAPI and hydroethidine fluorescence in both drug-treated and viable cells. Additionally, high concentrations of hydroethidine (50 µg/mL) were reported as being used by Chevalley *et al.,* 2010), but sufficient fluorescence was observed at as low as 1 µg/mL in this study. Using higher hydroethidine concentrations did not improve distinction between live/compromised parasites, and hence hydroethidine was discarded as a suitable vitality probe for use in this study.

3.4.2 – Relative killing speed assay on panel of antimalarials using vitality probes and fluorescence microscopy.

Although IC_{50} values for the standard antimalarial drugs used in this study have been reported, it was important to assess their effective concentrations on the laboratory strain of 3D7 *P. falciparum* to control for a series of factors: i) that the drug stocks used in this study were active; ii) that our laboratory stock of the 3D7 parasite strain had not altered its susceptibility to the drugs due to extensive sub-culturing; iii) that the routine culturing conditions and procedures employed here didn't result in altered drug sensitivity. Reassuringly, as reported in the relevant Results section, the IC_{50} values obtained agreed closely with published results, with the possible exception of methylene blue which appeared 6 times less active than reported (IC_{50} = 12 nM [this study] *vs.* 2 nM [Okombo *et al.,* 2012]) for reasons that are not apparent. It is further important to note that the 3D7 strain is a chloroquine sensitive strain which may not provide an accurate indication of chloroquine dose response in wild-type malaria parasites.

Studies have shown that chloroquine resistant strains can require a tenfold increase in concentration to provide 50% parasite viability inhibition as was, for example, witnessed by the Moneriz group when an IC_{50} of 190 nM was calculated for the chloroquine resistant strain *P. falciparum* Dd2 (Moneriz *et al.*, 2011).

An accurate IC_{50} for the individual compounds was required to determine the concentrations to be used in the relative speed of action experiments using the vitality probes. Two considerations went into the choice of using a 10x IC_{50} concentration for subsequent studies. Firstly, a sufficiently high concentration is required that will confidently compromise the viability of all the parasites in the test sample in all instances, considering the fluctuation in effective drug concentration that is typically found from one experiment to the next and is a normal consequence of the variables involved in working with live cells. Secondly, the concentration should ideally be sufficiently low for the results to reflect the normal mode of action of the drug in question, and not be a consequence of off-target effects (i.e. the compound inhibiting proteins and pathways unrelated to its primary target at high concentrations).

Calcein-AM and PI were selected as promising parasite viability markers for the relative killing speed experiments based on using gramicidin D as a model compound known to rapidly affect parasite viability (Khan *et al.*, 2012). The question was whether these probes would be useful in conjunction with the more conventional, standard antimalarial drugs for which the IC_{50} values were determined. In addition, during the optimization stage the probes were used individually. A second question was whether they could be used in combination to simultaneously detect and quantitate viable (calcein positive) and nonviable (PI positive) parasites in the same sample. In the experiments that were thus performed, parasites were incubated in parallel cultures with the standard antimalarials for eight hours, stained with a combination of calcein-AM and PI and viewed by fluorescence microscopy. Percentage

parasite viability could then be calculated from the ratio of viable (calcein positive) and nonviable (PI positive) parasites. Compounds with a more rapid speed of action would thus be expected to yield comparatively lower parasite viability at the 8-hour time-point.

Importantly, the calcein-AM and PI stains, used in combination, complemented each other well. Drug treatment saw a decrease in calcein-AM stained parasites which was mirrored by a complementary increase in PI staining, and no co-staining was observed. The probes could therefore be used to robustly distinguish and quantify viable/nonviable parasites in cultures treated with conventional antimalarials. Moreover, eight hours proved to be adequate for determining the comparative speeds of action of the individual drugs. IC_{50} assays (such as the pLDH assay employed in this study) typically evaluate the survival of parasites after 48 hour or longer incubations with drug compounds. The focus of this study was rather to develop a novel assay to determine relative antimalarial killing speed over a much shorter incubation period, and hence provide a means to further prioritize experimental compounds that are not only effective at low concentrations but are also rapid acting.

An eight-hour time point was selected since earlier and later time points did not provide as clear a distinction between test compounds in terms of relative killing speed. Therefore, the killing speed ranking observed in this assay is a measure of individual compound efficacy in an eight-hour period (similar to the six-hour period described by Ullah *et al.*, 2018). Although the assumption is made that this relative speed of action will be maintained over longer incubations (*i.e.* a reduction of parasite viability by 50% over 8 hours will translate into a reduction of a further 50% over the next 8 hours), this may not always be the case, as compound stability may be reduced over time and hence compromise its effectiveness. Furthermore, there may be a sub-population of parasites that are less susceptible to the rapid action of a compound which may in turn result in a plateau of killing speed over time. For example, in an extreme

conceptual case, if at the 8 hour time point 50% of parasites remain viable and the compound has completely degraded or the entire susceptible parasite sub-population has been killed, the parasite population will remain at 50% at longer time points and the reduction in parasite viability by the particular compound may be exceeded by compounds labelled as slower acting at 8 hours. A further drawback is that the assay only compares the killing speed of compounds in the trophozoite blood stage. Compounds that may be significantly more active in the ring stage may appear to be slower acting and vice-versa (compounds only active in the trophozoite stage will be slower acting if mixed cultures or exclusively ring stage cultures are used). If the assay is therefore employed as intended i.e. rapidly comparing the relative action speeds of medium sized compound libraries, it is clear that the more definitive PRR assay would still need to be employed to confirm the rapid action of selected compounds. Reassuringly, the same considerations apply to the BRRoK assay of Ullah *et al.* (2017) (reduction of luciferase levels measured at 6 hours in trophozoite stage cultures) who interrogated the MMV Malaria Box for fast vs. slow acting compounds and found results that correlated with the PRR assay (although, admittedly, only assessed using standard antimalarials).

Based on the proportion of remaining viable parasites at this time-point, the study drugs could be ranked as gramicidin D (2% remaining viability) > artemisinin (19%) > mefloquine (31%) > chloroquine (58%) > doxycycline (87%), which agrees very well with published studies (e.g. Khan *et al.*, 2012) and their known properties. This strongly suggests that the assay in this form (using fluorescence microscopy), can be used to rank the speed of action of experimental antimalarial compounds *vis-à-vis* each other.

The drugs selected for use in the pilot assay included some of those most commonly used (either currently or historically) to combat both the acute and chronic forms of malaria and hence are well known to be effective, as evidenced by the nanomolar IC_{50} values obtained in

the pLDH assays (except for doxycycline, used for prophylaxis rather than therapeutically, with a low micromolar IC_{50}).

The commonly prescribed semi-synthetic doxycycline is principally advocated for its potent antibacterial properties and only secondarily as an antimalarial, and in the latter case for prophylaxis. It is therefore not unexpected that its bactericidal mechanism may not correlate with its antimalarial efficacy. It has been established that the mechanism in bacteria involves the inhibition of protein synthesis at the ribosome, where the compound binds to the 30S small ribosome subunit preventing the further attachment of tRNA (Majewski, 2014). In *P. falciparum*, doxycycline was reported to disrupt nucleotide synthesis (Yeo *et al.*, 1998), as well as inhibit mitochondrial protein synthesis (Blum *et al.*,1984). A later study showed that doxycycline acts on the parasite apicoplast, although the effect had a late onset resulting in the slow action of the drug (Dahl *et al.*, 2006). In published studies, parasites were treated with doxycycline and assessed after 12 hours, after which parasite apicoplasts appeared morphologically intact and were capable of replicating their genomes for segregation into developing merozoites (Dahl *et al.*, 2006; Gailard *et al.*, 2015). It was observed that, instead of having a direct impact on the apicoplast, doxycycline disrupted the expression of apicoplast genes encoded by the nuclear genome. Hence doxycycline would not show an effect on existing apicoplast function, but instead apicoplasts inherited by daughter merozoites of doxycycline-treated parasites would contain insufficient levels of apicoplast-encoded proteins required for normal function (Dahl *et al.*, 2006; Gailard *et al.*, 2015). This loss in apicoplast function would ultimately result in parasite cell death, although this effect would be observed in the parasite life cycle after doxycycline treatment. This would explain the slow speed of action observed in doxycycline treated parasites in this study and suggests that there should be little effect on the parasite population over the course of an 8-hour incubation period.

Chloroquine, a member of the quinolines, was once the gold standard of malaria treatment until the emergence of chloroquine-resistant parasite strains (Meshnick and Dobson, 2001). Due to widespread resistance it has since become less used in isolation and instead has been combined with other drugs to create 'cocktails' to combat resistant strains. It is thought to disrupt the parasite machinery involved in haem detoxification and hence result in a build-up of toxic haem and resultant cell death (Chinappi *et al.,* 2010; Bounaadja *et al.,* 2017). As discussed in the Introduction (Chapter 1), chloroquine prevents the normal sequestration of haem (released in the food vacuole due to proteolysis of internalized host RBC hemoglobin) into an inert haemozoin crystal, causing an accumulation of haem and eventual parasite toxicity and lysis (Chinappi *et al.,* 2010; Bounaadja *et al.,* 2017; Francis *et al.,* 1997; Tewari *et al.,* 2017). This study showed chloroquine to be a relatively slow acting drug in comparison to the other test compounds. With a mean parasite viability of 58% after an 8-hour treatment (according to the microscopy analysis), just over half the parasite population showed viability sufficient enough to metabolize and retain calcein fluorescence and exclude PI, suggesting that the haem accumulation due to chloroquine action has a relatively slow cytotoxic effect compared, for example, to the actions of artemisinin and mefloquine. This conclusion correlated findings by Khan *et al.* (2012) in which chloroquine was found to exhibit a slow speed of antimalarial action using ATP and luciferase-based bioassays to measure the speed of drug action against *P. falciparum.* Presumably this indicates that more than 8 hours of haemoglobin digestion and haem accumulation is required for the latter to reach sufficient concentrations to kill the majority of the parasites, or that the mechanism of haem toxicity is exerted slowly. It further supports Ginsburg *et al.* (1998) who observed late onset of parasite cell death only after haem levels had reached critical levels.

Initially prescribed in Thailand as a combination therapy (mefloquine, sulfadoxine and pyrimethamine) in 1987, mefloquine has since been adapted for use in ACT (as artesunate-

mefloquine) to combat the increasing number of resistant malarial strains (Na-Bangchang *et al.,* 2007), in addition to its use as a prophylactic. As discussed in Chapter 1, as a member of the quinoline family it would perhaps be expected that mefloquine would have a similar mechanism (preventing the detoxification of haem) and thus similar killing speed as chloroquine in malaria parasites. This has been contradicted in various studies, e.g. combination therapies encompassing both drugs appear to provide a more effective outcome than either of the drugs alone which suggests a synergistic relationship (Sowunmi and Oduola, 1997), contrasting effects of chloroquine and mefloquine on hemoglobin endocytosis in malaria parasites (Hoppe *et al.,* 2004), inhibition of 80S ribosome GTPase activity by mefloquine (Wong *et al.*, 2017) and differential resistance mechanisms.

In this study, mefloquine was more rapid acting in comparison to chloroquine, with only 31% of remaining parasites being viable at the end of eight hours compared to 58% viable parasites after chloroquine treatment in the microscopy study. This makes mefloquine almost twice as effective over the same time period, and further suggests a differential mechanism between the two drugs. The significantly more rapid action of mefloquine compared to chloroquine was also reported by Khan *et al.* (2012) using ATP and luciferase-based assays.

More rapid acting than mefloquine (this difference became more marked in the flow cytometry and filter tube-based experiments) was methylene blue. Although not commonly used as a mainstream antimalarial and discontinued in malaria treatment owing to the side effect of turning urine blue (amongst others), it has since been used extensively to treat methemoglobinemia (Okombo *et al.,* 2012). Mechanistically it has been established that methylene blue acts as an electron acceptor from glutathione reductase whereby the then reduced version of methylene blue (leucomethylene blue) is transported into acidic vesicles (Blank *et al.,* 2012). Electrons are generated from the redox cycle which are then readily

transferrable to several oxidants in the malaria parasite e.g. haemoglobin metabolites like iron (III)-protoporphyrin (Ehrhardt *et al.,* 2013). The cycling of methylene blue in and out of these acidic vesicles in parasitized erythrocytes results in reduction of NADPH and subsequent oxidation of haematin with consequential inhibition of haemozoin formation and prevention of trophozoite metabolism and development (Blank *et al.,* 2012).

With the burgeoning problem of drug resistance, a real and current threat, there has since been increased interest in studying methylene blue (Dormoi *et al.,* 2012). Furthermore, this drug has been proven to be effective in significantly reducing gametocytaemia in studies conducted in Burkina Faso (Coulibaly *et al.,* 2009). It was determined that methylene blue was effective against both developing and mature gametocytes, thus having the potential to reduce transmission in malaria endemic regions (Coulibaly *et al.,* 2009).

The drug that showed the largest impact on the parasite population consistently was artemisinin, with a substantial loss of 89% of parasite viability after an 8-hour treatment in relation to an untreated control in the microscopy experiments. As summarized in Chapter 1, the mechanism of action of artemisinin has been debated for as long as its structure has been known. At present the primary mechanism of action is thought to be reduction of the endoperoxide bond in artemisinin in the iron-rich intracellular environment (primarily caused by the haem released during hemoglobin digestion in the parasite) creating an exponential increase in reactive oxygen species which leads to the breakdown of various cellular systems (Kavishe *et al.,* 2017). Although it is known that artemisinin and its derivatives have significantly shorter half-lives *in vivo* compared to other antimalarials, it is difficult to ascertain the exact critical point of the parasite population collapse.

It has been shown that the active metabolite of artemisinin has an elimination half-life of approximately one hour. However, it is not clear what the overall malaria parasite viability is

at this same time point (Krishna *et al.,* 2004). Sanz and colleagues assessed the *in vitro* killing speed of artemisinin, albeit their focus was on the parasite's ability to recover post-drug treatment and hence their first measurement of any reduction in vitality was at 24-hours, where an almost complete loss of population viability was observed (Sanz *et al.,* 2012). Using flow cytometry and the nucleic acid stain SYTO 61, the Klonis group (2013) observed the effect on the parasite after artemisinin treatment at specific points during the life cycle and noted a hypersensitivity to the drug of parasites less than eight hours old (Klonis *et al.,* 2013). Furthermore, it was demonstrated in the same study that short pulses of between one and six-hour doses of artemisinin were effective in causing significant reductions in viability, which constitutes the most rapid speed of action for any established antimalarial and correlates well with the killing speed observed in this study. The rapid elimination and consequent short half-life of artemisinin *in vivo* may thus be compensated for by its rapid speed of action, in addition to its clinical use in combination with partner drugs with longer half-lives (ACTs). This again highlights the utility of establishing the relative antimalarial speed of action of compounds as part of the drug development process.

3.4.3 - Adapting the fluorescence assay to flow cytometry.

The fluorescence microscopy-based bioassay was able to assess the changes in parasite staining patterns after eight hours of drug treatment by counting the ratio of viable (calcein positive/PI negative) vs. nonviable (calcein negative/PI positive) parasites in each sample. To explore an alternative, more rapid quantification method, the novel assay was adapted for analysis via flow cytometry.

Flow cytometry has long been established for use as a reliable and rapid method for parasite detection in human blood or malaria parasite culture samples (Pattanapanyasat *et al.,* 1992) as well as in *Plasmodium*-infected mice (Barkan *et al.,* 2000). More recently, this technique has

been used to measure individual drug efficacies against the *P. falciparum* parasite. In the parasite sexual life stage, gametocytes of transgenic GFP-expressing parasites of the 3D7 laboratory strain were detected and a panel of drugs, including chloroquine, were used to assess drug stress via flow cytometry (Wang *et al.*, 2014). Even more relevant is the fact that fluorescent probes have been used as indicators of drug stress for specific anti-gametocyte drugs using hydroethidine whereby only viable parasites retained the probe (Chevalley *et al.*, 2010), although in the present study hydroethidine accumulation in trophozoites appeared to be independent of parasite viability. Previous studies have been conducted making use of various fluorescent probes to measure parasitaemia of the *P. falciparum* asexual life stage using flow cytometry and these include Hoechst 33258 (Brown *et al.,* 1980), acridine orange (Whaun *et al.,* 1983), thiazole orange (Makler *et al.,* 1983) and hydroethidine (Wyatt *et al.,* 1991). This study made use of flow cytometry to develop a more rapid method for assessing the relative speed of action of antimalarial drugs using the vitality probes PI and calcein-AM, to exploit the promising results by fluorescence microscopy.

The drug concentrations of the panel as well as the probe staining concentrations remained identical to that of the fluorescence microscopy assay and direct comparisons could be made. The flow cytometry results obtained with the FACS Aria II instrument confirmed that the fluorescent vitality probes PI and calcein-AM could distinguish between live and dead parasites to measure antimalarial killing speeds and, importantly, the relative speed of action ranking of the panel of drugs mirrored that of the microscopy assay i.e. artemisinin > methylene blue > mefloquine > chloroquine > doxycycline. In comparing the two probes and assessing which provided the more accurate distinction between the panel of drugs as a measure of relative parasite killing speed, it could be argued that PI was the more sensitive vitality probe. It yielded the largest differences in peak fluorescence intensity between the different drug treated samples, allowing a more confident ranking to be achieved in comparison to calcein-AM. The

same trend was observed using the ACCURI flow cytometer. Nonetheless, using two probes with independent modes of accumulation on separate samples creates a means to control for the results obtained with any single probe.

Moving the assay from a single-sample platform in the FACS ARIA II to the Becton Dickinson ACCURI™ C6 Plus flow cytometer was motivated by the need to explore increasing assay throughput in order to assess larger compound collections. The ACCURI™ is capable of automated analysis of 96-well plates using a robotic arm, thus accelerating inter-sample analysis and ensuring samples are not left outside ideal culture conditions for extended periods of time as was the case with the single sample reads taken by the FACS ARIA II. Should the novel relative killing speed assay be employed in laboratories or in the field, the ACCURI™ would allow a more robust cross-referencing of the relative speeds of novel compounds from one study to the next. The automation, preselected compound and probe treatment parameters as well as preselected gating, ensures that any subjective nature of the analysis is kept to a minimum.

Control samples run alongside the panel of standard antimalarials in the ACCURI™ allowed for the gating limits to be set to isolate i) non-fluorescent parasites (Q1-LL), ii) parasites that are calcein-AM-positive only (Q1-UL), iii) parasites that are PI-positive only (Q1-LR), iv) parasites that are both calcein-AM-positive and PI-positive (Q1-UR). However, in a healthy parasite sample removed directly from ideal culture conditions and treated with calcein-AM, a significant proportion of the stained parasites were detected in Q1-UR (calcein-AM and PI-positive). The same applied to drug-treated parasites. This is unusual as many of the parasites in the sample were being detected as positive events for PI, although PI treatment was omitted in these samples. It is suggestive of cross-fluorescence (bleed-through) and an overlap of emission detection of calcein-AM and PI using a Becton Dickinson ACCURI™ C6 Plus. This

was not encountered in the fluorescence microscopy study, as no dual-staining of any cells was observed. The calcein-AM/PI probe combination is marketed in kit form by various manufacturers (e.g. Sigma-Aldrich and Alpha Laboratories) as an efficient way of identifying live/dead cells in culture. However, these kits are marketed for use with fluorescence microscopy and do not mention flow cytometry applications in the product literature. The excitation/emission maxima of calcein-AM (490/520) and PI (535/617) should be contrasting enough to exclude cross-fluorescence in flow cytometry, and the problem encountered may be specific to the ACCURI instrument used for the current study, which was not further investigated. Although not too problematic – fluorescence events recorded in Q1-UR and Q1-UL could be combined to detect calcein-positive parasites - it did suggest that using the probes in conjunction in co-stained samples would provide inaccurate data as no clear distinction would be possible between calcein-AM and PI-positive events. The probes were thus used separately in subsequent experiments.

In the case of the PI stained samples, the bleed-through phenomenon was not encountered - there was no-cross fluorescence of the PI-positive only events (Q1-LR) into the calcein-AM positive channels (Q1-UL or Q1-UR) using the control sample treated with fixative to compromise membrane integrity. In addition, with the panel of antimalarial drugs, PI produced a more robust differentiation between the speeds of action of the individual compounds. An additional advantage of PI as a vitality stain for malaria parasites is that it does not necessitate saponin lysis to remove RBC interference (although the saponin lysis step was included in this study if co-staining is to remain an option in future, optimized versions the FACS assay). Conceivably, a drawback of PI may be that an extremely potent compound could lead to degradation of parasite structural integrity to the extent where it may no longer be capable of registering as a PI positive event, thus leading to an underestimation of compromised parasites in a sample. Though not investigated, this contributed to the decision to continue using calcein-

AM for corroboration purposes in subsequent experiments (Chapter 4). Together, the two probes confirmed the previous rankings elucidated from fluorescence microscopy and earlier FACS i.e. gramicidin D > artemisinin > mefloquine > chloroquine > doxycycline.

3.4.4 - Filter tube-based assays.

To circumvent the requirement of a flow cytometer and produce a more "user-friendly" assay for wider dissemination, the possibility of using a multi-well fluorimeter to quantitate calcein-AM fluorescence in drug treated parasite populations was briefly explored. This approach was complicated by the need to remove calcein-AM present in uninfected RBCs by selective cell lysis using saponin. As such, a novel method for rapidly removing probe-stained parasites from lysed RBCs by centrifugation in filter tubes was considered. The rationale behind exploring filter tubes was that, in principle, it could be adapted to a medium throughput format using 96-well filter plates i.e. conceptually 96 samples could be simultaneously lysed in the filter-bottomed wells of a donor plate, followed by brief centrifugation in a plate centrifuge to rapidly remove the RBC cytoplasm from the intact parasites in the lysate. After lysis and removal of RBC cytoplasm by brief centrifugation, calcein-AM contained in viable parasites trapped on top of the filters could be extracted by adding Triton X-100 to lyse the parasites, followed by a second brief centrifugation and quantification of calcein-AM in the filtrate using a plate fluorimeter.

Although the ranking of the individual compounds in the panel using this method mirrored that of the microscopy and flow cytometry assays, significant technical problems were encountered. Use of saponin lysate volumes larger than 5 µL led to blockage of the filters and erratic inter-experimental results. This membrane clogging was likely due to cellular debris (RBC ghosts and intact parasites) after saponin lysis overloading the membrane filters. The centrifuge filter tubes used in the assay are most commonly used in pharmaceutical studies in the isolation of

smaller particles such as drugs and other inorganic matter and not necessarily for cellular substances such as residual calcein-AM fluorescence isolated from whole parasite cells (Velmurugan and Selvamuthukumar, 2014). The assay will require further development to circumvent the filter clogging problem. One possibility is to use filters with larger pore sizes (e.g. 1-2 µm as opposed to the 0.45 µm used here), coupled to optimization of cell density in the pRBC suspensions used in the assay. There are other means for removing the RBC lysate from saponin released parasites, notably centrifugation through a phthalate oil mixture (e.g. Khan *et al.*, 2012). However, this method is not adaptable to 96-well plates and requires extensive washing steps and was not pursued.

The problems encountered with the filter tube-based calcein-AM assay extended to the ATP assay, which also required the removal of RBC cytoplasm (and the ATP therein) by saponin lysis and centrifugation in the filter tubes, prior to lysis of the parasites trapped on the membrane filters and quantitation of their ATP content using a firefly luciferase-based commercial reagent. The parasite metabolizes glucose anaerobically and pyruvate is fermented to lactate to produce the required ATP for energy (Olszewski and Llinas, 2011). Measuring malaria parasite ATP levels as diagnostic of drug-induced stress was introduced by Khan *et al.* (2012). The latter study used centrifugation through phthalate oil cushions to separate parasites from RBC lysates but, as discussed above, filter tubes were employed in the current study to explore the possibility of improving throughput using 96-well filter plates. Interestingly, in the Khan *et al.* study, treatment of parasites with mefloquine and artemisinin led to an increase in ATP levels in 8 hours. Their assumption was that it represented increased metabolic activity by the parasite as part of its stress response to overcome detrimental drug effects - the resultant increase in metabolism, and hence ATP production, was proposed to act as a coping mechanism for any stress or cellular damage (Khan *et al.*, 2012; Barouch-Bentov, 2011). By contrast, in the present study ATP levels decreased over 8 hours of drug treatment to an extent that

correlated with the relative speed of drug action. Thus, the artemisinin > methylene blue > mefloquine > chloroquine > doxycycline ranking found with calcein-AM/PI staining and microcopy/flow cytometry analysis was reproduced. It is unclear whether *Plasmodium* parasite-associated ATP levels have been measured as an indication of drug stress in other studies outside of the Khan group. However, ATP levels have been used as indication of selective drug pressure in *Leishmania* parasites and similar results to this study were observed – ATP levels, as well as overall mitochondrial membrane potential, were reduced in drug treated parasites in relation to controlled wild-type models (Garcia-Hernandez *et al.,* 2012). This would then correlate to the decrease in ATP levels observed in this study.

Since the filter clogging phenomenon and consequent difficulties reproducing results inter-experimentally was also found with the ATP assay attempted in the present study, further optimization of both filter tube-based assays was not pursued, in favour of rather employing the flow cytometry assay with the ACCURI 96-well plate flow cytometer for the analysis of experimental compounds (Chapter 4).

3.5 – Conclusion

Changes in parasite staining patterns were quantitatively analysed by fluorescence microscopy and it was observed that a decrease in calcein-AM and increase in PI fluorescence was progressively seen moving from the expected (based on literature reports) slowest acting drug (doxycycline) through to the most rapid acting (artemisinin). These results strongly suggested that the assay was indeed capable of ranking antimalarial compounds based on their relative killing speeds. To increase throughput and quantification of the microscopy-based bioassay it was adapted for use in flow cytometry (initially in a FACS Aria II and then for increased throughput in a Becton Dickinson ACCURI^{TM} C6 Plus) and it was found that the ranking of the panel of drugs mirrored that of the microscopy assay i.e. artemisinin > methylene blue >

mefloquine > chloroquine > doxycycline. Adaptation of the calcein-AM assay for use in a plate reader using filter tubes to rapidly remove background RBC-associated fluorescence as well as alternatively using ATP as a measure of drug stress and associated speed of action provided results that agreed with the microscopy/flow cytometry analyses. These experiments were done as pilot assays as a preliminary to using 96-well filter plates to increase throughput and avoid the need for flow cytometry/microscopy analysis. However, failure to obtain robust inter-experimental reproducibility due to filter congestion caused these approaches to be discarded in favour of the calcein-AM/PI-based flow cytometry method for the analysis of experimental compounds (Chapter 4).

Chapter 4 – Application of the Calcein-AM/Propidium iodide Relative Speed of Action Analysis to Experimental Antimalarial Compounds

4.1 – Introduction

As it stands, the novel relative killing speed bioassay developed in Chapter 3 is fully quantifiable making use of flow cytometry and can assess compounds at medium throughput. The assay provided reproducible data on the ranking of a set of standard antimalarial compounds according to relative killing speed (doxycycline < chloroquine < mefloquine < artemisinin < gramicidin D) and this was based on the ratio of green fluorescent, calcein-positive (live) cells to red fluorescent, PI positive (dead) cells.

This chapter aimed at further validating the bioassay by testing its ability to rank separate sets of novel antimalarial compounds. Furthermore, it aimed to isolate/group novel compounds based on their synonymous mechanism. These compounds included a set of artemisinin analogs obtained from Prof. Richard Haynes (North West University), a set of indolyl-3-ethanone ethers obtained from Dr. Clint Veale (University of KwaZulu-Natal), and a set of compounds with previously demonstrated *in vitro* antimalarial activity intended as starting points for drug development contained in the 'Pathogen Box' supplied by the Medicines for Malaria Venture (MMV).

The PRR assay is the current standard by which the speed of antimalarial drug action is measured as it follows the regrowth of drug treated parasite populations to elucidate the precise killing speeds of these compounds. Although definitive, the assay requires prolonged culturing and is limited in throughput, with the shortened version still requiring 72-hours. To further investigate whether the fluorescent probes identify terminally compromised parasites and validate the findings of the Pathogen Box screen, a recovery assay was carried out. This

involved exposing parasites to the compounds for eight hours and measuring the ability of the compounds to recover from the exposure after an additional 40-hour incubation using the pLDH assay. The five slowest- and fastest- acting compounds present in the Pathogen Box according to the novel calcein-AM/PI-based assay were then scrutinized in the recovery assay to compare the killing speeds and assess the stringency of the novel assay.

4.2 – Materials and Methods

4.2.1 – Experimental compound assessment using calcein-AM/propidium iodide and flow cytometry

The set of standard antimalarial compounds (doxycycline, chloroquine, mefloquine, artemisinin and gramicidin D), novel artemisinin analogs and a set of indolyl-3-ethanone ether antimalarials were incubated with parasite cultures (2-5% parasitaemia, 2% haematocrit) in microfuge tubes at 10 µM (according to the data supplied with the MMV Pathogen Box, the average IC50s of the compounds against *P. falciparum* 3D7 is 0.9 µM) for eight hours. After the incubation the samples were stained with either calcein-AM (5 µg/mL) or PI (3.3 µg/mL) for 30 min followed by saponin lysis. Samples were resuspended in 0.5 mL culture medium before 0.2 mL was transferred to a 96 well, clear plate and analysed in a BD (Becton Dickenson) ACCURI™ C6 Plus flow cytometer. Control samples included paraformaldehyde/glutaraldehyde fixed samples treated independently with PI and calcein-AM as well as healthy parasite samples stained with either PI or calcein-AM. In the case of the Pathogen Box compounds, each was incubated with a parasite culture (2% parasitaemia, 2% haematocrit) in the well of a 96-well plate at 10 µM for eight hours. At the 7.5-hour mark the treated cultures were stained with either calcein-AM (5 µg/mL) or PI (3.3 µg/mL) for 30 min directly in the wells, saponin lysed and transferred to a BD ACCURI™ C6 Plus flow cytometer for analysis. Controls included gramicidin D treated and untreated samples both stained with either calcein-AM (5 µg/mL) or PI (3.3 µg/mL).

The calcein-AM was excited at 488 nm and emission recorded in the 530/30 filter channel, while the 622 nm laser was used to excite PI and emission recorded in the 660/20 filter channel. A total of 100 000 events were recorded for each sample and the data was analysed using Becton Dickinson Accuri C6 Plus (64-bit) software. Dot plots were generated depicting

parasite cell counts as a measure of fluorescent events – PI positive (indicating dead cells) and calcein-AM positive (indicating live cells). Sampling was automated via a robotic arm with a shaking procedure implemented between each sample read.

4.2.2 – Haemolysis assay

A trophozoite-stage parasite culture (2-5% parasitaemia, 2% haematocrit) was treated with a set of standard antimalarial compounds (doxycycline, chloroquine, mefloquine, artemisinin and gramicidin D), the novel artemisinin analogs and a set of indolyl-3-ethanone ether antimalarials in microfuge tubes at 10 µM for eight hours. In the case of the Pathogen Box compounds, the parasite cultures were incubated with each compound in the well of a 96-well plate at 10 µM for eight hours. Post treatment the samples were transferred to a Neubauer haemocytometer chamber for enumeration by light microscopy. Control samples included untreated pRBCs removed directly from routine culture conditions prior to enumeration as well as a sample of lysed RBCs (resuspended in saponin (0.1% [w/v] in PBS) to lyse the RBC membranes). The untreated pRBCs were used as indication of a healthy cell culture.

4.2.3 – Recovery assay

P. falciparum 3D7 parasites were cultured under sterile conditions as described (Chapter 3, 3.2.2). A parasite culture of between 2-5% parasitaemia and 2% haematocrit containing healthy, trophozoite stage parasites was transferred to 24-well plates at 1 mL per well. Control samples included RBCs and healthy, untreated pRBCs. Test samples were treated with 10 µM of the respective compounds which included a panel of standard antimalarials (doxycycline, chloroquine, mefloquine, artemisinin and gramicidin D) as well as the five fastest and five slowest acting compounds in the Pathogen Box. The plates were transferred to an airtight container and gassed with a special gas mixture (5% CO_2; 5% O_2; 90% N_2) before being placed in a 37^{o}C shaking incubator. After eight hours the plate was removed, the cells were transferred

to microfuge tubes and washed in culture medium (CM) to remove the compounds. CM (1 mL) was added to the drug treated parasite pellets and respective control pellets and the suspensions transferred back to 24 well plates after which they were returned to the air tight container, gassed and allowed to incubate at 37^{o}C for an additional 40 hours. Post incubation, the cells in the wells were resuspended and 20 µL transferred to a separate 96-well plate after which a pLDH assay was conducted as described in section 3.2.5 on each sample.

4.3 – Results

4.3.1 – Standard antimalarial assessment at 10 µM

The pilot relative killing speed assay generated a ranking of a set of standard antimalarial compounds all with well-established efficacies. Drug treatment in *P. falciparum* 3D7 parasites was done at 10x IC_{50} to provide a suitably parasiticidal concentration for each specific compound to induce a rapid and distinct response from the vitality probes. This was useful for the pilot assay due to the small number of compounds in the study. However, as a screening tool in the drug discovery arsenal with emphasis placed on increased throughput, it is less practical to test novel compounds in this manner. To avoid preparing separate concentrations of large quantities of varying compounds (depending on whether efficacy is known) and a resultant loss in throughput, a single concentration (10 µM) was adopted for all compounds scrutinized in the assay (according to the information provided with the MMV Pathogen Box, the average IC_{50} of the supplied compounds against *P. falciparum* 3D7 blood stages is approx. 0.9 µM). This concentration was first tested on the panel of standard antimalarials to ensure it was sufficiently parasiticidal and maintained the same relative killing speed ranking observed in the pilot assay which was done at 10x IC_{50}.

Briefly, trophozoite-stage parasites were treated with either artemisinin, doxycycline, chloroquine, mefloquine or gramicidin D for eight hours at 10 µM before staining with either calcein-AM (5 µg/mL) or PI (3.3 µg/mL) followed by saponin lysis. Samples were transferred to a 96 well, clear plate and analysed in a BD ACCURI™ C6 Plus flow cytometer. Control samples included paraformaldehyde/glutaraldehyde fixed samples treated independently with PI and calcein-AM as well as healthy parasite samples removed directly from ideal culture conditions prior to staining with either PI or calcein-AM. Dot plots for the control samples are shown in Fig. 41.

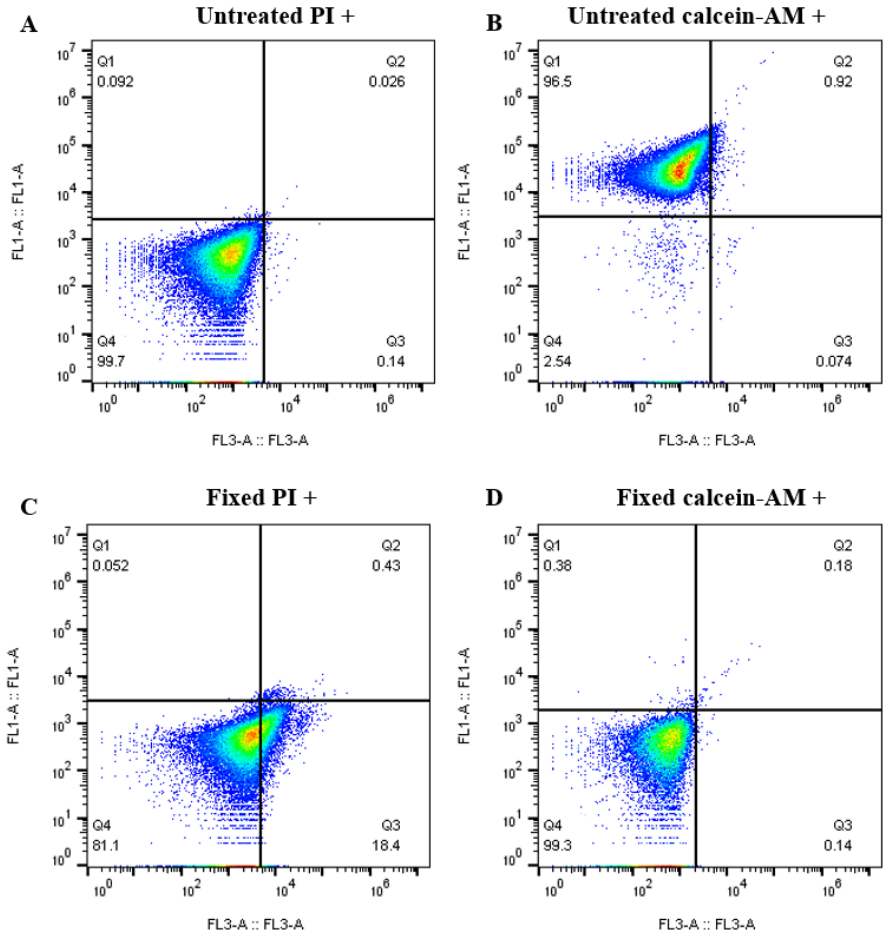

Figure 41: Dot plots for the control samples depicting 100 000 events per panel generated by a Becton Dickinson ACCURI™ C6 Plus flow cytometer. Panels A-D are representative of the four control samples in the relative killing speed assay for the standard antimalarials at 10 µM. Panel A – Healthy parasites treated with PI (3.3 µg/mL); Panel B –Healthy parasites treated with calcein-AM (5 µg/mL); Panel C – Parasites treated with a fixative (3% paraformaldehyde, 0.2% glutaraldehyde in PBS) prior to treatment with PI (3.3 µg/mL); Panel D – Parasites treated with a fixative prior to treatment calcein-AM (5 µg/mL). Saponin lysis was conducted in parasite samples to generate parasite lysates prior to analysis using FlowJo software (FlowJo, LLC, Ashland, Ore.).

The control samples performed as expected with healthy cell cultures showing large scale calcein-AM fluorescence (97% - combining quadrants Q1 and Q2 – Panel B) and negligible PI fluorescence (0% - combining Q2 and Q3 – Panel A). Cultures treated with a fixative resulted in dramatically reduced calcein-AM staining (0% - Panel D) and an increase in PI-positive events representing dead cells (19% - Panel C).

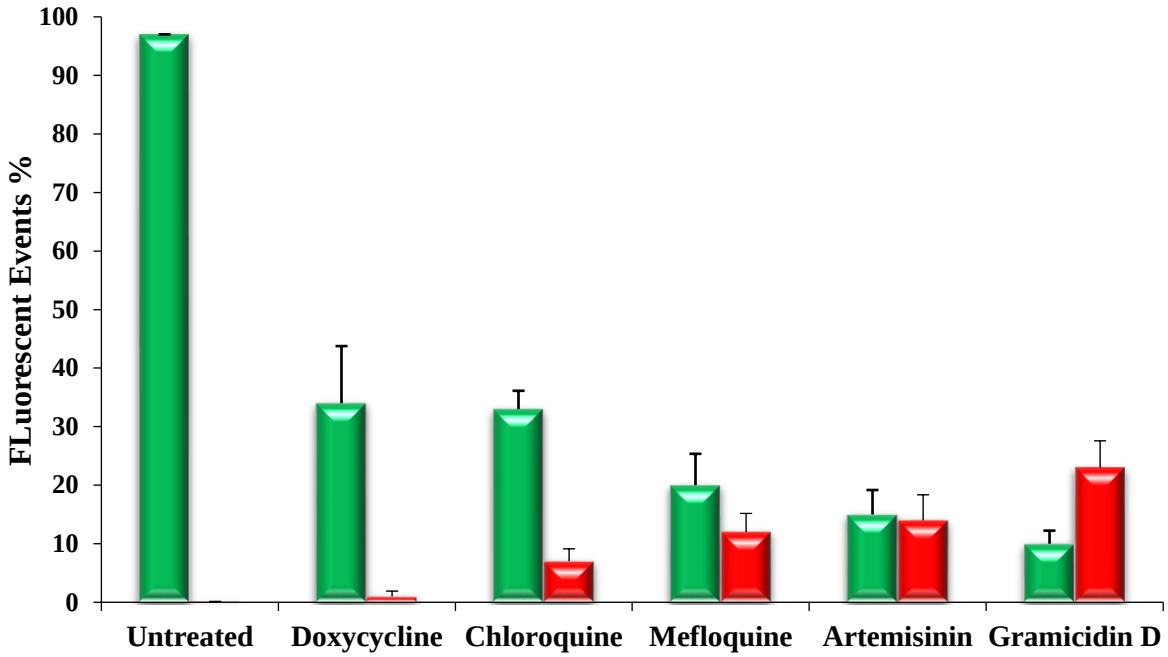

Figure 42: Mean fluorescent events recorded by Becton Dickinson ACCURI™ C6 Plus flow cytometer and representing 100 000 *P. falciparum* cells per sample after an eight-hour drug treatment at 10 µM. Samples were independently treated with either doxycycline, chloroquine, mefloquine, artemisinin and gramicidin D. Post treatment samples were stained with either PI (3.3 µg/mL) or calcein-AM (5 µg/mL) and then saponin lysed after which the number of live fluorescent cells (calcein-AM positive events) to dead (PI-positive events) were counted. Data is representative of three biological replicates each in duplicate and error bars indicate standard error of the mean.

The ranking of the standard compounds according to relative killing speed after an eight-hour treatment at 10 µM (Fig. 42) mirrored the ranking observed when each drug was used at 10x their IC_{50} (Chapter 3). Doxycycline proved to be the slowest acting compound with the highest number of calcein-positive parasites and lowest number of PI-positive parasites, while chloroquine, mefloquine, artemisinin and gramicidin D showed progressively greater impacts on parasite viability over the 8-hour treatment period. The associated dot plot figures for the standard antimalarials treated with calcein-AM or PI can be viewed in Appendix 14.

4.3.2 – Assessment of a set of novel artemisinin analogs

A set of artemisinin analogs (Fig. 43) prepared by the group of Prof. Richard Haynes (North West University) were the first experimental compounds to be assessed by comparing their speeds of action to artemisinin using the novel assay.

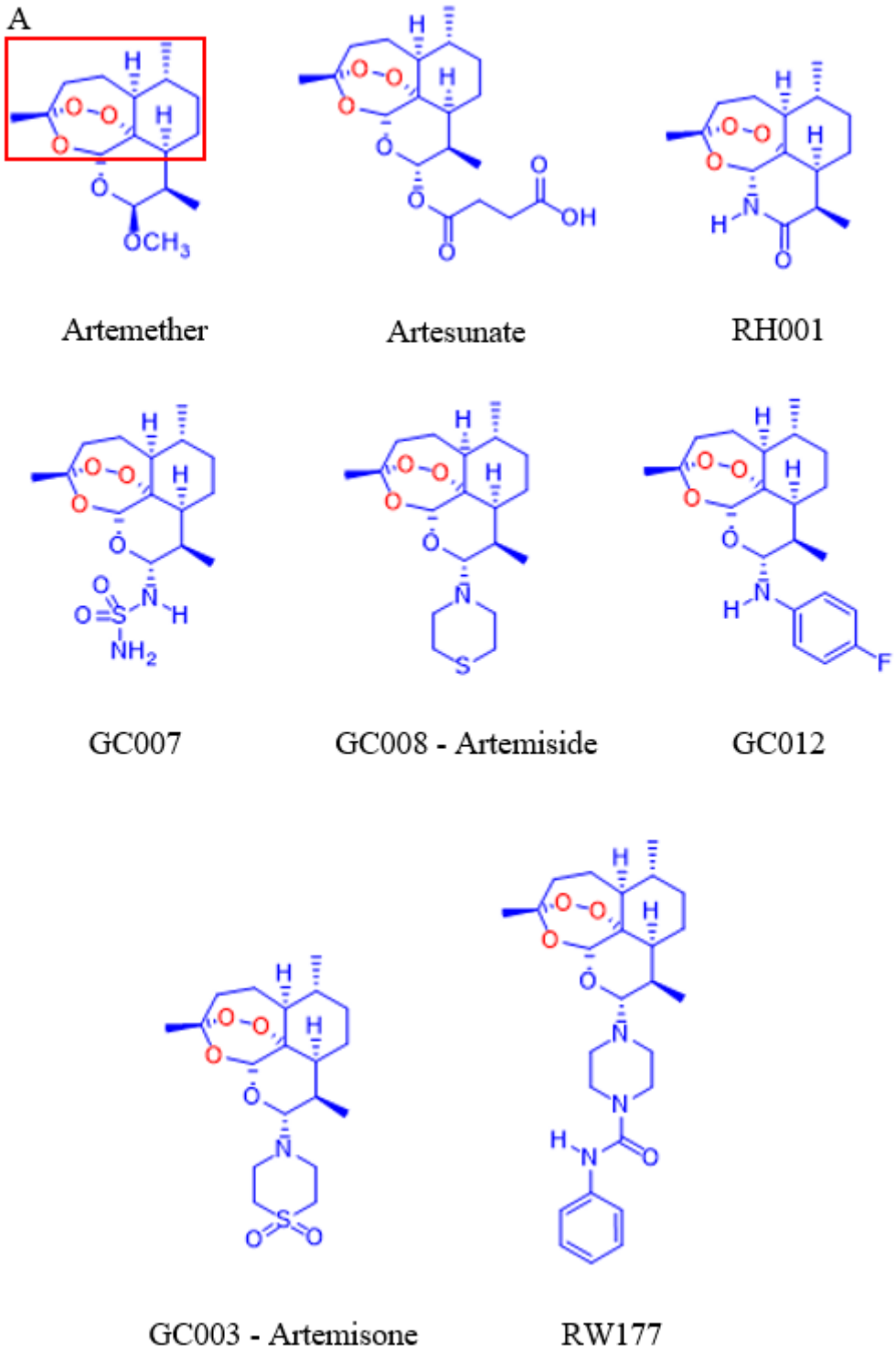

Figure 43: Chemical structures of the panel of novel artemisinin analogs acquired from Richard Haynes (North West University). Common structural elements include a sesquiterpene lactone bridged with an internal peroxide (shown by the boxed structure A for artemether).

Also included in the panel were the standard antimalarial compounds artemether and artesunate. Similar to the treatment with the panel of standard antimalarials, trophozoite-stage parasites were treated with each artemisinin analog for eight hours at 10 µM before staining with either calcein-AM (5 µg/mL) or PI (3.3 µg/mL) followed by saponin lysis. Samples were transferred to a 96 well, clear plate and analysed in a BD ACCURI™ C6 Plus flow cytometer (Fig. 44).

Calcein-AM staining showed more distinct differences across the compound killing speeds in relation to PI – a spread of 24.7% was obtained across the calcein-AM samples as opposed to just 4.6% across all the PI stained samples. This would suggest calcein-AM is a more sensitive probe in detecting the differences in drug stress across similar acting compounds in a single eight-hour time period. Since all the compounds share the sesquiterpene lactone and endoperoxide bridge (Fig. 43), it is likely that they would have similar modes (and thus speeds) of action. It was therefore encouraging to note that all the compounds caused a significant decrease in parasite viability (reduced calcein/increased PI positive events) over 8 hours that was comparable to that obtained with artemisinin. If the changes in calcein-AM staining is used as a guideline, the two artemisinin derivatives that are still widely used antimalarials, artesunate and artemether, produced contrasting killing speeds after an eight-hour treatment period. Artemether appeared decidedly slower with 32% of the recorded parasites being calcein-AM positive in relation to artesunate treatment yielding 16%. This suggests that artesunate is twice as effective in the same time and at a treatment concentration of 10 µM. Including the experimental artemisinin analogs, the relative killing speed as a measure of calcein-AM staining events would lead to a ranking (fastest to slowest) of: GC007 (7% calcein-AM positive events) > RH001 (9%) > GC012 (12%) > GC008 (13%) > artesunate (16%) > GC003 (19%) > artemisinin (19%) > RW177 (20%) > artemether (32%). The events (number of calcein-AM

positive cells recorded by the flow cytometer) were logged as a combined measure of quadrants Q1 and Q2 in each respective dot plot (Appendix 15).

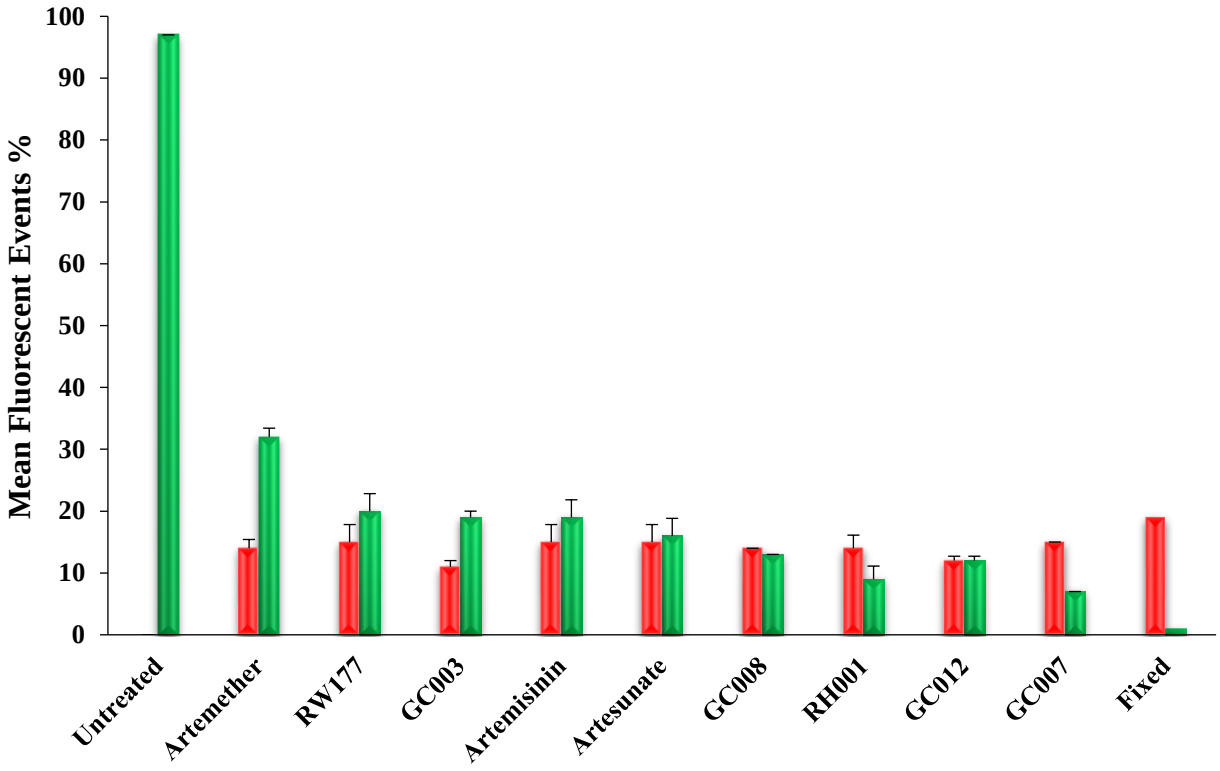

Figure 44: Mean fluorescent events recorded by Becton Dickinson ACCURI™ C6 Plus flow cytometer and representing 100 000 *P. falciparum* cells per sample after an eight-hour drug treatment at 10 µM. Samples were independently treated with either artesunate, artemether, artemisinin, or a set of novel artemisinin analogs – GC003, GC007, GC008, GC012, RH001 or RW177. Post treatment, samples were stained with either PI (3.3 µg/mL) or calcein-AM (5 µg/mL) after which the numbers of live (calcein-AM positive events) or dead (PI-positive events) cells were counted. Data is representative of three biological replicates each in duplicate and error bars indicate standard error.

Aside from a relatively higher number of calcein-AM positive events recorded after artemether treatment, there exists a similar trend in killing speeds across both the established and novel artemisinin compounds. This resulted in a confident ranking of the compounds being difficult to make when considering both the staining patterns observed for PI and for calcein-AM.

4.3.3 – Assessment of a set of indolyl-3-ethanone ether antimalarials

A set of indolyl-3-ethanone ethers that had previously been found to display sub-micromolar IC_{50} values against *P. falciparum* were obtained from Dr. Clint Veale (University of KwaZulu-Natal) for assessment in the relative killing speed assay. As previously described, they were subjected to the novel assay at 10 µM treatment concentration in *P. falciparum* cultures for eight hours. At this point in the protocol the individual samples would have been stained with either PI or calcein-AM prior to analysis. However, it was noted during treatment that the compounds appeared to be haemolytic (Fig. 45).

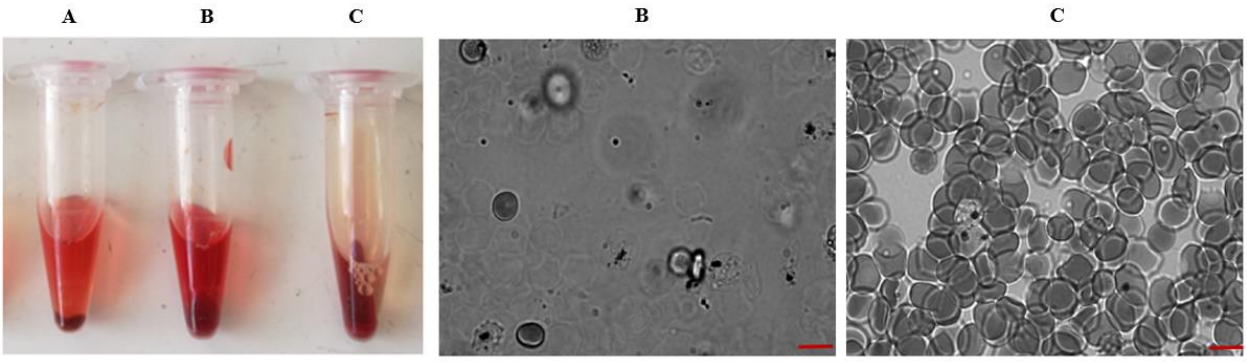

Figure 45: Qualitative examination of haemolysis observed post compound treatment in *P. falciparum*. A – gramidicin D; B – indolyl-3-ethanone ether (code: RLC01-066); C – Artemisinin. Parasite samples were treated with compound at 10 µM for eight hours and microscopy images were obtained using a Zeiss AxioVert fluorescence microscope. Scale bars represent 5 µm. The highest degree of haemolysis can be observed with treatment of RLC01-066 (B) in comparison to gramicidin D (A) and artemisinin (C).

A qualitative comparison of haemolytic activity was conducted by comparing the opacity of the supernatant of drug treated, parasite samples. Artemisinin treatment yielded a relatively clear supernatant displaying no haemolysis after eight hours whereas a cloudy, red supernatant is observed after treatment with a high concentration of gramicidin D (10 µM) in the same time. The experimental indolyl-3-ethanone ethers (RLC01-066 is shown as a representative – Fig. 45 B) yielded significant haemolysis with treatment at 10 µM in the same time and provided an opaque supernatant in relation to gramicidin D and artemisinin. This was

confirmed using microscopy where large scale haemolysis could be seen in the RLC01-066 treated sample (there appeared to be RBC 'ghosts' remaining) in comparison to the artemisinin treated sample which shows intact RBCs. To quantify this observation a haemolysis assay was designed and conducted on the compounds. Given that extensive haemolysis may affect compound speed of action, the assay was also conducted across the standard antimalarial panel and the novel artemisinin analogs described in sections 4.3.1 and 4.3.2 respectively to compare the haemolytic activity.

Parasite samples were treated with each compound in the standard antimalarial panel, each of the novel artemisinin analogs, as well as each of the indolyl-3-ethanone ethers at 10 µM for eight hours. Post drug treatment the samples were transferred to a Neubauer haemocytometer chamber for enumeration by light microscopy. Control samples comprised untreated RBCs and saponin lysed RBC samples (Fig. 46).

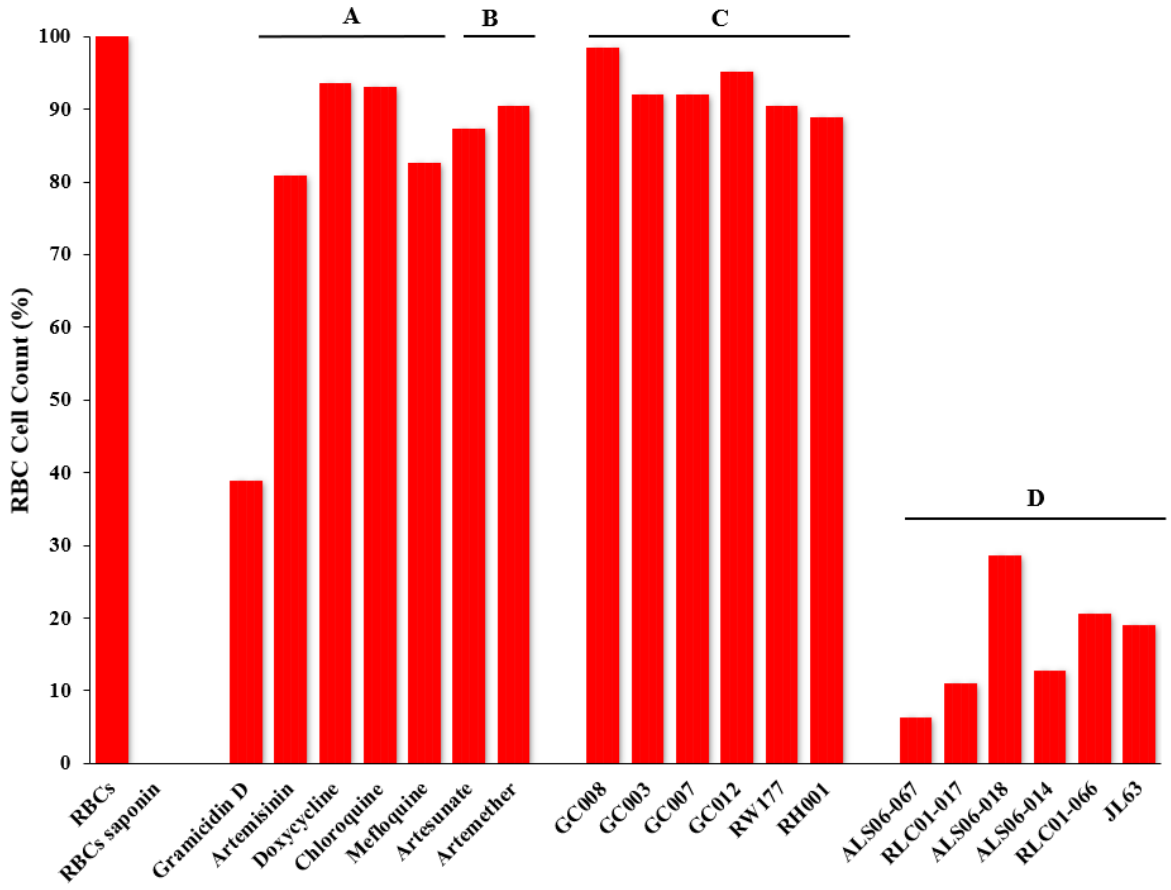

Figure 46: RBC counts indicative of haemolysis observed post-treatment with the individual compounds at 10 µM for eight hours. Untreated RBCs and saponin lysed RBCs acted as positive and negative baselines for cell counts respectively. Compounds included the standard antimalarial panel (set A), two artemisinin derivatives (artemether and artesunate – set B), novel artemisinin analogs (set C) and indolyl-3-ethanone ethers (set D). RBC counts were converted to a percentage relative to the counts obtained with untreated RBCs.

The haemolysis observed after treatment with the indolyl-3-ethanone ethers in the qualitative analysis (Fig. 46) was mirrored during the quantitative study. Little haemolysis was encountered under drug stress using the standard antimalarial panel (with the exception of Gramicidin D, which is known to be a membrane-active peptide) and artesunate, artemether and the novel artemisinin analogs (sets A, B and C). This contrasted with the large scale haemolysis observed after treating with the indolyl-3-ethanone ethers (set D). This provided a dilemma as the antimalarial activity that these compounds have been found to possess could potentially be a result of RBC lysis. As such these compounds were not put forward for testing

in the novel relative killing speed assay, and it also motivated the inclusion of hemolysis assays in the analysis of subsequent experimental compounds (the Pathogen Box).

4.3.4 – Assessment of the MMV 'Pathogen Box'

The 'Pathogen Box' is an initiative funded by the Medicines for Malaria Venture (MMV) containing 400 diverse compounds that all have previously been shown to act against one or more of the organisms responsible for neglected diseases, predominantly kinetoplastids (*Trypanosoma brucei, T. cruzi* and *Leishmania spp.*;70 compounds) and *Mycobacterium tuberculosis* (116 compounds) and is provided as an open source resource to drug discovery scientists. Relevant to this study, it contains 124 compounds categorized as antimalarials. The aim of the work described in this section was to assess the relative killing speeds of the latter compounds via the novel assay and hence identify the most rapid acting that can be prioritized for further study.

Trophozoite stage parasites were treated in parallel with each of the 124 antimalarial compounds supplied by the MMV in the Pathogen Box for eight hours at 10 µM before staining with either calcein-AM (5 µg/mL) or PI (3.3 µg/mL). Samples were then analysed in a BD ACCURI™ C6 Plus flow cytometer. Of the compounds analysed, the five slowest and five fastest acting were identified and their PI/calcein-AM fluorescent events compared (Fig. 47). A comprehensive ranking of all the compounds tested in the Pathogen Box is tabulated in Appendix 16 and 17.

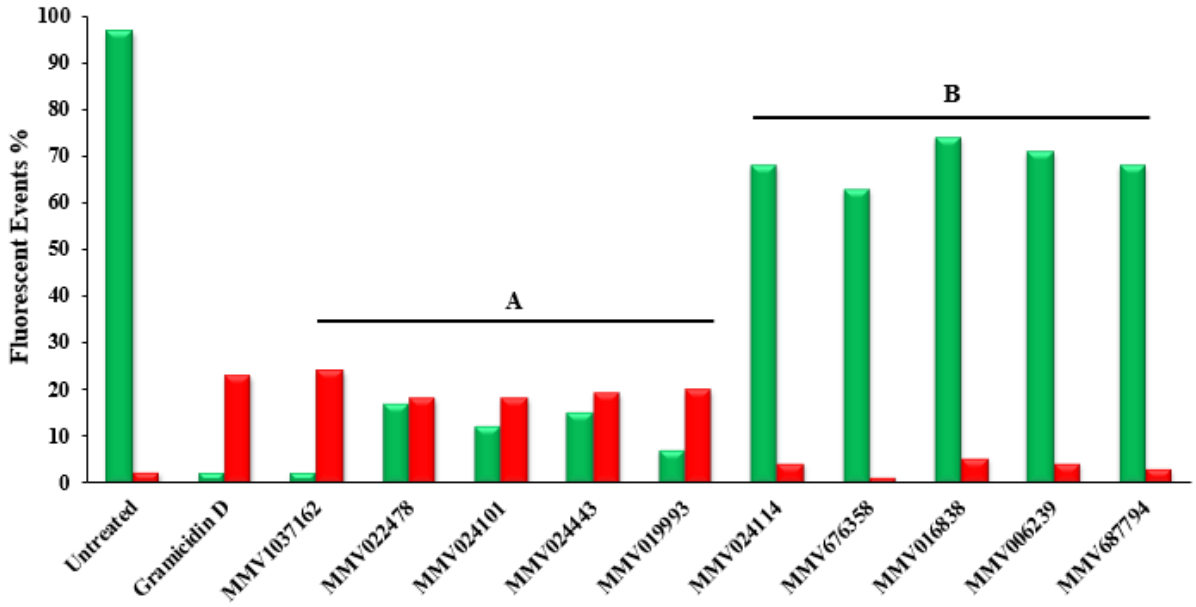

Figure 47: Fastest and slowest acting antimalarial compounds in the Pathogen Box according to the PI/calcein-AM fluorescent event ratios. The five quickest acting compounds (A) exhibited a larger number of PI fluorescent events after eight hours of drug treatment at 10 µM in comparison to the five slowest acting with a larger number of calcein-AM fluorescent events (B). Control samples included an untreated control culture as well as a gramicidin D treated sample.

There was a significant contrast in the effect on parasite viability over 8 hours of the five slowest acting compounds tested in the Pathogen Box and the five fastest. The slowest compounds (Fig. 47, Panel B) recorded an average of 69% of the total number of fluorescent cells counted to be calcein-AM positive as opposed to 11% across the five most rapid acting (Panel A). A similar trend was observed for the PI fluorescent events albeit in reverse. Interestingly, the most rapid acting parasiticidal compound (MMV1037162) provided PI/calcein-AM staining ratios that closely resembled that of gramicidin D.

The chemical structures of the ten identified compounds were obtained to assess whether the relative speed of antimalarial action observed in the flow cytometry study could be attributed to any specific chemical characteristics, as well as to identify any structural commonalities amongst the fastest acting and slowest acting compounds (Fig. 48 and 49 respectively). An

interesting observation was a shared Bromine residue between all five structures of the slowest acting compounds, although consulting the literature did not provide any clues as to possible reasons for this.

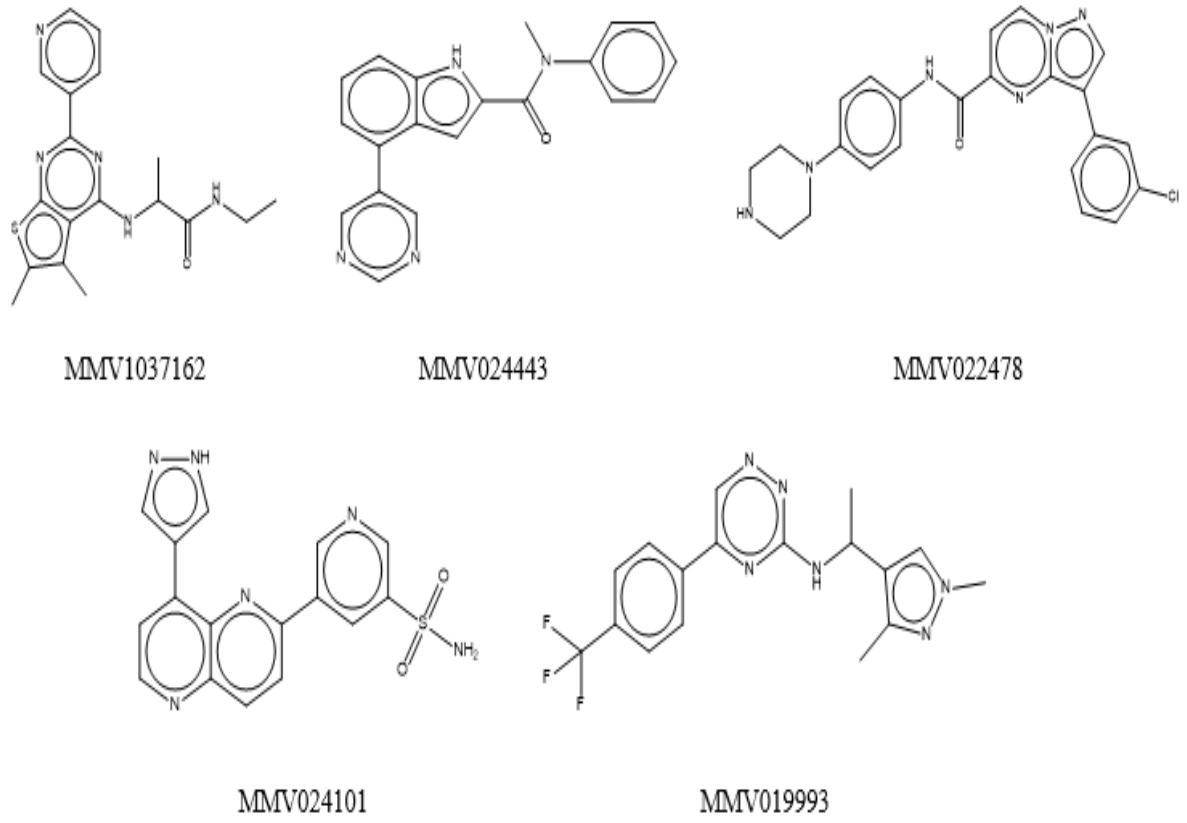

Figure 48: Chemical structures of the five most rapidly parasiticidal compounds according to the novel fluorescent probe assay identified by their MMV Pathogen Box code.

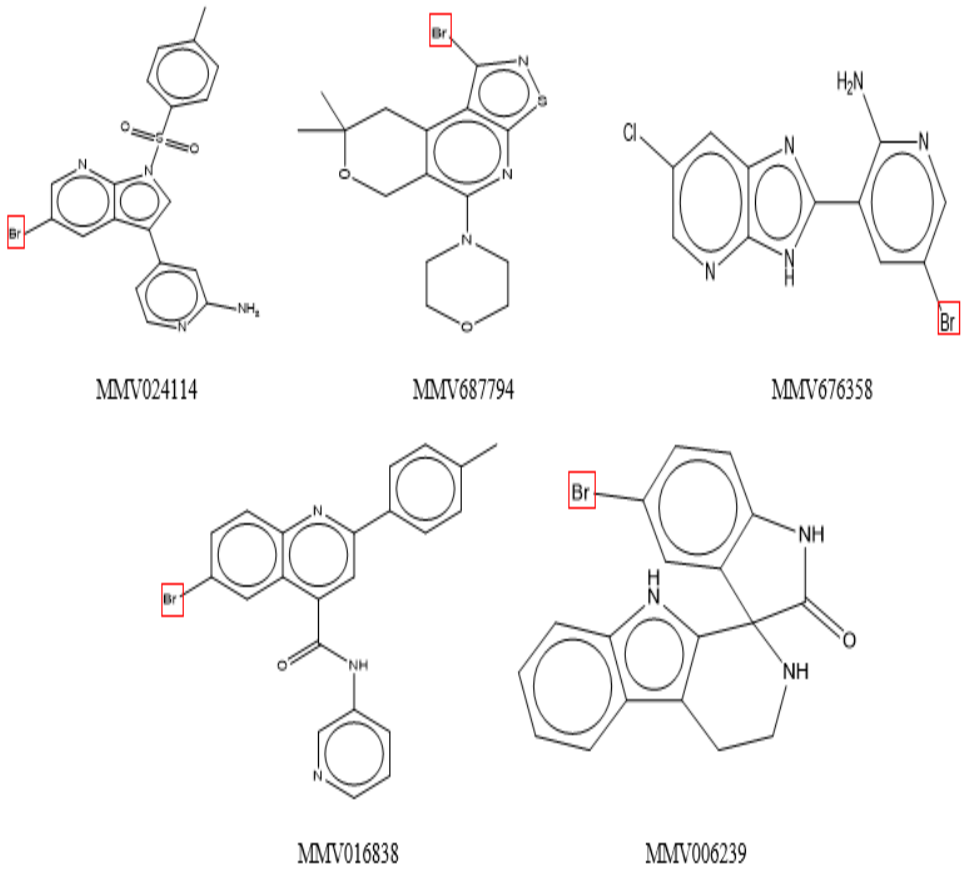

Figure 49: Chemical structures of the five slowest acting parasiticidal compounds according to the novel fluorescent probe assay identified by their MMV Pathogen Box code. A Bromine residue (highlighted) is common throughout the structures.

An additional consideration was whether the relative speeds of action of the compounds reflected their IC_{50} values against *P. falciparum* 3D7 strain parasites (given that they were all tested at a fixed concentration of 10 µM). As shown in Table 6, rapid vs. slow action was not dependent on the IC_{50} values of the compounds reported by the MMV Pathogen Box (http://www.pathogenbox.org). In fact, the most rapid acting compound (MMV1037162) is reported as being the least potent (highest IC_{50} value), which emphasizes that drug potency does not necessarily translate into rapid action.

Table 6: Slowest vs. fastest acting compounds in the Pathogen Box according to the relative killing speed assay and their associated IC_{50}'s.

Slowest acting compounds	*P. falciparum* 3D7 IC_{50} (μM)	Fastest acting compounds	*P. falciparum* 3D7 IC_{50} (μM)
MMV024114	0.6	MMV1037162	2.0
MMV687794	0.3	MMV024443	0.7
MMV676358	1.5	MMV022478	0.8
MMV016838	0.12	MMV024101	0.6
MMV006239	1.3	MMV019993	0.1

To further confirm that the activity and relative speed of action of the compounds tested in the Pathogen Box were not due to any haemolytic effects, the compounds were subjected to the haemolysis assay. As described in section 4.3.3, RBCs (2% haematocrit) were treated with each of the 124 antimalarial compounds in the Pathogen Box at 10 μM for eight hours. After drug treatment, the samples were transferred to a Neubauer haemocytometer chamber for enumeration. Control samples comprised untreated RBCs (negative control) and saponin lysed RBC samples (positive control). Of particular interest was whether the five most rapid acting compounds identified exerted their rapid action by extensive haemolysis, as was found for the indolyl-3-ethanone ethers. The results of the haemolysis assay for these five compounds compared to the slowest acting compounds are shown in Fig. 50. A comprehensive ranking of the haemolytic effects of all the compounds tested in the Pathogen Box is tabulated in Appendix 18.

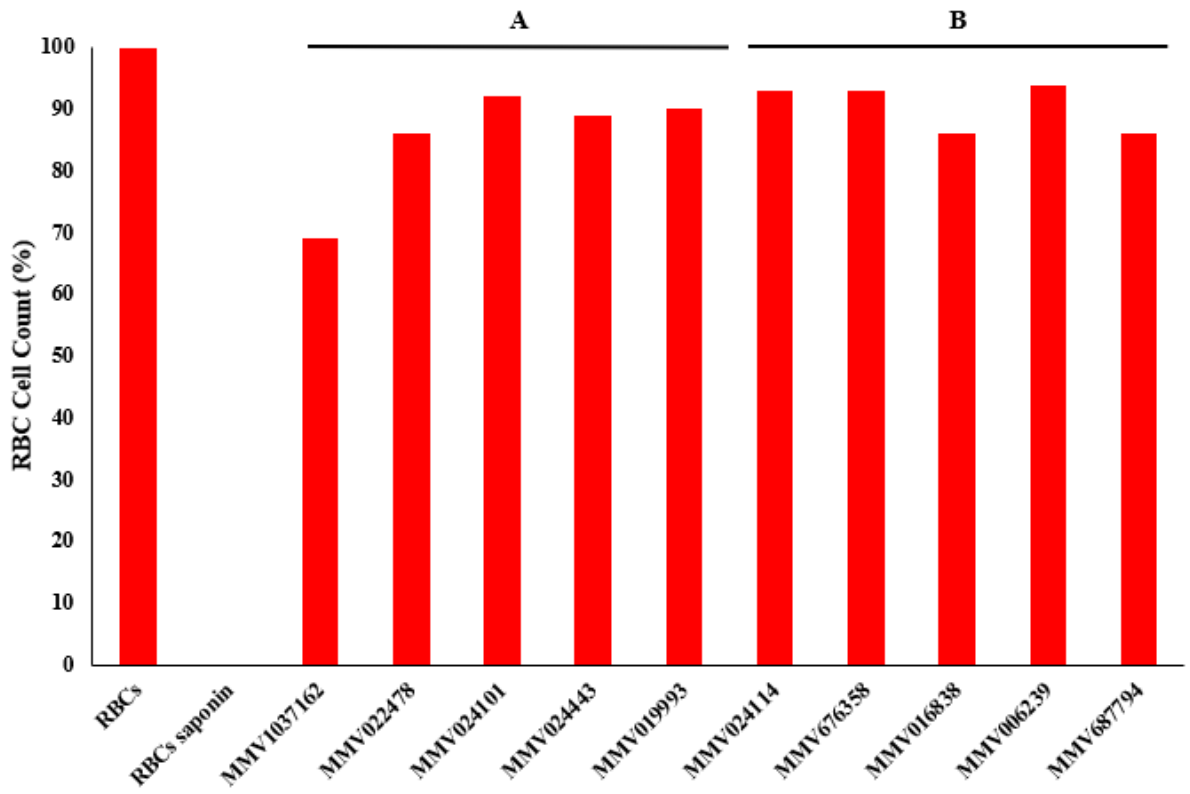

Figure 50: Haemolysis assay of the five most rapid and five slowest acting Pathogen Box antimalarial compounds identified in the novel relative speed-of-action assay. RBCs were incubated with the compounds at 10 µM for 8 hours and counted in a Neubauer chamber (haemocytometer). The graph shows the percentage of intact RBCs (relative to the untreated control) of the five fastest acting set of compounds (A) and the five slowest acting (B). Untreated RBCs and saponin lysed RBCs acted as positive and negative baselines for cell counts respectively.

In contrast to the indolyl-3-ethanone ethers that showed large scale haemolysis after treatment (Fig. 46), the five compounds identified to be the most rapid acting (as well as the five slowest) in the Pathogen Box showed no extensive haemolysis as a basis for their rapid action.

4.3.5 – Recovery assay

To be able to confidently determine whether the reductions in parasite viability observed in the novel relative killing speed assay were accurate indications of compromised vitality and thus validate the Pathogen Box analysis, a recovery assay was conducted. The principle of the assay is to determine to what extent parasites in a drug treated population can recover after 40 hours

from a limited period of drug treatment (eight hours in this study) in a single life cycle. A similar approach to gauge the relative speed of action of antimalarials was used by Khan *et al.* (2011), Ullah *et al.* (2017) and Paguio *et al.* (2011), except in the latter two studies SYBR Green was used to measure parasite levels after the drug-free incubation period, instead of pLDH. Khan *et al.* exposed parasites for 6 hours followed by a 48 hour recovery period, Ullah *et al.* exposed the parasites to drugs for 6 hours followed by a 42 hour recovery period and Paguio *et al.* exposed for 6 hours followed by 48 hours recovery.

4.3.5.1 – Recovery assay using standard antimalarials

Initial assessment of the recovery assay and its correlation with the calcein-AM/PI flow cytometry analyses involved using the panel of standard antimalarial compounds. Early trophozoite stage cultures were treated with each drug at 10 µM for eight hours. Following treatment, the drugs were removed by washing with CM and culturing was continued for a further 40 hours to complete the 48-hour life cycle. Residual parasite levels in the cultures were then assessed using the pLDH assay and compared to untreated control cultures (Fig. 51).

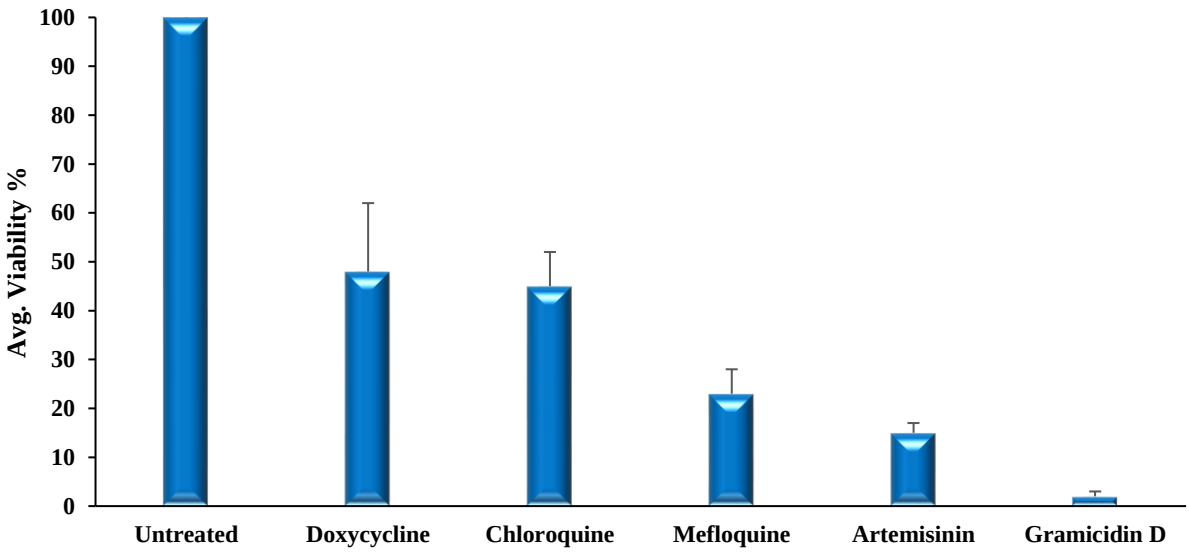

Figure 51: Recovery assay conducted on standard antimalarial compounds. Trophozoite-stage parasites were incubated with the standard compounds at 10 µM for 8 hours, followed by washing to remove the compounds and culturing for an additional 40 hours. A pLDH assay was carried out to determine parasite levels. Comparisons were made to an untreated control of healthy parasites and results are expressed as percentage viability relative to the control. Each data point represents mean ± standard deviation. Data is representative of three biological replicates each in duplicate and error bars indicate standard error

After the 40-hour recovery period gramicidin D treatment showed a negligible parasite viability of 2% in relation to the untreated control followed by artemisinin at 15% which are indicative of rapid speeds of action in 8 hours. Mefloquine ranked third in the panel with 23% viability with chloroquine and doxycycline ranking in fourth and fifth with viabilities of 45% and 48% respectively.

Overall this indicates that, although parasite viability after exposure to each drug was not exactly replicated in each of the assays performed in this study, the relative ranking of the speed of action in the respective assays (fluorescence microscopy, flow cytometry and recovery assays) remained the same: gramicidin D > artemisinin > mefloquine > chloroquine > doxycycline.

4.3.5.2 – Recovery assay using the slowest and fastest acting compounds in the Pathogen Box

To validate the observed relative killing speeds of the Pathogen Box compounds in the novel assay they were compared to the recovery assay to account for any recrudescence observed across a single parasite life cycle. The assay was conducted on the five slowest and five most rapid acting compounds found in the Pathogen Box. As with the standard antimalarials, the ten Pathogen Box compounds were incubated with trophozoite-stage parasite cultures at 10 μM for eight hours, followed by a further 40-hour incubation of the samples without drug before assessing parasite levels in the cultures using the pLDH assay. The remaining parasite viability in each drug-treated sample was expressed as a percentage relative to an untreated control (Fig. 52).

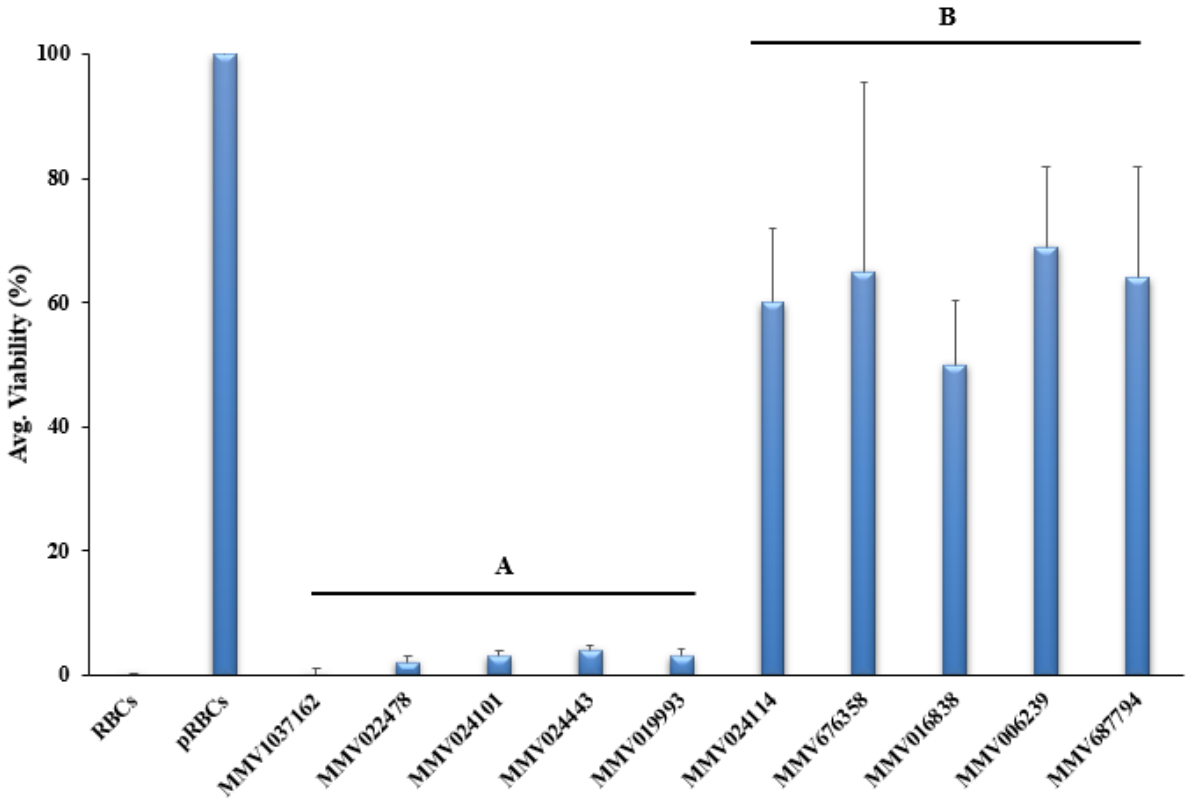

Figure 52: Pathogen Box recovery assay conducted on the 5 slowest and 5 most rapid acting antimalarial compounds in the Pathogen Box. Trophozoite-stage cultures were treated with each of the compounds at 10 µM for 8 hours, the compounds removed by washing, and culturing continued for an additional 8 hours before performing a pLDH assay to determine parasite levels in the cultures. Panel A – the five fastest acting compounds according to the novel assay. Panel B – the five slowest acting. Control samples of unparasitized RBCs and untreated pRBCs acted as negative and positive controls respectively. Results are expressed as percentage viability relative to the untreated pRBCs. Each data point represents mean ±standard deviation Data is representative of one biological sample, in duplicate and error bars indicate standard deviation.

The results obtained provided significant support for the validity of the flow cytometry relative speed of action analysis carried out on the Pathogen Box antimalarial compounds. The parasite cultures exposed for 8 hours to the 5 most rapid acting compounds identified in the earlier screen essentially failed completely to recover during the next 40 hours. By contrast, the 8-hour exposure to the slowest acting compounds only reduced parasite recovery by approx. 40% compared to untreated control cultures.

4.4 – Discussion

4.4.1 – Standard antimalarial assessment at 10 µM

In chapter 3, the relative speed of action of the panel of standard antimalarials was assessed by flow cytometry after an 8-hour incubation at 10 times their IC_{50} concentrations and yielded a ranking of doxycycline < chloroquine < mefloquine < artemisinin < gramicidin D. For the assessment of larger numbers of experimental compounds as was done in this chapter, a fixed concentration of 10 µM was selected. This is similar to concentrations used by others to screen the Pathogen Box for activity against 3D7 *P. falciparum*, *Trypansoma brucei*, *Trypanosoma cruzi* and *Leishmania donovani* (5 – 10 µM; Duffy *et al.*, 2017), *Toxoplasma gondii* and *T. brucei* (10 µM; van Voorhuis *et al.*, 2016), *T. brucei* (10 µM; Veale and Hoppe, 2018), *Giardia lamblia* and *Cryptosporidium parvum* (16 µM; Hennessey *et al.*, 2018) and *P. falciparum* digestive vacuoles (10 µM; Tong *et al.*, 2018). Admittedly this concentration is higher than - antimalarial activity, as opposed to activity against other pathogens, notably when larger compound libraries are used. As an example, a high-throughput screening campaign to identify effective antimalarial compounds undertaken by GlaxoSmithKlein was carried out on *P. falciparum* at 2 µM and led to the identification of 13,000 hits (from an original library of nearly two million compounds) (Gamo *et al.*, 2010).

The studies described above focused on compound efficacy, i.e. discriminating between active and inactive compounds, and not on relative speed of action. As such, it was necessary to ensure that a 10 µM treatment concentration would be suitable to provide a ranking of compounds according to relative killing speed. This was further motivated by the average IC_{50} of the Pathogen Box compounds (as supplied by the MMV) against blood stage 3D7 parasites of 0.9 µM. In addition, Ullah *et al.* (2017) used a maximal treatment concentration of 81xIC_{50} when assessing their panel of drugs for relative speed of action. Therefore, malaria parasites were

subjected to the panel of standard antimalarials at 10 µM (as opposed to 10 x IC_{50} in Chapter 3) for eight hours and their relative killing speed re-assessed using flow cytometry. Reassuringly, the ranking of the compounds was reproduced – the doxycycline treated sample had the highest ratio of calcein/PI positive cells through chloroquine, mefloquine, artemisinin and finally gramicidin D with the lowest calcein/PI positive cells. In fact, a more confident ranking of the compounds could be observed at 10 µM due to the larger differences in calcein and PI positive events. It is however acknowledged that 10 µM may be too low a concentration to see any druggable affect by doxycycline (IC_{50} ~ 12 µM) and hence may provide false assumptions on the compounds rate.

An aspect of the flow cytometry analyses that was encountered with the assessment of the standard antimalarials as well as the experimental compounds (artemisinin derivatives and Pathogen Box) was that, while calcein-AM produced relatively large changes in calcein-positive events after treatment, the same could not be said of PI. This was also found with the aldehyde-fixed control parasites. A healthy parasite sample stained with calcein-AM recorded a total cell count of 97% calcein-positive events while a sample that was treated with the fixative prior to staining saw only 0.5% remaining calcein-positive. Similarly, parasites treated with rapid acting artemisinin and gramicidin D produced a decrease in calcein positive events to 15% and 10% respectively. By contrast, fixed parasites recorded only 19% PI positive events (vs. 0.17% for control parasites), while artemisinin and gramicidin D produced 14% and 23% respectively. A possible explanation is that the fixative and drugs were not only compromising membrane permeability, but also effecting the integrity of the parasites themselves in such a way that only certain parasites remained morphologically sufficiently intact to retain the probe and be registered as PI-positive events. However, based on the microscopy and FACS analyses in Chapter 3 where PI behaved as a robust stain for compromised parasites, a problem may have been optimal detection of PI-stained parasites by the ACCURI flow cytometer used.

Nonetheless, as long as it was borne in mind that approx. 20% was the maximum percentage PI-positive events that would be recorded, PI continued to be employed in subsequent experiments as a useful companion to calcein-AM to compare the speeds of action of compounds.

4.4.2 – Assessment of a set of novel artemisinin analogs

To further explore the utility of the assay, its ability to rank novel antimalarial compounds according to their relative killing speeds was assessed. A series of artemisinin analogs from Prof. Richard Haynes (North West University) were obtained for scrutiny in the assay. Artemisinin and its derivatives are still considered the frontline of defense against modern, resistant malaria (Ahirrao *et al.,* 2016; Kapoti *et al.,* 2018) and since their introduction to the malaria drug discovery arsenal, artemisinin's have been the most effective and rapidly acting of the commonly used antimalarials (Haynes *et al.,* 2006). As discussed previously, there is an alarming emergence of resistance to ACTs. The kelch propeller domain of the gene K13 is a marker of artemisinin resistance and *P. falciparum* isolates collected in Vietnam between 2009 and 2016 resulted in the observation of eight separate point mutations in this domain which is associated with reduced effectiveness of dihydroartemisinin (DHA), particularly in ring-stage parasites (Thuy-Nhien *et al.,* 2017). The development of artemisinin derivatives by the Haynes group and others is an attempt to address resistance, as well as the relatively short *in vivo* half-life of artemisinin.

Structurally the compounds investigated in the panel share the artemisinin core structure of a sesquiterpene lactone bridged with an internal endoperoxide and differentiate in their side chains. As discussed earlier, a multitude of mechanisms of action have been proposed for artemisinin since its discovery, but currently it is widely thought that artemisinin thrives in the iron-rich intracellular environment of the parasite, causing the rapid haem-mediated production

of free radicals which can lead to the prompt breakdown of various cellular systems within the parasite and result in a rapid cell death compared to other antimalarials (Kavishe *et al.*, 2017). Since the endoperoxide bridge is responsible for this mechanism, the derivatives tested in this study should share the same mode of action. It is therefore encouraging that they displayed a rapid speed of action comparable to that of artemisinin, suggesting that although their pharmacokinetics may differ, their pharmacodynamics may result in similar mechanisms of action resulting in similar killing speeds.

If decreases in calcein positive parasites is taken as a yardstick, with the exception of artemether, all the compounds appeared slightly faster acting than artemisinin, with the derivative GC007 being the most rapid. A cautionary note, however, is that the concentration that the panel was tested at was 10 µM. Artemisinin has an IC_{50} of < 20 nM according to this study with other studies showing the novel derivatives to have IC_{50}'s in the same range – 3-54 nM for GC007, GC012 and GC003 (artemisone) (Muller *et al.*, 2015). Therefore 10 µM would have significant toxic effects on the parasites and may result in off-target effects.

The panel consisted of eight compounds, two of which are clinically used – artesunate and artemether. The latter derivatives have been well studied and are currently administered as part of ACTs in the form of Coartem (artemether combined with lumefantrine) or as Coarsucam/Winthrop (artesunate combined with amodaquine) (Gilmore *et al.*, 2014). Artesunate was discovered to be the first water-soluble artemisinin derivative and has been used to treat both severe and uncomplicated forms of malaria (Lin *et al.*, 1995; Jung *et al.*, 2002). However, it was found that in an aqueous environment artesunate became quickly unstable and as such the synthesis of more stable derivatives was prioritized. One such derivative was artemether which contains an ether linkage as opposed to artesunate's ester and boasted greater stability in relation to artesunate, improving the *in vivo* half-life of artesunate

(< 1 hour) to 3 hours (Makanga and Krudshood, 2009; Ahirrao *et al.,* 2018). An active metabolite of artemisinins in dihydroartemisinin (DHA) which is two to three times more active than either artemether and artesunate and conversion of artemether to DHA is less effective than the same conversion for artesunate (Suputtamongkol *et al.,* 2001). Clinical trials have shown artesunate to outperform artemether by displaying a more rapid clearance speed of the parasite and at a 29% lower dose than that of artemether (Suputtamongkol *et al.*, 2001). Duffey *et al.* (2018) recognized the need to not only prioritize research into novel antimalarials with differing modes of action (leading, hopefully, to fewer paths to resistance) but more so to prioritize rapid-acting novel compounds. The group identified artesunate as currently the most effective and most rapidly parasiticidal antimalarial on the market using a modification of the PRR assay. It is therefore interesting that in the current study, based on calcein-AM staining, artesunate appeared to be twice as rapid acting as artemether and also slightly faster than artemisinin.

Two compounds in the artemisinin analogue panel (GC003 and GC008 – artemisone and artemiside, respectively) have already been extensively studied as novel antimalarials and have been used in murine models as well as in clinical trials. Artemisone is a synthetic derivative developed by Prof. Haynes (and collaborators) and after showing promise has since been acquired by Indian pharmaceutical company Cipla. It has a lower IC_{50}, higher bioavailability and longer half-life than artemisinin (Nagelschmitz *et al.,* 2008) and in preclinical trials appears to be more effective than artesunate in the treatment of cerebral malaria (Waknine-Grinberg *et al.,* 2010; Golenser *et al.,* 2017), although there are concerns of neurological and auditory side effects including ataxia and slurred speech (Bhagavathula *et al.,* 2016). Artemiside is produced through the same reaction as artemisone and is in fact its precursor. In some cases, artemiside activity has been shown to outperform that of artemisone and other artemisinin derivatives both in *Plasmodium* culture as well as using murine models (Guo *et al.,* 2012). Both compounds are

able to act against the asexual and sexual life stage of the parasite at low nanomolar ranges and both have recently shown synergism with methylene blue (Coertzen *et al.*, 2018). In the flow cytometry assay, artemiside and artemisone were seen to display comparable speeds of action.

Ultimately it can be said that, in comparison to the staining patterns of both calcein-AM and PI in artemisinin treated parasites, the compounds in the panel display similar speeds of action after eight-hours, the most effective arguably being GC007. Important to note is that the novel compounds do appear to be an improvement (even if slight) over artemisinin in terms of killing speed – a respectable characteristic considering that artemisinin is still regarded as one of the most rapid acting antimalarials.

4.4.3 – Assessment of a set of indolyl-3-ethanone ethers

The indolyl-3-ethanone ethers (donated by C. Veale, Univ. KwaZulu-Natal) were assessed since they have been found to have antimalarial IC_{50} values in the 0.1 – 0.2 µM range (Lunga *et al.*, 2018) and, based on *in silico* docking studies, there is a possibility that they bind to an interesting target - 7,8-dihydro-6-hydroxymethylpterin-pyrophosphokinase (HPPK), an enzyme in the folate synthesis pathway (C. Veale, personal communication). Of the sulfonamide group of antimalarials the most commonly used is sulfadoxine which targets the parasites dihydropterate synthase (DHPS) and, although still used as a treatment in sub-Saharan Africa, has been shown to have reduced efficacy due to parasite resistance (Baraka *et al.*, 2017). Alternative targets in the folate synthesis pathway (a pathway absent from human hosts and therefore an ideal parasite-specific drug target) that have been exploited include dihydrofolate reductase (DHFR) which is inhibited by the antimalarials pyrimethamine and proguanil, but also often contains drug-resistant mutations (Hurwitz *et al*., 1981). Although yet to be validated as a malaria drug target, HPPK (which exists as a bi-functional enzyme with DHPS in *P.*

falciparum) has been the focus of antimicrobial drug discovery projects, notably in *E. coli* and *S. aureus* (Dennis *et al.*, 2016).

During drug treatment it was noted that the compounds had a haemolytic effect on the host RBCs. This was confirmed initially by qualitative observation and then quantitively using a cell count approach after drug treatment in comparison to untreated samples as well parasite samples treated with the artemisinin analogs and the standard antimalarial panel. Explanations for this could encompass several possibilities, including direct binding to and destabilization of the lipid membrane of RBCs. Gramicidin was first utilized as an antimicrobial peptide able to link to and change the composition of cellular membranes resulting in permeabilization and resultant apoptosis (Liou *et al.,* 2015). Finally, it was also observed that gramicidin was responsible for the formation of hydroxyl radicals (previously observed to be the primary cause of death in gramicidin treated *Staphylococcus aureus*) (Liou *et al.,* 2015). However, without further investigation it is impossible to narrow down the exact cause of the lysis observed via the indolyl-3-ethanone ethers. In addition, the haemolysis also does not appear to be a consistent feature of these compounds. In the original study (Lunga *et al.* 2018), no haemolysis was detected and the compounds were non-toxic to HeLa cells at concentrations as high as 500 µM. If the compounds have an inherent tendency to bind to and compromise the integrity of cell membranes, the latter would not have been the case. Studies have shown that some novel compounds may exhibit haemolytic effects as was the case with a set of 9-anilinoacridine compounds that had shown to be promising agents against the parasite's DNA topoisomerase II (in this case at concentrations < 4 µM) (Auparakkitanon *et al.*, 2003). However, at the time of writing no other evidence could be found that attributed RBC lysis as a downside of targeting HPPK.

4.4.4 – Assessment of the MMV 'Pathogen Box'

Towards the end of 2015 the MMV launched a project funded by the Bill and Melinda Gates foundation entitled 'The Pathogen Box' which made a series of compounds and small molecules that had been prescreened by the MMV and its partners available to research groups worldwide for further study (http://www.pathogenbox.org). The intention is that these 400 compounds and the subsequent research generated around them would invigorate momentum towards the discovery of novel drugs against a variety of the neglected diseases. Being open source, this would likely improve the prospect of novel drugs reaching the market. The compounds in the Pathogen Box have previously shown to be effective killing agents using phenotypic screens rather than target-based approaches against each respective pathogen due to the unknown mechanisms of action for the majority of the compounds. Therefore, the Pathogen Box is also provided as a resource to identify new infectious disease targets such that similar compounds may in the future be developed as novel killing agents in their own right using target-based drug discovery approaches.

A large section of the compounds in the Pathogen Box encompassed the most promising compounds found in the 'Malaria Box' – the project launched by the MMV in 2012 and that preceded the Pathogen Box. These compounds were acquired for scrutiny in the novel relative killing speed assay developed in this study. The compounds had already shown significant promise as suitably parasiticidal against malaria parasites at low concentration ranges. A question that arises and was addressed in this study was how the compounds compare to each other with regards to speed of action. A further objective was to determine if the assay in its current form is able to identify fast and slow acting compounds in a larger collection of compounds.

The novel relative killing speed assay was carried out on the series of 124 antimalarial compounds at 10 µM and for eight hours and stained with either calcein-AM or PI before analysis by flow cytometry. As it was noted in previous flow cytometry assays that calcein-AM showed cross-fluorescence into the PI gating channels, samples were not dual stained to avoid any false PI-positive fluorescent parasites after treatment. Of the 124 samples the five slowest and five fastest acting compounds were identified and directly compared to show the potential of the novel assay. The five slowest acting compounds all had a high number of calcein-positive fluorescent cells and low number of PI positive cells after the eight-hour treatment period (averaging of 69% and 3% of the fluorescent events, respectively). If compared to the panel of standard antimalarials this would suggest that these compounds were acting at a slower speed than even doxycycline. In contrast the five fastest acting compounds (averaging 11% calcein-positive and 20% PI-positive cells) compared favorably with artemisinin and gramicidin D, the two fastest acting compounds in the standard antimalarial panel.

The results suggested that MMV1037162 was the most rapidly acting of the antimalarial compounds in the Pathogen Box. Previous studies have shown this compound to be effective in both the asexual parasite stage as well as in gametocytes (one of only five compounds in the Pathogen Box observed to be gametocidal by Duffy *et al.*, 2017). Of particular importance is that the Duffy group noticed haemolysis when assaying blood samples of MMV1037162 treated parasites (the only Pathogen Box compound reported to exhibit this property in their study. To corroborate this, MMV1037162 showed the largest degree of haemolysis in the cell-count assay performed in this study (69% remaining RBC count relative to untreated controls, compared to 86% of the second most haemolytic compound). This may suggest that the rapid onset of parasite death observed in the relative killing speed assay may be attributed to some extent to RBC lysis.

To date, little has been reported on the remaining compounds identified to be the fastest and slowest acting antimalarial compounds in the Pathogen Box. Of the fastest, MMV024443 is an indole-2-carboxamide which has been shown to target the *Plasmodium falciparum* calcium-dependent kinase 1 (CDPK1) (Crowther *et al.,* 2016) while MMV022478 has been shown to also show efficacy against *T. brucei brucei* at low micromolar concentrations (Borbely *et al.,* 2010). MMV022478 is a pyrazolo pyrimidine derivative which has been shown to inhibit mammalian NADPH oxidase 4 (Borbely *et al.,* 2010).

Of the slowest acting, MMV024114 has been linked to folate biosynthesis whereby the compound has been shown to significantly reduce folate metabolism via a mechanism that is not currently known. Subsequent resistance mutations have been observed in *pfcrt* and *pfabcl3* which relate to the development of an efflux-based form of resistance by treated parasites (Cowell *et al.,* 2018). Interestingly, although stated to do so in the Pathogen Box supporting information file, MMV016838 was found not to be active in assays conducted by the Cowell group (2018) against either the asexual or gametocyte stages (Cowell *et al.,* 2018). This could correlate with its identification as one of the slowest acting compounds according to the relative killing speed assay in this study.

In a study conducted by Dennis et al (2018), MMV006239 behaved similarly to KAE609, a *Pf*ATP4 inhibitor, and caused alkalinisation of the parasite cytosol at concentrations < 1 µM (Dennis *et al.,* 2018). It was also noted that MMV006239 shared certain similar structural elements to KAE609 which falls into a group of spiroindolone antimalarials (Dennis *et al.,* 2018). In this study however, it was observed to be one of the slowest acting compounds. It was noted in the Rottman study that the observations on killing speed and efficacy were made in schizont-stage parasites and this could explain why the killing speed was observed to be slower in the relative killing speed assay (the assay focused on trophozoite-stage cultures).

4.4.5 – Recovery assay

In this chapter, the calcein-AM and PI flow cytometry assay was found to be able to rank a small panel of standard antimalarials according to their expected speeds of action, to show that a set of artemisinin analogs that all contain the sesquiterpene lactone endoperoxide structure and likely share the same mechanism of action are all able to rapidly affect parasite viability at speeds comparable to artemisinin, and to identify the fastest vs. slowest acting antimalarial compounds in the Pathogen Box. An important consideration that remained was to attempt to gauge the accuracy and validity of the assay in general, and of the Pathogen Box analysis in particular, by using an independent methodology. With the PRR assay, Sanz *et al.* (2012) have championed the principle of measuring regrowth of parasites after an exposure to drug for a defined period of time (recrudescence) as a means for determining antimalarial speed of action. In order to account for parasite recrudescence in a single life cycle, a recovery assay (which shortens the drug exposure time to 8 hours and measures parasite regrowth using a pLDH assay 40 hours later), was used to assess the results obtained with the standard antimalarial drugs and Pathogen Box compounds. A similar approach was used by Khan *et al.* (2012), Ullah *et al.* (2017) and Paguio *et al.* (2011), to assess the relative speed of action of antimalarials, although the latter two studies employed the SYBR Green assay to measure parasite levels after the drug-free incubation period.

Parasite cultures were treated with each respective drug in the standard antimalarial panel or the 5 fastest and 5 slowest acting Pathogen Box compounds for eight hours after which samples were returned to culture and remaining parasite viability assessed after 48 hours. Reassuringly, in the case of the standard antimalarials, the comparative speeds of action found agreed with previous experiments. Interestingly, the parasites able to recover from doxycycline treatment were only 1% more than that observed after chloroquine treatment. It was observed using

microscopy and FACS that doxycycline was significantly slower acting in relation to chloroquine (and the other drugs in the panel). This would be a concern in determining the killing speeds of slower acting antimalarials (such as doxycycline) that only show visible effect on parasites in the life cycle immediately following that in which drug stress is applied, as has been proposed for drugs acting on the apicoplast of the parasite. Fortunately, this does not diminish the novel killing speed assay in which the aim was to achieve a ranking of antimalarials such that the most rapid could be identified.

In the case of the Pathogen Box compounds, the five fastest acting compounds yielded an average viability of 5% in comparison to an average of 60% for the five slowest acting compounds. Interestingly, this correlates reasonably well with the percentage of parasites that were positive for calcein (i.e. viable) in the flow cytometry analysis – 11% (on average) for the rapid acting compounds and 69% for the slow acting compounds. Overall, the net viabilities appeared to be lower than the average fluorescent events observed in the flow cytometry study. This could relate to fewer parasites being able to fully recover after drug treatment and complete a second life cycle, even though they were still sufficiently viable to retain calcein after 8 hours. A consideration of the assay is that it would not detect parasites that have survived the drug exposure and only start proliferating after 48 hours. Nevertheless, overall the five fastest acting compounds identified via flow cytometry using PI and calcein-AM could be robustly distinguished from the five slowest acting when assessed via the recovery assay.

4.5 – Conclusion

Using calcein-AM and PI as vitality indicators, the assay produced reproducible fluorescence data on the set of standard antimalarial compounds used to treat samples of *P. falciparum* parasites at 10 µM for eight hours. As was the case in Chapter 3 (at 10xIC_{50}) the compounds were ranked in order of killing speed from doxycycline being the slowest to artemisinin the

fastest. A series of artemisinin analogs obtained from Prof. Richard Haynes (North West University) were scrutinized in the assay with comparable staining patterns observed across both the novel compounds and the parent drug – artemisinin. This implied the compounds had similar speeds (and potentially mechanism) of action. Assessment of a set of novel potential HPPK inhibitors obtained from Dr. Clint Veale (University of KwaZulu-Natal) was hindered due to the onset of haemolysis during early stages of drug treatment. Investigation into a set of 124 antimalarial-like compounds obtained as a subsection of the Pathogen Box supplied by the MMV yielded ten 'hit' compounds that were explored further in this study. Five of these compounds were significantly more rapid acting in relation to the panel and five were significantly slower. Of the five rapid acting compounds, MMV1037162 was identified as the most efficient after eight hours although some minor haemolysis was noted (and confirmed by Duffy *et al.*, 2017). The novel assay was compared to a recovery assay to measure parasite recrudescence over a single life cycle and these results mirrored what was observed in the relative killing speed assay and hence validate these observations, further confirming the development of a novel, accurate, improved-throughput, quantifiable, relative drug killing-speed bioassay.

Chapter 5 – Concluding Discussion

Although both curable and preventable, malaria remains one of the diseases with the widest impact, with just over half the world's population living in regions at risk of infection. Of these areas many overlap with some of the poorest economic and social climates where access to means of prophylaxis and therapy can be difficult and the cost of antimalarial medication is not feasible in relation to income. With the emergence of large-scale resistance to existing drugs (most notably to artemisinin in recent years – the last line of defense in the antimalarial arsenal) there has been renewed effort in the discovery/development of novel antimalarial compounds. These efforts have been championed by both public and private partnerships including the Medicines for Malaria Venture and the Bill and Melinda Gates Foundation and have resulted in the discovery of thousands of novel natural/synthetic compounds. The generation of these large compound libraries led to their use in high-throughput screening (primarily phenotypic, although in some cases target-based) to group compounds based on similar efficacy or hypothesized target/mechanism. However, due to the complexity, cost and high attrition of the drug development process, many of these compounds remain in databases and literature unpursued, while instead focus has been placed on developing drug cocktails of existing antimalarials to develop new combination drug therapies. Due to ongoing as well as emerging resistance coupled with the area-specific issues associated with malaria endemic regions (e.g. the requirement for multiple dosages to affect parasite clearance), new antimalarials should ideally have the fastest possible speed of action in order to maximize efficacy and minimize the potential for resistant parasite selection and dissemination.

Defining parameters for the next-generation antimalarials have been laid out by Burrows *et al.* and prioritize speed of action for novel candidate compounds targeting the asexual stage parasite (TCP-1s). A TCP-1 compound is a critical component of SERCaP and hence

techniques are required with which to rapidly identify fast-acting antimalarial-like compounds. Previous assays developed by Sanz *et al.* (PRR assay) and Le Manach *et al*. pushed forward this agenda and although being important additions to the malaria drug discovery arsenal, they remain slow and/or low-throughput. The BRRoK assay assessed a compound's initial cytocidal action (within six-hours) such that compounds may be benchmarked against a panel of existing antimalarials for which killing speeds are known. In this way a relative speed of kill could be achieved as a means to triage a compounds speed of action against the minimal requirements for ideal TCP-1 candidates. Similar to the BRRoK assay, the assay described in this thesis involves exposing trophozoite stage parasites to antimalarial compounds for eight-hours, after which parasite viability is determined using fluorescent vitality probes and flow cytometry

Of the four probes chosen for assessment in the pilot assays, calcein-AM and propidium iodide provided the most robust and reproducible data when it came to staining viable and nonviable mammalian cells respectively. Using fluorescence microscopy, a panel of eight anticancer compounds were assayed against HeLa cells and ranked according to killing speed based on the staining patterns observed using the two probes. The assay aimed to essentially separate the compounds into groups of slow-, medium- and rapid-acting instead of defining exact time points of cell clearance. The ranking obtained from the microscopy assay resulted in a novel Arf6 inhibitor (nav2729) showing the quickest efficacy, and the C-terminal Hsp90 inhibitor novobiocin having the slowest speed (in relation to compounds in the panel). Interestingly, these results were mirrored using calcein-AM to measure relative killing speeds of the same set of compounds in a plate reader, which accelerates data acquisition by avoiding fluorescence microscopy analysis and cell counting and improves throughput by using 96-well plates. By including more compounds in the panel and using this fluorescent probe-based assay to group them according to relative killing speed, a library of compounds can be generated where the most rapid acting can be prioritized for further study. This may have relevance to cancer drug

discovery. If the mechanism of action of test compounds are known (as was the case in this study), the assay could be used to identify targets that are likely to have the most rapid effect on cancer cell viability. Although HeLa cells were used as a model system in this study, there is no *a priori* reason why it may not be applicable to other cancer cell types and may also be employed to compare the speed of action of compounds on cancer vs. normal cell lines. Related to the latter point, conceptually an additional application could be to assess the relative speed of activity of cytotoxic compounds. For example, if a compound has a rapid relative antimalarial speed of action but exerts cytotoxicity over a longer period, it could provide a "therapeutic window" of activity (provided the pharmacokinetic behavior of the compound is appropriate, *i.e.* short half-life). An interesting finding was that the commonly used resazurin (Alamar Blue) cytotoxicity assay could also rank the compounds according to relative speed of action when used at shorter time-points. The difference was that the assay detected cytotoxic effects - a decrease in the ability of the cells to reduce resazurin to resorufin, likely reflecting compromised metabolic activity - earlier than the fluorescent probes, which rely on a disruption of membrane impermeability. While the latter likely represents a terminal degradation of cell viability, the question remains whether the decreased reducing potential of the cells revealed by resazurin is irreversible. This can be investigated in future studies (e.g. using a cell recovery assay similar to the PRR assay) and might make the resazurin assay more attractive to labs established in the field or the poorer malaria endemic regions where access to the costlier fluorescence probes and a fluorescence microscope/fluorescence plate reader may be problematic.

Using the same fluorescent vitality probes in malaria parasites provided similar indications on cellular vitality as was observed in mammalian cells. Calcein-AM and PI were able to rapidly (in relation to current assays) and quantitatively (using both fluorescence microscopy and flow cytometry) separate a panel of standard antimalarial compounds based on relative killing speed.

The results reflected expected efficacy speeds (based on literature reports) whereby doxycycline showed little effect in an eight-hour treatment window in comparison to the fastest acting compound and current gold standard for malaria treatment, artemisinin. Adaptations of the assay to a plate reader using filter tubes did not prove fruitful, which may represent a challenge in implementing this assay in malaria endemic regions with the necessity for flow cytometry or fluorescence microscopy analysis. From this perspective, it may be useful in future to re-visit the methodological approach used and attempt to develop a plate reader-based assay using the probes. In principle, throughput and data acquisition time may also be improved by using a high-content analysis fluorescence microscope. However, high-content imaging platforms are likely to be even more inaccessible for routine analysis than fluorescence microscopes or flow cytometers.

When assaying a set of novel antimalarial compounds, the assay proved sensitive enough to separate a panel of artemisinin analogs based on relative killing speed. Although the speeds were similar, as would be expected from compounds with similar scaffolds, subtle differences in the staining patterns of both calcein-AM and PI suggested that artemether was the slower acting, compared to GC007 and GC012 which appeared both faster acting than artemisinin. Nonetheless, it is encouraging in terms of the validity of the assay that all these endoperoxide-containing sesquiterpene lactones (which included artesunate) revealed rapid speeds of action comparable to artemisinin. When investigating the antimalarial compounds found in the Pathogen Box, a group of five compounds were identified as being significantly slower than the rest in the panel, as well as five compounds that were significantly faster. This is important, as knowing which of the compounds in the panel are more rapid acting could ensure swift relief from patient symptoms, minimize the occurrence of mutations potentially leading to drug resistance mechanisms and could also reduce dosages required for complete parasite clearance. A cautionary note was that the most rapid acting compound (MMV1037162) also displayed

hemolysis (corroborating a similar finding by Duffy *et al.*, 2017) and argues for the inclusion of hemolysis assays when assessing speed of action. Importantly, analysis of the five most rapid and five slowest identified Pathogen Box compounds using a modified PRR assay (assessing parasite re-growth after an 8-hour drug exposure by a pLDH assay) confirmed their rapid vs. slow speeds of action. The assay also confirmed the ranking of the standard antimalarials obtained previously. It provides a reassuring validation of the Pathogen Box analysis and the novel calcein-AM/PI flow cytometry assay method used.

To increase throughput to screening larger compound libraries, a group in 2015 developed a killing speed assay that incorporated fluorescent dyes and flow cytometry to assess a set of standard antimalarial compounds as well as 20 compounds from the 'Malaria Box' (MMV) (Linares *et al.,* 2015). Parasites were cultured in the presence of the compounds for 24- and 48-hours before removing the drug and adding a sample of erythrocytes pre-labelled with CFDA-SE (an intracellular dye capable of staining the erythrocyte cytosol) to differentiate them from pre-drug-treated erythrocytes. The ability of the parasites to reestablish infection in labeled erythrocytes was then tracked after tagging the parasite DNA with Hoechst DNA stain and quantification via dual-staining flow cytometry. The ability of the test compounds to clear the parasites in 24- or 48-hours was determined by counting the number of dual-stained parasitized erythrocytes which would have resulted only after the establishment of new infections (Linares *et al.,* 2015). Essentially, thus, like the PRR assay, it measures the ability of parasites to recover from an initial period of drug exposure. This is an improvement on existing assays in terms of increased throughput potential using 96-well plates with each well containing a different compound. However, in the assay developed in this thesis study, all wash steps were circumvented (the above assay requires wash steps to remove drug) and cells were treated with drugs, stained with the vitality probes and saponin lysed by directly adding the appropriate reagents to the plate wells and then transferring the plate to the flow cytometer. Additionally,

the time it takes to perform the above assay from start to data acquisition compared to the assay described in this thesis is greatly improved (relative killing speed assessments obtainable in 8 hours vs 96 hours).

As cautioned by Sanz *et al.*, the assay does not rely on metabolic activity or enzyme/DNA content as surrogates for parasite viability, but detects compromised membrane permeability. Although not formally tested, this likely represents a terminal disruption of parasite viability. As with the BRRoK assay, it allows results to be obtained in less than a day as well as the simultaneous evaluation of multiple compounds. An advantage over the BRRoK assay is that it does not require the preparation of transgenic parasites expressing firefly luciferase. However, caveats it shares with the BRRoK assay is that it does not consider possible stage-specificity of compounds (trophozoites are used in all instances). For example, the speed of action of compounds that act preferentially on ring stages may be underestimated or undetectable, while compounds that have little or no activity in the ring stage may be identified as fast acting in the assay, but have a compromised speed of action when used *in vivo* (depending on the stage the parasites are in when the compound is administered). In addition, unlike the PRR assay, the assay does not determine the absolute speed of action of individual compounds, but the comparative speed of action vis-à-vis other experimental compounds and standard antimalarials. Nonetheless, it does allow a preliminary selection of potentially fast acting experimental compounds from larger collections for further studies. These may include medicinal chemistry projects to optimise efficacy and pre-clinical performance, mode of action studies to identify targets (clearly the targets of compounds that have fast actions may be particularly important for maintaining parasite viability), as well as a more thorough investigation of the speeds of action of the compounds using the PRR assay.

A recent study by Duffey (2018) described the discovery of a novel amicarbalide derivative, SC83288, for the treatment of severe malaria. Of pertinence to this study is the emphasis placed by the researches on prioritizing the discovery of novel antimalarials that are effective at low nanomolar concentrations coupled with rapid killing speeds. Therefore, when assessing SC83288, both efficacy, as well as clearance speed, were evaluated before being deemed a suitable candidate antimalarial for trials in murine models. The killing speed of the compound was scrutinized using both the Le Manach and Linares methods mentioned above which resulted in the process being significantly low in throughput as well as labour-intensive (Duffey *et al.,* 2018). Nevertheless, this study showcased the current focus of researchers to not only find attractive new compounds to add to the drug discovery arsenal, but the importance being placed on speed of efficacy. Novel assay techniques, such as the one proposed in this study, will aid researchers in making quicker decisions on novel compound killing speeds and quicken the drug development process in terms of prioritizing rapid acting compounds. This study has also provided data on the relative killing speeds of novel antimalarial compounds found in the Pathogen Box which may act as benchmark references for future studies and form the basis of the next generation of fast acting antimalarials that could be used to combat modern, resistant malaria.

Appendix

1. Thawing solution A – 10% NaCl solution

In 1 mL of sterile water, 100 mg of NaCl (Sigma-Aldrich, Germany) was solubilised and filter sterilised in a 0.22 µm filter and stored at 4^{o}C.

2. Thawing solution B – 1% NaCl solution

In 5 mL of sterile water, 50 mg of NaCl (Sigma-Aldrich, Germany) was solubilised and filter sterilised in a 0.22 µm filter and stored at 4^{o}C.

3. Fresh RBC's

Blood was extracted from volunteers in SGVac K2EDTA 9 mL collection vials after ethical approval was signed by the volunteer using compliance forms approved by the Rhodes University ethics committee. Immediately after extraction the blood was transferred to a 50 mL falcon tube and placed at 4^{o}C until two layers were clearly visible – the serum layer containing plasma and white blood cells and the lower layer containing the fresh RBC's. The serum layer was aspirated leaving behind the RBC pellet. The pellet was washed in CM and centrifuged at 3000 rpm for 5 min to further isolate and remove any residual serum. A 2 mL layer of CM was left above the fresh RBC pellet and the tube was placed at 4^{o}C for use up to two weeks.

4. Complete culture medium – CM

In a sterile 50 mL falcon tube, 2 g of glucose (Sigma-Aldrich, Germany) and 2.5 g of AlbuMax II (Life Technologies, USA) were solubilised in 50 mL of RPMI 1640 medium with 25 mM Hepes and 2 mM L-glutamine (Lonza, Belgium). In an Eppendorf tube, 44 mg of Hypoxanthine (Sigma-Aldrich, Germany) was added to 1 mL of 1 M NaOH before being transferred to the 50 mL falcon tube. After the glucose and AlbuMax had completely solubilised, 300 µL of

Gentamicin (50 mg/mL – Lonza, Belgium) was added and the final solution filter sterilized through a 0.22 µM filter before being added to 450 mL of RPMI 1640 medium and stored at 4^{o}C.

5. Giemsa stain

A 5% working solution of Giemsa was prepared from 5 mL Giemsa solution (Sigma-Aldrich, Germany) in 45 mL of 1 X phosphate-buffered saline in a 50 mL falcon tube and wrapped in tin foil to minimize light exposure.

6. Sorbitol solution – 5%

In a 50 mL falcon tube, 2.5 g of D-Sorbitol (Sigma-Aldrich, Germany) was solubilised in 50 mL of distilled water and filter sterilized through a 0.22 µM filter before being stored at 4^{o}C.

7. Drug stock solutions

A panel of standard anti-malarial drug compounds were purchased from Sigma-Aldrich, Germany and solubilized to a concentration of 20 mM as per the following profile – chloroquine and doxycycline in sterile water, mefloquine and artemisinin in methanol, methylene blue in ethanol and gramicidin D & S in DMSO. These stock solutions were stored at -20^{o}C. Intermediate solutions were prepared on the day of use as per the IC_{50} profile of each drug.

8. Vitality probe solutions

Vitality probes including TMRE, PI, hydroethidine and calcein-AM were purchased from Sigma-Aldrich, Germany and solubilized to a concentration of 1 mM in DMSO. These stock solutions were stored at -20^{o}C.

9. Malstat solution

In 80 mL of sterile distilled water, 4 g of L-lactate (Sigma-Aldrich, Germany), 1.32 g of Trizma base (Sigma-Aldrich, Germany), and 22 mg of 3-acetylpyridine nicotinamide adenine dinucleotide (APAD; Sigma-Aldrich, Germany) was solubilized. The pH of the solution was adjusted to 9 and 400 µL of Triton-X 100 was added. The volume was adjusted to 200 mL and stored at 4^{o}C.

10. NBT/PES solution

In 100 mL of sterile distilled water, 160 mg of nitro blue tetrazolium (NBT; Sigma-Aldrich, Germany) and 8 mg of phenazine ethosulphate (PES; Sigma-Aldrich, Germany) was solubilized and stored at 4^{o}C in a Schott bottle wrapped in tin foil to minimize light exposure.

11. CellTitre-Glo reagent

The CellTitre-Glo Luminescent Cell Viability Assay kit (Promega, Madison, WI) provided a buffer and substrate which were combined and aliquoted equally into Eppendorf tubes. The aliquots were stored at -20^{o}C in tin foil to minimize light exposure.

12. Visual comparison of the anticancer compound rankings across each time point for assays conducted in Chapter 2

A - Fluorescence microscopy-based relative killing speed assay.

B - Plate-based fluorescence assay.

C - ATP Assay.

D - Resazurin-based *in vitro* cytotoxicity assay.

<u>8 Hours:</u>

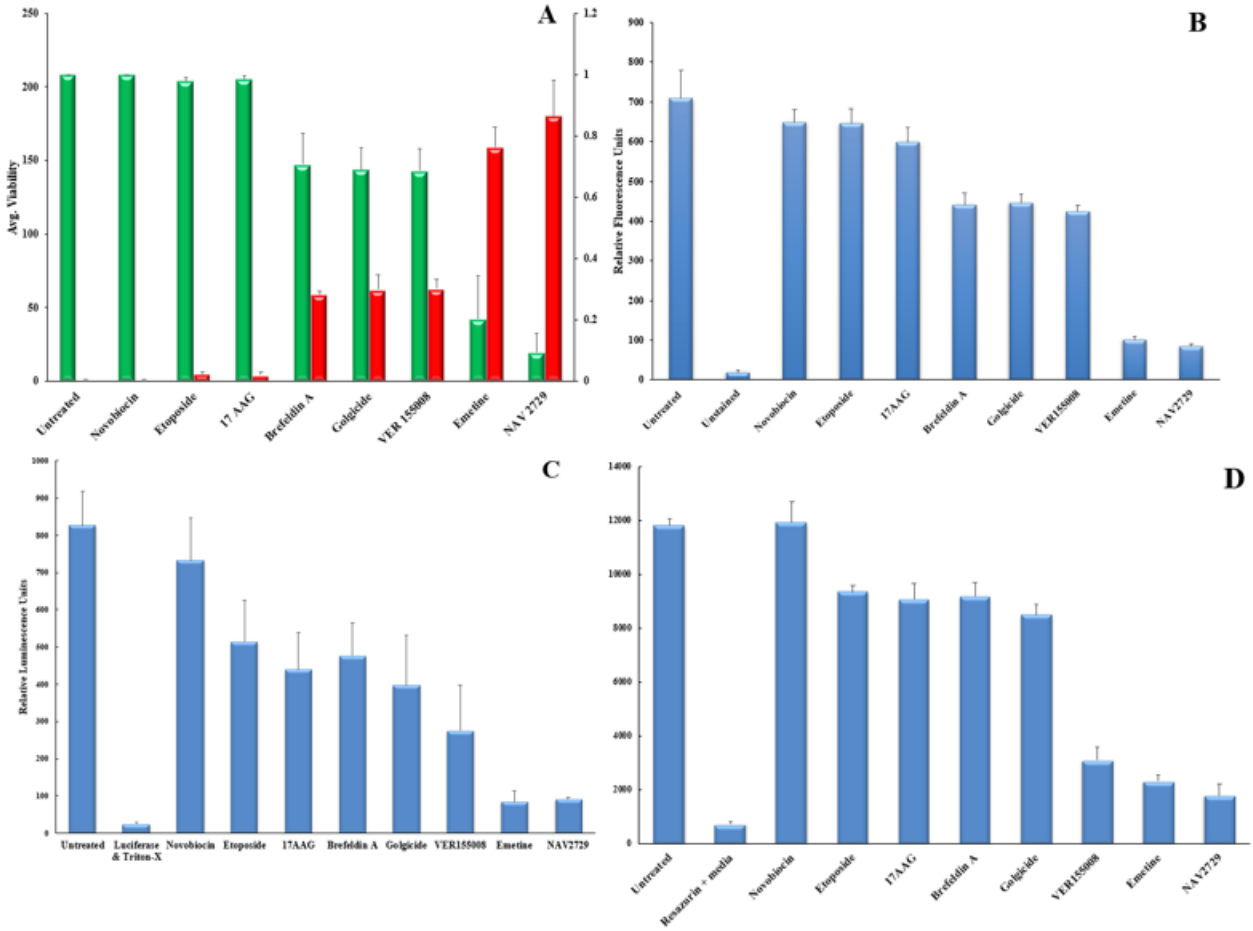

16 hours:

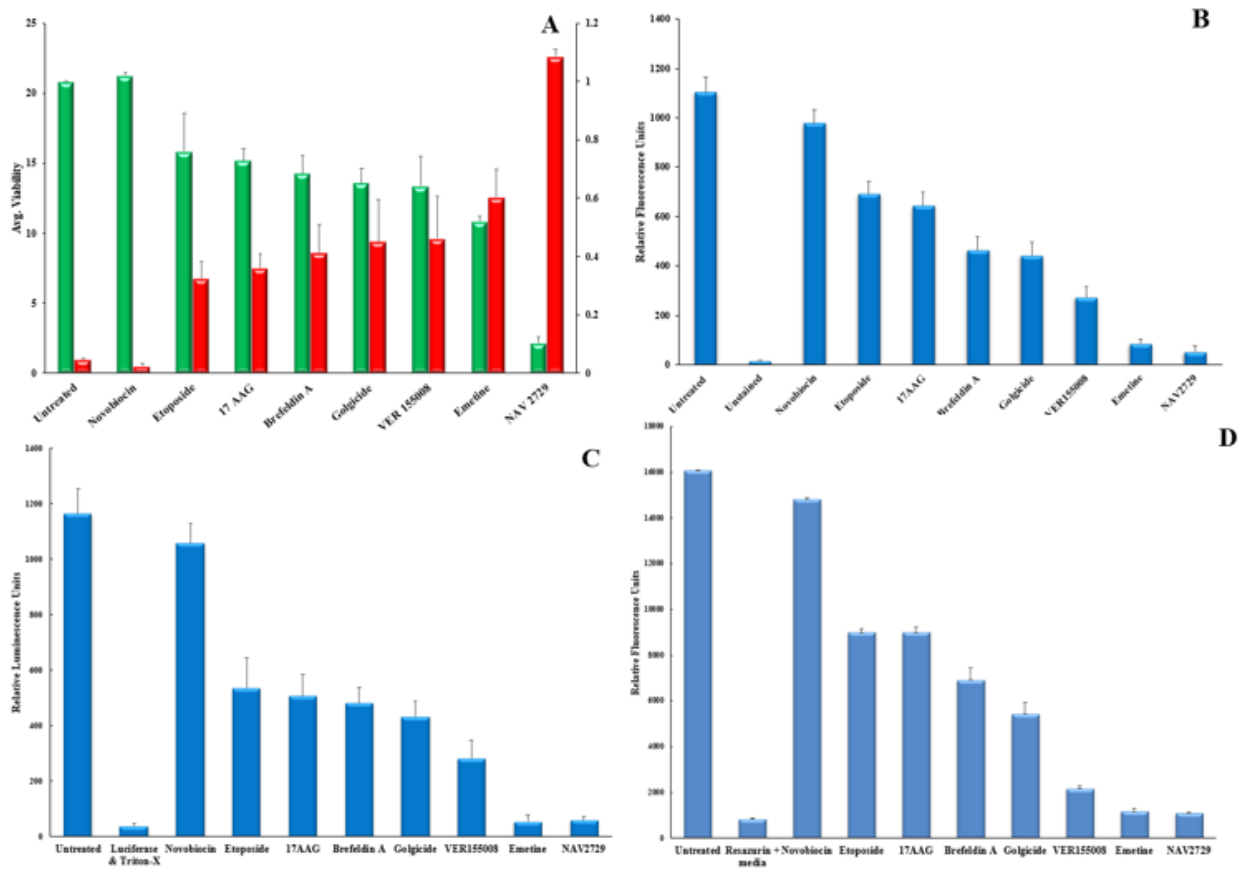
A
Avg. Viability
Untreated
Novobiocin
Etoposide
17 AAG
Brefeldin A
Golgicide
VER 155008
Emetine
NAV 2729
B
Relative Fluorescence Units
Untreated
Unstained
Novobiocin
Etoposide
17AAG
Brefeldin A
Golgicide
VER155008
Emetine
NAV2729
C
Relative Luminescence Units
Untreated
Luciferase & Triton-X
Novobiocin
Etoposide
17AAG
Brefeldin A
Golgicide
VER155008
Emetine
NAV2729
D
Relative Fluorescence Units
Untreated
Resazurin + media
Novobiocin
Etoposide
17AAG
Brefeldin A
Golgicide
VER155008
Emetine
NAV2729

24 hours:

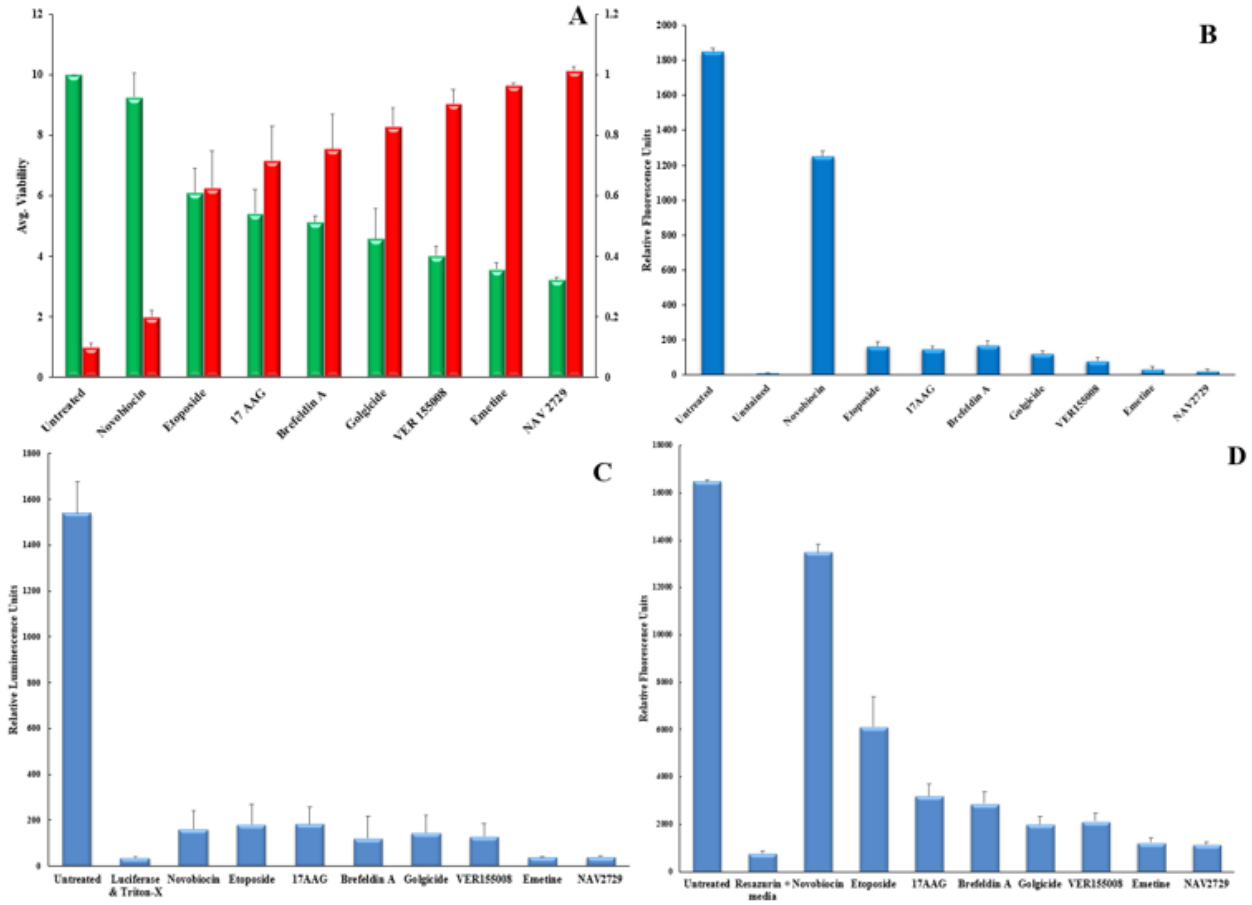
A
Avg. Viability
Untreated
Novobiocin
Etoposide
17 AAG
Brefeldin A
Golgicide
VER 155008
Emetine
NAV 2729
B
Relative Fluorescence Units
Untreated
Unstained
Novobiocin
Etoposide
17AAG
Brefeldin A
Golgicide
VER155008
Emetine
NAV2729
C
Relative Luminescence Units
Untreated
Luciferase & Triton-X
Novobiocin
Etoposide
17AAG
Brefeldin A
Golgicide
VER155008
Emetine
NAV2729
D
Relative Fluorescence Units
Untreated
Resazurin + media
Novobiocin
Etoposide
17AAG
Brefeldin A
Golgicide
VER155008
Emetine
NAV2729

13. Dot plots for the relative speed of action analysis on the antimalarial standards in Chapter 3 using PI or calcein-AM and a Becton Dickinson ACCURI™ C6 Plus flow cytometer.

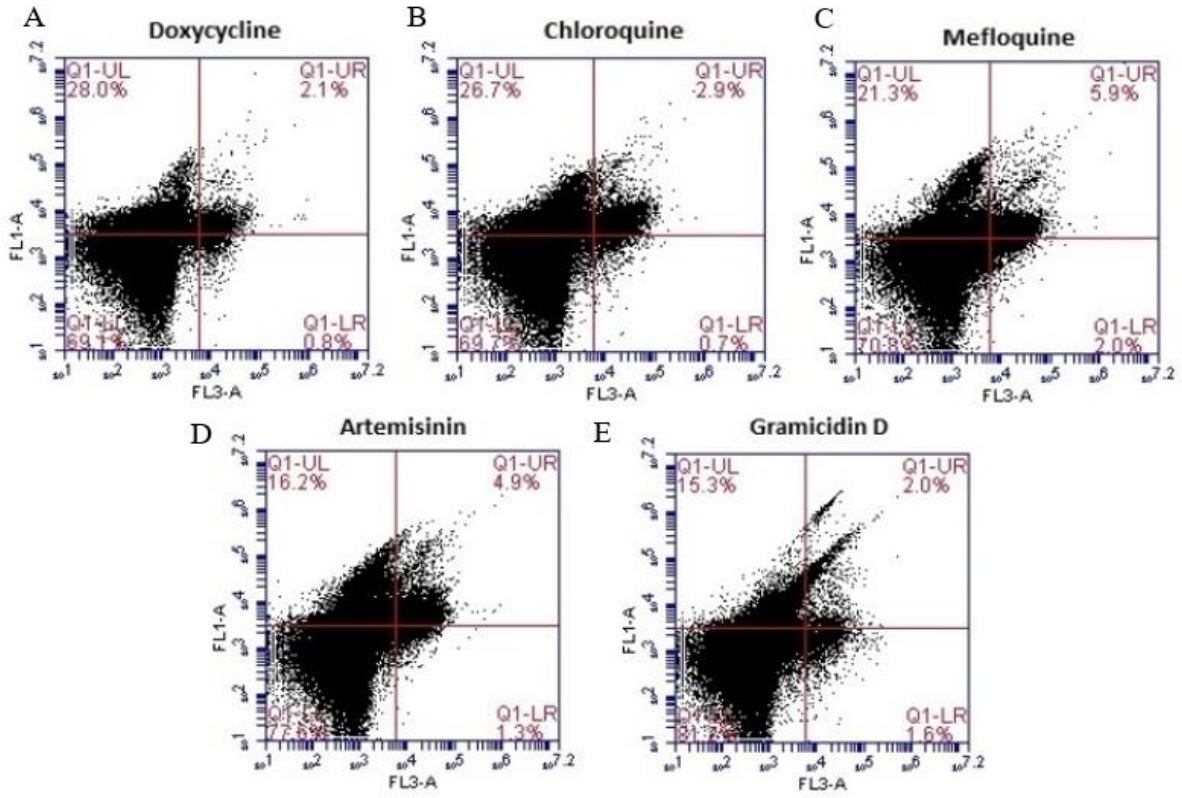

Dot plots for the antimalarial standards for the calcein-AM study depicting 100 000 events per panel generated by a Becton Dickinson ACCURI™ C6 Plus flow cytometer. Parasite samples were treated with doxycycline (A – 120 µM), chloroquine (B – 125 nM), mefloquine (C – 95 nM), artemisinin (D – 160 nM) or gramicidin D (E – 10 nM) for eight hours, stained with calcein-AM (5 µg/mL) and saponin (0.1%) lysed. Analysis conducted using the FlowJo software (FlowJo, LLC, Ashland, Ore.).

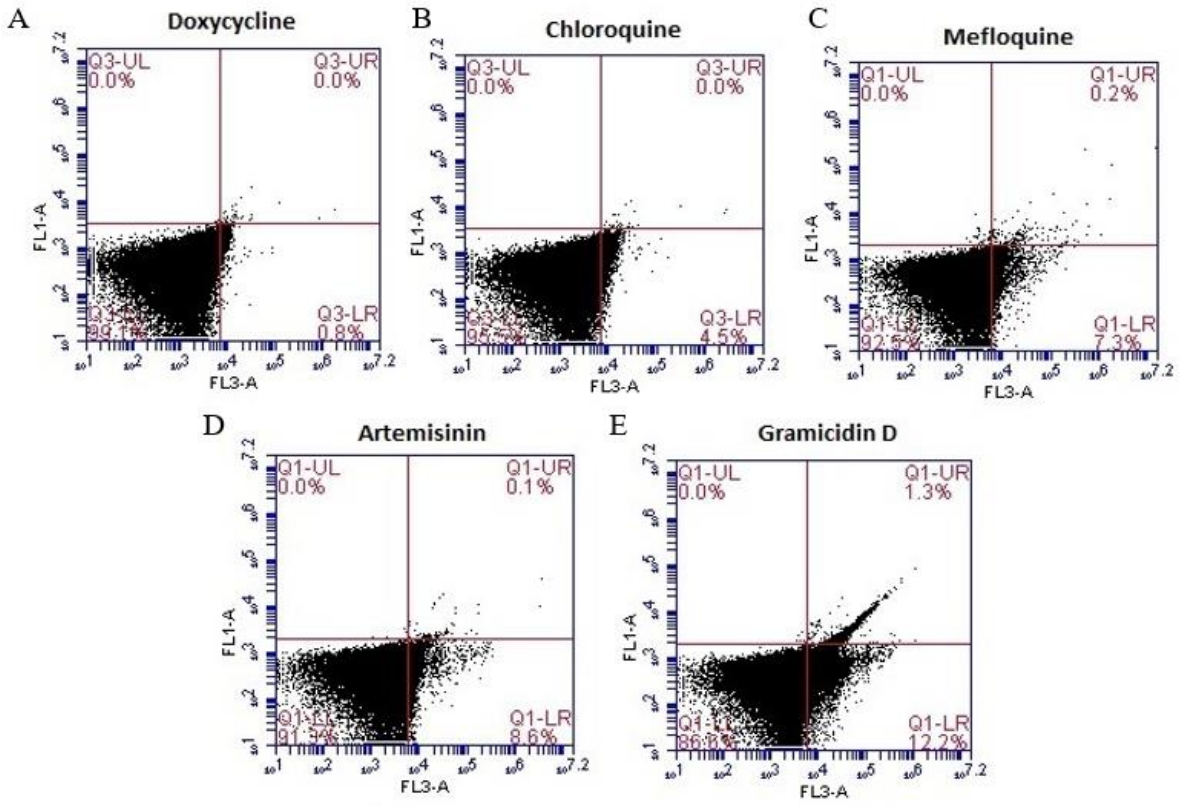

Dot plots for the antimalarial standards for the PI study depicting 100 000 events per panel generated by a Becton Dickinson ACCURI™ C6 Plus flow cytometer. Parasite samples were treated with doxycycline (A – 120 µM), chloroquine (B – 125 nM), mefloquine (C – 95 nM), artemisinin (D – 160 nM) or gramicidin D (E – 10 nM) for eight hours, stained with PI (3.3 µg/mL) and saponin (0.1%) lysed. Analysis conducted using the FlowJo software (FlowJo, LLC, Ashland, Ore.).

14. Dot plots for the relative speed of action analysis on the antimalarial standards in Chapter 4 using PI or calcein-AM and a Becton Dickinson ACCURI^{TM} C6 Plus flow cytometer.

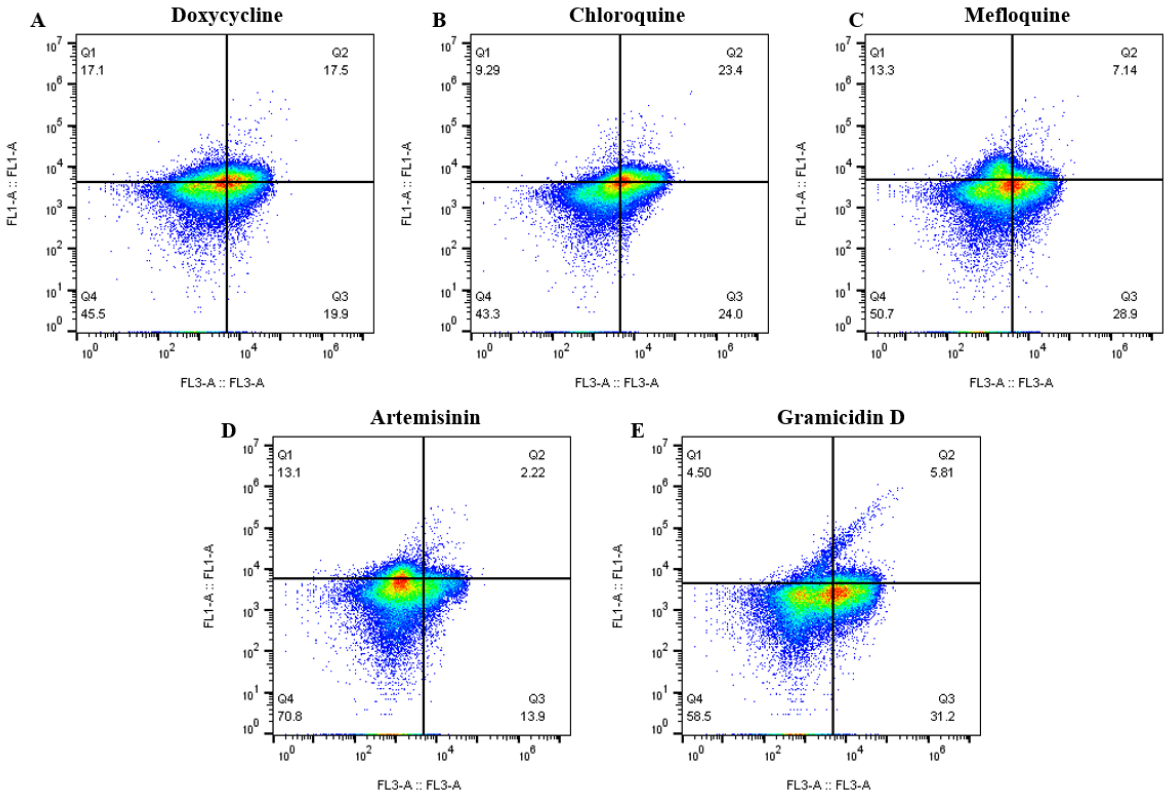

Dot plots for the antimalarial standards for the calcein-AM study depicting 100 000 events per panel generated by a Becton Dickinson ACCURI^{TM} C6 Plus flow cytometer. Parasite samples were treated with doxycycline (A), chloroquine (B), mefloquine C), artemisinin (D) or gramicidin D (E) at 10 µM for eight hours, stained with calcein-AM (5 µg/mL) and saponin (0.1%) lysed. Analysis conducted using the FlowJo software (FlowJo, LLC, Ashland, Ore.).

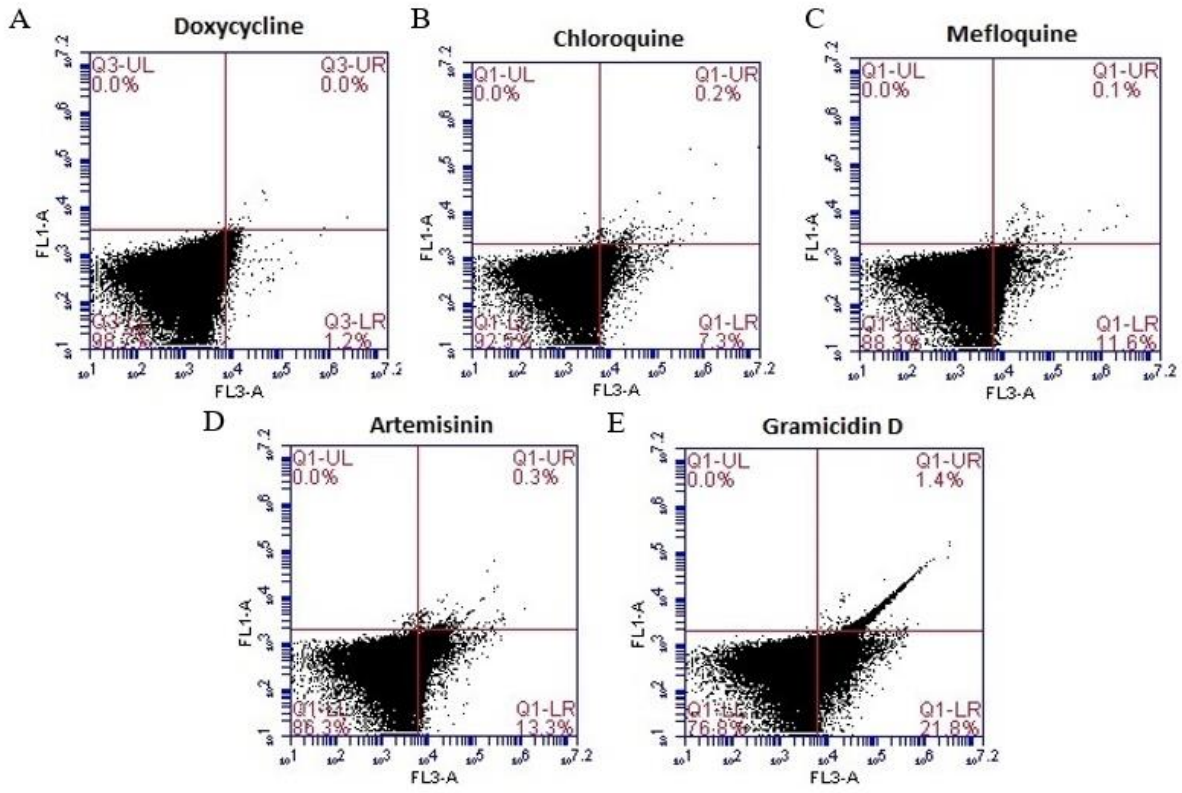

Dot plots for the antimalarial standards for the PI study depicting 100 000 events per panel generated by a Becton Dickinson ACCURI™ C6 Plus flow cytometer. Parasite samples were treated with doxycycline (A), chloroquine (B), mefloquine (C), artemisinin (D) or gramicidin D (E) at 10 µM for eight hours and stained with PI (3.3 µg/mL). Analysis conducted using the Becton Dickinson Accuri C6 Plus (64-bit) software.

15. Dot plots for the relative speed of action analysis on the novel artemisinin analogs in Chapter 4 using PI or calcein-AM and a Becton Dickinson ACCURI™ C6 Plus flow cytometer.

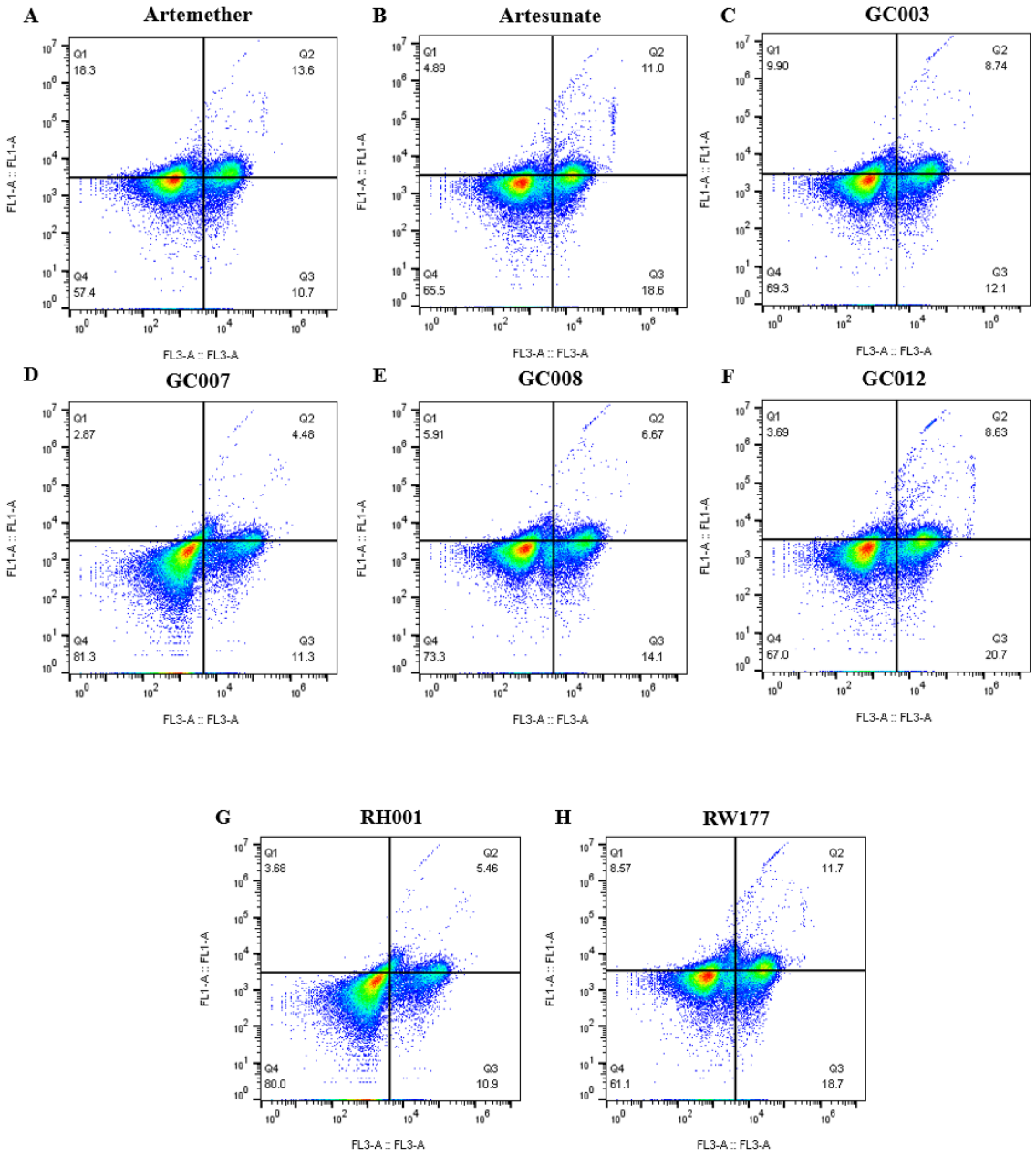

Dot plots for the novel artemisinin analogs in the calcein-AM study depicting 100 000 events per panel generated by a Becton Dickinson ACCURI™ C6 Plus flow cytometer. Parasite samples were treated with a set of artemisinin analogs (GC003, GC007, GC008, GC012, RH001 and RW177) at 10 µM for eight hours, stained with calcein-AM (5 µg/mL) and saponin (0.1%) lysed. Artemether and artesunate were also used to treat a set of *P. falciparum* parasite samples under the same conditions for comparative purposes. Analysis conducted using the FlowJo (v10.4.1) software.

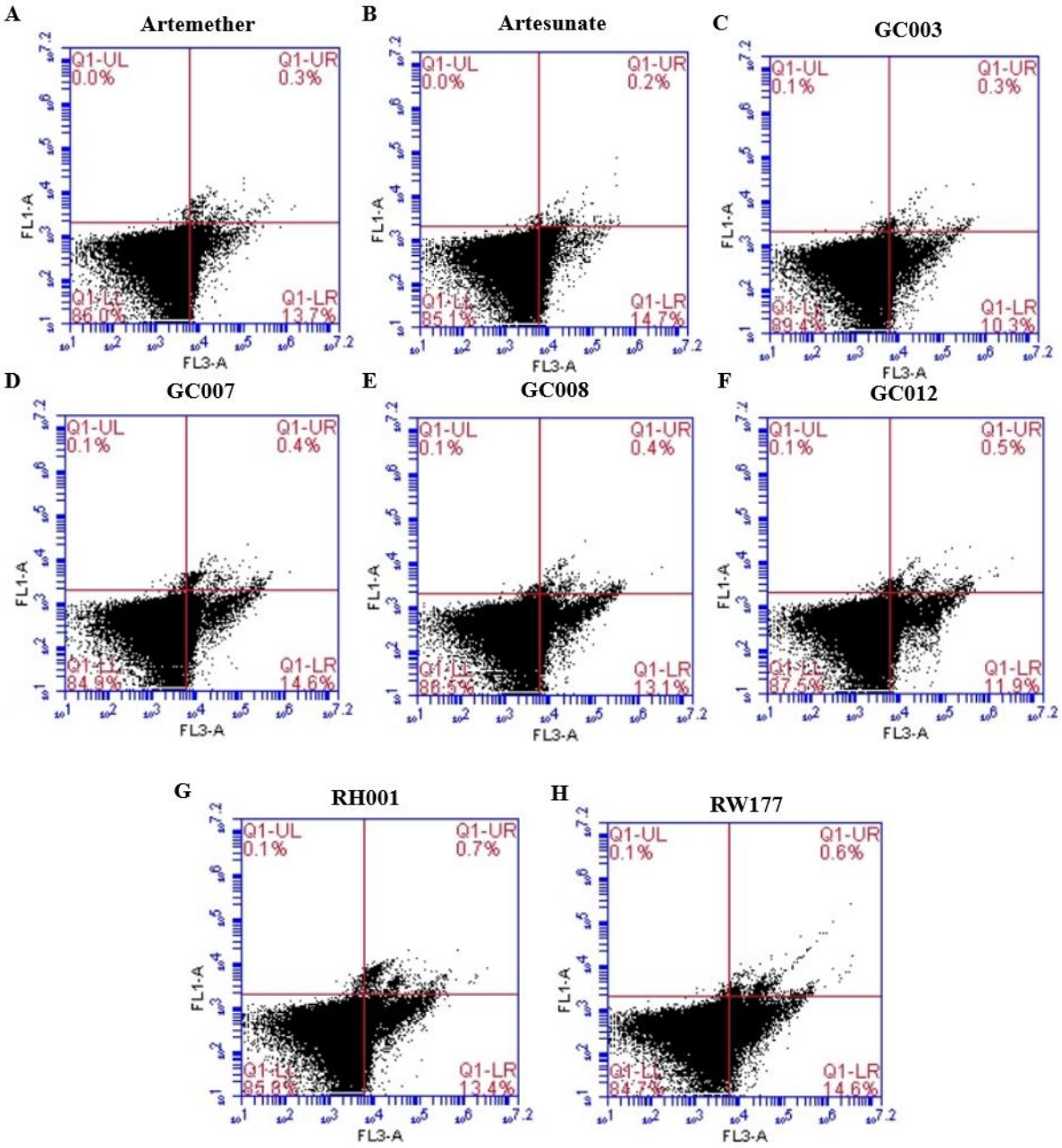

Dot plots for the novel artemisinin analogs in the PI study depicting 100 000 events per panel generated by a Becton Dickinson ACCURI™ C6 Plus flow cytometer. Parasite samples were treated with a set of artemisinin analogs (GC003, GC007, GC008, GC012, RH001 and RW177) at 10 µM for eight hours and stained with PI (3.3 µg/mL). Artemether and artesunate were also used to treat a set of *P. falciparum* parasite samples under the same conditions for comparative purposes. Analysis conducted using the Becton Dickinson Accuri C6 Plus (64-bit) software.

16. Ranking of the compounds in the Pathogen Box as a measure of relative killing speed according to the number of calcein-AM staining events in relation to an untreated control (ranked fastest to slowest).

Calcein-AM (%)	Compound	Rank	Calcein-AM (%)	Compound	Rank	Calcein-AM (%)	Compound	Rank
2	MMV1037162	1	41	MMV020520	49	49	MMV001059	95
7	MMV019993	2	41	MMV024035	50	50	MMV084603	96
12	MMV024101	3	42	MMV010764	50	50	MMV676605	97
15	MMV024443	4	42	MMV020710	50	50	MMV676269	98
17	MMV022478	5	42	MMV019721	50	50	MMV009135	99
30	MMV1088520	6	42	MMV016136	50	50	MMV085499	100
30	MMV020670	7	42	MMV676442	50	50	MMV023985	101
30	MMV007133	8	42	MMV019807	51	51	MMV020388	102
30	MMV011229	9	42	MMV560185	51	51	MMV024195	103
31	MMV007920	10	42	MMV007471	51	51	MMV007803	104
32	MMV1028806	11	43	MMV019234	51	51	MMV011691	105
32	MMV023370	12	43	MMV676528	51	51	MMV676877	106
32	MMV1019989	13	43	MMV020391	51	51	MMV020165	107
32	MMV023388	14	43	MMV085230	52	52	MMV006901	108
33	MMV062221	15	44	MMV007638	53	53	MMV000907	109
34	MMV676350	16	44	MMV006833	53	53	MMV019742	110
34	MMV020982	17	44	MMV026490	53	53	MMV008439	111
34	MMV1029203	18	44	MMV026550	55	55	MMV019189	112
34	MMV010576	19	44	MMV011765	59	59	MMV634140	113
34	MMV688980	20	45	MMV687246	61	61	MMV028694	114
35	MMV1030799	21	45	MMV676260	61	61	MMV020289	115
35	MMV021375	22	45	MMV663250	62	62	MMV676270	116
36	MMV026468	23	45	MMV392832	62	62	MMV026313	117
36	MMV023953	24	46	MMV085210	62	62	MMV022236	118
36	MMV676881	25	46	MMV026356	62	62	MMV407834	119
36	MMV393144	26	46	MMV022029	63	63	MMV676358	120
37	MMV024829	27	46	MMV020081	68	68	MMV687794	121
38	MMV011903	28	46	MMV023860	68	68	MMV024114	122
38	MMV020623	29	46	MMV023949	71	71	MMV006239	123
38	MMV020120	30	46	MMV023233	74	74	MMV016838	124
38	MMV020136	31	46	MMV084864	78			
38	MMV024397	32	47	MMV019087	79			
38	MMV007625	33	47	MMV020320	80			
39	MMV006372	34	47	MMV024406	81			
39	MMV020591	35	47	MMV085071	82			
39	MMV020512	36	47	MMV023183	83			
39	MMV020517	37	47	MMV023227	84			
39	MMV032967	38	47	MMV019551	85			
39	MMV011511	39	48	MMV020321	86			
39	MMV010545	40	48	MMV000858	87			
40	MMV021057	41	48	MMV676380	88			
40	MMV020537	42	48	MMV032995	89			
40	MMV019838	43	48	MMV024937	90			
40	MMV020152	44	49	MMV026020	91			
40	MMV031011	45	49	MMV006741	92			
40	MMV020291	46	49	MMV009054	93			
40	MMV667494	47	49	MMV019790	94			

17. Ranking of the compounds in the Pathogen Box as a measure of relative killing speed according to the number of PI staining events in relation to an untreated control (ranked fastest to slowest).

PI (%)	Compound	Rank	PI (%)	Compound	Rank	PI (%)	Compound	Rank
24	MMV1037162	1	4	MMV009054	48	3	MMV023183	95
20	MMV019993	2	4	MMV008439	49	3	MMV020165	96
19	MMV024443	3	4	MMV1019989	50	3	MMV667494	97
18	MMV022478	4	4	MMV010576	51	3	MMV023227	98
18	MMV024101	5	4	MMV024829	52	3	MMV020289	99
9	MMV000907	6	4	MMV024035	53	3	MMV676270	100
9	MMV020512	7	4	MMV687246	54	3	MMV026313	101
9	MMV1029203	8	4	MMV023860	55	3	MMV084864	102
8	MMV1028806	9	4	MMV019790	56	2	MMV676350	103
7	MMV010764	10	4	MMV009135	57	2	MMV020537	104
7	MMV019234	11	4	MMV011765	58	2	MMV006833	105
7	MMV676442	12	4	MMV023388	59	2	MMV085071	106
7	MMV022236	13	4	MMV028694	60	2	MMV019551	107
7	MMV011691	14	4	MMV010545	61	1	MMV084603	108
6	MMV019189	15	4	MMV634140	62	1	MMV006372	109
6	MMV085210	16	4	MMV407834	63	1	MMV020520	110
6	MMV020388	17	3	MMV011903	64	1	MMV024397	111
6	MMV007803	18	3	MMV020591	65	1	MMV021375	112
5	MMV020120	19	3	MMV020623	66	1	MMV023370	113
5	MMV676605	20	3	MMV019721	67	1	MMV031011	114
5	MMV007638	21	3	MMV019838	68	1	MMV023949	115
5	MMV020710	22	3	MMV020152	69	1	MMV024937	116
5	MMV020517	23	3	MMV560185	70	1	MMV024195	117
5	MMV019807	24	3	MMV019087	71	1	MMV007133	118
5	MMV020321	25	3	MMV020320	72	1	MMV676358	119
5	MMV019742	26	3	MMV000858	73	0	MMV006901	120
5	MMV020391	27	3	MMV006741	74	0	MMV062221	121
5	MMV676380	28	3	MMV1030799	75	0	MMV024114	122
5	MMV026468	29	3	MMV1088520	76	0	MMV676269	123
5	MMV020670	30	3	MMV023953	77	0	MMV663250	124
5	MMV026356	31	3	MMV032967	78			
5	MMV007471	32	3	MMV011511	79			
5	MMV022029	33	3	MMV007625	80			
5	MMV020291	34	3	MMV020081	81			
5	MMV026490	35	3	MMV024406	82			
5	MMV026550	36	3	MMV085230	83			
5	MMV023233	37	3	MMV676260	84			
5	MMV001059	38	3	MMV032995	85			
5	MMV016838	39	3	MMV085499	86			
5	MMV392832	40	3	MMV023985	87			
4	MMV026020	41	3	MMV676877	88			
4	MMV020982	42	3	MMV676881	89			
4	MMV021057	43	3	MMV688980	90			
4	MMV020136	44	3	MMV011229	91			
4	MMV016136	45	3	MMV393144	92			
4	MMV676528	46	3	MMV007920	93			
4	MMV006239	47	3	MMV687794	94			

18. Ranking of the compounds in the Pathogen Box as a measure of haemolytic effects in relation to an untreated control (ranked most haemolytic to least).

RBC Count	Compound	Rank	RBC Count	Compound	Rank	RBC Count	Compound	Rank
579	MMV011511	1	897	MMV020512	47	914	MMV1019989	93
602	MMV020520	2	897	MMV026468	48	915	MMV023949	94
696	MMV1037162	3	897	MMV006833	49	915	MMV011765	95
857	MMV663250	4	897	MMV026550	50	917	MMV024035	96
859	MMV676350	5	898	MMV023233	51	917	MMV007920	97
862	MMV019807	6	899	MMV000858	52	919	MMV062221	98
868	MMV016838	7	899	MMV020670	53	919	MMV028694	99
869	MMV022478	8	899	MMV024443	54	920	MMV024195	100
869	MMV687794	9	899	MMV019551	55	921	MMV020537	101
870	MMV020120	10	900	MMV1028806	56	921	MMV024406	102
870	MMV667494	11	900	MMV020591	57	924	MMV024101	103
872	MMV676528	12	900	MMV020391	58	926	MMV024829	104
872	MMV020289	13	900	MMV031011	59	926	MMV085071	105
874	MMV000907	14	900	MMV026313	60	926	MMV001059	106
876	MMV023227	15	901	MMV006741	61	927	MMV688980	107
878	MMV007133	16	901	MMV023953	62	928	MMV019234	108
878	MMV023183	17	901	MMV026490	63	928	MMV016136	109
879	MMV006372	18	901	MMV019790	64	929	MMV019742	110
879	MMV022236	19	901	MMV007803	65	932	MMV026020	111
880	MMV020623	20	902	MMV010764	66	932	MMV010576	112
880	MMV020320	21	902	MMV020982	67	934	MMV560185	113
880	MMV024114	22	902	MMV022029	68	936	MMV021375	114
883	MMV676605	23	902	MMV407834	69	936	MMV687246	115
884	MMV676877	24	903	MMV007625	70	936	MMV011229	116
885	MMV006901	25	903	MMV676269	71	941	MMV393144	117
885	MMV032967	26	904	MMV019087	72	942	MMV1030799	118
886	MMV084603	27	904	MMV023985	73	942	MMV676358	119
887	MMV676380	28	904	MMV676881	74	943	MMV006239	120
887	MMV009135	29	905	MMV019838	75	950	MMV019189	121
887	MMV676270	30	905	MMV1088520	76	953	MMV010545	122
890	MMV032995	31	905	MMV020291	77	954	MMV019721	123
891	MMV009054	32	905	MMV085230	78	960	MMV676442	124
893	MMV007471	33	905	MMV020165	79			
893	MMV011691	34	906	MMV019993	80			
894	MMV020710	35	906	MMV634140	81			
894	MMV023370	36	907	MMV007638	82			
894	MMV026356	37	907	MMV020517	83			
894	MMV024937	38	907	MMV020321	84			
895	MMV1029203	39	907	MMV023860	85			
895	MMV020081	40	907	MMV676260	86			
895	MMV392832	41	909	MMV011903	87			
896	MMV020136	42	912	MMV021057	88			
896	MMV024397	43	912	MMV020152	89			
896	MMV008439	44	912	MMV085210	90			
896	MMV085499	45	912	MMV020388	91			
896	MMV023388	46	913	MMV084864	92			

References

1. Abdul-Ghani, R., Farag, H.F., Allam, A.F. (2013) Sulfadoxine-pyrimethamine resistance in *Plasmodium falciparum*: a zoomed image at the molecular level within a geographic context. *Acta Tropica* **125**(2): 163-190.
2. Abkarian, M., Massiera, G., Berry, L., Rogues, M., Braun-Breton, C. (2011) A novel mechanism for egress of malarial parasites from red blood cells. *Blood* **117**(15): 4118-4124.
3. Agbenyega, T., Angus, B.J., Bedu-Addo, G., Baffoe-Bonnie, B., Guyton, T., Stacpoole, P.W., Krishna, S. (2000) Glucose and lactate kinetics in children with severe malaria. *The Journal of Clinical Endocrinology and Metabolism* **85**(4): 1569-1576.
4. Agnandji, S.T., Lell, B., Fernandes, J.F., Abossolo, B.P., Methogo, B.G., Kabwende, A.L., Adegnika, A.A., MOrdmuller, B., Issifou, S., Kremsner, P.G. (2012) A phase 3 trial of RTS,S/ASO1 malaria vaccine in African infants. *The New England Journal of Medicine* **367**(24): 2284-2295.
5. Ahirrao, P., Batra, D., Jain, U.K. (2016) Artemisinin, a potential antimalarial drug: Current status. *Journal of Chemical and Pharmaceutical Research* **8**(7): 624-636.
6. Ahmann, F.R., Garewal, H.S., Schifman, R., Celniker, A., Rodney, S. (1987) Intracellular adenosine triphosphate as a measure of human tumor cell viability and drug modulated growth. *In vitro Cellular and Developmental Biology* **23**(7): 474-480.
7. Allan, R.K., Mok, D., Ward, B.K., Ratajczak, T. (2006) Modulation of chaperone function and cochaperone interaction by novobiocin in the c-terminal domain of Hsp90: Evidence that coumarin antibiotics disrupt Hsp90 dimerization. *The Journal of Biological Chemistry* **281**(11): 7161-7171.

8. Atanasov, A.G., Waltenberger, B., Pferschy-Wenzig, E., … Stuppner, H. (2015) Discovery and resupply of pharmacologically active plant-derived natural products: A review. *Biotechnology Advances* **33**(8): 1582-1614.

9. Anderson, T.J., Nair, S., Jacobzone, C., Zavai, A., Balkan, S. (2003) Molecular assessment of drug resistance in *Plasmodium falciparum* from Bahr El Gazal province, Sudan. *Tropical Medicine and International Health* **8**(12): 1068-1073.

10. Angus, B.J., Chotivanich, K., Udomsangpetch, R., White, N.J. (1997) In vivo removal of malaria parasites from red blood cells without their destruction in acute falciparum malaria. *Blood* **90**(5): 2037-2040.

11. Antoine, T., Fisher, N., Amewu, R., O`Neill, P.M., Ward, S.A., Biaginin, G.A. (2013) Rapid kill of malaria parasites by artemisinin and semi-synthetic endoperoxides involved ROS-dependent depolarization of the membrane potential. *Journal of Antimicrobial Chemotherapy* **69**(4): 1005-1016.

12. Atieli, H.E., Zhou, G., Afrane, Y., Lee, M.C., Mwanzo, I., Githeko, A.K., Yan, G. (2011) Insecticide-treated net (ITN) ownership, usage, and malaria transmission in the highlands of western Kenya. *Parasites and Vectors* **4**(113): doi: 10.1186/1756-3305-4-113.

13. Auparakkitanon, S., Noonpakdee, W., Ralph, R.K., Denny, W.A., Wilairat, P. (2003) Antimalarial 9-anilinoacridine compounds directed at hematin. *Antimicrobial Agents and Chemotherapy* **47**(12): 3708-3712.

14. Autino, B., Noris, A., Russo, R., Francesco, C. (2012) Epidemiology of malaria in endemic areas. *Mediterranean Journal of Hematology and Infectious Diseases* **4**(1): e2012060.

15. Bae, J., Munshi, A., Li, C., Samur, M., Rao, P., Mitsiades, C., Anderson, K.C., Munshi, N.C. (2013) Heat shock protein 90 is critical for the regulation of phenotype and

functional activity of human T lymphocyte and NK cells. *The Journal of Immunology* **190**(3): 10.4049/jimmunol.1200593.

16. Baldacci, P., Menard, R. (2004) The elusive malaria sporozoite in the mammalian host. *Molecular Biology* **54**(2): 298-306.

17. Balint, G.A. (2001) Artemisinin and its derivatives: An important new class of anti-malarial agents. *Pharmacology and Therapeutics* **90**: 261-265.

18. Bamji, Z.D., Washington, K.N., Akinboye, E., Bakare, O., Kanaan, Y.M., Copeland, R.L. (2015) Apoptotic effects of novel dithiocarbamate analogs of emetine in prostate cancer cell lines. *Anticancer research* **35**(9) 4723-4732.

19. Bandyopadhyay, U., Das, D., Berjee, R.K. (1999) Reactive oxygen species: Oxidative damage and pathogenesis. *Current Science* **7**(1): 65-74.

20. Baniecki, M. L., D. F. Wirth, and J. Clardy. (2007) High-throughput *Plasmodium falciparum* growth assay for malaria drug discovery. *Antimicrobial Agents and Chemotherapy* **51**(2): 716–723.

21. Bannister, L.H., Hopkins, J.M., Fowler, R.E., Krishna, S., Mitchell, G.H. (2000) A brief illustrated guide to the ultrastructure of the *Plasmodium falciparum* asexual blood stages. *Parasitology Today* **16**(10): 427-433.

22. Barkan, D., Ginsburg, H., Golenser, J. (2000) Optimisation of flow cytometric measurement of parasitaemia in plasmodium infected mice. *International Journal for Parisitology* **30**(5): 649 - 653.

23. Baraka, V., Delgado-Ratto, C., Nag, S., Ishengoma, D.S., Madebe, R.A., Mavoko, H.M., Nabasumba, C., Lutumba, P., Alifrangis, M., van Geertruyden, J. (2017) Different origin and dispersal of sulfadoxine-resistant *Plasmodium falciparum* haplotypes between Eastern Africa and Democratic Republic of Congo. *Internation Journal of Antimicrobial Agents* **49**(4): 456-464.

24. Barouch-Bentov, R. (2011) Mechanisms of Drug-Resistance in Kinases. *Expert Opinion on Investigational Drugs* **20**(2): 153-208.

25. Beard, J. (2006) DDT and human health. *Science of the Total Environment* **355**(1-3): 78-89.

26. Bennett, T. N., M. Paguio, B. Gligorijevic, C. Seudieu, A. D. Kosar, E. Davidson, and P. D. Roepe. (2004) Novel, rapid, and inexpensive cell-based quantification of anti-malarial drug efficacy. *Antimicrobial Agents and Chemotherapy* **48**(5): 1807–1810.

27. Bhagavathula, A.S., Elnour, A.A., Shehab, A. (2016) Alternatives to currently used antimalarial drugs: in search of the magic bullet. *Malaria Journal* **5**(103): doi: 10.1186/s40249-016-0196-8.

28. Bhatia, S., Diedrich, D., Frieg, B., Ahlert, H. … Hauer, J. (2018) Targeting Hsp90 dimerization via the C terminus is effective in imatinib-resistant CML and lacks the heat shock response. *Blood* **132**(3): 307-320.

29. Birkholtz, L., Coetzer, T.L., Mancama, D., Leroy, D., Alano,P. (2016) Discovering new transmission-blocking anti-malarial compounds: challenges and opportunities. *Trends in Parasitology* **32**(9): 669-681.

30. Bisht, K.S., Bradbury, C.M., Mattson, D., Kaushal, A., Sowers, A., Markovina, S., Ortiz, K.L., Sieck, L.K., Isaacs, J.S., Brechbiel, M.W., Mitchell, J.B., Neckers, L.M., Gius, D. (2003) Geldanamycin and 17-allylamino-17-demethoxygeldanamycin potentiate the in vitro and in vivo radiation response of cervical tumour cells via the heat shock protein 90-mediated intracellular signalling and cytotoxicity. *Cancer Research* **63**(24): 8984-8995.

31. Black, R.E., Morris, S.S., Bryce, J. (2003) Where and why are 10 million children dying every year? *The Lancet* **361**: 2226-2234.

32. Blackman, M.J., Corrie, J.E.T., Croney, J.T., Kelly, G., Eccleston, J.F., Jameson, D.M. (2002) Structural and biochemical characterization of a fluorogenic rhodamin-labeled malarial protease substrate. *Biochemistry* **41**: 12244-12252.

33. Blank O., Daviourd-Charvet, E., Elhabiri, M. (2012) Interactions of the antimalarial drug methylene blue with methemoglobin and heme targets in *Plasmodium falciparum*: a physico-biochemical study. *Antioxidants and Redox Signaling* **17**(4): 544-554.

34. Bligh, E.G., Dyer, W.J. (1959) A rapid method of total lipid extraction and purification. *Canadian Journal of Biochemistry and Physiology* **37**(8): 911-917.

35. Blum, J.J., Yayon, A., Friedman, S., Ginsburg, H. (1984) Effects of mitochondrial protein synthesis inhibitors on the incorporation of isoleucine into *Plasmodium falciparum in vitro*. *Journal of Protozoology* **31**(3): 475-479.

36. Bourinbaiar, A.S., Coleman, C.F. (1997) The effect of gramicidin, a topical contraceptive and antimicrobial agent with anti-HIV activity, against herpes simplex viruses type 1 and 2 in vitro. *Archives of Virology* **142**(11): 2225-2235.

37. Brossi, A., Venugoplan, B., Dominguez Gerpe, L., Yeh, H. J., Flippen-Anderson, J. L., Buchs, P., Luo, X. D., Milhous, W., Peters, W. (1988) Arteether, a new anti malarial drug: synthesis and anti-malarial properties. *Journal of Medicinal Chemistry* **31**(3): 645 - 650.

38. Burke, J.E., Inglis, A.J., Perisic, O., Masson, G.R. … Williams, R.L. (2014) Structures of PI4KIIIβ complexes show simultaneous recruitment of Rab11 and its effectors. *Science* **344**(6187): 1035-1038.

39. Burketova, L., Trda, L., Ott, P.G., Valentova, O. (2015) Bio-based resistance inducers for sustainable plant protection against pathogens. *Biotechnology Advances* **33**(6): 994-1004.

40. Briolant Briolant, S., Wurts, N., Zettor, A., Rogier, C., Pradines, B. (2010) Susceptibility of Plasmodium falciparum isolates to doxycycline in associated with pftetQ sequence polymorphisms and pftetQ and pfmdt Copy Numbers. *Journal of Infectious Diseases* **201**(1): 153 - 159.

41. Bronner, P.G., Tiono, A.B., Oudraogo, A. … Bousema, T. (2016) Single low dose primaquine to reduce gametocyte carriage and *Plasmodium falciparum* transmission after artemether-lumefantrine in children with asymptomatic infection: a randomized, double-blind, placebo-controlled trial. *BMC Medicine* **14**(40): doi: 10.1186/s12916-016-0581-y.

42. Brostin, D., Mitofan, L., Palii, C., Estaquier, J., Montreuil. J. (2005) Novel fluorescence assay using calcein-AM for the determination of human erythrocyte viability and aging. *Journal of the International Society for Analytical Cytology* **66**(1): 78-84.

43. Brown, A.C. (2017) An overview of herb and dietary supplement efficacy, safety and government regulations in the United States with suggested improvements. *Food and Chemical Toxicology* **107**(Part A): 449-471.

44. Boissiere, A., Arnathau, C., Duperray, C., Berry, L., Lachaud, L., Renaud, F., Durand, P., Prugnolle, F. (2012) Isolation of *Plasmodium falciparum* by flow-cytometry: implications for single-trophozoite genotyping and parasite DNA purification for whole-genome high-throughput sequencing of archival samples. *Malaria Journal* **11**(163).

45. Bolscher, J.M., Koolen, K.M., van Gemert, G.J., van de Vegte-Bolmer, M.G., Bousema, T., Leroy, D., Saurwein, R.W., Dechering, K.J. (2015) A combination of new screening assays for prioritization of transmission-blocking antimalarials reveals distinct dynamics of marketed and experimental drugs. *The Journal of Antimicrobial Chemotherapy* **70**(5): 1357-1366.

46. Borbely, G., Szabadkai, I., Horvath, Z., Marko, P., Varga, Z., Breza, N., Baska, F., Vantus, T., Huszar, M., Geiszt, M., Hunyady, L., Buday, L., Orfi, L., Keri, G. (2010) Small-molecule inhibitors of NADPH Oxidase 4. *Journal of Medicinal Chemistry* **53**(18): 6758-6762.

47. Boroughs, L.K., Antonyak, M.A., Johnson, J, L., Cerione, R.A. (2011) A unique role for heat shock protein 70 and its binding partner tissue transglutaminase in cancer cell migration. *The Journal of Biological Chemistry* **286**(43): 37094-37107.

48. Bounaadja, L., Schmitt, M., Albrecht, S., Mouray, E., Tarnus, C., Florent, I. (2017) Selective inhibition of PfA-M1, over PfA-M17, by an amino-benzosuberone derivative blocks malaria parasites development in vitro and in vivo. *Malaria Journal* **16**: 382.

49. Brown, G.V., Battye, F.l., Howard, R.J. (1980) Seperation of stages of *Plasmodium falciparum*-infected cells by means of a fluorescence-activated cell sorter. *The American Journal of Tropical Medicine and Hygiene* **29**:1147-1149.

50. Bruneel, F., Tulbach, F., Corne, P., Megarbarne, B., Mira, J.P. … Wolff, M. (2010) Severe imported *falciparum* malaria: a cohort study in 400 critically ill adults. *PLoS One* **5**(10): e13236.

51. Bucana, C., Saiki, I., Nayar, R. (1986) Uptake and Accumulation of the Vital Dye Hydroethidine in the Neoplastic Cells/ *The Journal of Histochemistry and Cytochemistry* **34**(9): 1109-1115.

52. Budina-Kolomets, A., Balaburski, G.M., Bondar, A., Beeharry, N., Yen, T., Murphy, M.E. (2014) Comparison of the activity of the three different Hsp70 inhibitors on apoptosis, cell cycle arrest, autophagy inhibition, and Hsp90 inhibition. *Cancer Biology and Therapy* **15**(2): 194-199.

53. Burrows, J.N., Leroy, D., Lotharius, J., Waterson, D. (2011) Challenges in antimalarial drug discovery. *Future Medicinal Chemistry* **3**(11): 1401-1412.

54. Burrows, J.N., van Huijsduijnen, R.H., Mohrle, J.J., Oeuvray, C., Wells, T.N. (2013) Designing the next generation of medicines for malaria control and eradication. *Malaria Journal* **12**(187): doi: 10.1186/14752875-12-187.

55. Cabatchnik, Z.I., Glickstein, H., Milgram, P., Breuer, W. (1996) A fluorescence assay for assessing chelation of intracellular iron in a membrane model system and in mammalian cells. *Analytical Biochemistry* **233**(2): 221-227.

56. Cabrera, M., Cui, L. (2015) *In vitro* activities of primaquine-schizonticide combinations on asexual blood stages and gametocytes of *Plasmodium falciparum*. *Antimicrobial Agents and Chemotherapy* **59**(12): 7650-7656.

57. Campo, B., Vandal, O., Wesche, D.L., Burrows, J.N. (2015) Killing the hypnozoite – drug discovery approaches to prevent relapse in *Plasmodium vivax*. *Pathogens and Global Health* **109**(3): 107-122.

58. Carlson, R.P., Taffs, R., Davison, W.M., Stewart, P.S. (2008) Anti-biofilm properties of chitosan-coated surfaces. *Journal of Biomaterials Science, Polymer Edition* **19**(8): 1035-1046.

59. Carvalho, L., Luque-Ortega, J.R., Manzano, J.I., Castanys, S., Rivas, L., Gamarro, F. (2010) Tafenoquine, an antiplasmodial 8-aminoquinoline, targets *Leighmania* respiratory complex III and induces apoptosis. *Antimicrobial Agents and Chemotherapy* **54**(12): 5344-5351.

60. Cerebrospinal fluid kynurenine and kynurenic acid concentrations are associated with coma duration and long-term neurocognitive impairment in Ugandan children with cerebral malaria. *Malaria Journal* **16**(303): doi: 10.1186/s12936-017-1954-1.

61. Chevalley, S., Coste, A., Lopez, A., Pipy, B., Valentin, A. (2010) Flow cytometry for the evaluation of anti-plasmodial activity of drugs on Plasmodium falciparum gametocytes. *Malaria Journal* **9**(49).

62. Chamani, E., Rabbani-Chadegani, A., Zahraei, Z. (2014) Spectroscopic detection of etoposide binding to chromatin components: the role of histone proteins. *Spectrochimica Acta Part A: Molecular and Biomolecular Spectroscopy* **133**: 292-299.

63. Chan, G.K.Y., Kleinheinz, T.L., Peterson, D., Moffat, J.G. (2013) A simple high-content cell cycle assay reveals frequent discrepancies between cell number and ATP and MTS proliferation assays. *PLoS One* **8**(5) doi: 10.1371/journal.pone.0063583.

64. Chaudhury, S., Regules, J.A., Darko, C.A., Dutta, S., Wallqvist, A., Waters, N.C., JOngert, E., Lemiale, F., Bergmann-Leitner, E.S. (2017) Delayed fractional dose regimen of the RTS,S/AS01 malaria vaccine candidate enhances an IgG4 response that inhibits serum opsonophagocytosis. *Scientific Reports* **7**(1): 7998.

65. Chavain, N., Vezin, H., Dive, D., Touati, N., Paul, J.F., Buisine, E., Biot, C. (2008) Investigation of the redox behavior of ferroquine, a new antimalarial. *Molecular Pharmaceutics* **5**(5): 710-716.

66. Chen, W., ten Berge, D., Brown, J., Ahn, S., Hu, L.A., Miller, W.E., Caron, M.G., Barak, L.S., Nusse, R., Lefkowitz, R.J. (2003) Dishevelled 2 recruits beta-arrestin 2 to mediate Wnt5A–stimulated endocytosis of Frizzled 4. *Science* **301**(5638): 1391-1394.

67. Chen, I., Poirot, E., Newman, M., Kandula, D., Shah, R., Hwang, J., Cohen, J.M., Gosling, R., Rooney, L. (2015) An assessment of the supply, programmatic use, and regulatory issues of single low-dose primaquine as a *Plasmodium falciparum* gametoicytocide for sub-Saharan Africa. *Malaria Journal* **14**(204): doi: 10.1186/s12936-015-0714-3.

68. Chimaka, V.U., Karolina, A.A., Christophides, G.K., Vlachou, D. (2017) *Plasmodium berghei* PIMMS2 promotes ookinete invasion of the *Anopheles gambiae* mosquito midgut. *Infection and Immunity* **85**(8): doi: 10.1128/IAI.00139-17 [ahead of print].

69. Chinnapi, M., Via, A., Marcatili, P., Tramontano, A. (2010) On the mechanism of chloroquine resistance in *Plasmodium falciparum*. *PLoS Once* **5**(11): e14064.

70. Chitarra, L.G., Breeuwer, P., Abee, T., Bulk, R.W. (2006) The use of fluorescent probes to assess viability of the plant pathogenic bacterium *Clavibacter michiganensis* subsp. *michaganesis* by flow cytometry. *Fitopatologia Brasilieria* **31**(4): 349-356.

71. Clark, M., Fisher, N.C., Kasthuri, R., Hand, C.C. (2013) Parasite maturation and host serum iron influence the labile iron pool of erythrocyte stage *Plasmodium falciparum*. *British Journal of Haematology* **161**(2): 262-269.

72. Collins, T.J., Berridge, M.J., Lipp, P., Bootman, M.D. (2002) Mitochondria are morphologically and functionally heterogeneous within cells. *The EMBO Journal* **21**(7): 1616 – 1627.

73. Collins, C.R., Hackett, F., Atid, J., Tan, M.S.Y., Blackman, M.J. (2017) The *Plasmodium falciparum* pseudoprotease SERA5 regulates the kinetics and efficiency of malaria parasite egress from host erythrocytes. *PLoS Pathogens* **13**(7): e1006453.

74. Combrinck, J.M., Mabotha, T.E., Ncokazi, K.K., Ambele, M.A., Taylor, D., Smith, P.J., Hoppe, H.C., Egan, T.J. (2013) Insights into the role of heme in the mechanism of action of anti-malarials. *ACS Chemical Biology* **8**(1): 133-137.

75. Combs, A.B., Pan, S.J. (1992) Emetine inhibits glycolysis in isolated, perfused rat hearts. *Cardiovascular Toxicology* **3**(4): 311-318.

76. Comer, S.B., Vielhauer, G.A., Manthe, C.A., Chagaturu, V.K., Szabla, K., Matts, R.L., Donnelly, A.C., Blagg, B.S.J., Holzbeierlein, J.M. (2010) Characterization of a novel novobiocin analogue as a putative C-terminal inhibitor of heat shock protein 90 in prostate cancer cells. *Europe PMC* **70**(1): 27-36.

77. Contreras, C.E., Rivas, M.A., Dominguez, J., Charris, J., Palacios, M., Bianco, N.E., Blanca, I. (2004) Stage-specific activity of potential anti-malarial compounds measured

in-vitro by flow-cytometry in comparison to optical microscopy and hypoxanthine uptake. *Memorias do Instituto Oswaldo Cruz* **99**(2): 179 – 184.

78. Corbett, Y., L. Herrera, J. Gonzalez, L. Cubilla, T. L. Capson, P. D. Coley, T. A. Kursar, L. I. Romero, and E. Ortega-Barria. (2004) A novel DNA-based microfluorimetric method to evaluate anti-malarial drug activity. *American Journal of Tropical Medicine and Hygiene* **70**(2): 119–124.

79. Coulibaly, B. Zoungrana, A., Mockenhaupt, F.P., Schirmer, R.H., Klose, C., Mansmann, U., Meissner, P.E., Muller, O. (2009) Strong gametocidal effect of methylene blue-based combination therapy against falciparum malaria: a randomized controlled trial. *PLoS ONE* **4**(5): e5318.

80. Cowell, A.N., Istvan, E.S., Lukens, A.K., Gomez-Lorenzo, M.G., Vanaerschot, M… … Winzeler, E.A. (2018) Mapping the malaria parasite druggable genome by using *in vitro* evolution and chemogenomics. *Science* **359**(6372): 191-199.

81. Cowman, A.F., Crabb, B.S. (2006) Invasion of red blood cells by malaria parasites. *Cell* **124**(4): 755-766.

82. Cox, F.E.G. (2010) History of the discovery of the malaria parasites and their vectors. *Parasites and Vectors* **3**(5).

83. Cravo, P.V.L., Carlton, J.M.R., Hunt, P., Bisonei, L., Padua, R.A., Walliker, D. (2003) Genetics of mefloquine resistance in the rodent malaria parasite *Plasmodium chabaudi*. *Antimicrobial agents and Chemotherapy* **47**(2): 709-718.

84. Crowder, G.J., Hillesand, H.K., Keyloun, K.R., Reid, M.C., Lafuente-Monasterio, M.J., Ghidelli-Disse, S., Leonard, S.E., He, P., Jones, J.C., Krahn, M.M., Mo, J.S., Dasari, K.S., Fox, A.M.W., Ojo, K.K. (2016) Biochemical screening of five protein kinases from *Plasmodium falciparum* against 14 000 cell-active compounds. *PLoS One* **11**(3): e0149996.

85. Cruickshank, S.J., Hopperstad, M., Younger, M., Connors, B.W., Spray, D.C., Srinivas, M. (2004) Potent block of Cx36 and Cx50 gap junction channels by mefloquine. *PNAS* **101**(33): 12364-12369.

86. Cruz, L.N., Juliano, M.A., Budu, A., Juliano, L., Holder, A.A., Blackman, M.J., Garcia, C.R.S. (2012) Extracellular ATP triggers proteolysis and cytosolic Ca^{2+} rise in *Plasmodium berghei* and *Plasmodium yoelii* malaria parasties. *Malaria Journal* **11**(69).

87. Cspregi, R., LemLi, B., Kunsagi-Mate, S., Szente, L., Koszegi, T., Nemeti, B., Poor, M. (2018) Complex formation of resorufin and resazurin with B-cyclodextrins: Can cyclodextrins interfere with a resazurin cell viability assay? *Molecules* **23**(2): pii: E382.

88. Cui, L., Su, X.Z. (2009) Discovery, mechanisms of action and combination therapy of artemisinin. *Expert Review of Anti-infective Therapy* **7**(8): 999-1013.

89. Czenkaska, E.M. (2011) Assessment of cell proliferation with resazurin-based fluorescent dye. *Methods in Molecular Biology* **740**: 27-32.

90. Dahl, E.L., Schock, J.L., Shenai, B.R., Gut, J., DeRisi, J.L., Rosenthal, P.J. (2006) Tetracyclines specifically target the apicoplast of the malaria parasite *Plasmodium falciparum*. *Antimicrobial Agents and Chemotherapy* **50**(9): 3124 – 3131.

91. Dahlstrom, S., Veiga, M.I., Martensson, A., Bjorkman, A., Gil, J.P. (2009) Polymorphism in PFMRP1 (*Plasmodium falciparum* multidrug resistance protein 1) amino acid 1466 associated with resistance to sulfadoxine-pyrimethamine treatment. *Antimicrobial Agents and Chemotherapy* **53**(6): 2553-2556.

92. De, D., Krogstad, F.M., Cogswell, F.B., Krogstad, D.J. (1996) Aminoquinolines that circumvent resistance in *Plasmodium falciparum in vitro. American Journal of Tropical Medicine and Hygiene* **55**(6): 579-583.

93. De Boer, C., Meulman, P.A., Wnuk, R.J., Peterson, D.H. (1970) Geldanamycin, a new antibiotic. *The Journal of Antibiotics* **23**(9): 442-447.

94. De Ryker, M., Thomas, J., Riley, J., Brough, S.J., Miles, T.J., Gray, D.W. (2016) Identification of trypanocidal activity for known clinical compounds using the new *Trypanosoma cruzi* hit-discovery screening cascade. *PLoS Neglected Tropical Diseases* **10**(4): e0004584.

95. Delves, M.J., Plouffe, D., Scheurer, C., Meister, S., Wittlin, S., Winzeler, E.A., Sinden, R.E., Leroy, D. (2012) The activities of current antimalarial drugs on the life cycle stages of *Plasmodium*: A comparative study with human and rodent parasites. *PLoS Medicine* **9**(2): e1001169.

96. Delves, M.J., Straschil, U., Ruecker, A., Miguel-Blanco, C., Marques, S., Dufour, A.C., Baum, J., Sinden, R.E. (2016) Routine *in vitro* culture of *P. falciparum* gametocytes to evaluate novel transmission blocking interventions. *Nature Protocols* **11**(9): 1668-1680.

97. Delves, M.J., Miguel-Blanco, C., Matthews, H., Molina, I., Ruecker, A. … Baum, J. (2018) A high throughput screen for next-generation leads targeting malaria parasite transmission. *Nature Communications* **9**(1): 3805.

98. Desjardins, R.E., Canfield, C.J., Haynes, J.D., Chulay, J.D. (1979) Quantitative assessment of anti-malarial activity in vitro by semiautomated microdilution technique. *Antimicrobial Agents and Chemotherapy* **16**: 710-718.

99. Demanga, C.G., Eng, J.W., Gardiner, D.L., Roth, A., Butterworth, A., Adams, J.H., Trenholme, K.R., Dalton, J.P. (2017) The development of sexual stage malaria gametocytes in a wave bioreactor. *Parasites and Vectors* **10**: 216.

100. Deniaud, A., Sharaf el dein, A., Maillier, E., Poncet, D., Kroemer, G., Lemaire, C., Brenner, C. (2008) Endoplasmic reticulum stress induces calcium-dependent permeability transition, mitochondrial outer membrane permeabilization and apoptosis. *Oncogene* **27**: 285-299.

101. Dennis, M.L., Pitcher, N.P., Lee, M.D., DeBono, A.J., Wang, Z.C., Harjani, J.R., Rahmani, R., Cleary, B., Peat, T.S., Baell, J.B., Swarbrick, J.D. (2016) Stuctural basis for the selective binding of inhibitors to 6-hydroxymethyl-7,8-dihydropterin pyrophosphkinase from *Staphylococcus aureus* and *Eschericia coli*. *Journal of Medicinal Chemistry* **59**(11): 5248-5263.

102. Dennis, A.S.M., Rosling, J.E.O., Lehane, A.M., Kirk, K. (2018) Diverse antimalarials from whole-cell phenotypic screens disrupt malaria parasite ion volume homeostasis. *Scientific Reports* **8**(8795).

103. Dennis, A.S.M., Lehane, A.M., Ridgway, M.C., Holleran, J.P., Kirk, K. (2018) Cell swelling induced by the antimalarial KAE609 (cipargamin) and other *Pf*ATP4-associated antimalarials. *Antimicrobial Agents and Chemotherapy* **62**(6): doi: 10.1128/AAC.00087-18.

104. Dias, N., Lima, N. (2002) A comparative study using fluorescence-based and a direct-count assay to determine cytotoxicity in *Tetrahymena pyriformis. Research in Microbiology* **153**: 313-322

105. Diedrich, D., Wildner, A.C., Silveira, T.F., Silva, G.N.S., Santos, F., do Canto, V.P., Gosmann, G., Bergold, A.M., Zimmer, A.R., Netz, P.A. (2018) SERCA plays a crucial role in the toxicity of a betulinic acid derivative with potential antimalarial activity. *Chemico-Biological Interactions*: doi: 10.1016/j.cbi.2018.03.014. [Epub ahead of print].

106. Dodonova, S.O., Aderhold, P., Kopp, J., Ganeva, I., Rohling, S., Hagen, W.J.H., Sinning, I., Wieland, F., Briggs, J.A.G. (2017) 9 Å structure of the COPI coat reveals that the Arf1 GTPase occupies two contrasting molecular environments. *eLife* **6**: doi: 10.7554/eLife.26691.

107. Dondorp, A.M., Yeung, S., White, L., Nguon, C., Day, N.P., Socheat, D., von Seidlein, L. (2010) Artemisinin resistance: current status and scenarios for containment. *Nature Reviews Microbiology* **8**(4): 272-280.

108. Dormoi, J., Pascual, A., Briolant, S., Amalvict, R., Charras, S., Baret, E., des Etages, E.H., Ferraud, M., Pradines, B. (2012). Proveblue (methylene blue) as an anti-malarial agent: in vitro synergy with dihydroartemisinin and atorvastatin. *Antimicrobial Agents and Chemotherapy* **56**(6): 3467 – 3469.

109. Dorn, A., Vippagunta, S.R., Matile, H., Jacquet, C., Vennerstrom, J.L., Ridley, R.G. (1998) An assessment of drug-haematin binding as a mechanism for inhibition of haematin polymerization by quinoline anti-malarials. *Biochemical Pharmacology* **55**(6): 727-736.

110. Du, X., Mi, R., Qu, Q., Qu, Y., Yue, T. (2008) Effects of geldanamycin on expression of Bcl-2 in human cervical cancer HeLa cells. *Chinese Journal of Clinical Oncology* **5**: 113-117.

111. Duffey, M., Sanchez, C.P., Lanzer, M. (2018) Profiling of the anti-malarial candidate SC83288 against artemisinins in *Plasmodium falciparum*. *Malaria Journal* **17**(121): doi: 10.1186/s12936-018-2279-4.

112. Duffy, S., Avery, V.M. (2013) Identification of inhibitors of *Plasmodium falciparum* gametocyte development. *Malaria Journal* **12**(408): doi: 10.1186/1475-2975-12-408.

113. Duffy, S., Sykes, M.L., Jones, A.J., Shelper, T.B., Simpson, M., Lang, R., Poulsen, S., Sleebs, B.E., Avery, V.M. (2017) Screening the Medicines for Malaria Venture Pathogen Box across multiples pathogens reclassifies starting points for open-source drug discovery. *Antimicrobial Agents and Chemotherapy* **61**(9): doi: 10.1128/AAC.00379-17.

114. Durrant, D.E., Morrison, D.K. (2018) Targeting the Raf kinases in human cancer: the Raf dimer dilemma. *British Journal of Cancer* **118**: 3-8.

115. Ebstie, Y.A., Abay, S.M., Tadesse, W.T., Ejigu, D.A. (2016) Tafenoquine and its potential in the treatment and relapse prevention of *Plasmodium vivax* malaria: the evidence to date. *Drug Design, Development and Therapy* **26**(10): 2387-2399.

116. Eckstein-Ludwig, U., Webb, R.J., van Goethem, D.A., East, J.M., Lee, A.G., Kimura, M., O'Neill, P.M., Bray, P.G., Ward, S.A., Krishna, S. (2003) Artemisinin's target the SERCA of *Plasmodium falciparum*. *Nature* **424**(6951): 957-961.

117. Egan, T.J. (2006) Chloroquine and primaquine: combining old drugs as a new weapon against *falciparum* malaria. *Trends in Parasitology* **22**(6): 235-237.

118. Ehrhardt, K., Davioud-Charvet, E., Ke, H., Vaidya, A.B., Lanzer, M., Deponte, M. (2013) The antimalarial activities of methylene blue and the 1,4-napthoquinone 3-[4-(trifluoromethyl)benzyl]-menadione are not due to the inhibition of the mitochondrial electron transport chain. *Antimicrobial Agents and Chemotherapy* **57**(5): 2114-2120.

119. Elloso, M.M., van der Hyde, H.C., vande Waa, J.A., Manning, D.D., Weidanz, W.P. (1994) Inhibition of *Plasmodium falciparum* in vitro by human gamma delta T cells. *Journal of Immunology* **153**(1): 1187-1194.

120. Emter, R., Natsch, A. (2015) A fast resazurin-based live viability assay is equivalent to the MTT-test in the KeratinoSens assay. *Toxicology in vitro* **29**(4): 688-693.

121. Enderle, T.H., Ogletree, D.F., ChemLa, D.S., Magowan, C., Weiss, S. (1997) Membrane specific mapping and colocalization of malarial and host skeletal proteins in the *Plasmodium falciparum* infected erythrocyte by dual-color near-field scanning optical microscopy. *Proceedings of the National Academy of Sciences* **94**: 520-525.

122. Engelbrecht, D., Coetzer, T.L. (2012) The walking dead: Is hydroethidine a sutiable viability dye for intra-erythrocytic *Plasmodium falciparum*. *Parasitology International* **61**(4): 731-734.

123. Enserink, M. (2010) If Artemisnin Drugs Fail, Whats Plan B? *Science* **328**: 846.

124. Ernst, K., Liebscher, M., Mathea, S., Granzhan, A., Schmid, J., Popoff, M.R., Ihmels, H., Barth, H., Schiene-Fischer, C. (2016) A novel Hsp70 inhibitor prevents cell intoxication with the actin ADP-ribosylating *Clostridium perfringens* iota toxin. *Scientific Reports* 6: 20301.

125. Esposito, B.P., Epsztejn, S., Breuer, W., Cabantchik, Z.I. (2002) A review of fluorescence methods for assessing labile iron in cells and biological fluids. *Analytical Biochemistry* **304**(1): 1-18.

126. Esposito, A., Choimet, J., Skepper, J.N., Mauritz, J.M.A., Lew, V. (2010) Quantitative imaging of human red blood cells infected with *Plasmodium falciparum*. *Biophysical Journal* **99**: 953-960.

127. Eyase, F.L., Akala, H.M., Ingasia, L., … Johnson, J.D. (2013) The role of *Pfmdr1* and *Pfcrt* in changing chloroquine, amodiquine, mefloquine and lumefantrine susceptibility in Western-Kenya *P. falciparum* samples during 2008-2011. *PLoS One* **8**(5): e64299.

128. Fadaka, A., Ajiboye, B., Ojo, O., Adewale, O., Olayide, I., Emuowhochere, R. (2017) Biology of glucose metabolization in cancer cells. *Journal of Oncological Sciences* **3**(2): 45-51.

129. Fall, B., Diawara, S., Sow, K., Baret, E., Diatta, B., Fall, K.B., Mbaye, P.S., Fall, F., Dieme, Y., Rogier, C., Wade, B., Bercion, R., Pradines, B. (2011) Ex vivo susceptibility of Plasmodium falciparum isolates from Dakar, Senegal, to seven standard anti-malarial drugs. *Malaria Journal* **10**:310

130. Farber, S., Diamond, L., Mercer, R.D. (1948) Temporary remissions in acute leukemia in children produced by folic acid antagonist, 4-aminopteroyl-glutamic acid (aminopterin). *The New England Journal of Medicine* **238**: 787-793.

131. Favuzza, P., Guffart, E., Tamborini, M., Schere, B., Dreyer, A.M., Rufer, A.C., Erny, J., Hoernschemeyer, J., Thoma, R., Schmid, G., Gsell, B., Lamelas, A., Benz, J., Joseph, C., Matile, H., Pluschke, G., Rudolph,M.G. (2017) Structure of the malaria vaccine candidate antigen CyRPA and its complex with a parasite invasion inhibitory antibody. *eLife* **6**: doi: 10.7554/eLife.20383.

132. Ferru, E., Giger, K., Pantaleo, A., Campanella, E., Grey, J., Ritchie, K., Vono, R., Turrini, F., Low, P.S. (2011) Regulation of membrane-cytoskeletal interactions by tyrosine phosphorylation of erythrocyte band 3. *Blood* **117**(22): 5998-6006.

133. Fillinger, U., Lindsay, S.W. (2011) Larval source management for malaria control in Africa: myths and reality. *Malaria Journal* **10**: 353.

134. Fitch, C.D., Chevli, R., Banyal, H.S., Phillips, G., Pfaller, M.A., Krogstad, D.J. (1982) Lysis of Plasmodium falciparum by ferriprotoporphyrin IX and a chloroquine-ferriprotoporphyrin IX complex. *Antimicrobial Agents and Chemotherapy* **21**(5): 819 – 822.

135. Fitch, C. D. (2004) Ferriprotoporphyrin IX, phospholipids, and the anti-malarial actions of quinoline drugs. *Life Sciences* **74**(16): 1957 – 1972.

136. Fivelman, Q.L., McRobert, L., Sharp, S., Taylor, C.J., Saeed, M., Swales, C.A., Sutherland, C.J., Baker, D.A. (2007) Improved synchronous production of *Plasmodium falciparum* gametocytes *in vitro*. *Molecular and Biochemical Parasitology* **154**: 119-123.

137. Fleischer, B. (2004) Editorial: 100 years ago: Giemsa's solution for staining of plasmodia. *Tropical Medicine and International Health* **9**: 755.

138. Francis, S.E., Sullivan, D.J., Goldberg, D.E. (1997) Hemoglobin metabolism in the malaria parasite *Plasmodium falciparum*. *Annual Review of Microbiology* 51: 97-123.

139. Fredhold, B.B., Cunha, R.A., Svenningsson, P. (2003) Pharmacology of adenosine A2A receptors and the therapeutic applications. *Current Topics in Medicinal Chemistry* **3**(4): 413-426.

140. Fry, M., Pudney, M. (1992) Site of action of the antimalarial hydroxynaphthoquinone, 2-[trans-4-(4'-chlorophenyl) cyclohexyl]-3-hydroxy-1,4-naphthoquinone (566C80). *Biochemical Pharmacology* **43**(7): 1545-1553.

141. Fu, X., Wan, S., Lyu, Y,L., Liu, L.F., Qi, H. (2008) Etoposide induces ATM-dependent mitochondrial biogenesis through AMPK activation. *PLoS One.* **3**(4): e2009.

142. Fu, y., Tilley, L., Kenny, S., Klonis, N. (2010) Dual labeling with a far-red probe permits analysis of growth and oxidative Stress in *P. falciparum*-infected RBCs. *Cytometry* **77A**: 253-263.

143. Gailard, T., Madamet, M., Pradines, B. (2015) Tetracyclines in malaria. *Malaria Journal* **14**: 445.

144. Garcia, C.H.S., Depoix., D., Queiroz, R.M.L., Souza, J.M.F., Fontes, W., Sousa, M.V., Santos, M.D.M., Carvalho, P.C., Grellier, P., Charneau, S. (2017) Dynamic molecular events associated to *Plasmodium berghei* gametogenesis through proteomic approach. *Journal of Proteomics*: doi: 10.1016/j.jprot.2017.11.009 [ahead of print]

145. Garcia-Hernandez, R., Manzano, J.I., Castanys, S., Garnarro, F. (2012) *Leishmania donovani* develops resistance to drug combinations. *Neglected Tropical Diseases* **6**(12): e1974.

146. Garewal, H.S., Ahmann, F.R., Schifman, R.B., Celniker, A. (1986) ATP assay: ability to distinguish cytostatic from cytocidal anticancer drug effects. *Journal of the National Cancer Institute* **77**(5): 1039-1045.

147. Gamo, F.J., Sanz, L.M., Vidal, J., de Cozar, C., Alvarez, E., Lavandera, J.L., Vanderwall, D.E., Green, D.V., Kumar, V., Hasan, S., Brown, J.R., Peishoff, C.E., Cardon, L.R., Garcia-Bustos, J.F. (2010) Thousands of chemical starting points for antimalarial lead identification. *Nature* **465**(7296): 305-310.

148. Geary, T., Jense, J.B. (1983) Lack of Cross-resistance to 4-Aminoquinolines in Chloroquine-Resistant *Plasmodium falciparum in vitro*. *The Journal of Parasitology* **69**(1): 97-105.

149. Gebru, T., Lalremruata, A., Kremsner, P., Mordmuller. B., Held, J. (2017) Life-span of in vitro differentiated *Plasmodium falciparum* gametocytes. *Malaria Journal* **16**(330): doi: 10.1186/s12936-017-1986-6.

150. Gedik, C.M., Collins, A.R. (1990) Comparison of effects of fostriecin, novobiocin, and camptothecin, inhibitors of DNA topoisomerases, on DNA replication and repair in human cells. *Nucleic Acids Research* **18**(4): 1007-1013.

151. Gelb, M.H. (2007) Drug discovery for malaria: a very challenging and timely andeavor. *Current Opinion in Chemical Biology* **11**: 440-445.

152. Gelhaus, C., Jacobs, T., Andra, J., Leippe, M. (2008) The antimicrobial peptide NK-2, the core region of mammalian NK-Lysin, kills intraerythrocytic *Plasmodium falciparum*. *Antimicrobial Agents and Chemotherapy* **52**(5): 1713-1720.

153. Gelman, M.S., Kannegaard, E.S., Kopito, R.R. (2002) A principal role for the proteasome in endoplasmic reticulum-associated degradation of misfolded intracellular cystic fibrosis transmembrane conductance regulator. *Journal of Biological Chemistry* **277**(14): 11709-11714.

154. Gilead, Z., Becker, Y. (1971) Effect of emetine on ribonucleic acid biosynthesis in HeLa cells. *European Journal of Biochemistry* **23**: 143-149.

155. Gilmore, K., Kopetzki, D., Lee, J.W., Horvath, Z., McQuade, T., Seidel-Morgenstern, A., Seeberger, P.H. (2014) Contiuous synthesis of artemisinin-derived medicines. *Chemical Communications* **50**(84): 12652-12655.

156. Ginsburg, H., Deharo, E. (2011) A call for using natural compounds in the development of new anti-malarial treatments- An introduction. *Malarial Journal* **10**(Suppl.1).

157. Giovanella, F., Ferreira, G.K., de Pra, S.D.T. … de Souza, R.P. (2015) Effects of primaquine and chloroquine on oxidative stress parameters in rats. *Anais da Academia Brasileira de Ciências* **87**(2).

158. Glickstein, H., El, R.B., Shvartsman, M., Cabantchik, Z.I. (2005) Intracellular labile iron pools as direct targets of iron chelators: a fluorescence study of chelator action in living cells. *Blood* **106**(9): 3242-3250.

159. Gnana, P.K., Guida, T., Alfano, L., Avilla, E., Santoro, M., Carlomagno, F., Melillo, R.M. (2013) Molecular mechanism of 17-allyamino-17-demethoxygeldanamycin (17-AAG)-induced AXL receptor tyrosine kinase degradation. *Journal of Biological Chemistry* **288**(24): 17481-17494.

160. Golenser, J., Bucholz, V., Bagheri, A., Nasereddin, A., Dzikowski, R., Guo, J., Hunt, N.H., Eyal, S., Vakruk, N., Greiner, A. (2017) Controlled release of artemisone for the treatment of experimental cerebral malaria. *Parasites and Vectors* **10**(117): doi: 10.1186/s13071-017-2018-7.

161. Goodman, C.D., Siregar, J.E., Mollard, V., Vega-Rodriquez, J. … McFadden, G.I. (2016) Parasites resistant to the antimalaria atovaquone fail to transmit by mosquitoes. *Science* **352**(6283): 349-353.

162. Goodman, C.D., Buchanan, H.D., McFadden, G.I. (2017) Is the mitochondrion a good malaria drug target? *Trends in Parasitology* **33**(3): 185-193.

163. Graciotti, M., Alam, M., Solyakov, L., Schmid, R., Burley, G., Bottrill, A.R., Doerig, C., Cullis, P., Tobin, A.B. (2014) Malaria Protein Kinase CK2 (*Pf*CK2) shows novel mechanisms of regulation. *PLoS One* **9**(3): e85391.

164. Grandesso, F., Guindo, O., Woi Messe, L., Makarimi, R., Traore, A., Dama, S., Laminou, I.M., Rigal, J., de Smet, M., Oukem-Boyer, O.M., O., Doumbo, O.K., Djimde, A., Etard, J.F. (2018) Efficacy of artesunate-amodiaquine, dihydroartemisinin-piperaquine and artemether-lumefantrine for the treatment of uncomplicated *Plasmodium falciparum* malaria in Maradi, Niger. *Malaria Journal* **17**(1): doi: 10.1186/s12936-018-2200-1.

165. Greenwood, B. (2017) Elimination of malaria: halfway there. *Transactions of the Royal Society of Tropical Medicine and Hygiene* **111**(1): 1-2.

166. Grimberg, B.T., Jaworska, M.M., Hough, L.B., Zimmerman, P.A., Phillips, J.G. (2009) Addressing the malaria drug resistance challenge using flow cytometry to discover new anti-malarials. *Bioorganic and Medicinal Chemistry Letters* **19**(18): 5452-5457.

167. Grimberg, B.T. (2011) Methodology and application of flow cytometry for investigation of human malaria parasites. *Journal of immunological methods* **367**:1-16.

168. Grimberg, B.T., Mehlotra, R.K. (2011). Expanding the anti-malarial drug arsenal-Now, but how? *Pharmaceuticals (Basel, Switzerland)* **4**(5): 681-712.

169. Grenert, J.P., Sullivan, W.P., Haystead, T.A., Clark, J., Mimnaugh, E., Krutzsch, H., Ochel, H.J., Schulte, T.W., Sausville, E., Neckers, L.M., Toft, D.O. (1997) The amino-terminal domain of heat shock protein 90 (hsp90) that binds geldanamycin is an ATP/ADP switch domain that regulates hsp90 conformation. *The Journal of Biological Chemistry* 272(38): 23842-23850.

170. Grollman, A.P. (1968) Effects of emetine on protein and nucleic acid biosynthesis in HeLa cells. *Journal of biological chemistry* **243**(15): 4089-4094.

171. Grollman A.P., Jarkovsky Z. (1975) Emetine and Related Alkaloids. In: Corcoran J.W., Hahn F.E., Snell J.F., Arora K.L. (eds) Mechanism of Action of Antimicrobial and Antitumor Agents. Antibiotics, vol 3. Springer, Berlin, Heidelberg.

172. Guo, W., Reigan, P., Siegel, D., Zirrolli, J., Gustafson, D., Ross, D. (2005) Formation of 17-allyamino-17-demethoxygeldanamycin (17-AAG) hydroquinone by NAD(P)H: quinone oxidoreductase 1: role of 17-AAG hydroquinone in heat shock protein 90 inhibition. *Cancer Research* **65**(21): 10006-10015.

173. Gural, N., Mancio-Silva, L., Miller, A.B., Galstian, A., Butty, V.L., Levine, S.S., Patrapuvich, R., Desai, S.P., Mikolajczak, S.A., Kappe, S.H.I., Fleming, H.E., March, S., Sattabongkot, J., Bhatia, S.N. (2018) *In vitro* culture, drug sensitivity, and transcriptome of *Plasmodium vivax* hypnozoites. *Cell Host and Microbe* **23**(3): 395-406.

174. Guo, J., Guiguemde, A.W., Bentura-Marciano, A., Clark, J., Haynes, R.K., Chan, W.C., Wong, H.N., Hunt, N.H., Guy, R.K., Golenser, J. (2012) Synthesis of artemiside and its effects in combination with conventional drugs against severe murine malaria. *Antimicrobial Agents and Chemotherapy* **51**(1): 163-173.

175. Guo, Z., Li, Y., Zhang, D., Ma, J. (2017) Axl inhibition induces the antitumor immune response which can be further potentiated by PD-1 blockade in the mouse cancer models. *Oncotarget* **8**(52): 89761-89774.

176. Hamdoun, A.M., Cherr, G.N., Roepke, T.A., Epel, D. (2004) Activation of multidrug efflux transporter activity at fertilization in sea urchin embryos (*Strongylocentrotus purpuratus*). *Developmental Biology* **276**(2): 452-462.

177. Hammerstein, A.F., Wylie, P.G. (2016) Accurate cytotoxicity and proliferation determination: Advantages of a high-throughput phenotypic approach over ATP luminescence assays. *Assays and Drug Development Techniques* **14**(7): 407-415.

178. Hancock, R.E.W. (1987) Role of porins in outer membrane permeability. *Journal of Bacteriology* **169**: 929-933.

179. Hande, K.R. (199) Etoposide: four decades of development of a topoisomerase II inhibitor. *European Journal of Cancer* **34**(10): 1514-1521.

180. Hany, D., Shokouh-amiri, H., Zibari, G.B. (2017) Amebiasis and other parasitic infections. *Blumgart`s surgery of the liver, biliary tract and pancreas.* Memorial Sloan Kettering`s Cancer Centre, New York, pp 1083-1101.

181. Hartwig, C.L., Rosenthal, A.S., D'Angelo J., Griffin, C.E., Posner, G.H., Cooper, R.A. (2009) Accumulation of artemisinin trioxane derivatives within neutral lipids of Plasmodium falciparum malaria parasites is endoperoxide-dependent. *Biochemical Pharmacology* **77**(3): 322 – 326.

182. Hay, S.I., Guerra, C.A., Gething, P.W., Patil, A.P., Tatem, A.J., Noor, A.M., Kabaria, C.W., Manh, B.H., Elyazar, I.R.F., Brooker, S., Smith, D.L., Moyeed, R.A., Snow, R.W. (2009) A world malaria map: *Plasmodium falciparum* endemicity in 2007. *Plose One* **6**(3).

183. Haynes, R.H., Fugmann, B., Stetter, J., Rieckmann, K., Heilmann, H.D., Chan, H.W. … Romer, A. (2006). Artemisone—a highly active antimalarial drug of the artemisinin class. *Angewandte Chemie* **45**(13): 2082-2088.

184. Held, J., Supan, C., Salazar, C.L., Tinto, H., Bonkian, L.N., Nahum, A., Moulero, B., Sie, A., Coulibaly, B., Sirima, S.B., Siribie, M., Otsyula, N., Otieno, L., Abdallah, A.M., Kimutai, R., Bouyou-Akotet, M., Kombila, M., Koiwai, K., Cantalloube, C., Din-Bell, C., Djeriou, E., Waitumbi, J., Mordmuller, B, Ter-Minassian, D., Lell, B., Kremsner, P.G. (2015) Ferroquine and arteseunate in African adults and children with *Plasmodium falciparum* malaria: a pahse 2, multicenter, randomized, double-blind, dose-randing, non-inferiority study. *Lancet Infectious Diseases* **15**(12): 1409-1419.

185. Helms, J.B., Rothman, J.E. (1992) Inhibition by brefeldin A of a Golgi membrane enzyme that catalyses exchange of guanine nucleotide bound to ARF. *Nature* **360**: 352-254.

186. Hemmer, C.J., Lehr, H.A., Westphal, K., Unverricht, M., Kratzius, M., Reisinger, E.C. (2005) *Plasmodium falciparum* Malaria: reduction of endothelial cell apoptosis *in vitro*. *Infection and Immunity* **75**(3): 1764-1770.

187. Hennessey, K.M., Rogiers, I.C., Shih, H.W., Hulverson, M.A., Choi, R., McCloskey, M.C., Whitman, G.R., Barret, L.K., Merrit, E.A., Paredez, A.R., Ojo, K.K. (2018) Screening of the pathogen box for inhibitors with dual efficacy against *Giardia lamblia* and *Cryptosporidium parvum*. *PLoS Neglected Tropical Diseases* **12**(8): e0006673.

188. Hien, T.T. (1994) An overview of the clinical use of artemisinin and its derivatives in the treatment of falciparum malaria in Viet Nam. *Transactions of the Royal Society of Tropical Medicine and Hygiene* **88**(Suppl 1): S7-S8.

189. Hiraoka, Y., Kimbara, K. (2002) Rapid assessment of the physiological status of the polychlorinated biphenyl degrader *Comamona testeroni* TK102 by flow cytometry. *Applied and Environmental Microbiology* **68**(4): 2031-2035.

190. Ho, S.W., Tsui, Y.T., Wong, TT., Cheung, S.K., Goggins, W.B., Yi, L.M., Cheng, K.K., Baum, L. (2013) Effects of 17-allyamino-17-demethoxygeldanamycin (17-AAG) in transgenic mouse models of frontotemporal lobar degeneration and Alzheimers disease. *Translational neurodegeneration* **2**(1): doi: 10.1186/2047-9158-2-24.

191. Houstekm J., Klement, P., Hermanska, J., Houstkova, H., Hansikova, H., Van den Bogert, C., Zeman, J. (1995) Altered properties of mitochondrial ATP-synthase in patients with a T→G mutation in the ATPase 6 (subunit a) gene at position 8993 of mtDNA. *Biochimica et Biophysica Acta* **1271**(2-3): 349-357.

192. Hoppe, H.C., van Schalkwyk, D.A., Wiehart, U.I.A., Meredith, S.A., Egan, J., Weber, B.W. (2004) Anti-malarial quinolines and artemisinin inhibit endocytosis in *Plasmodium falciparum*. *Antimicrobial Agents and Chemotherapy* **48**(7): 2370-2378.

193. Humphreys, D., Davidson, A.C., Hume, P.J., Makin, L.E., Koronakis, V. (2013) ARf6 coordinates actin assembly through the WAVE complex, a mechanism by *Salmonella* to invade host cells. *PNAS* **110**(42): 16880-16885.

194. Hurwitz, E.S., Johnson, D., Campbell, C.C. (1981) Resistance of *Plasmodium falciparum* malaria to sulfadoxine-pyrimethamine ('Fansidar') in a refugee camp in Thailand. *Lancet* **1**(8229): 1068-1070.

195. Infanger, M., Kossmehl, P., Shakibaei, M., Bauer, J., Kossmehl-Zorn, S., Cogoli, A., Curcio, F., Okshe, A., Wehland, M., Kreutz, R., Paul, M., Grimm, D. (2006) Simulated weightlessness changes the cytoskeleton and extracellular matrix proteins in papillary thyroid carcinoma cells. *Cell and Tissue Research* **324**(2): 267-277.

196. Internet 2: Detect and monitor viability of 3D tumour spheroids. Nexcelom Bioscience Ltd, Manchester, United Kingdom. Retrieved from: http://www.nexcelom.co.uk/celigo/3D_3_viability-of-3D-tumor-spheroids.php [Accessed: 20/02/17].

197. Jacobberger, J.W., horna, P.K., Hare, J.D. (1992) Cell cycle analysis of asexual stages of erythrocytic malaria parasties. *Cell Proliferation* **25**: 431-445.

198. Jamil, S., Lam, I., Majd, M., Tsai, S., Duronio, V. (2015) Etoposide induces cell death via mitochondrial-dependent actions of p53. *Cancer Cell International* **15**: 79.

199. Jang, J.W., Kim, J.Y., Yoon, J., Yoon, S.Y., Cho, C.H., Han, E.T., An, S.S.A., Lim, C.S. (2013) Flow cytometric enumeration of parasitaemia in cultures of *Plasmodium falciparum* stained with SYBR Green I and CD235A. *The Scientific World Journal* **536723**: doi: 10.1155/2014/536723.

200. Janneck, L., Koyfman, A., Takayesu, J.K. (2011) Clinical review of malaria for the emergency physician. *African Journal of Emergency Medicine* **3**(1): 126-130.

201. Jang, Y.Y., Cho, D., Kim, S.K., Shin, D.J., Park,M.H., Lee, J.J., Shin, M.G., Shin, J.H., Suh, S.P., Ryang, D.W. (2012) An improved flow cytometry-based natural killer cytotoxicity assay involving calcein AM staining of effector cells. *Annals of Clinical & Laboratory Science* **42**(1): 42-9.

202. Jang, J.W., Kim, J.Y., Yoon, J., Yoon, S.Y., Cho, C.H., Han, E.T., An, S.S., Lim, C.S. (2014) Flow cytometric enumeration of parasitaemia in cultures of *Plasmodium falciparum* stained with SYBR Green I and CD235A.

203. Jelokhani-Niaraki, M., Kondejewski, L.H., Farmer, S.W., Hancock, R.E., Kay, C.M., Hodges, R.S. (2000) Diastereoisomeric analogues of gramicidin S: Structure, biological activity and interaction with lipid bilayers. *Biochemical Journal* **349**: 747-755.

204. Jensen, J.M., Trager, W. (1977) Plasmodium falciparum in Culture: Use of outdated erythrocytes and description of the candle jar method. *Journal of Parisitology* **63**(5): 883 – 886.

205. Jimenez, A., Carrasco, L., Vazguez, D. (1977) Enzymic and nonenzymic translocation by yeast polysomes. Site of action of a number of inhibitors. *Biochemistry* **16**(21): 4727-4730.

206. Johnson, J.D., Dennull, A., Gerena, L., Lopez-Sanchez, M., Roncal, N.E., Waters, N.C. (2007) Assessment and continued validation of the malaria SYBR Green I-based fluorescence assay for use in malaria drug screening. *Antimicrobial Agents and Chemotherapy* **51**(6): 1926-1933.

207. Jones, M., Mercer, A.E., Stocks, P.A., La Pensee, L.J. … O'Neill, P.M. (2009) Antitumour and antimalarial activity of artemisinin-acridine hybrids. *Biooragnic and Medicinal Chemistry Letters* **19**(7): 2033-2037.

208. Josling, G.A., Llinas, M. (2015) Sexual development in *Plasmodium* parasites: knowing when it's time to commit. *Nature Reviews* **13**(9): 573-587.

209. Jovel, I.T., Bjorkman, A., Roper, C., Martensson, A., Ursing, J. (2017) Unexpected selections of *Plasmodium falciparum* polymorphisms in previously treatment-naïve areas after monthly presumptive administration of three different antimalarial drugs in Liberia 1976-1978. *Malaria Journal* **16**(1): 113.

210. Jurczyszyn, A., Zebzda, A., Czepiel, J., Perucki, W., Bazan-Socha, S., Cibor, D., Owczarek, D., Majka, M. (2014) Geldanamycin and its derivatives inhibit the growth of myeloma cells and reduce the expression of the MET receptor. *Journal of Cancer* **5**(6): 480-490.

211. Kakhlon, O., Cabantchik, Z.I. (2002) The labile iron pool: characterization, measurement, and participation in cellular processes. *Free Radical Biology and Medicine* **33**(8): 1037-1046.

212. Kapoti, D.S., Singh, S., Luqman, S., Bhakuni, R.S. (2018) Synthesis of novel 1,2,3-triazole based artemisinin derivatives and their antiproliferative activity. *New Journal of Chemistry* **42**: 5978-5995.

213. Katsu, T., Ninomiya, C., Kuroko, M., Kobayashi, H., Hirota, T., Fujita, Y. (1988) Action mechanism of amphipathic peptides gramicidin S and melittin on erythrocyte membrane. *Biochimica et Biophysica Acta* **939**(1): 57-63.

214. Karbwang, J., Bangchang, K.N., Thanavibul, A., Bunnag, D., Chongsuphajaisiddhi, T., Harinasuta, T. (1992) Comparison of oral artemether and mefloquine in acute uncomplicated *falciparum* malaria. *The Lancet* **340**(8830): 1245-1248.

215. Karl, S., Wong, R.P.M., St Pierre, T.G., Davis, T.M.E. (2009) A comparative study of a flow-cytometry-based assessment of *in vitro Plasmodium falciparum* drug sensitivity. *Malaria Journal* **8**(294): doi: 10.1186/1475-2875-8-294.

216. Kavishe, R.A., Koenderink, J.B., Ailfrangis, M. (2017) Oxidative stress in malaria and artemisinin combination therapy: Pros and Cons. *The FEBS Journal*. **284**(16): 2579-2591.

217. Kee, A.J., Bryce, N.S., Yang, L., Polishchuk, E., Schevzov, G., Weigert, R., Polishchul, R., Gunning, P.W., Hardeman, E.C. (2017) ER/Golgi trafficking is facilitated by unbranched actin filaments containing Tpm4.2. *Cytoskeleton (Hoboken, N.J.)* **74**(10): 379-389.

218. Kenthirapalan, S., Waters, A.P., Matuschewski, K., Kooij, T.W. (2012) Flow cytometry-assisted rapid isolation of recombinant *Plasmodim berghei* parasites exemplified by functional analysis of aquaglyceroporin. *International Journal of Parasitology* **42**(13-14): 1185-1192.

219. Kesely, K.R., Pantaleo, A., Turrini, F.M., Olupot-Olupot, P., Low, P.S. (2016) Inhibition of an erythrocyte tyrosine kinase with imatinib prevents *Plasmodium falciparum* egress and terminates parasitaemia. *PLoS One* **11**(10): e0164895.

220. Khan, T., van Brummelen, A.C., Parkinson, C.J., Hoppe, H.C. (2012) ATP and luciferase assays to determine the rate of drug action in in vitro cultures of Plasmodium falciparum. *Malaria Journal* **11**:369

221. Khanaani, J., Ginsburg, H. (1989) Metabolic interconnection between the human malaria parasite *Plasmodium falciparum* and its host erythrocyte: Regulation of ATP levels by means of an adenylate translocator and adenylate kinase. *The Journal of Biological Chemistry* **264**(6): 3194-3196.

222. Kikuta, S., Watanabe, S.J., Sato, R., Gusev, O., Nesemelov, A., Sogame, Y., Cornette, R., Kikawada, T. (2017) Towards water-free biobanks: long-term dry preservation at room temperature of desiccation-sensitive enzyme luciferase in air-dried insect cells. *Scientific Reports* **7**(1): doi: 10.1038/s41598-017-06945-y.

223. Klausner, R.D., Donaldson, J.G., Lippincott-Schwartz, J. (1992) Brefeldin A: insights into the control of membrane traffic and organelle structure. *The Journal of Cell Biology* **116**(5): 1071-1080.

224. Klausner, R., Alonso, P. (2004) An attack on all fronts. *Nature* **430**(7002): 930-931.

225. Klayman, D.L. (1985) Qinghaosu (artemisinin): an anti-malarial drug from China. *Science* **228**: 1049-1055.

226. Klonis, N., Xie, S.C., McCaw. J.M., Crespo-Ortiz, M.P., Zaloumis, S.G., Simpson, J.A., Tilley, L. (2013). Altered temporal response of malaria parasites determines differential sensitivity to artemisinin. *Proceedings of the National Academy of Sciences of the United States of America* **110**(13): 5157-5162.

227. Koita, O.A., Sangare, L., Miller, H.D., Sissako, A. … Krogstad, D.J. (2017) AQ-13, an investigational antimalarial, versus artemether plus lumefantrine for the treatment of uncomplicated *Plasmodium falciparum* malaria: a randomized, phase 2, non-inferiority clinical trial. *The Lancet. Infectious Diseases.* **17**(12): 1266-1275.

228. Kondejewski, L.H., Farmer, S.W., Wishart, D.S., Hancock, R.E., Hodges, R.S. (1996) Gramicidin S is active against both gram-positive and gram-negative bacteria. *International Journal of Peptide and Protein Research* **47**(6): 460-466.

229. Kondratskyi, A., Kondratska, K., Vanden Abeele, F., Gordienko, D. … Prevarskaya, N. (2017) Ferroquine, the next generation antimalarial drug, has antitumor activity. *Scientific Reports* **7**(1): 15896.

230. Krishan, A. (1975) Rapid flow cytofluorimetric analysis of mammalian cell cycle by propidium iodide staining. *Journal of Cell Biology* **66**:188-193.

231. Krishna, S., Uhlemann, A., Haynes, R. (2004) Artemisinins: mechanisms of action and potential for resistance. *Drug Resistance Updates* **7**(4-5): 233-244.

232. Krishnamoorthy, G.P., Guida, T., Alfano, L., Avilla, E., Santoro, M., Carlomagno, F., Melillo, R.M (2013) Molecular mechanism of 17-allyamino-17-demethoxygeldanamycin (17-AAG)-induced AXL receptor tyrosine kinase degradation. *Journal of Biological Chemistry* **288**(24): 17481-17494.

233. Krogstad, D.J., Gluzman, I.Y., Kyle, D.E., Oduloa, M.J., Martin, S.K., Milous, W.K., Schlesinger, P.H. (1987) Efflux of chloroquine from *Plasmodium falciparum*: mechanism of chloroquine resistance. *Science* **238**: 1283-1285.

234. Krogstad, D.J., Shlesinger, P.H., Herwaldt, B.L. (1988) Anti-malarial agents: Mechanism of chloroquine resistance. *Antimicrobial Agents and Chemotherapy*. **32**(6): 799-801.

235. Kublin, J.G., Cortese, J.F., Njunju, E.M., Mukadam, R.A.G., Wirima, J.J., Nazembe, P.N., Djimde, A.A., Kouriba, B., Taylor, T.E., Plowe, C.V. (2003) Reemergence of chloroquine-sensitive *Plasmodium falciparum* malaria after cessation of chloroquine use in Malawi. *The Journal of Infectious Diseases* **187**(12): 1870-1875.

236. Kuhen, K.L., Chatterjee, A.K., Rottman, M., Gagaring, K. (2014) KAF156 is an antimalarial clinical candidate with potential for use in prophylaxis, treatment, and prevention of disease transmission. *Antimicrobial Agents and Chemotherapy* **58**(9): 5060-5067.

237. Kumar, K., Giribhattanavar, P., Sagar, C., Patil, S. (2018) A rapid and simple resazurin assay to detect minimum inhibitory concentrations of the first-line drugs for *Mycobacterium tuberculosis* isolated from cerebrospinal fluid. *Journal of Global Antimicrobial Resistance* **12**: 157-161.

238. Lakshmana, V., Bray, P.G., Verdier-Pinard, D., Johnson, D.J., Horrocks, P., Muhle, R.A., Alakpa, G.E., Hughes, R.H., Ward, S.A., Krogstad, D.J., Sidhu, A.B.S., Fidock,

D.A. (2005) A critical role for PfCRT K76T in *Plasmodium falciparum* verapamil-reversible chloroquine resistance. *The EMBO Journal* **24**(13): 2294-2305.

239. Lai, Y., Xing, L., Poda, G.I., Hu, Y. (2007) Structure-activity relationships for interaction with multidrug resistance protein 2 (ABCC2/MRP2): The role of the torsion angle for a series of biphenyl-substituted heterocycles. *Drug metabolism and disposition* **35**(6): 937-945.

240. Lambros, C., Vanderberg, J. (1979) Synchronization of *Plasmodium falciparum* erythrocytic stages in culture. *Journal of Parisitology* **65**(3): 418 – 420.

241. Lanteri, C.A., Chaorattanakawee, S., Lon, C., Saunders, D.L., Rutvisuttinunt, W., Yingyuen, K., Bathurst, I., Ding, X, C.D., Tyner, S.D. (2014) *Ex vivo* activity of endoperoxide antimalarials, including artemisone and arterolane, against multidrug-resistant *Plasmodium falciparum* isolates from Cambodia. *Antimicrobial Agents and Chemotherapy* **58**(10): 5831-5840.

242. Laroche, G., Giguere, P.M., Dupre, E., Dupuis, G., Parent, J.L. (2007) The N-terminal coiled-coil domain of the cytohesin/ARNO family of guanine nucleotide exchange factors interacts with Galphaq. *Molecular and cellular biochemistry* **306**(1-2): 141-152.

243. Lasonder, E., Treeck, M., Alam, M., Tobin, A.B. (2012) Insights into the *Plasmodium falciparum* schizont phosphor-proteome. *Microbes and Infection* **14**(10): 811-819.

244. Lebedeva, I.V., Pande, P., Patton, W.F. (2011) Sensitive and specific fluorescent probes for functional analysis of the three major types of mammalian ABC transporters. *PLOS One* **6**(7): e22429.

245. Lee, S.A., Kim, Y.J., Lee, C.S. (2013) Brefeldin A induces apoptosis by activating the mitochondrial and death receptor pathways and inhibits focal adhesion kinase-mediated cell invasion. *Basic and Clinical Pharmacology* **113**: 329-338.

246. Leitgeb, A.M., Charunwatthana, P., Rueangveerayut, R., Uthaisin, C. … Dondorp, A.M. (2017) Inhibition of merozoite invasion and transient de-sequestration by sevurapin in humans with *Plasmodium falciparum* malaria. *PLoS One* **12**(12): e0188754.

247. Leong, F.J., Jain, J.P., Feng, Y., Goswani, B., Stein, D. (2018) A phase 1 evaluation of the pharmacokinetic/pharmacodynamic interaction of the anti-malarial agents KAF156 and piperaquine. *Malaria Journal* **17**(7): doi: 10.1186/s12936-017-2162-8.

248. Leroy, D., Campo, B., Ding, X.C., Burrows, J.N., Cherbuin, S. (2014) Defining the biology component of the drug discovery strategy for malaria eradication. *Trends in Parasitology* **30**(10): 478-490.

249. Li, W., Mo, W., Shen, D., Sun, L., Wang, J., Lu, S., Gitschier, J.M., Zhou, B. (2005). Yeast model uncovers dual roles of mitochondria in the action of artemisinin. *PLoS GENETICS* **1**(3): e36.

250. Lin, Z.P., Johnson, D.R., Finch, R.A., Belinsky, M.G., Kruh, G.D., Sarotelli, A.C. (2002) Comparitive study of the importance of multidrug resistance-associated protein 1 and P-glycoprotein to drug sensitivity in immortalized mouse embryonic fibroblasts. *Molecular Cancer Therapeutics* **1**(12): 1105-1114.

251. Linares, M., Viera, S., Crespo, B., Franco, V., Gomez-Lorenzo, M.G., Jimenez-Diaz, M.B., Angulo-Barturen, I., Sanz, L.M., Gamo, F. (2015) Identifying rapidly parasiticidal antimalarial drugs using a simple and reliable *in vitro* viability fast assay. *Malaria Journal* **14**(441): doi: 10.1186/s12936-015-0962-2.

252. Linden, L., Schaar, H.M., Lanke, K.H.W., Neyts, J., Kuppeveld, F.J.M. (2010) Differential effects of the putative GBF1 inhibitors Golgicide A and AG1478 on Enterovirus replication. *Journal of Virology* **84**(15): 7535-7542.

253. Liu, J., Gluzman I.Y., Drew, M.E., Goldberg, D.E. (2005). The role of *Plasmodium falciparum* food vacuole plasmepsins. *The Journal of Biological Chemistry* **280**: 1432 – 1437.

254. Liu, J., Hung, Y., Yang, C., Chen, Y. (2015) The antimicrobial activity of gramicidin A is associated with hydroxyl radical formation. *PLoS One* **10**(1): e0117065.

255. Llanos-Cuentas, A., Casapia, M., Chuquiyauri, R., Hinojosa, J.C. … Duparc, S. (2018) Antimalarial activity of single-dose DSM265, a novel *Plasmodium* dihydroortate dehydrogenase inhibitor, in patients with uncomplicated *Plasmodium falciparum* or *Plasmodium vivax* malaria infection: a proof-of-concept, open-label, phase 2a study. *The Lancet. Infectious Diseases* **18**(8): 874-883.

256. Loew, L.M., Tuft, R.A., Carrington, W., Fay, F.S. (1993) Imagine in five dimensions: time-dependent membrane potentials in individual mitochondria. *Biophysical Journal* **65**(6): 2396-2407.

257. Loo, C.S.N., Lam, N.S.K., Yu, D., Su, X., Lu, F. (2017) Artemisinin and its derivatives in treating protozoan infections beyond malaria. *Pharmacological Research* **117**: 192-217.

258. Lopez, M.L., Vommaro, R., Zalis, M., de Souza, W., Blair, S., Segura, C. (2010) Induction of cell death on *Plasmodium falciparum* asexual blood stages by *Solanum nudum* steroids. *Parasitology International* **59**: 217-225.

259. Loria, P., Miller, S., Foley, M., Tilley, L. (1999) Inhibition of the peroxidative degradation of haem as the basis of action of chloroquine and other quinolone anti-malarials. *Biochemical Journal* **339**(Pt 2): 363-370.

260. Luchsinger, C., Aguilar, M., Burgos, P.V., Ehrenfeld, P., Mardones, G.A. (2018) Functional disruption of the Golgi apparatus protein Arf1 sensitizes MDA-MB-231

breast cancer cells to the antitumor drugs Actinomycin D and Vinblatine through ERK and AKT signaling. *PLoS One* **13**(4): e0195401.

261. Luhrmann, A., Tholke, J., Behn, I., Schumann, J., Tiegs, G., Hauschildt, S. (1998) Immunomodulating properties of the antibiotic novobiocin in human monocytes. *Antimicrobial agents and chemotherapy* **42**(8): 1911-1916.

262. Lunga, M.J., Chisango, R.L., Weyers, C., Isaacs, M., Taylor, D., Edkins, A.L., Khanye, S.D., Hoppe, H.C., Veale, C.G.L. (2018) Expanding the SAR of nontoxic antiplasmodial indolyl-3-ethanone ethers and thioethers. *ChemMedChem* **13**(13): 1353-1362.

263. Luo, X.G., Zou, J.N., Wang, S.Z., Zhang, T.C., Xi, T. (2010) Novobiocin decreases SMYD3 expression and inhibits the migration of MDA-MB-231 human breast cancer cells. *IUBMB Life* **62**(3): 194-199.

264. Lyman, G., DeVincenzo, J.P. (1967) Determination of pictogram amounts of ATP using the luciferin-luciferase enzyme system. *Analytical Biochemistry* **21**(3): 435-443.

265. Lyons, A.B., Parish, C. R. (1994) Determination of lymphocyte division by flow cytometry. *J Immunol Methods* 171:131–137.

266. Mace, K.E., Mwandama, D., Jafali, J., Luka, M., Filler, S.J., Sande, J., Ali, D., Kachur, S.P., Mathanga, D.P., Skarbinski, J. (2011) Adherence to treatment with artemether-lumefantrine for uncomplicated malaria in rural Malawi. *Clinical Infectious Diseases* **53**(8): 772 – 779.

267. Majewski, M. (2014) A current opinion on the safety and efficacy of doxycycline including parenteral administration – a review. *Polish Annals of Medicine* **21**(1): 57 – 62.

268. Makanga, M., Krudshood, S. (2009) The clinical efficacy of artemether/lumefrantrine (Coartem). *Malaria Journal* **8**(suppl 1): S5.

269. Maitland, K. (2015) Management of severe pediatric malaria in resource-limited settings. *BioMed Central* **13**(42): 1-27.

270. Makler, M.T., Hinrichs, D.J. (1993) Measurement of the lactate dehydrogenase activity of Plasmodium falciparum as an assessment of parasitemia. *American Journal of Tropical Medicine and Hygiene* **48**(2): 205-210.

271. malERA Consultative Group on Drugs (2011) A research agenda for malaria eradication: drugs. *PLoS Medicine* **8**: e1000402.

272. Maloney, A., Workman, P. (2002) Hsp90 as new therapeutic target for cancer therapy: the story unfolds. *Expert Opinion on Biological Therapy* **2**(1): 3-24.

273. Manfredi, G., Yang, L., Gajewski, C.D., Mattiazzi, M. (2002) Measurements of ATP in mammalian cells. *Methods* **26**(4): 316-326.

274. Marchetti, R.V., Lehane, A.M., Shafik, S.H., Winterberg, M., Martin, R.E., Kirk, K. (2015) A lactate and formate transporter in the intraerythrocytic malaria parasite, *Plasmodium falciparum*. *Nature Communications* **6**: 6721.

275. Marcu, M.G., Chadli A., Bouhouche, I., Catelli, M., Neckers, L.M. (2000) The heat shock protein 90 antagonist novobiocin interacts with a previously unrecognised ATP-binding domain in the carboxyl terminus of the chaperone. *Journal of Biologial Chemistry* **275**(47): 37181-37186.

276. Martinez, S. M., Kingston, S., Ngor, A., Chaput, J.C., Vinay, N.J., Korch, S.B. (2018) Direct delivery of a synthetic ATP binding protein reduces ATP and induces apoptosis in Hela cells. *AACR Annual Meeting 2018* **78**(13): doi: 10.1158/1538-7445.AM2018-452.

277. Martinkova, M., Mezeiova, E., Fabisikova, M., Gonda, J., Pilatova, M., Mojzis, J. (2015) Total synthesis of pachastrissamine together with its 4-epi-congener via [3,3-

sigmatropic rearrangements and antiproliferative/cytotoxic evaluation. *Carbohydrate Research* **402**: 6-24.

278. McCarthy, J.S., Lotharius, J., Ruckle, T., Chalon, S. … Mohrle, J.J. (2017) Safety, tolerability, pharmacokinetics, and activity of the novel long-acting antimalarial DSM265L a two-part first-in-human phase 1a/1b randomized study. *The Lancet. Infectious Diseases* **17**(6): 626-635.

279. McConnell, J., Wang, Y., McAlpine, S. (2015) Targeting the C-Terminus of Hsp90 as a cancer therapy. In: McAlpine, S., Edkins, A. (eds) *Heat Shock Protein Inhibitors. Topics in Medicinal Chemistry* **19**. Springer, Cham.

280. McFarlin, B., Gary, M.A. (2017) Flow cytometry what you see matters: Enhanced clinical detection using image-based flow cytoimetry. *Methods* **112**(1): 1-8.

281. McMillian, M.K., Li, L., Parker, J.B., Patel, L., Zhong, Z., Gunnet, J.W., Powers, J.W., Johnson, M.D. (2002) An improved resazurin-based cytotoxicity assay for hepatic cells. *Cell Biology and Toxicology* **18(**3): 157-173.

282. McNamaria, D.T., Kasehagen, L.J., Grimberg, B.T., Cole-Tobian, J., Collins, W.E., Zimmerman, P.A. (2006) Diagnosing infection levels of four human malaria parasite species by a polymerase chain reaction/ligase detection reaction fluorescent microsphere-based assay. *The American Journal of Tropical Medicine and Hygiene* **74(**3): 413-421.

283. McNamara, C.W., Lee, M.C.S., Lim, C.S., … Winzeler, E.A. (2013) Targeting *Plasmodium* phosphatidylinositol 4-kinase to eliminate malaria. *Nature* **504(**7479): 248-253.

284. Mehta, M., Sonawat, H.M., Sharma, S. (2006) Glycolysis in *Plasmodium falciparum* results in modulation of host enzyme activities. *Journal of Vector Borne Diseases* **43(**3): 95-103.

285. Meshnick, S.R., Yand, Y., Lima, V., Kuypers, F., Kamchonwongpaisan, S., Yuthavong, Y. (1993) Iron-dependent free radical generation from the antimalarial agent artemisinin. *Antimicrobial Agents and Chemotherapy* **37**(5): 1108-1114.

286. Meshnick, S.R., Dobson, M.J. (2001) *The History of Anti-malarial Drugs*. Anti-malarial chemotherapy: Mechanisms of action, resistance, and new directions in drug discovery. Humana Press, Totowa, New Jersey, USA: 15-25.

287. Miller, L.H., Good, M.F., Milon, G. (1994) Malaria Pathogenesis. *Science* **264**:1878-1883.

288. Miguel-Blanco, C., Molina, I., Bardera, A.I., Diaz, B., Heras, L., Lozano, S., Gonzalez, C., Rodriguez, J., Delves, M.J., Ruecker, A., Colmearejo, G., Viera, S., Martinez, M.S., Fernandez, E., Baum, J., Sinden, R.E., Herreros, E. (2017) Hundreds of dual-stage antimalarial molecules discovered by a functional gametocyte screen. *Nature Communications* **8**: 15160.

289. Mikolajczak, S.A., Vaughan, A.M., Kangwanrangsan, N., Roobsoong, W., Fishbaugher, M., Timamnuaychok, N., Rezakhani, N., Lakshmana, V., Singh, N., Kaushansky, A., Camargo, N., Baldwin, M., Lindner, S.E., Adams, J.H., Sattabongkot, J., Kappe, S.H.I. (2015) *Plasmodium vivax* liver stage development and hypnozoite persistence in human liver-chimeric mice. *Cell Host and Microbe* **17**(4): 526-535.

290. Misumi, Y., Miki, K., Takatsuki, A., Tamura, G., Ikehara, Y. (1986) Novel blockade by brefeldin A of intracellular transport of secretory proteins in cultured rat hepatocytes. *The Journal of Biological Chemistry* **261**(24): 11398-11403.

291. Mishra, M., Mishra, V.K., Kashaw, V., Iyer, A.K., Kashaw, S.K. (2017) Comprehensive review on various strategies for antimalarial drug discovery. *European Journal of Medicinal Chemistry* **125**(5): 1300-1320.

292. Mithra, M., Mishra, V.K., Kasahw, V., Iyer, A.K., Kashaw, S.K. (2017) Comprehensive review on various strategies for antimalarial drug discovery. *European Journal of Medicinal Chemistry* **125**(5): 1300-1320.

293. Mohammed, A., Ndaro, A., Kalinga, A., Manjurano, A., Mosha, J.F., Mosha, D.F., van Zwetselaar, M., Koenderink, J.B., Mosha, F.W., Alifrangis, M., Reyburn, H., Roper, C., Kavishe, R.A. (2013) Trends in chloroquine resistance marker, Pfcrt-K76T mutation ten years after chloroquine withdrawl in Tanzania. *Malaria Journal* **12**(415): doi: 10.1186/1475-2875-12-415.

294. Molina-cruz, A., Canepa, G.E., Barillas-Mury, C. (2017) *Plasmodium P47:* a key gene for malaria transmission by mosquito vectors. *Current Opinion in Microbiology* **40**: 168-174.

295. Mombo-Ngoma, G., Remppis, J., Sievers, M., Manego, Z., Endamne, L., Lell, B., Hutchinzon, D., Kremsner, P. (2016) Fosmidomycin-piperaquine as a non-artemsinin-based combination for acute uncomplicated *Plasmodium falciparum* malarial. *BMJ Global Health* **2**(2).

296. Moneriz, C., Marin-Garcia, P., Bautista, J.M., Diez, A., Puyet, A. (2009) Haemoglobin interference and increased sensitivity of fluorimetric assays for quantification of low-parasitaemia *Plasmodium* infected erythrocytes. *Malaria Journal* **8**(279): doi: 10.1186/1475-2875-8-279.

297. Moneriz, C., Marin-Garcia, P., Garcia-Granados, A., Bautista, J.M., Diez, A., Puyet, A. (2011) Parasitostatic effect of maslinic acid. I. growth arrest of *Plasmodium falciparum* intraerythrocytic stages. *Malaria Journal* **10**:82.

298. Montecucco, A., Zanetta, F., Biamonti, G. (2015) Molecular mechanisms of etoposide. *Experimental and Clinical Sciences* **14**: 95-108.

299. Moore, B.R., Laman, M., Salman, S., Batty, K.T., Page-Sharp, M., Hombhanje, F., Manning, L., Davis, T.M. (2016) Napthoquine: An emerging candidate for artemisinin combination therapy. *Drugs* **76**(7): 789-804.

300. Morris, C.A., Duparc, S., Borghini-Fuhrer, I., Jung, D., Shin, C.S., Fleckstein, L. (2011) Review of the clinical pharmacokinetics of artesunate and its active metabolite dihydroartemisinin following intravenous, intramuscular, oral or rectal administration. *Malaria Journal* **10**(263): doi: 10.1186/1475-2875-10-263.

301. Mossallam, S.F. (2010) Detection of some intestinal protozoa in commercial fresh juices. *Journal of the Egyptian Society of Parasitology* **40**(1): 135-149.

302. Moyo, P., Botha, M.E., Nondaba, S., Niemand, J., Maharaj, V.J., Eloff, J.N., Louw, A.I., Birkholtz, L. (2016) In vitro inhibition of *Plasmodium falciparum* early and late stage gametocyte viability by extracts from eight traditionally used South African plant species. *Journal of Ethnopharmacology* **185**(5): 235-242.

303. Muller, I.B., Hyde, J.E. (2010) Antimalarial drugs: modes of action and mechanisms of parasite resistance. *Future Microbiology* **5**(12): 1857-1873.

304. Muller, J., Balmer, V., Winzer, P., Rahman, M., Manser, V., Haynes, R.K., Hemphill, A. (2015) *In vitro* effects of new artemisinin derivatives in *Neospora caninum*-infected human fibroblasts. *International Journal of Antimicrobial Agents* **46**(1): 88-93.

305. Mungthin, M., Bray, P.G., Ridley, R.G., Ward, S.A. (1998) Central role of haemoglobin degradation in mechanisms of action of 4-aminoquinolines, quinolone methanols, and phenanthrene methanols. *Antimicrobial Agents and Chemotherapy* **42**(11): 2973-2977.

306. Mutai, B.K., Waitumbi, J.N. (2010) Apoptosis stalks *Plasmodium falciparum* maintained in continuous culture condition. *Malaria Journal* **9**(Suppl 3): S6.

307. Myint, P.T., Shwe, T. (1987) A controlled clinical trial of artemether (qinghaosu derivative) versus quinine in complicated and severe *falciparum* malarial. *Transactions of the Royal Society of Tropical Medicine and Hygiene* **81**(4): 559-561.

308. Nagelschmitz, J., Voith, B., Wensing, G., Roemer, A., Fugmann, B., Haynes, R.K., Kotecka, B.M., Rieckmann, Edstein, M.D. (2008) First assessment in humans of the safety, tolerability, pharmacokinetics, and *ex vivo* Pharmacodynamic antimalarial activity of the new artemisinin derivative artemisone. *Antimicrobial Agents and Chemotherapy* **52**(9): 3085-3091.

309. Narain, U., Sall, C. (2016) Methodology for valuing the health impacts of air pollution: discussion of challenges and proposed solutions. Washington D.C. World Bank Group.

310. Nayak, M.S.,Yang, J.M., Hait, W.N. (2007) Effect of a single nucleotide polymorphism in the murine double minute 2 promoter (SNP309) on the sensitivity to topoisomerase II-targeting drugs. *Cancer Research* **67**(12): 5831-5839.

311. Naydenov, N.G., Harris, G., Morales, V., Ivanov, A.I. (2012) Loss of membrane trafficking protein αSNAP induces non-canonical autophagy in human epithelia. *Cell Cycle* **11**(24): 4613-4625.

312. Neckers, L., Workman, P. (2012) Hsp90 molecular chaperone inhibitors: are we there yet? *Clinical Cancer Research* **18**(1): 64-76.

313. Neu, H.C. (1987) The biochemical basis of antimicrobial and bacterial resistance. *The bulletin of the New York Academy of Medicine* **63**(3): 295-317.

314. Nir-Paz, R., Prevost, M.C., Nicolas, P., Blanchard, A., Wroblewski, H. (2002) Susceptibilities of *Mycoplasma fermentans* and *Mycoplasma hyorhinis* to membrane-active peptides and enrofloxacin in human tissue cell cultures. *Antimicrobial Agents and Chemotherapy* **46**(5): 1218-1225.

315. Nixon, G.L., Moss, D.M., Shone, A.E., Lalloo, D.G., Fisher, N., O'Neill, P.M., Ward, S.A., Biagini, G.A. (2013) Antimalarial pharmacology and therapeutics of atovaquone. *The Journal of Antimicrobial chemotherapy* **68**(5): 977-985.

316. Nosten, F., Luxemburger, C., ter Kuile, F.O., Woodrow, C., Eh, J.P., Chongsuphajaisddhi, T., White, N.J. (1994) Treatment of multidrug-resistant Plasmodium falciparum malaria with 3-day artesundate-mefloquine combination. *Journal of Infectious Diseases* **170**(4): 971-977.

317. Nosten, F., Kuile, E., Maelankiri, L., Chongsuphajaisiddhi, T., Nopdonrattakoon, L., Tangkitchot, S., Bourdreau, E., Bunnag, D., White, N.J. (1994) Mefloquine prophylaxis prevents malaria during pregnancy: a double-blind, placebo-controlled study. *Journal of Infectious Diseases* **169**: 595-603.

318. Nosten, F., van Vugt, M., Price, R., Luxemburger,C., Thway, K.L., Brockman, A., McGready, R., ter Kuile, F., Looareesuwan, S., White, N.J. (2000) Effects of artesunate-mefloquine combination on incidence of *Plasmodium falciparum* malaria and mefloquine resistance in western Thailand: a prospective study. *Lancet* **356**(9226): 297-302.

319. Nzila, A. (2006) The past, present and future of antifolates in the treatment of *Plasmodium falciparum* infection. *Journal of Antimicrobial Chemotherapy* **57**(6): 1043-1054.

320. O`Neill, P.M., Barton, V.E., Ward, S.A. (2010) The molecular mechanism of action of artemisinin - the debate continues. *Molecules* **15**(3): 1705-1721.

321. Ohashi, Y., Iijima, H., Yamaotsu, N., Yamazaki, K., Sato, S., Okamura, M., Sugimoto, K., Dan, S., Hirono, S., Yamori, T. (2011) AMF-26, a novel inhibitor of the Golgi system, targeting ADP-ribosylation Factor 1 (Arf1) with potential for cancer therapy. *Journal of Biological Chemistry* **287**(6): 3885-3897.

322. Okell, L.C., Griffin, J.T., Roper, C. (2017) Mapping sulphadoxine-pyrimethamine-restitant *Plasmodium falciparum* malaria in infected humans and in parasite populations in Africa. *Scientific Reports* **7**(1): doi: 10.1038/s41598-017-06708-9.

323. O'Brien, M.C., Bolton, W.E. (1995) Comparison of cell viability probes compatible with fixation and permeabilization for combined surface and intracellular staining in flow cytometry. *Cytometry* **19**: 243-255.

324. O`Hayre, M., Vazguez-Prado, J., Kufareva, I., Stawiski, E.W., Handel, T.M., Sehagiri, S., Gutkind, J.S. (2013) The emerging mutational landscape of G proteins and G-protein-coupled receptors in cancer. *Nature Reviews. Cancer* **13**(6): 412-424.

325. O'Neill, P.M., Barton, V.E., Ward, S.A. (2010) The molecular mechanism of action of artemisinin – The debate continues. *Molecules* **15**(3): 1705-1721.

326. O`Reilly, C.M., Fogarty, K.E., Drummond, R.M., Tuft, R.A., Walsh, J.V. (2003) Quantitative analysis of spontaneous mitochondrial depolarizations. *Biophyscial Journal* **85**(5): 3350-3357.

327. Obermann, W.M., Sondermann, H., Russo, A.A., Pavletich, N.P., Hartl, F.U. (1998) In vivo function of Hsp90 is dependent on ATP binding and ATP hydrolysis. *The Journal of Cell Biology* **143**(4): 901-910.

328. Ochel, H., Eichhorn, K., Gadermann, G. (2001) Geldanamycin: the prototype of a class of antitumor drugs targeting the heat shock protein 90 family of molecular chaperones. *Cell Stress Chaperones* **6**(2): 105-112.

329. Oiknonomou, C.M., Jensen, G.J. (2017) Cellular Electron Cryotomography: Toward structural biology in situ. *Annual Review of Biochemistry* **86**: 873-896.

330. Olszewski, K.L., Llinas, M. (2011) Central carbon metabolism of Plasmodium parasites. *Molecular and Biochmical Parasitology* **175**(2): 95-103.

331. Pacifici, G.M. (2018) Clinical pharmacology of the antimalarial quinine in children. *International Journal of Pediatrics* **6**(4): 7451-7465.

332. Paguio, M.F., Bogle, K.L., Roepe, P.D. (2011) *Plasmodium falciparum* resistance to cytocidal versus cytostatic effects of chloroquine. *Molecular and Biochemical Parasitology* **178**(1-2): 1-6.

333. Painter, H.J., Morrisey, J.M., Vaidya, A.B. (2010) Mitochondrial electron transport inhibition and viability of intraethryocytic *Plasmodium falciparum*. *Antimicrobial Agents and Chemotherapy* **54**(12): 5281-5287.

334. Pandey, A.V., Tekwani, B.L., Singh, R.L., Chauhan, V.S. (1999) Artemisinin, an endoperoxide anti-malarial, disrupts the hemoglobin catabolism and heme detoxification systems in malarial parasite. *The Journal of Biological Chemistry* **274**: 19383 – 19388.

335. Pantaleo, A., Ferru, E., Carta, F., Mannu, F., Giribaldi, G., Vono, R., Lepedda, A.J., Pippia, P., Turrini, F. (2010) Analysis of changes in tyrosine and serine phosphorylation of red cell membrane proteins induced by *P. falciparum* growth. *Proteomics* **10**(19): 3469-3479.

336. Paquet, T., Le Manach, C., Cabrera, D.G., Younis, Y. … Chibale, K. (2017) Antimalarial efficacy of MMV390048, an inhibitor of *Plasmodium* phosphatidylinositol 4-kinase. *Science Translational Medicine* **9**(387): doi: 10.1126/scitranslmed.aad9735.

337. Pasini, E.M. Ierssel, D., Vial, H.J., Kocken, C.H.M. (2013) A novel live-dead staining methodology to study malaria parasite viability. *Malaria Journal* **12**(190): doi: 10.1186/1475-2875-12-190.

338. Pattanapanyasat, K., Webster, H.K., Udomsangpetch, R., Wanachiwanawin, W., Yongvanitchit, K. (1992) Flow cytometric two-color staining technique for

simultaneous determination of human erythrocyte membrane antigen and intracellular malarial DNA. *Cytometry* **13**(2): 182 – 187.

339. Peatey, C.L., Leroy, D., Gardiner, D.L., Trenholme, K.R. (2012) Anti-malarial drugs: How effective are they against *Plasmodium falciparum* gametocytes? *Malaria Journal* **11**: 34.

340. Pegoraro, S., Duffey, M., Otto, T.D., Wang, Y., Rosemann, R., Baumgartner, R., Fehler, S.K., Lucantoni, L., Avery, V.M., Moreno-Sabater, A., Mazier, D., Vial, H.J., Strobl, S., Sanchez, C.P., Lanzer, M. (2017) SC83288 is a clinical development candidate for the treatment of severe malaria. *Nature Communications* **8**(14193): doi: 10.1038/ncomms14193.

341. Pena, F.J., Martin-Muno, P./, Ortega-Ferrusola, C. (2017) Advances in flow cytometry in basic and applied equine andrology. *Animal Reprodcution* **14**(1): 136-142.

342. Pfaller, M.A., Krogstad, D.J., Parquette, A.R., Nguyen-Dinh, P. (1982) Plasmodium falciparum: stage-specific lactate production in synchronized cultures. *Experimental parasitology* **54**(3): 391-396.

343. Phyo, A.P., Jittamala, P., Nosten, F.H., Pukrittayakamee, S., Imwong, M., White, N.J., Duparc, S., Macintyre, F., Baker, M., Mohrle, J.J. (2016) Antimalarial activity of artefenomel (OZ439), a novel synthetic antimalarial endoperoxide, in patients with *Plasmodium falciparum* and *Plasmodium vivax* malaria: an open-label phase 2 trial. The *Lancet. Infectious Diseases* **16**(1): 61-69.

344. Pluess, B., Tanser, F.C., Lengeler, C., Sharp, B.L. (2010) Indoor residual spraying for preventing malaria. *The Cochrane Database of Systematic Reviews* **4**: CD006657.

345. Ponsford, M.J., Medana, I.M., Prapansilp, P., Hien, T.T., Lee, S.J., Dondorp, A.M., Esiri, M.M., Day, N.P., White, N.J., Turner, G.D. (2012) Sequestration and

microvascular congestion are associated with coma in human cerebral malaria. *Journal of Infectious Diseases* **205**(4): 663-671.

346. Putnam, K.P., Bombick, D.W., Doolittle, D.J. (2002) Evaluation of eight *in vitro* assays for assessing the cytotoxicity of cigarette smoke condensate. *Toxicology in vitro* **16**(5): 599-607.

347. Qi, X., Wang, F., Mortensen, M., Wertz, R., Chen, G. (2018) Targeting an oncogenic kinase/phosphatase signaling network for cancer therapy. *Acta Pharmaceutica Sinica B* **8**(4): 511-517.

348. Rajabi, H., Kufe, D. (2017) MUC1-C oncoprotein integrates a program of EMT, epigenetic reprogramming and immune evasion in human carcinomas. *Biochimica et Biophysica Acta* **1868**(1): 117-122.

349. Rautenbach, M., Eyeghe-Bickong, H.A., Vlok, N.M., Stander, M., de Beer, A. (2012) Direct surfactin-gramicidin S antagonism supports detoxification in mixed producer cultures of *Bacillus subtilis* and *Aneurinibacillus migulanus*. *Microbiology* **158**: 3072-3082.

350. Reader, J., Botha, M., Theron, A., Lauterbach, S.B., Rossouw, C., Engelbrecht, D., Wepener, M., Smit, A., Leroy, D., Mancama, D., Coetzer, T.L., Birkholtz, L. (2015) Nowhere to hide: interrogating different metabolic parameters of *Plasmodium falciparum* gametocytes in a transmission blocking drug discovery pipeline towards malaria elimination. *Malaria Journal* **14**(213): doi: 10.1186/s12936-015-07018-z.

351. Ridley, R. (2001) Malaria Drug Development. *Malaria in Africa: Emerging Prevention and Control Strategies.* Report from AAAS Annual Meeting, San Francisco.

352. Rodriguez-Corrales, J.A., Josan, J.S. (2017) Resazurin live cell assay: Setup and fine-tuning for reliable cytotoxicity results. *Proteomics for Drug Discovery* **1647**: 207-219.

353. Rogers, L. (2012) The rapid cure of amoebic dysentery and hepatitis by hypodermic injections of soluble salts of emetine. *British Medical Journal* **1**(2686): 1424-1425.

354. Rolling, T., Agbenyega, T., Krishna, S., Kremsner, P.G., Cramer, J.P. (2015) Delayed haemolysis after artesunate treatment of severe malaria – review of the literature and perspective. *Travel Medicine and Infectious Disease* **13**(2): 143-149.

355. Rollo, I.M. (1975) Drugs used in chemotherapy of amebiasis. *The pharmacological basis of therapeutics*. Macmillan, New York, pp 1074-1078.

356. Rossi, G., Vernaeve, L., van den Bergh, R., Nguon, C., Debackere, M., Peiri, A.C., Van, V., Khim, N., Kim, S., Eam, R., Ken, M., Khean, C., de Smet, M., Menard, D., Kindermans, J.M. (2018) Closing in on the reservoir: Proactive case detection in high-risk groups as a strategy to detect *Plasmodium falciparum* asymptomatic carriers in Cambodia. *Clinical Infectious Diseases*: doi: 10.1093/cid/cix1064 [ahead of print].

357. Roth, J.M., Sawa, P., Omweri, G., Osoti, V., Makio, N., Bradley, J., Bousema, T., Schallig, H.D.F.H., Mens, P.F. (2018) *Plasmodium falciparum* gametocyte dynamics after pyronaridine-artesunate or artemether-lumefantrine treatment. *Malaria Journal* **17**(1): 223.

358. Rottman, M., McNamara, C., Yeung, B.K.S., Lee, M.C.S., Zou, B… … Diagana, T.T. (2010) Spiroindolones, a new and potent chemotype for the treatment of malaria. *Science* **329**(5996): 1175-1180.

359. Rueangweerayut, R., Bancone, G., Harrell, E.J. … Green, J.A. (2017) Hemolytic potential of tafenoquine in female volunteers heterozygous for glucose-6-phosphate dehydrogenase (G6PD-deficiency) (G6PD Mahidol Variant) versus G6PD-normal volunteers. *American Journal of Tropical Medicine and Hygiene* **97**(3): doi: 10.4269/ajtmh.16-0779.

360. Saibil, H. (2013) Chaperone machines for protein folding, unfolding and disaggregation. *Nature Reviews Molecular Cell Biology* **14**(10): 630-642.

361. Sanz, L.M., Crespo, B., De-Corzar, C., Ding, X.C., Llergo, J., Burrows, J.N., Garcia-Bustos, J.F., Gamo, F.J. (2012) *P. falciparum in vitro* killing rates allow to discriminate between different anti-malarial mode-of-action. *Plos One* **7**(2): e30949.

362. Saenz, J.B., Sun, W.J., Chang, J.W., Li, J., B.B., Gray, N.S., Haslam, D.B. (2009) Golgicide A reveals essential roles for GBF1 in Golgi assembly and function. *Nature Chemical Biology* **5**(3): 157-165.

363. Savage, M.L., Olah, I., Scott, T.R. (1992) Plasma cell proliferation in the chicken harderian gland. *Cell Proliferation* **25**(4): 337-344.

364. Schlecht, R., Scholz, S.R., Dahmen, H., Wegner, A., Sirrenberg, C., Musli, D., Bomke, J., Eggenweiler, H.M., Mayer, M.P., Bukau, B. (2013) Functional analysis of Hsp70 inhibitors. *PLoS One* **8**(11): e78443.

365. Schlienger, S., Campbell, Claing, A. (2014) Arf1 regulates the Rho/MLC pathway to control EGF-dependent breast cancer cell invasion. *Molecular Biology of the cell* **25**(1): 17-29.

366. Schulte, T.W., Akinaga, S., Murakata, T., Agatsuma, T., Sugimoto, S., Nakano, H., Lee, Y.S., Simen, B.B., Argon, Y., Felts, S., Toft, D.O., Neckers, L.M., Sharma, S.V. (1999). Interaction of radicicol with members of the heat shock protein 90 family of molecular chaperones. *Molecular Endocrinology* **13**(9): 1435-1448.

367. Sedegah, M., Kim, Y., Ganeshan, H., Huang, J., Belmonte, M., Abot, E., Banania, J.G., Farooq, F., McGrath, S., Peters, B., Sette, A., Soisson, L., Diggs, C., Doolan, D.L., Tamminga, C., Villasante, E., Hollingdale, M.R., Richie, T.L. (2013) Identification of minimal human MHC-resticred CD8+ T-cell epitopes within the *Plasmodium falciparum* circumsporozoite protein (CSP). *Malaria Journal* **12**: 185.

368. Seemann, N., Welling, A., Rustenbeck, I. (2017) The inhibitor of connexin Cx36 channels, mefloquine, inhibits voltage-dependent Ca^{2+} channels and insulin secretion. *Molecular and Cellular Endocrinology:* [in press].

369. Shao, R.G., Shimizu, T., Pommier, Y. (1996) Brefeldin A is a potent inducer of apoptosis in human cancer cells independently of p53. *Experimental Cell Research* **227**(2): 190-196.

370. Sharaf el dein, O., Gallerne, C., Deniuad, A., Lemaire, C. (2009) Role of the permeability transition pore complex in lethal inter-organelle crosstalk. *Bioscience* **14**(9): 3465-3482.

371. Sharma, S., Bharti, R.S., Bhardwaj, N., Anvikar, A.R., Valecha, N., Mishra, N. (2017) Correlation of *in vitro* sensitivity of chloroquine and other antimalarials with the partner drug resistance to *Plasmodium falciparum* malaria in selected sites of India. *Indian Journal of Medical Microbiology* **35**(4): 485-490.

372. Shen, B. (2015) A new golden age of natural products drug discovery. *Cell* **163**(6): 1297-1300.

373. Sikora, A., Michalski, R., Hardy, M., Ouari, O., Adamus, J., Marcinek, A., Zielonka, J., Kalyanaraman, B. (2017) N,N.N′,N′-tetramethylhydroethidine (TMHE) - in search for better probes for the detection of superoxide radical anion: P-061. *Free Radical Biology and Medicine* **108**(Supplement 1): S38.

374. Singh, G., Jayanarayan, K.G., Dey, C.S. (2005) Novobiocin induces apoptosis-like cell death in topoisomerase II over-expressing arsenite resistant *Leishmania donovani*. *Molecular and Biochemical Parasitology* **141**(1): 57-69.

375. Singh, S., Carpenter, A.E., Genovesio, A. (2011) Increasing the content of high-content screening. *Journal of Biomolecular Screening* **19**(5): 640-650.

376. Singh, N., Barnes, S.J., Kennedy, S., Adams, J.H. (2017) Experimental evaluation of cryopreservative solutions to maintain *in vitro* and *in vivo* infectivity of *P. berghei* sporozoites. *PLoS One* **12**(5): e0177304.

377. Sirenko, O., Mitlo, T., Hesley, J., Luke, S., Owens, W., Cromwell, E.F. (2015) High-content assays for characterizing the viability and morphology of 3D cancer spheroid cultures. *Assay and Drug Development Technologies* **13**(7): 402-414.

378. Sissoko, M.S., Healy, S.A., Katile, A., Omaswa, F., Zaidi, I., Gabriel, E.E., … Duffy, P.E. (2017) Safety and efficacy of PfSPZ vaccine against plasmodium falciparum via direct venous inoculation in healthy malaria-exposed adults in Mali: a randomized, double-blind phase 1 trial. *The Lancet infectious diseases* **17**(5): 498-509.

379. Skrzypek, R., Callaghan, R. (2017) The 'pushmi-pullyo' of resistance to chloroquine in malaria. *Essays in Biochemistry* **61**(1): 167-175.

380. Smilkstein, M., Sriwilaijaroen, N., Kelly, J.X., Wilairat, P., Riscoe, M. (2004) Simple and inexpensive fluorescence-based technique for high-throughput anti-malarial drug screening. *Antimicrobial Agents and Chemotherapy* **48**(5): 1803-1806.

381. Smith, D.H., Davis, B.D. (1966) Mode of action of Novobiocin in *Eschericia coli*. *Journal of Bacteriology* **93**(1): 71-79.

382. Spangenberg, T., Burrows, J.N., Howalczyk, P., McDonald, S., Wells, T.N., Willis, P. (2013) The open access malaria box: A drug discovery catalyst for neglected diseases. *PLoS One* **8**(6): e62906.

383. Solyakov, L., Halbert, J., Alam, M.M., Semblat, J.P. … Doerig, C. (2011) Global kinomic and phosphor-proteomic analyses of the human malaria parasite *Plasmodium falciparum*. *Nature Communications* **2**: 565.

384. Soubeyrand, S., Pope, L., Hache, R.J.G. (2010) Topoisomerase Iiα-dependent induction of a persistent DNA damage response in response to transient etoposide exposure. *Molecular Oncology* **4**(1): 38-51.

385. Sowunmi, A., and Oduala, A.M.J. (1997) Comparative efficacy of chloroquine/chlorpheniramine combination and mefloquine for the treatment of chloroquine-resistant Plasmodium falciparum malaria in Nigerian children. *Transactions of the Royal Society of Tropical Medicine and Hygiene* **91**(6): 689 – 693.

386. Spillman, N.J., Allen, R.J., McNamara, C.W., Yeung, B.K., WInzeler, E.A., Diagana, T.T., Kirk, K. (2013) Na (+) regulation in the malaria parasite *Plasdmodium falciparum* involves the cation ATPase *Pf*ATP4 and is the target of the spiroindolone antimalarials. *Cell Host and Microbe* **13**(2): 227-237.

387. Spillman, N.J., Kirk, K. (2015) The malaria parasite cation ATPase *Pf*ATP4 and its role in the mechanism of action of a new arsenal of antimalarial drugs. *International Journal of Parasitology. Drugs and Drug Resistance* **5**(3): 149-162.

388. Srivastava, A., Philip, N., Hughes, K.R., Gergiou, K., MacRae, J.I., Barret, M.P., Creek, D.J., McConville, M.J., Waters, A.P. (2016) Stage-specific changes in *Plasmodium* metabolism required for differentiation and adaptation to different host and vector environments. *PLoS Pathogens* **12**(12): e1006094.

389. Stadelmann, B., Rufener, R., Aeschbacher, D., Spiliotis, M., Gottstein, B., Hemphill, A. (2016) Screening of the open source malaria box reveals early lead compound for the treatment of alveolar echinococcosis. *PLoS Neglected Tropical Diseases* **10**(3): e0004535.

390. Stanojcic, S., Kuk, N., Ullah, I., Sterkers, Y., Merrick, C.J. (2017) Single-molecule analysis reveals that DNA replication dynamics vary across the course of schizogony in the malaria parasite *Plasmodium falciparum*. *Scientific Reports* **7**(1): 4003.

391. Stewart, C.C., Stewart, S.J. (1994) Cell preparation for identification of leukocytes. *Methods in Cell Biology* **41**: 39-59.

392. Sullivan, D.J., Gluzman, I.Y., Russel, D.G., Goldberg, D.E. (1996) On the molecular mechanism of chloroquine's antimalarial action. *Proceedings of the National Academy of Sciences of the United States of America* **93**(21): 11865-11870.

393. Sullivan, D.J., Matile, H., Ridley, R.G., Goldberg, D.E. (1998) A common mechanism for blockade of heme polymerization by anti-malarial quinolones. *The Journal of Biological Chemistry* **273**(47): 31103-31107.

394. Sullivan, D.J. (2013) Timing is everything in artemisinin action. *Proceedings of the National Academy of Sciences of the United States of America* **110**(13): 4866 – 4867.

395. Sullivan, D.J. (2017) Quinolines block heme crystal step growth. *Proceedings of the National Academy of Sciences* **114**(29): 7483-7485.

396. Sun, J., Liao, J.K. (2004) Induction of angiogenesis by heat shock protein 90 mediated by protein kinase Akt and endothelial nitric oxide synthase. *Arteriosclerosis, thrombosis and vascular biology* **24**(12): 2238-2244.

397. Supputtamongkol, Y., Newton, P.N., Angus, B., Teja-Isavadharm, P., Keeratithakul, D., Rasameesoraj, M., Pukrittayakamee, S., White, N.J. (2001) A comparison of oral artesunate and artemether antimalarial bioactivities in acute *falciparum* malaria. *British Journal of Clinical Pharmacology* **52**(6): 655-661.

398. Suzuki, T., Fujikura, K., Higashiyama, T., Takata, K. (1997) DNA staining for fluorescence and laser confocal microscopy. *Journal of Histochemistry and Cytochemistry* **45**(1): 49-53.

399. Swanson, P.A., Hart, G.T., Russo, M.V., Nayak, D., Yazew T., Pena, M., Khan, S.M., Janse, C.J., Pierce, S.K., Mcgavern, D.B. (2016) CD8+ T Cells induce fatal brainstem

pathology during cerebral malaria via luminal antigen-specific engagement of brain vasculature. *Plos Pathogens* **12**(12): e1006022.

400. Sydor, J.R., Normant, E., Pien, C., Porter, J.R. … Tong, J.K. (2006) Development of 17-allyamino-17-demethoxygeldanamycin hydroquinone hydrochloride (IPI-504), an anti-cancer agent directed against Hsp90. *PNAS* **103**(46): 17408-17413.

401. Sypniewska, P., Duda, J.F., Locatelli, I., Althaus, C.R., Althaus, F., Genton, B. (2017) Clinical and laboratory predictors of death in African children with features of severe malaria: a systematic review and meta-analysis. *BMC Medicine* **15**(147): doi: 10.1186/s12916-017-0906-5.

402. Tarning, J., Rijken, M.J., McGready, R., Phyo, A.P., Hanpithakpong, W., Day, N.P., White, N.J., Nosten, F., Lindegardh, N. (2012) Population pharmacokinetics of dihydroartemisinin and piperaquine in pregnant and nonpregnant women with uncomplicated malaria. *Antimicrobial Agents and Chemotherapy* **56**(4): 1997-2007.

403. Tatuch, Y., Robinson, B.H. (1993) The mitochondrial DNA mutation at 8993 associated with NARP slows the rate of ATP synthesis in isolated lymphoblast mitochondria. *Biochemical and Biophysical Research Communications* **192**(1): 124-128.

404. ter Kuile, F., White, N.J., Holloway, P., Pasvol, G., Krishna, S. (1993) Plasmodium falciparum: in vitro studies of the pharmacodynamics properties of drugs used for the treatment of severe malaria. *Experimental Parastiology* **76**(1): 85-95.

405. Tenopoulou, M., Kurz, T., Doulias, P.T., Galaris, D., Brunk, U.T. (2007) Does the calcein-AM method assay the total cellular 'labile iron pool' or only a fraction of it? *Biochemistry Journal* **403**(2): 261-266.

406. Tewari, S.G., Prigge, S.T., Reifman, J., Wallqvist, A. (2017) Using a genome-scale metabolic network model to elucidate the mechanism of chloroquine action in

Plasmodium falcaiparum. *International Journal for Parastiology: Drugs and Drug Resistance* **7**(2): 138-146.

407. Thomas, D., Tazerouni, H., Sundararaj, K.G.S., Cooper, J.C. (2016) Therpeutic failure of primaquine and need for new medicines in radical cure of *Plasmodium vivax*. *Acta Tropica* **160**: 35-38.

408. Thuy-Nhien, N., Tuyen, N.K., Tong, N.T., Vy, N.T., Thanh, N.V., Van, H.T., Huong-Thu, P., Quang, H.H., Boni, M.F., Dolecek, C., Farrar, J., Thwaites, G.E., Miotto, O., White, N.J., Hien, T.T. (2017) K13 propeller mutations in *Plasmodium falciparum* populations in regions of malaria endemicity in Vietnam from 2009 to 2016. *Antimicrobial Agents and Chemotherapy* **61**(4): doi: 10.1128/AAC.01578-16.

409. Tizifa, T.A., Kabaghe, A.N., McCann, R.S., van den Berg, H., Vugt, M.V., Phiri, K.S. (2018) Prevention efforts for malaria. *Current Tropical Medicine Reports:* doi: 10.1007/s40475-018-0133-y.

410. Tong, J.X., Chandramohanadas, R., Tan, K.S. (2018) High-content screening of the Medicines for Malaria Venture pathogen box for *Plasmodium falciparum* digestive vacuole-disrupting molecules reveals valuable starting points for drug discovery. *Antimicrobial Agents and Chemotherapy* **62**(3): doi: 10.1128/AAC.02031-17.

411. Tonnang, H.E.Z., Kanagalawe, R.Y.M., Yanda, P.Z. (2010) Predicting and mapping malaria under climate change scenarios: the potential redistribution of malaria vectors in Africa. *Malaria Journal* **9**:111.

412. Trager, W., Jensen, J.B. (1976) Human malaria parasites in continuous culture. *Science* **193**(4254): 673-675.

413. Ullah, I., Sharma, R., Biagini, G.A., Horrocks, P. (2017) A validated bioluminescence-based assay for the rapid determination of the initial rate of kill for discovery antimalarials. *The Journal of Antimicrobial Chemotherapy* **72**(3): 717-726.

414. Van Voorhuis, W.C., Adams, J.H., Adelfio, R., Ahyong, V., Akabas, M.H., Alano, P. … Willis, P.A. (2016) Open Source drug discovery with the malaria box compound collection for neglected diseases and beyond. *PLoS Pathogens* **12**(7): e1005763.

415. van Vugt, M., Leonardi, E., Phaipun, L., Slight, T., Thway, K.L., McGready, R., Brockman, A., Villegas, L., Looareesuwan, S., White, N.J., Nosten, F. (2002) Treatment of uncomplicated multidrug-resistant *falciparum* malaria with artesunate-atovaquone-proguanil. *Clinical Infectious Diseases* **35**: 1498-1504.

416. Vangapandu, S., Jain, M., Kaur, K., Patil, P., Patel, S.R., Jain, R. (2007) Recent advances in anti-malarial drug development. *Medicinal Research Reviews* **23**(10): 2829-2843.

417. Varela, M.L., Razakandrainibe, R., Aldebert, D., Barale, J.C., Jambou, R. (2014) Cytometric measurement of *in vitro* inhibition of *Plasmodium falciparum* field isolates by drugs: a new approach for re-invasion inhibition study. *Malaria Journal* **13**(110): doi: 10.1186/1475-2875-13-110.

418. Vazquez-Memije, M.E., Shanske, S., Santorelli, F.M., Kranz-Eble, P., DeVivo, D.C., DiMauro, S. (1998) Comparative biochemical studies of ATPases in cells from patients with the T8993G or T8993C mitochondrial DNA mutations. *Journal of Inherited Metabolic Disease* **21**(8): 829-836.

419. Veale, C.G., Hoppe, H.C. (2018) Screening of the pathogen box reveals new starting points for anti-trypanosomal drug discovery. *MedChemComm* **9**: 2037-2044.

420. Velmurugan, R., Selvamuthukumar, S. (2014) Unsatisfied processing conditions in making ifosfamide nanostructured lipid carriers: Effects of various formulation parameters on particle size, entrapment efficiency, and drug loading capacity. *Journal of Pharmaceutical Negative Results* **5**(1): 8 -12.

421. Vennerstrom, J.L., Nuzum, E.O., Miller, R.E., Dorn, A., Gerena, L., Dande, P.A., Ellis, W.Y., Ridley, R.G., Milhous, W.K. (1999) 8-Aminoquinolines active against blood stage *Plasmodium falciparum in vitro* inhibit hematin polymerization. *Antimicrobial Agents and Chemotherapy* **43**(3): 598-602.

422. Verhoef, H., Veenemans, J., Mwangi, M.N., Prentice, A.M. (2017) Saftey and benefits of interventions to increase folate status in malaria-endemic areas. *British Journal of Haemotology* **177**(6): 905-918.

423. Vesey, G., Narai, J., Ashbolt, N., Williams, K., Veal, D. (1994) Detection of specific microorganism in environmental samples using flow cytometry. *Methods in Cell Biology* **42**: 489-522.

424. Vickers, A.A., Chopra, I., O`Neill, A.J. (2007) Intrinsic novobiocin resitance in *Staphylococcus saprophyticus*. *Antimicrobial agents and chemotherapy* **51**(12): 4484-4485.

425. de Vries, P.J., Dien, T.K. (1996) Clinical pharmacology and therapeutic potential of artemisinin and its derivatives in the treatment of malaria. *Drugs* **52**(6): 818-836.

426. Waknine-Grinberg, J.H., Hunt, N., Bentura-Marciano, A., McQuillan, J.A., Chan, H.W., Chan, W., Barenholz, Y., Haynes, R.K., Golenser, J. (2010) Artemisone effective against murine cerebral malaria. *Malaria Journal* **9**(227): doi: 10.1186/1475-2875-9-227.

427. Walker, J.V., Nitiss, J.L. (2002) DNA topoisomerase II as a target for cancer chemotherapy. *Cancer Investigation* **20**(4): 570-589.

428. Walker, P.G., Floyd, J., Ter Kuile, F., Cairns, M. (2017) Estimated impact on birth weight of scaling up intermittent preventative treatment of malaria in pregnancy given sulphadoxine-pyrimethamine resistance in Africa: A mathematical model. *PLoS Medicine* **14**(2): e1002243.

429. Wallber, F., Tenev, T., Meier, P. (2016) Analysis of apoptosis and necroptosis by fluorescence-activated cell sorting. *Cold Spring Harbor Protocols* **2016**(4): doi: 10.1101/pdb.prot087387.

430. Walsh, J.J., Coughlan, D., Heneghan, N., Gaynor, C., Bell, A. (2007) A novel artemisinin-quinine hybrid with potent anti-malarial activity. *Bioorganic and Medicinal Chemistry Letters* **17**(13): 3599-3602.

431. Wanders, R.J., Ruiter, J.P., Wijburg, F.A., Zeman, J., Klement, P., Houstek, J. (1996) Prenatal diagnosis of systematic disorders of the respiratory chain in the cultured chorionic villus fibroblasts by study of ATP-synthesis in digitonin-permeabilized cells. *Journal of Inherited Metabolic Disease* **19**(2): 133-136.

432. Wang, Z., Liu, M., Liang, X., Siriwat, S., Li, X., Chen, X., Parker, D.M., Miao, J., Cui, L. (2014) A flow cytometry-based quantitative drug sensitivity assay for all *Plasmodium falciparum* gametocyte stages. *PLos ONE* **9**(4): e93825.

433. Wang, J., Zhang, C.J., Chia, W.N., Loh, C.C.Y., Li, Z., Lee, Y.M., He, Y., Yuan, L., Lim, T.K., Liu, M., Liew, C.X., Lee, Y.Q., Zhang, J., Lu, N., Lim, C.T., Hua, Z., Liu, B., Shen, H., Tan, K.S.W., Lin, Q. (2015) Haem-activated promiscuous targeting of artemisinin in *Plasmodium falciparum*. *Nature Communications* **6**: 10111.

434. Wani, W.A., Jameel, E., Baig, U., Mumtazuddin, S., Hun, L.T. (2015) Ferroquine and its derivatives: New generation of antimalarial agents. *European Journal of Medicinal Chemistry* **101**: 534-551.

435. Waxse, B., Sendupta, P., Hesketh, G.G., Lippincott-Schwartz, J., Buss, F. (2017) Myosin VI facilitates connexion 43 gap junction accretion. *Journal of Cell Science*, doi: 10.1242/jcs.199083.

436. Wellems, T.E., Hayton, K., Fairhurst, R.M. (2009) The impact of malaria parasitism: from corpuscules to communities. *Journal of Clinical Investigation* **119**(9): 2496-2505.

437. Wellems, T.E., Hayton, K., Fairhurst, R.M. (2009) The impact of malaria parasitism: from corpuscules to communities. *Journal of Clinical Investigation* **119**(9): 2496-2505.

438. Wells, T.N., Hooft van Huijsduijnen, R. (2015) Ferroquine: welcome to the next generation of antimalarials. *The Lancet. Infectious Diseases* **15**(12): 1365-1366.

439. Wendel, B.S., He, C., Wu, D., Hernandez, S.M., Ma, K.Y., Liu, E.W., Xiao, J., Crompton, P.D., Pierce, S.K., Ren, P., Chen, K., Jiang, N. (2017) Accurate immune repertoire sequencing reveals malaria infection driven antibody lineage diversification in young children. *Nature Communications* **8**(1): doi: 10.1038/s41467-017-00645-x.

440. Whaun, J.M., Rittershaus, C. (1983) Rapid identification and detection of parasitized human red cells by automated flow cytometry. *Cytometry* **4**(2): 117 – 122.

441. White, N.J. (1994) Clinical pharmacokinetics and pharmacodynamics of artmisinin and derivatives. *Transactions of the Royal Society of Tropical Medicine and Hygiene* **88**(Suppl 1): S41-S43.

442. White, N.J. (2010) Artemisinin resistance – the clock is ticking. *The Lancet* **376**: 2051-2052.

443. White, M.T., Bejon, P., Olotu, A., Griffin, J.T., Riley, E.M., Kester, K.E., Ockenhouse, C.F., Ghani, A.C. (2013) The relationship between RST,S vaccine-induced antibodies, CD4+ T cell responses and protection against *Plasmodium falciparum* infection. *PLoS One* **8**(4): e61395.

444. White, N.J., Pukrittayakamee, S., Phyo, A.P., Rueangweerayut, R. … Leong, F.J. (2015) Spiroindolone KAE609 for *falciparum* and *vivax* malaria. *New England Journal of Medicine* **371**(5): 403-410.

445. White, N.J. (2017) Malaria parasite clearance. *Malaria Journal* **16**: 88.

446. White, N.J., Duong, T.T., Uthaisin, C., Nosten, F., Phyo, A.P. … Leong, F.J. (2017) Antimalarial activity of KAF156 in *falciparum* and *vivax* malaria. *New England Journal of Medicine* **375**(12): 1152-1160.

447. Whitesell, L., Shifrin, S.D., Schwab, G., Neckers, L.M. (1992) Benzoquinonoid ansamycins possess selective tumorcidal activity unrelated to src kinase inhibition. *Cancer Research* **52**(7): 1721-1728.

448. Wissing, F., Sanchez, C.P., Rohrback, P., Ricken, S., Lanzer, M. (2002) Illumination of the malaria parasite *Plasmodium falciaprum* alters intracellular pH. *The Journal of Biological Chemistry* **277**(40): 37747-37755.

449. Wong, W., Bai, X., Sleebs, B.E., Triglia, T., Brown, A., Thompson, J.K., Jackson, K.E., Hanssen, E., Marapan, D.S., Fernandez, I.S., Ralph, S.A., Cowman, A.F., Scheres, S.H.W., Baum, J. (2017) Mefloquine targets the *Plasmodium falciparum* 80S ribosome to inhibit protein synthesis. *Nature Microbiology* **2**(17031): doi: 10.1038/nmicrobiol.2017.31.

450. World Health Organization. (2018). World malaria report 2018. World Health Organization. http://www.who.int/iris/handle/10665/275867. License: CC BY-NC-SA 3.0 IGO

451. Wu, D.L., Wang, G.X., Tang, D.H. (2001) Observation on the effect of napthoquine phosphate on the control of malaria in Qiongzhong County, Hainan Province. *China Tropical Medicine* **1**(3): 216-217.

452. Wu, L., Chen, X., Huang, L., Tian, J., Ke, F., Xu, J., Chen, Y., Zheng, M. (2015) A novobiocin derivative, XN4, inhibits the proliferation of chronic myeloid leukemia cells by inducing oxidative DNA damage. *PLOS One* **10**(4): e0123314.

453. Wyatt, C.R., Goff, W., Davis, W.C. (1991) A flow cytometric method for assessing vialbity of intraerythrocytic hemoparasites. *Journal of Immunological Methods* **140**(1): 23-30.

454. Yang, H., Lee, M., Park, I., Jeon, H., Choi, J., Seo, S., Kim, S., Koh, G.H., Park, K., Lee, D.H. (2017) HSP90 inhibitor (NVP-AUY922) enhances the anti-cancer effect of BCL-2 inhibitor (ABT-737) in small cell lunch cancer expressing BCL2. *Cancer Letters* **411**: 19-26.

455. Yayon, A., Cabantichik, Z.I., Ginsburg, H. (1985) Susceptibility of human malaria parasites to chloroquine is pH dependent. *PNAS* **82**(9): 2784-2788.

456. Yazon, A., Cabantchik, Z.I., Ginsburg, H. (1984) Identification of the acidic compartments of *Plasmodium falciparum*-infected human erythrocytes as the target of the anti-malarial drug chloroquine. *EMBO* **3**(11): 2695-2700.

457. Yeo, A.E., Rieckmann, K.H., Christopherson, R.I. (1998) Indirect inhibition by antibiotics of nucleotide and deoxynucleotide biosynthesis in *Plasmodium falciparum*. *Southeast Asian Journal of Tropical Medicine and Public Health* **29**(1): 24-26.

458. Yoo, J.H., Shi, D.S., Grossman, A.H., Sorensen, L.K., Tong, Z., MLeynek, T.M., Rogers, A., Zhu, W., Richards, J.R., Winter, J.M., Zhu, J., Dunn, C., Bajji, A., Shenderovich, M., Meuller, A.L., Woodman, S.E., Harbour, J.W., Thomas, K.R., Odelberg, S.J., Ostanin, K., Li, D.Y. (2016) ARF6 is an actionable node that orchestrates oncogenic GNAQ signaling in uveal melanoma. *Cancer Cell* **29**(6): 889-904.

459. Yoo, S.M., Cerione, R.A., Antonyak, M.A. (2017) The Arf-GAP and protein scaffold Cat1/Git1 as a multifaceted regulator of cancer progression. *Small GTPases* **5**: 1-9.

460. Young, R.D., Rathod, P.K. (1993) Clonal viability measurements on Plasmodium falciparum to assess in vitro schizonticidal activity of leupeptin, chloroquine, and 5-fluoroorotate. *Antimicrobial Agents and Chemotherapy* **37**(5): 1102-1107.

461. Zeeman, A.M., Lakshminarayana, S.B., van der Werff, N., Klooster, E.J. … Kocken, C.H. (2016) PI4 kinase is a prophylactic but not radical curative target in *Plasmodium vivax*-type malaria parasites. *Antimicrobial Agents and Chemotherapy* **60**(5): 2858-2863.

462. Zhang, J., Krugliak, M., Ginsburg, H., (1999) The fate of ferriprotorphyrin IX in malaria infected erythrocytes in conjunction with the mode of action of anti-malarial drugs. *Molecular and Biochemical Parasitology* **99**(1): 129-141.

463. Zhang, J.X., Li, H., Chan, C.F., Lan, R., Chan, W.L., Law, G.L., Wong, W.K., Wong, K.L. (2012) A potential water-soluble ytterbium-based porphyrin-cyclen dual bio-probe for Golgi apparatus imaging and photodynamic therapy. *Chemical Communications* **48**: 9646-9648.

464. Zhang, M., Gallego-Delgado, J., Fernandez-Arias, C., Waters, N.C., Rodriguez, A., Tsuji, M., Wek, R.C., Nussenzweig, V., Sullivan, W.J. (2017) Inhibiting the *Plasmodium* eIF2α kinase PK4 prevents artemisinin-induced latency./ *Cell Hot and Microbe* **22**(6): 766-776.

465. Zielonka ,J., Zhao, H., Xu, Y., Kalyanaraman. (2005) Mechanistic similarities between oxidation of hydroethidine by Fremy's salt and superoxide: Stopped-flow optical and EPR studies. *Free Radical Biology & Medicine* **39**: 853-863.